

**A novel evolutionary approach for the discovery of small
bioactive molecules**

George Karageorgis

Submitted in accordance with the requirements for the degree of

Doctor of Philosophy

The University of Leeds

School of Chemistry

January, 2015

The candidate confirms that the work submitted is his own, except where work which has formed part of jointly-authored publications has been included. The contribution of the candidate and the other authors to this work has been explicitly indicated below. The candidate confirms that appropriate credit has been given within the thesis where reference has been made to the work of others. Further details of the jointly-authored publications and the contributions of the candidate and the other authors to the work are included below.

“Efficient discovery of Androgen Receptor modulators by Activity-Directed Synthesis” George Karageorgis, Stuart Warriner and Adam Nelson, *Nature Chemistry*, 2014, **6**, 872-876.

A.N. and S.W. conceived, designed and supervised the project. G.K. undertook the experimental work. A.N., S.W. and G.K. analysed the results and wrote the paper.

This copy has been supplied on the understanding that it is copyright material and that no quotation from the thesis may be published without proper acknowledgement.

The right of George Karageorgis to be identified as author of this work has been asserted by him in accordance with the Copyright, Designs and Patents Act 1988.

© 2015 The University of Leeds and George Karageorgis

Acknowledgements

Reaching the final stages of this PhD project I cannot but think back to its beginning, where Adam and Stuart proposed that, instead of taking on any other project, maybe I should have tried my hands on this one. In all honesty, I did not quite think it through before I agreed and it has turned to one of the most joyful things of my life so far. I am immensely indebted to both Adam and Stuart for entrusting me with this project and will forever be grateful for their support, guidance and mentoring in both, my academic as well as life endeavors.

I was blessed with having loving parents who supported me in every possible way and taught me to chase my ambitions and push myself to achieve all that I can. My Father passed on to me his scientific sense of curiosity, structured and methodic thinking, hard-working nature and spontaneous personality whilst my Mother her courage, perseverance and patience; personality traits which all proved to be very useful throughout this period of my life. Their endless love and support has given me the courage to reach this far, and probably go a lot further. I cannot forget my brothers, who made me look at the bright side of things, even if there wasn't one, giving me courage to push forward.

Fellow students and colleagues in Chemistry, G56 deserve my appreciation and gratefulness, especially for putting up with my horrible jokes, my explosively loud Cypriot presence and awkward moments following my miserably failed attempts to grasp the concept and basis of sarcasm. More specifically, Dr Thomas James (TOJ) who also as a *deus ex machina* helped my lovely wife in her job search, Dr Mark Dow (MD) who taught me how to properly do a column, Dr Richard Doveston (Ricardo), Dr Philip Craven (Phil) and Dr James Firth (Colin) for useful discussions on Chemistry and NMR, Dr Giorgia Magnatti, Dr Alun Myden (A-dogg) Dr Charles-Hugues Lardeau, and George Burslem for fun times in the lab, and of course Steven Kane (Phteven) for numerous discussions about movies, photography, chemical literature and introducing me to squash. It took me three months to begin to understand his accent but as it turned out, English

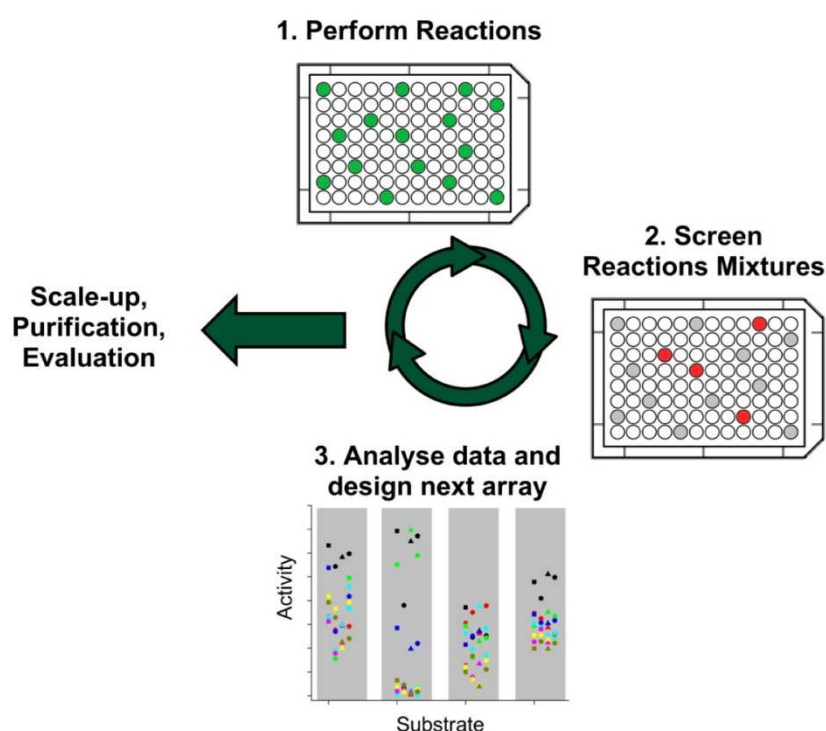
is neither his or mine first language. Not least, Dr James Murray, Dr Dan Williamson and Dan Foley for fun times and discussions to go with a cold pint. Everyone made life in the lab a joy even when things weren't going as expected and for that I will always be thankful.

Last but not least, I would like to thank my beautiful wife, Maria, who believed in me, and followed me to the UK as my girlfriend before agreeing to marry me. Her love, comfort and support helped put me through the difficult times and kept me focused on what mattered. She always recognised the significance of my work and her taking pride in what I do, drove me forward. The occasional home-made chocolate cake was merely a bonus. *Καρδούλα μου, ευχαριστώ.*

Abstract

Current approaches for the discovery of bioactive molecules tend to treat all molecules in large collections with the same significance regardless of their ultimate biological activity. Furthermore, these approaches exploit a limited palette of reliable well-working reactions, that have been optimised for the preparation of individual compounds.

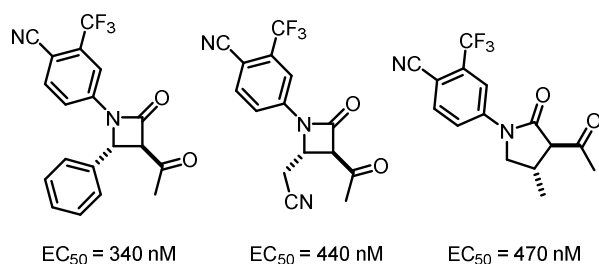
This thesis describes the development of a new discovery approach – Activity-Directed Synthesis. The approach aims to merge the discovery of small bioactive molecules with the emergence of a synthetic route. In this regard Activity-Directed Synthesis may be analogous with the evolution of biosynthetic pathways as is observed in Nature.



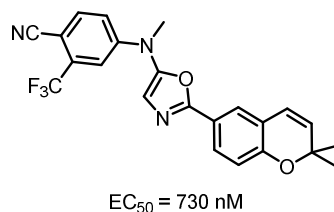
For the implementation of Activity-Directed Synthesis, a well-studied chemical toolbox – metal carbenoid chemistry – that has been underutilised in bioactive molecule discovery was used. The approach was demonstrated in the discovery of novel chemotypes of small bioactive molecules that agonise the Androgen Receptor. Both intra- and intermolecular reactions were exploited in sequential rounds of carbenoid reactions which had many alternative outcomes. Three iterative rounds of screening crude reaction

mixtures and design of subsequent reaction arrays enabled the rapid discovery of reactions that yielded bioactive products. Hence small-molecule modulators of the Androgen Receptor, based on scaffolds with no previously annotated activity were discovered.

Intramolecular reaction products



Intermolecular reaction products



A total of 272 microreactions was performed in the case of intramolecular reactions and a total of 326 microreactions was performed in the case of intermolecular reactions. In the case of the intramolecular chemistry, it was demonstrated retrospectively that the approach enabled the parallel optimisation of both the structure of bioactive molecules and the routes for their synthesis. In the case of the intermolecular chemistry, it was demonstrated that non-exhaustive reaction arrays could still lead to the discovery of sub-micromolar modulators of the Androgen Receptor, greatly improving the efficiency of Activity-Directed Synthesis.

Table of Contents

Acknowledgements	i
Abstract	iii
Table of Contents	v
Abbreviations	viii
1. Chapter 1 Evolutionary approaches for the discovery of bioactive molecules	1
1.1. Introduction	1
1.2. Current approaches in bioactive molecule discovery	3
1.2.1. DNA-encoded libraries	5
1.2.1.1. DNA-recorded libraries	5
1.2.1.2. DNA-templated libraries.....	8
1.3. Activity-Directed Synthesis.....	11
1.4. Selection of a chemical toolbox for activity-directed synthesis....	14
1.5. Selected Biological Target: The Androgen Receptor	19
1.5.1. The Structural and Chemical Biology of the Androgen Receptor	19
1.5.2. Androgen receptor ligands: agonists, antagonists and Selective AR modulators (SARMs).....	22
1.6. Project Outline.....	25
1.7. Summary.....	27
2. Chapter 2 Synthesis of diazo substrates for intramolecular metal-catalysed carbenoid reactions	28
2.1. Development of methods for the preparation of diazo-compounds.....	28
2.1.1. Development of a synthetic approach using a model system	29
2.1.2. Development of a synthetic methodology for the preparation of aryl diazo-acetamides	31
2.2. Preparation of the diazo-butanamide and acetamide precursors	33
2.2.1. Preparation of the diazo-compounds	35
2.3. Summary.....	40
3. Chapter 3 Establishment of a high-throughput assay	42
3.1. Invitrogen TR-FRET Androgen Receptor Biochemical Assay	42
3.2. Establishing the plate reader set-up.....	44

3.2.1.	Determination of the activity of known agonists and antagonists.....	46
3.3.	Metal scavenging studies.....	47
3.4.	Determination of the activity of the diazo precursors.....	48
3.5.	Summary.....	49
4.	Chapter 4 Exploitation of intramolecular reactions in the Activity-Directed Synthesis of androgen receptor agonists	50
4.1.	Reaction array 1.....	50
4.2.	Reaction array 2.....	52
4.3.	Reaction array 3.....	55
4.4.	Scale up.....	58
4.4.1.	Reactions from diazo substrate 17a	59
4.4.2.	Reactions from diazo substrate 17b	60
4.4.3.	Reactions from diazo substrate 17i	61
4.5.	Evaluation of the isolated products.....	62
4.6.	Synthesis of β -lactam 25 via an alternative route.....	63
4.7.	Retrospective exploration of the basis of the emergence of Activity-Directed Synthesis.....	64
4.7.1.	Quantitative HPLC.....	64
4.7.2.	Diversity of products.....	65
4.8.	Summary.....	69
5.	Chapter 5 Exploitation of Intermolecular Reactions in the Activity-Directed Synthesis of Androgen Receptor Agonists.....	72
5.1.	Synthesis of diazo amide substrates for intermolecular reactions.....	72
5.2.	Selection of co-substrates for the intermolecular reactions.....	75
5.3.	Intermolecular reaction array 1.....	79
5.4.	Intermolecular reaction array 2.....	82
5.5.	Intermolecular reaction array 3.....	87
5.6.	Scale-up.....	90
5.6.1.	Reactions identified in reaction array 1.....	92
5.6.2.	Reactions identified in reaction array 2.....	93
5.6.3.	Reactions identified in reaction array 3.....	94
5.7.	Biological and structural assessment of isolated compounds.....	95
5.7.1.	Biological evaluation of isolated compounds.....	95
5.7.2.	Structural evaluation of active modulators.....	98
5.8.	Summary.....	99

6.	Chapter 6 Conclusions and Future Work.....	101
6.1.	Conclusions.....	101
6.1.1.	Activity-Directed Synthesis exploiting intramolecular reactions.....	101
6.1.2.	Activity-Directed Synthesis exploiting intermolecular reactions.....	101
6.2.	Future work	102
6.2.1.	Retrospective exploration of the intermolecular reaction arrays.....	102
6.2.2.	Crystallographic Studies	103
6.2.3.	Further Future Work.....	103
7.	Chapter 7 Experimental Section	106
7.1.	Instrumentation and General Information.....	106
7.2.	Experimental Procedures	107
7.2.1.	Experimental procedures for organic compounds	107
7.2.2.	Compound Data	110
7.2.3.	Experimental procedures for assaying individual compounds or reaction mixtures from intra- or intermolecular reaction arrays	155
7.2.4.	Experimental procedure for the metal scavenging studies	159
7.2.5.	Experimental procedure for quantitative HPLC analysis of product mixtures containing the β -lactam 25	162
8.	References.....	163

Abbreviations

Ac	acetyl
ADS	Activity-Directed Synthesis
ap.	apparent
AR	Androgen Receptor
AR LBD	Androgen Receptor Ligand-binding Domain
Ar	aromatic
Bn	benzyl
b	broad
conc.	concentrated
COSY	correlation spectroscopy
δ	chemical shift
d	doublet
dd	double doublet
DHT	5 α -Dihydrotestosterone
DMF	<i>N,N'</i> -dimethylformamide
DMSO	Dimethyl sulfoxide
dq	double quartet
dt	double triplet
<i>e.g.</i>	<i>example gratia</i> ; for example
<i>etc.</i>	<i>et cetera</i> ; and so forth
ES	electrospray ionisation
Et	ethyl
EtOAc	ethyl acetate
ether	diethylether
hept	heptet

HMBC	heteronuclear multiple bond correlation experiment
HMQC	heteronuclear multiple-quantum coherence experiment
HRMS	high resolution mass spectrometry
<i>i.e.</i>	<i>id est</i> , that is
IR	infrared
<i>J</i>	spin-spin coupling constant
LC-MS	liquid chromatography mass spectrometry
m	multiplet
Me	methyl
MeCN	acetonitrile
m.p.	melting point
<i>m/z</i>	mass to charge ratio
MS	mass spectrometry
NMR	nuclear magnetic resonance
nOe	Nuclear Overhauser Effect
NOESY	Nuclear Overhauser Effect Spectroscopy
<i>p</i> -ABSA	<i>para</i> -acetamidobenzenesulfonylazide
petrol	petroleum spirit
Ph	Phenyl
ppm	parts per million
q	quartet
R_f	retention factor
rot	rotamer
rt	room temperature
s	singlet
t	triplet

TE	Testosterone
<i>tert</i>	tertiary
THF	tetrahydrofuran
TLC	thin layer chromatography
TR-FRET	Time Resolved Förster Resonance Energy Transfer
<i>via</i>	by way of

1. Chapter 1

Evolutionary approaches for the discovery of bioactive molecules

Synthetic and naturally occurring small bioactive molecules are of immense value both as tools for chemical biology and starting points for drug discovery.¹ This chapter outlines current approaches for the discovery of bioactive molecules, and emerging evolutionary approaches. This description is followed by an overview of the proposed project in which an evolutionary approach to bioactive molecule discovery – activity-directed synthesis – was developed.

1.1. Introduction

Advances in molecular and biological sciences have provided a dramatically improved understanding of many biological mechanisms and diseases at the molecular level.² However, the discovery of biologically active molecules suited to study these mechanisms is lagging.³ It can be argued that this gap between these two aspects of drug discovery is not due to a lack of the necessary synthetic methods but, rather, a lack of tools to select which molecules should be synthesised.²⁻³

Historically, chemists have often initiated bioactive molecule discovery using high-throughput screening (HTS) of a large collection of compounds as a starting point. This process can identify active compounds or classes of compounds with similar scaffolds or three-dimensional structures. Subsequent determination of Structure-Activity Relationships (SARs) indicates the structural features which contribute most to the displayed activity. To establish SARs, a focused set of molecules is usually prepared; each molecule purified usually in series and tested usually in parallel to identify the most active molecules. These molecules are submitted to further evaluation *in vitro* and *in vivo*. Test results are used to confirm the desired bioactivity, the mechanism of action, and provide feedback for further structural optimisation. An illustrative example is shown in Figure 1.1.

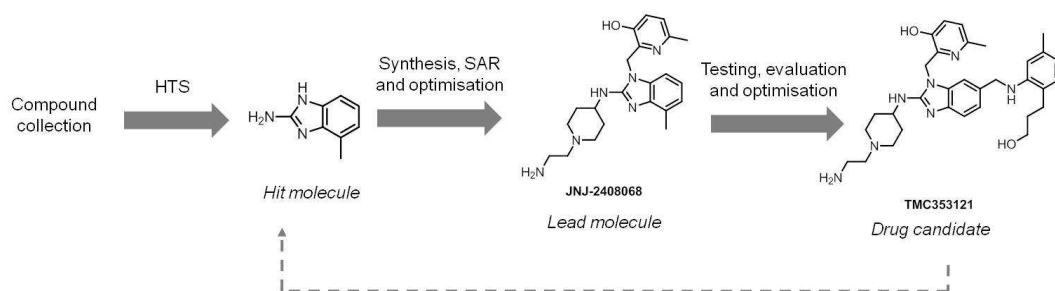


Figure 1.1: Illustrative example of a bioactive molecule discovery in drug discovery. HTS highlights hit molecules which are then optimised and tested.

SAR studies and combinatorial chemistry have been proven successful in generating promising drug candidates.⁴ Nevertheless, this approach is highly empirical and time consuming. Equal resource is invested in all molecules regardless of their ultimate biological activity because each stage – molecular design, synthesis purification and testing – is undertaken in isolation. Furthermore, chemists tend to exploit a limited palette of reliable well-working reactions, optimised for the preparation of a single, pure compound.⁵ This bias has led to a historically uneven exploration of the chemical space and may inadvertently limit the diversity of the structures being investigated.⁶

In sharp contrast, Nature applies a highly efficient evolutionary approach from which bioactive natural products ultimately emerge. Nucleic acids are transcribed and translated to give biosynthetic enzymes which use simple bioavailable small molecules to synthesise constellations of more elaborate structures: natural products. If the natural products have a beneficial effect for the host organism, the latter lives on to inherit these characteristics. Through iterative rounds of cell survival and selection, ultimately biosynthetic pathways emerge to yield natural products with beneficial functions. This approach led to the emergence of bioactive products and associated synthetic pathways in parallel (Figure 1.2).

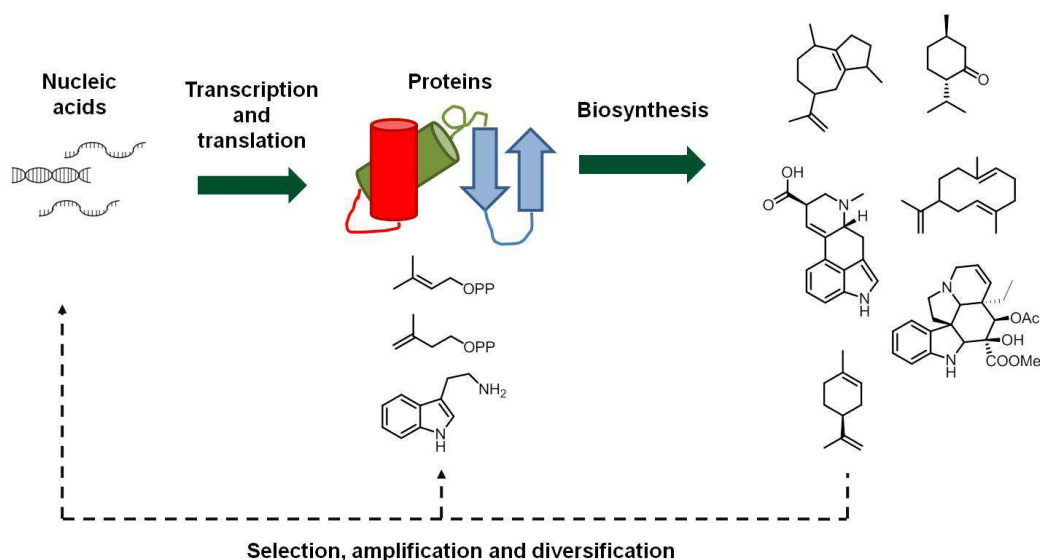


Figure 1.2: Evolution of biosynthetic pathways. Nature generates bioactive molecules through iterating rounds of selection based on cell-survival.

1.2. Current approaches in bioactive molecule discovery

The biological activity and structural diversity which are displayed by natural products have stimulated researchers to incorporate selection strategies inspired by Nature into *in vitro* approaches for the discovery of bioactive molecules. These approaches outlined below attempt to drive efficient selection of biologically active compounds from large or putative libraries based on biological activity. Some also introduce elements of feedback into molecule optimisation.

Dynamic Combinatorial Chemistry (DCC) has emerged as an approach that enables the synthesis of molecules from building blocks to be directed on the basis of their affinity for a target protein. In DCC, a library of building blocks armed with functionalities which allow reversible bond formation, is incubated with a target protein. The target then templates the assembly of productive combinations of building blocks to yield a molecule that forms a stable protein-ligand complex. Despite the fact that DCC has been proven successful in several cases,⁷ it has significant limitations, such as the requirement for stoichiometric amounts of the target protein and the need to conduct reversible chemical reactions in conditions under which the target

protein is stable. These limitations can also restrict the potential diversity of the bioactive products.

An alternative approach which directly linked cell survival with the presence of a bioactive molecule was developed by Benkovic and co-workers. A systematic approach for discovering genetically selected cyclic peptide modulators of protein-protein interactions (PPIs) was developed.⁸ The approach exploits split-intein ligations,⁹ and leads to the formation of genetically-encoded intracellular libraries of cyclic peptides (Figure 1.3.A). These libraries of cyclic peptides are then screened using a reverse two-hybrid system. Here, cell growth is coupled to the desired bioactivity, e.g. the disruption of a specific PPI (Figure 1.3.B). If the targeted PPI is not disrupted, the transcription of genes necessary for cell survival in a specific growth medium is prevented. The ability of the cyclic peptide to function as a PPI inhibitor is thereby directly linked to the survival of the host cell.

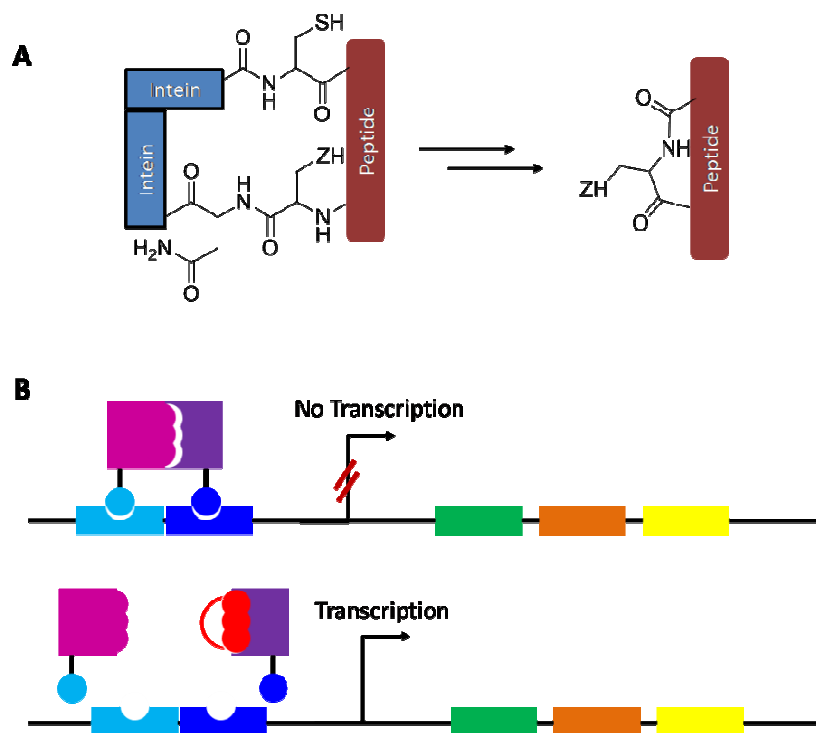


Figure 1.3: **A.** Simplified illustration of the split-intein ligation system to create a library of cyclic amides. **B.** Illustration of the reverse two-hybrid system. Disruption of the PPI (pink and purple protein) results in the transcription of a gene cluster (green, brown and yellow codons) necessary for cell survival (Adapted from *Nat. Protocols* 2007, 2, 1126).

Genetic expression and selection occur simultaneously mimicking the naturally-imposed selection pressure. Benkovic's group has demonstrated the applicability of their method on a range of targets such as the disruption of the homodimerisation of a HIV-1 protease⁸ and AICAR transformylase,¹⁰ as well as inhibition of a DAM methyltransferase in *E. Coli*.⁹ This system is able to utilise the natural synthetic pathways of the host organism to produce vast numbers of different cyclic peptides and mimic Nature's effective selection and amplification features *via* cell survival. However, this system is only able to produce peptidic molecules and can only be exploited in the discovery of cyclic peptides.

1.2.1. DNA-encoded libraries

A recent approach which can integrate some evolutionary aspects into bioactive molecule discovery approaches involves DNA-encoded libraries. These libraries are classed into two categories: DNA-recorded and DNA-templated libraries.

1.2.1.1. DNA-recorded libraries

In DNA-recorded libraries, DNA duplex tags or strands are used to record the history of the synthesis and enable deconvolution of the structure of the synthesised molecule using DNA sequencing. The generation of the library starts from a chemically functionalised DNA template. An initial pool is split into several batches and different chemical reactions with various building blocks are performed; at each step of the synthesis, a DNA tag which indicated the transformation used is enzymatically attached in order to track the synthesis, before the sub-pools are re-combined. Clark and co-workers¹¹ have reported the discovery of a novel, p38 MAP kinase inhibitor using the approach. The initial free amine group was conjugated with a DNA duplex template. In only four cycles of splitting, reacting, tagging and pooling a library of over 800 million members was generated (Figure 1.4).

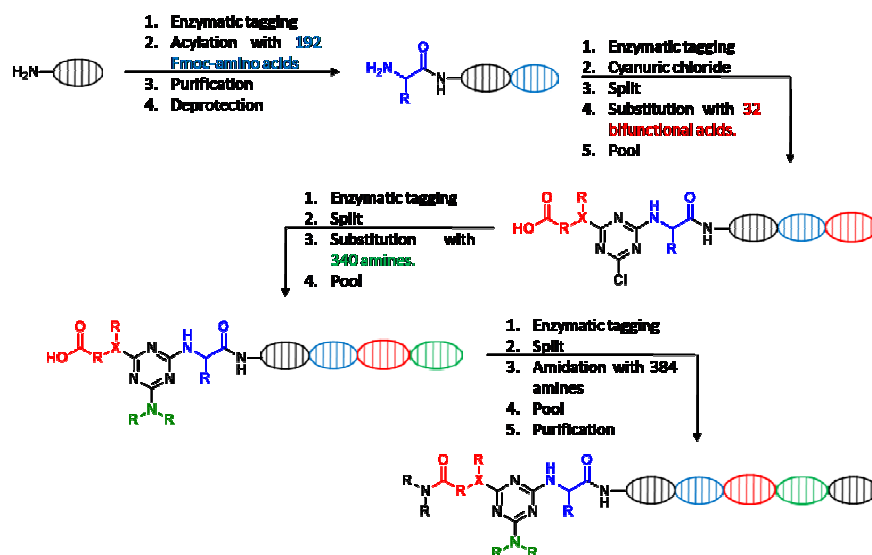


Figure 1.4: Generation of a DNA-recorded library using a “split-tag-and-pool” combinatorial approach. A DNA-tag is enzymatically attached at each step to record the history of the synthesis (Adapted from *Nat. Chem. Biol.* 2009, 5, 647).

An aliquot of the library was incubated with the immobilised protein and non-binding molecules were then washed away. The protein was then denatured and the binding molecules were retrieved. PCR was used to amplify the DNA sequences of the binding molecules which were then and incubated with a fresh sample of protein. After only three iterative rounds of incubation and selection of the DNA sequences by PCR, potent inhibitors of the same scaffold family were identified (Figure 1.5), whose structures were revealed by sequencing of the corresponding DNA sequences.

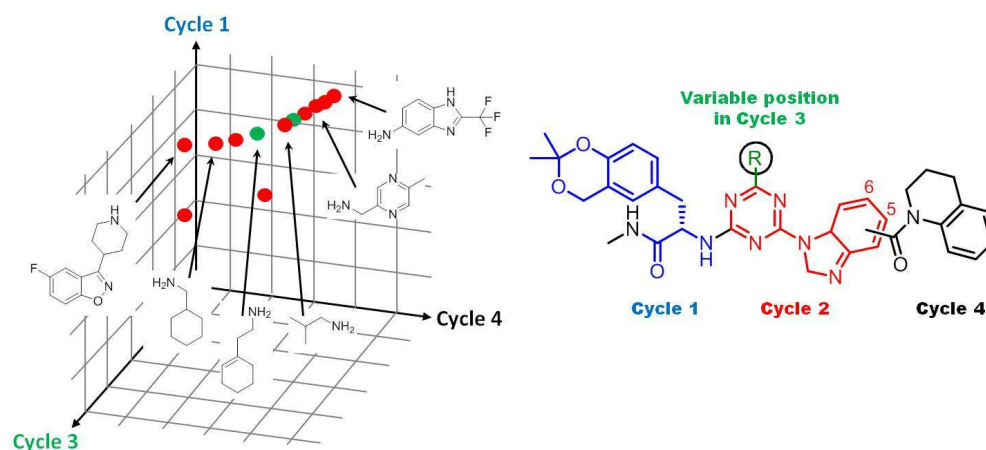


Figure 1.5: Three-dimensional SAR diagram illustrating compounds which bind to p38 MAPK (left). All hits share a common scaffold, varying only at the position of the triazine ring (right) (Adapted from *Nat. Chem. Biol.* 2009, 5, 647).

Re-synthesis of the hit compounds as individual molecules confirmed both their inhibitory actions against the p38 MAPK and their nanomolar binding potency. Furthermore, a crystal structure of one of the hit compounds bound to p38 MAPK revealed that the DNA template was unlikely to affect the compound binding in any way, since the DNA-linking carboxamide was found to be exposed to solvent.

Undertaking a related approach, Neri and co-workers exploited DNA-encoded libraries of fragments in combination with the concept of DCC.¹² These encoded self-assembling chemical libraries comprise various small molecular fragments attached to different single-stranded DNA, containing a common hybridisation region and a unique label. The DNA-tag enables both the assembly of fragments and their identification (Figure 1.6). Neri's group has reported the application of this approach in the discovery of pairs of fragments that bind to trypsin,^{12a,13} MMP-3¹³ and streptavidin.¹⁴ Although efficient this approach is not evolutionary as there is no possibility for mutations to vary the structure of the fragments or ligands. Also, this approach identifies combinations of fragments which still need to be linked together in order to synthesise a potentially bioactive molecule. Additional effort is thus required to identify an appropriate linkage between the two fragments.

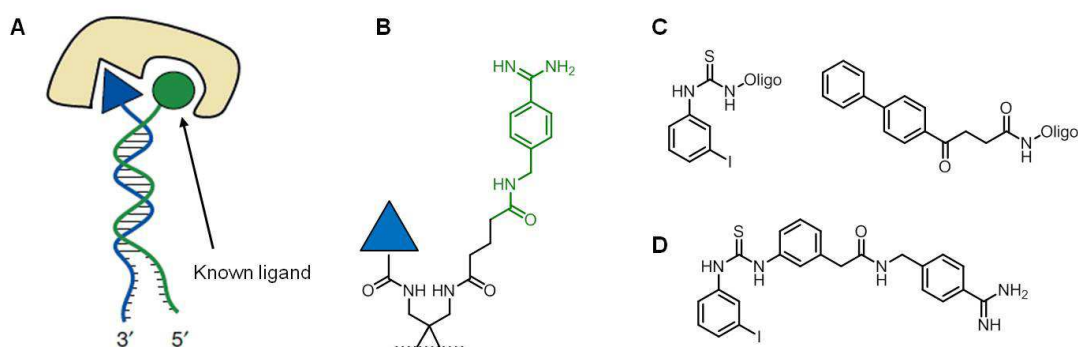


Figure 1.6: Application of the ESAC library on trypsin. **A:** A known ligand was used as a warhead. **B:** Chemical structure of the known ligand and linker to the DNA oligos when assembled. A library of 620 small molecules was screened (blue triangle). **C:** Examples of small molecules selected. **D:** New molecule synthesised with nanomolar inhibitory activity against trypsin. A suitable linker needs to be identified to link the two fragments.

1.2.1.2. DNA-templated libraries

In contrast to DNA-recorded libraries, DNA-templated libraries rely on the recognition and hybridisation properties of nucleic acids to encode the synthesis: reactants are brought into close proximity, thus increasing their effective concentration and the rate of the reaction, enabling the DNA to encode the structure of the synthesised molecule. Work carried out mainly by Liu and co-workers has demonstrated that this templated concept can be implemented to perform a wide range of chemical transformations including reactions in organic solvents,¹⁵ stereoselective reactions¹⁶ and multi-step reactions.¹⁷

The sequence specific hybridisation properties of DNA-templates assure that at low concentrations, reactions between mismatched DNA templates will not occur. In this sense, each DNA-template can be considered as a virtual “nano-vessel”. This aspect of DNA-templated synthesis sets the basis for the generation of DNA-templated libraries, as parallel reactions can be performed in a single reaction vessel and libraries of compounds can be prepared as a whole. DNA-templates and reagents can be pooled together and the individual building blocks will only react as directed by DNA sequence specificity. The intermediates can be purified as a whole library and be submitted to the next round of reactions in order to introduce different levels of structural diversity and generate the full library (Figure 1.7).

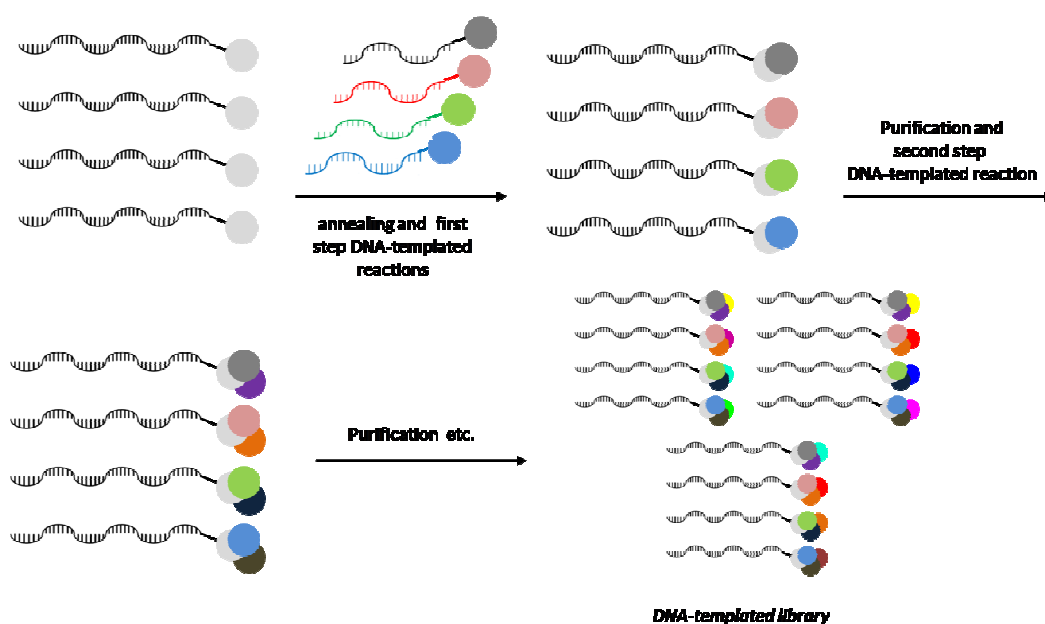


Figure 1.7: Generation of a DNA-templated library. Parallel reactions occur in the same vessel, programmed by the sequence specificity of the DNA-templates.

To eliminate complications stemming from low concentration factors, PCR amplification and DNA-sequencing can be used to identify the structures of highly-active molecules that are present in low concentration. Liu and co-workers have demonstrated the applications of their approach by preparing two DNA-templated macrocyclic fumaramide libraries; a small library of 65 members^{17b} and a larger one containing 13 824 different members (Figure 1.8A).¹⁸ Liu's group used the small library for a proof-of-concept study.¹⁹ The DNA-conjugated library members were amplified by PCR before and after selection. After only three selection rounds, a 10^3 -fold enrichment was observed for some molecules, which allowed the amplification of high affinity binding molecules present in low concentration. This enrichment of the overall library population with more active binders demonstrated the viability of the selection-based screening and DNA-templated libraries. Although evolution of structure would be possible in principle, by introducing mutations to the DNA template, such an example has not yet been demonstrated experimentally.

Liu's methodology has been commercialised by the company Ensemble Discovery applying the principles of DNA-templated libraries in drug discovery.²⁰ After screening and selection against a biological target, potent molecules are identified by PCR amplification and DNA sequencing.

The selection data are used for the design of the next generation optimised library providing an aspect of evolution to this promising drug discovery approach.

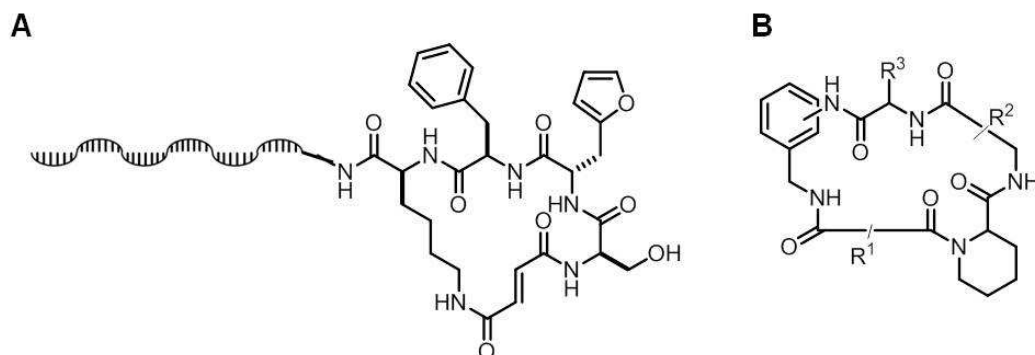


Figure 1.8: Macrocyclus prepared using DNA-templated synthesis. **A:** macrocyclic furamide structures with DNA oligo attached. **B:** Example of an Ensemblin macrocycle able to inhibit a certain protein-protein interaction.

Nature has developed a wide range of biologically active small molecules by imposing selection pressure on constellations of natural products derived from a set of available starting materials. This process generates molecules whose high affinity and specificity for their designated biological targets increases over iterating rounds of cell-survival. Achieving the combination of both the selection and evolution aspects, *i.e.* a methodology mimicking Nature's approach is extremely challenging to implement. Current approaches implement methods which enable the selection of active molecules from a large set of possible combinations.^{9-14,21} However, few of these approaches exploit the evolutionary aspects that characterise Nature's approach, *i.e.* utilising the activity of a group of products as feedback element in an iterative manner.

1.3. Activity-Directed Synthesis

The aim of the project was the development of a new chemical evolutionary approach for the discovery of novel bioactive molecules. It was envisaged that the new approach would be able to focus on active molecules rather than treating all molecules with the same significance. Furthermore, in contrast to current approaches where synthesis and selection occur in isolation of each other, the new approach aims to bring the synthesis of molecules and their screening together, much like its observed in biosynthetic pathways. It was hypothesised that it should be possible to mimic the evolutionary process of Nature by replacing metabolites with starting materials susceptible to different chemical transformations, and biosynthetic proteins with chemical catalysts and reagents.

As shown in Figure 1.9, the methodology would exploit arrays of reactions with inherently unpredictable outcome to produce mixtures of products. After removing the catalyst by scavenging and the solvent by evaporation, the crude product mixtures would be dissolved in buffer and screened, thus identifying reactions that yield bioactive products. The results would be analysed to inform the design of a subsequent reaction array. The process would be repeated with the subsequent array being screened at a lower concentration in order to impose selection pressure onto the system. Finally, promising reactions would be performed to scale in order to isolate the products, characterise and evaluate their biological activity.

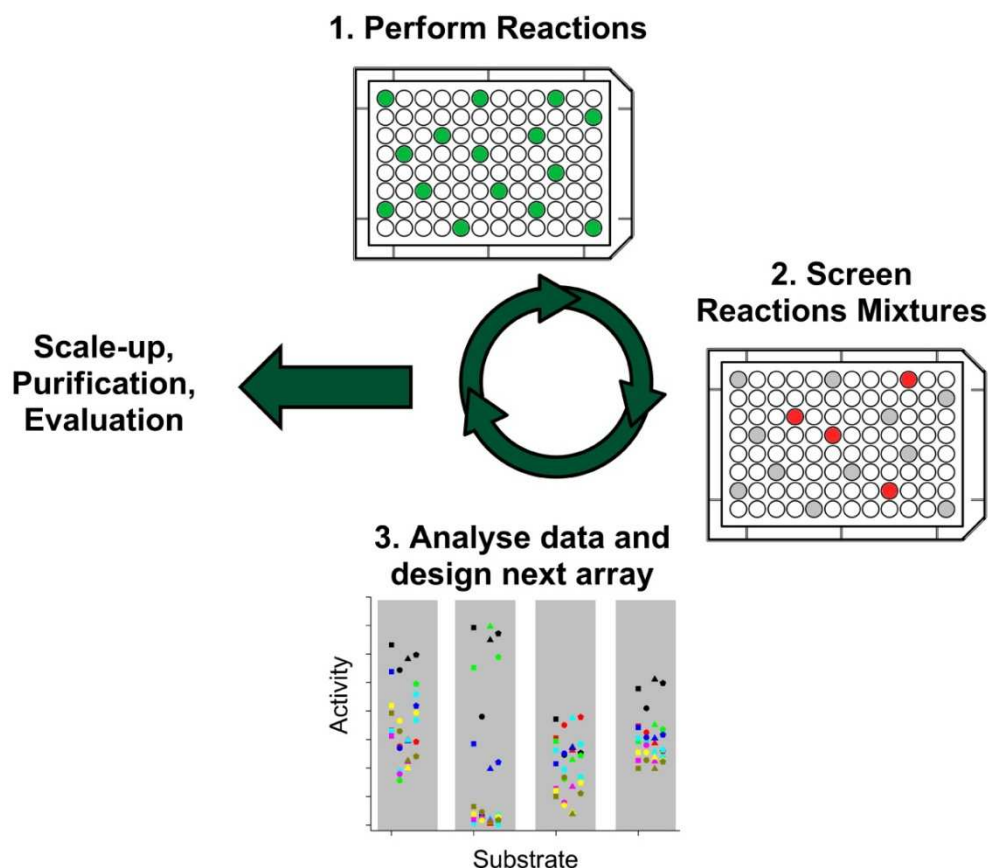


Figure 1.9: Illustrative diagram describing Activity-Directed Synthesis. Such an approach would bring together all the stages in the discovery of bioactive molecules, and facilitate the parallel emergence of an associated synthetic route.

By exploiting reactions with multiple possible outcomes rather than predictable and optimised chemical reactions, generating mixtures of diverse products rather than just a single compound, this process will allow the rapid and facile identification of molecules active against a desired biological target. Evolutionary feedback would be utilised through the analysis of the information from the screening of a first reaction array to design a second reaction array. Such an approach would, in principle, allow the optimisation of both the structure of the active component as well as a route for its synthesis simultaneously.

Methods exploiting the possibilities of multiple reaction pathways have been applied for the discovery of novel chemical reactions or metal catalysts.²² For example, Hartwig and co-workers,^{22d} utilised GC-MS as a screening method to identify three novel metal-catalysed reactions using a

HTS 384-well plate setup. Small molecule substrates were added to the rows of the well plate and mixed with different metal catalysts and ligands added to the columns of the plate. After the reactions were conducted, GC-MS was used to identify the formation of products, the mass of which was significantly greater than that of the small molecule substrates. Products identified with positive biological activity using the suggested approach would be re-synthesised and tested individually to confirm their potency.

A related approach to bioactive ligand discovery, dubbed synthetic fermentation was recently published by Huang *et al.*²³ Multiple simple building blocks (isoxazolidine-based monomers) reacted in a well plate setup, with α -ketoacids to form β -amides. Initiating and terminating building blocks could only be functionalised on one end whilst elongating building blocks could be functionalised on either end (Figure 1.10A). Thus the range of oligomers produced was critically dependent on the combination of building blocks used. The elongated amide was capped with a terminating building block to cease the elongation process. As the synthetic process occurs in aqueous solution, the synthetic culture containing mixtures of products of different lengths, can be directly assayed against a desired biological target. By preparing mixtures with overlapping building blocks, the structure of the active compound can be deconvoluted by simple combinatorial strategies. The same principles of evolutionary feedback, miniaturisation and crude testing were applied in order to ferment up to 6000 non-natural oligopeptides from which a micromolar inhibitor of a HCV protease was identified (Figure 1.10). This approach enables direct testing of a reaction mixture containing more than one possibly active products. However the inherent limitation is that it requires aqueous chemistry, greatly diminishing the range of transformations that may be exploited.

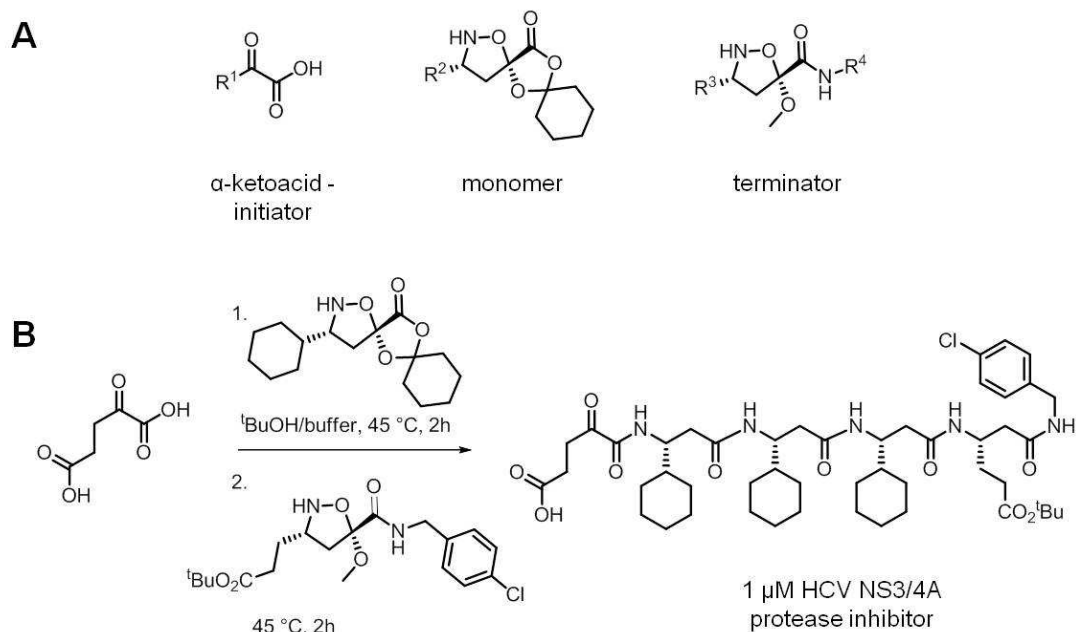


Figure 1.10: Example of Huang *et al.* synthetic fermentation of β -olipeptides. **A:** Simple building blocks are used in a combinatorial way to generate mixtures of multiple products. **B:** Example of the *in situ* preparation of an active molecule.

1.4. Selection of a chemical toolbox for activity-directed synthesis

Current approaches for the discovery of bioactive molecules tend to exploit a limited palette of reliable well-working reactions, optimised for the preparation of a single, pure compound.⁵ Thus the existing chemical toolbox is not suited for this project. A new chemical toolbox is needed in order to overcome the limitations of conventional approaches in chemical connectivity^{5,24} and to produce mixtures of products instead of single products.

The starting materials used were diazo-carbonyl compounds which were suitable for the purposes of this project for several reasons. First, diazo-compounds decompose in the presence of metal catalysts to generate highly reactive carbenoid species. (Figure 1.11) Commonly used metals include Cu, Co, Pd and Fe however the most abundantly studied class of metal catalysts are Rh catalysts. The carbenoid intermediates can undergo a plethora of different transformations.²⁵ C-H, O-H, N-H insertions, cyclopropanations and cascade cycloaddition processes, have all been

reported in both intra- and intermolecular reactions, affording the formation of diverse molecular scaffolds (Figure 1.12).²⁵⁻²⁶

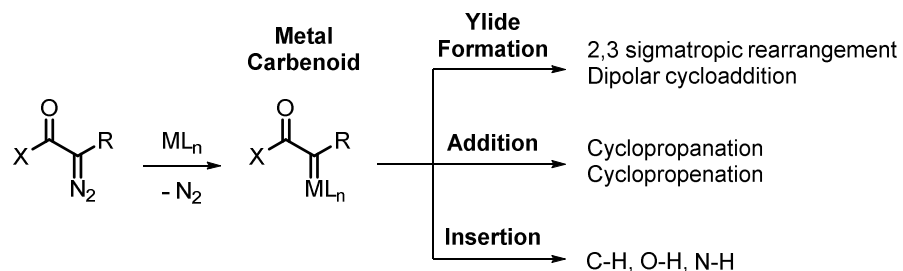


Figure 1.11: Formation of metal-carbenoid species after treatment with metal catalyst. These intermediates are highly reactive and can undergo a plethora of transformations.

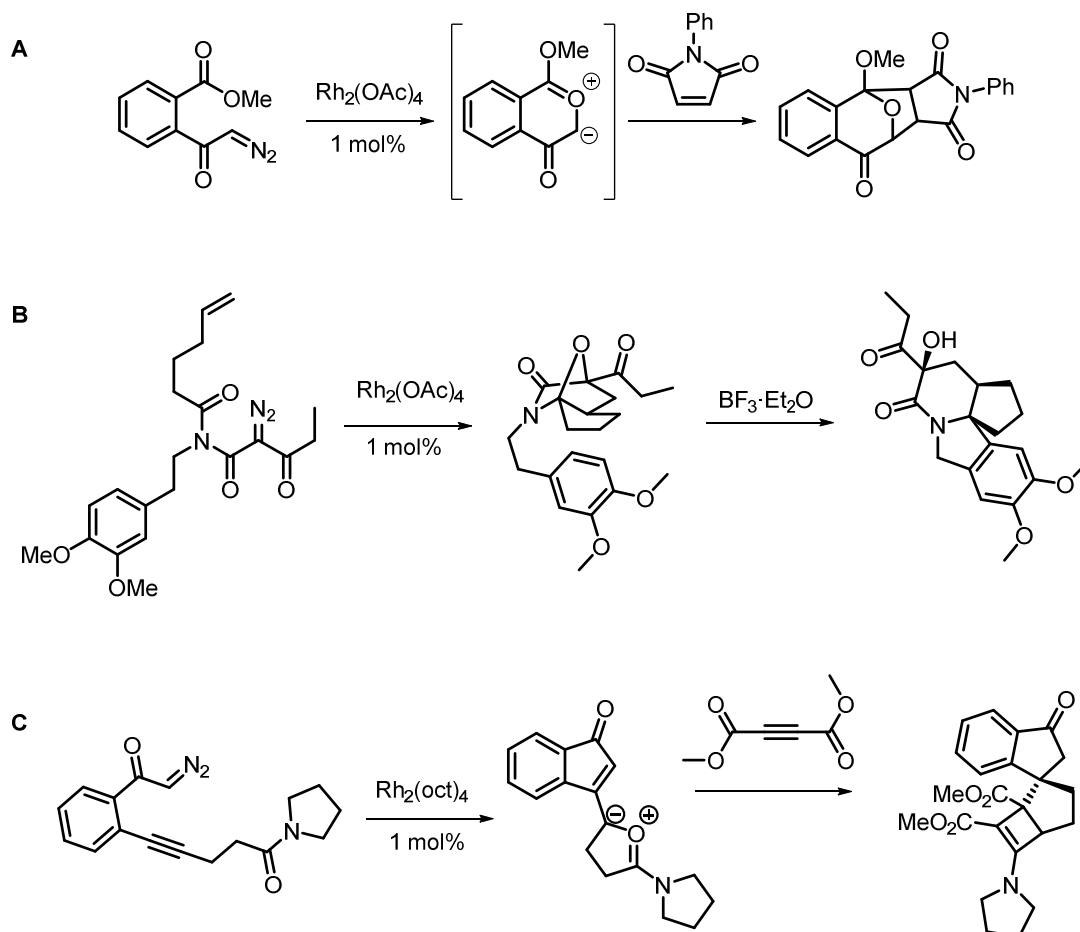


Figure 1.12: Examples of $\text{Rh}^{(\text{II})}$ carbenoid chemistry. **A:** carbonyl ylide and intermolecular cycloaddition. **B:** isomünchnone intramolecular cycloaddition and π -cyclisation. **C:** merged alkyne metathesis and tandem cyclisation.

Moreover, the reactivity of the carbenoid species can be finely tuned to favour the formation of one possible product over one or two other possible co-products. The tunability stems from the interactions of the molecular orbitals of the metal, the ligands and the carbene. In the case of rhodium catalysts which have been more extensively studied, the HOMO of the sp^2 -hybridised carbene interacts with the LUMO of the rhodium-ligand complex resulting in the formation of a σ -bond. The stability of the carbenoid though depends on the ligands of the catalyst which can donate or withdraw electrons from the metal and affect the degree in which it can participate in π -back donating bonding (Figure 1.13).

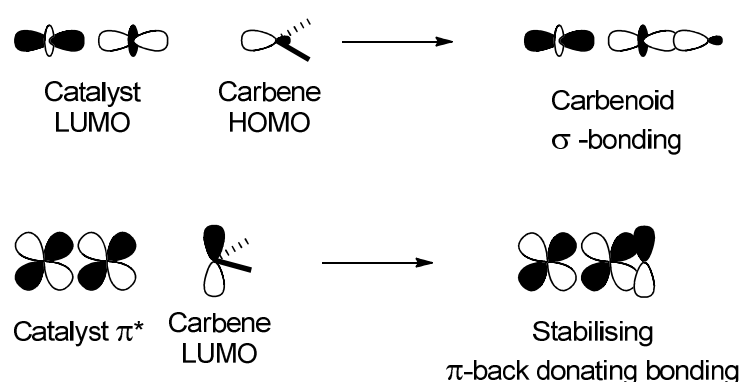


Figure 1.13: Molecular orbital interactions between the metal catalyst and the carbene to form the reactive carbenoid. The stability of the carbenoid is mostly affected by the electron density donated by the catalyst ligands through π -back donating bonding.

The more electron-density the ligand adds to the catalyst, the more stable the carbenoid and *vice versa*, affecting the relative rate of the various transformations.²⁷ Apart from the catalyst's ligands, the substituents of the carbenoid carbon atom can also influence the stability of the carbenoid formed through either steric and conformational or electronic effects.²⁸ In a representative example, the diazoacetamide **1** can undergo an intramolecular cyclopropanation/rearrangement cascade to give product **2**, or a C-H bond insertion to give product **3** (Figure 1.14).²⁶ Similarly, the diazo-compound **4** can give both the C-H insertion and the cyclopropanation products **5** and **6** respectively. In both cases, changing the ligands resulted in favouring the formation of one product over the other.

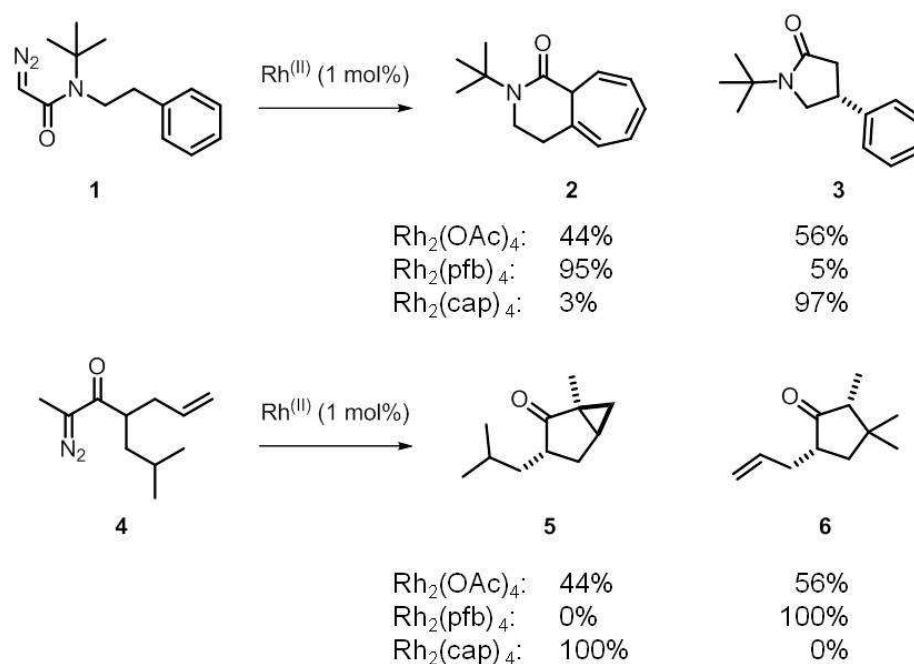


Figure 1.14: Effects of Rh^{III} catalysts on reaction selectivity; cyclisation/rearrangement (product **2**) against C-H insertion (product **3**) (top) and cyclopropanation (product **5**) against C-H insertion (product **6**) (bottom).

Furthermore, a variety of chiral catalysts has been developed allowing for stereoselective control over the formation of chiral products²⁸⁻²⁹ as well as increasing the range of ligands used. These catalysts were developed based on chiral ligands and may be classed in three major groups: acetates, carboxamides and phosphates (Figure 1.15). Depending on the substitution pattern around the carbene carbon, different groups of catalysts have different effects of the reaction outcome, as described above.

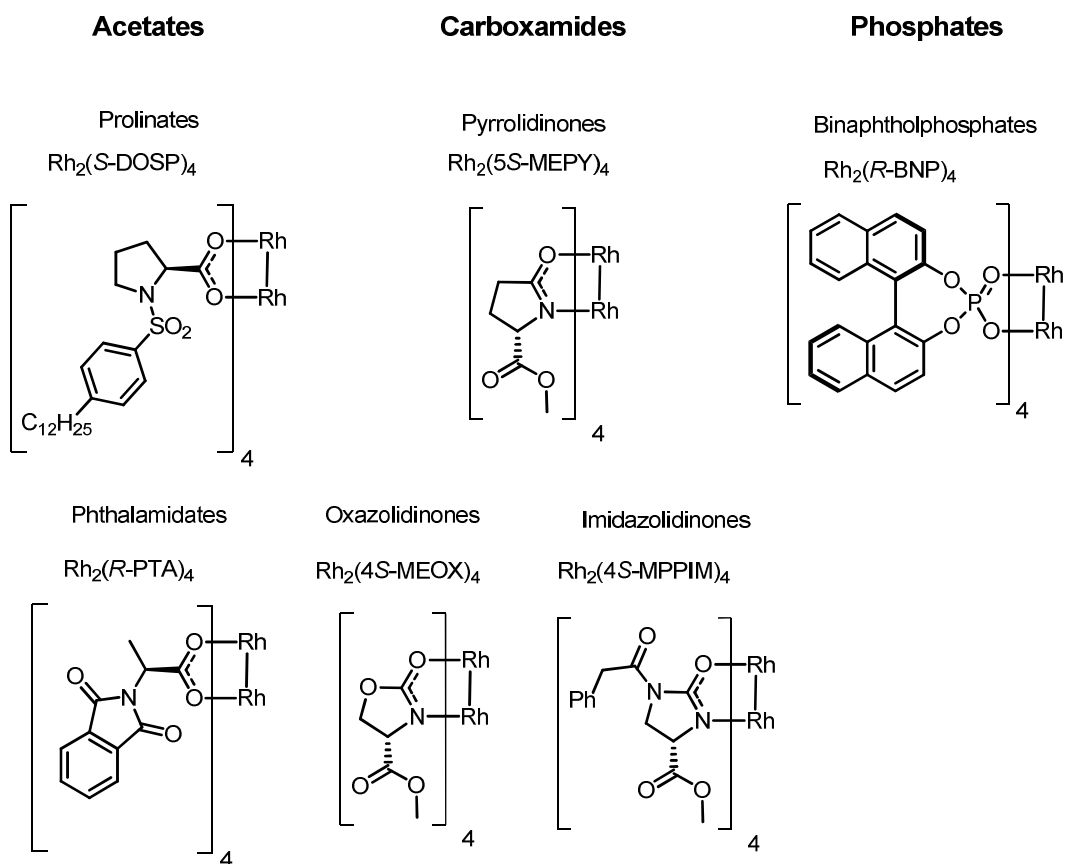


Figure 1.15: Structures of representative examples of chiral $\text{Rh}^{(\text{II})}$ catalysts. The three distinct groups, acetates, carboxamides and phosphates can be subdivided further based on the core of the ligand used.

Being able to generate different scaffolds from the same starting materials by changing the $\text{Rh}^{(\text{II})}$ catalyst is an ideal aspect for the purpose of this project, as a crude reaction mixture may contain more than one potentially bioactive molecules. Furthermore the tunability of the carbenoid chemistry may enable the optimisation of the synthetic route in parallel with the selection of the most active component.

1.5. Selected Biological Target: The Androgen Receptor

1.5.1. The Structural and Chemical Biology of the Androgen Receptor

The androgen receptor (AR) is a member of the steroid and nuclear receptor superfamily, which acts as an intracellular transcriptional factor. Its function is modulated by the binding of androgenic hormones (testosterone or dihydrotestosterone) which induce conformational changes affecting both receptor-protein and receptor-DNA interactions. The AR is crucial for the expression and development of male sexual characteristics. Numerous mutations of the AR have been identified and associated with disease such as prostate cancer and Androgen Insensitivity Syndrome.³⁰

The AR gene is approximately 90 kb long and encodes a protein of 919 amino acids, divided into three functional domains (Figure 1.16): the *N*-terminal domain (NTD) which has a modulatory function, the DNA-binding domain (DBD) and the *C*-terminal ligand-binding domain (LBD). A small hinge region is located between the DBD and the LBD. A nuclear localisation signal spans over the DBD and the hinge region, responsible for the translocation of the protein from the cytoplasm to the nucleus.

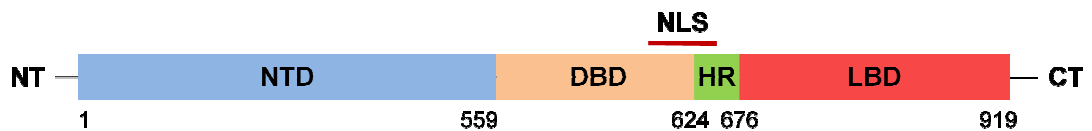


Figure 1.16: Graphical representation of the AR protein domains. NT: *N*-terminus; NTD: *N*-terminal domain; DBD: DNA-binding domain; HR: hinge region; LBD: Ligand-binding domain; NLS: nuclear localisation signal; CT: *C*-terminus.

The unbound AR is mainly located in the cytoplasm. Upon ligand binding, the conformational changes induced result in the dimerisation, phosphorylation and translocation of the AR into the nucleus.³⁰ Once in the nucleus, the AR binds onto the DNA through its hormone response element (HRE), located in the promoter of AR gene targets, resulting in the recruitment of the transcriptional machinery and activating AR-regulated gene expression (Figure 1.17).

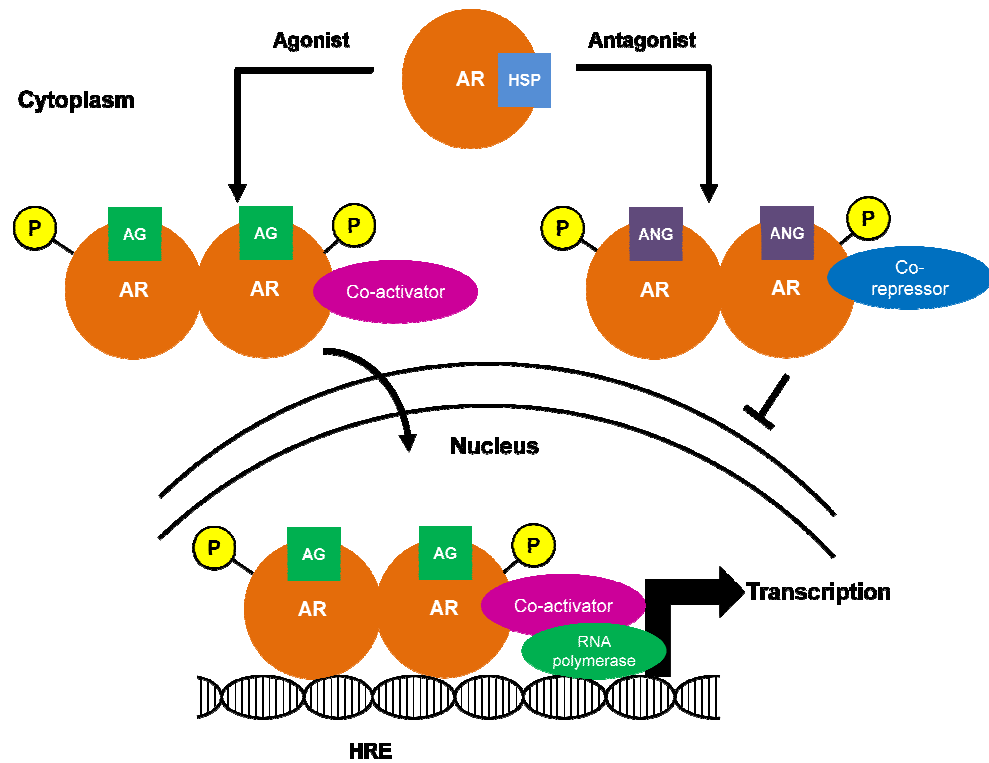


Figure 1.17: Cartoon schematic of the transcriptional pathway induced by the activated androgen receptor. Upon binding of an agonist, the receptor dimerises and is phosphorylated. It then enters the nucleus where it recruits the transcriptional machinery. If an antagonist binds, the conformational changes result in the recruitment of a co-repressor which prevents the transcriptional process. AR: Androgen receptor, HSP: heat shock protein, AG: agonist, ANG: antagonist, P: phosphorylation, HRE: hormone response element.

The AR LBD consists of 11 α -helices, arranged in three layers (Figure 1.18). Ligand-propagated conformational changes in the LBD result in the formation of a functional activation region on the surface of the LBD, necessary for the interaction of the AR and co-activator recruitment during transcriptional activation.

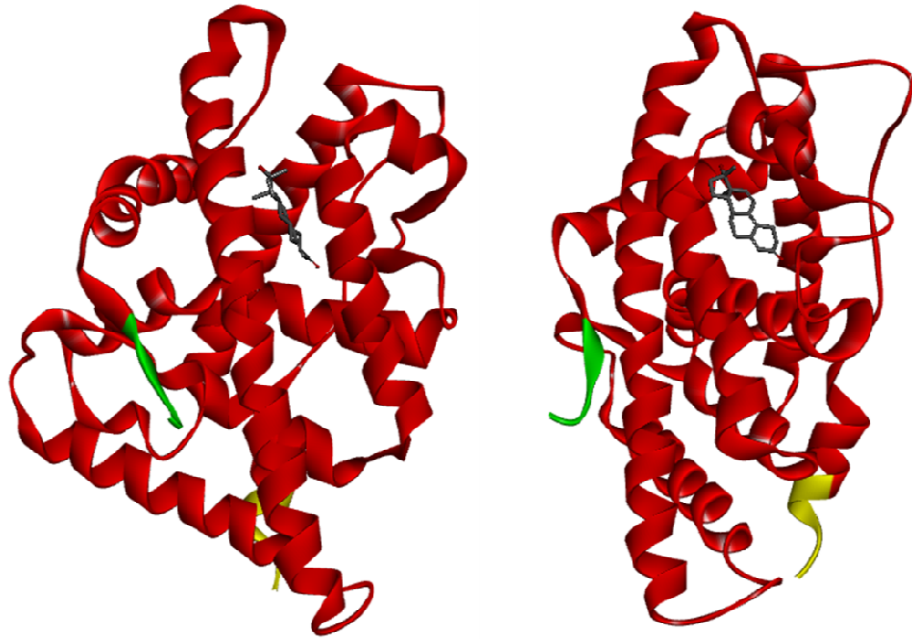


Figure 1.18: The androgen receptor ligand-binding domain crystal structure (Resolution: 2.0 Å) with DHT bound; front (left) and side (right) view (PDB: 1I37). The LBD consists of 11 α -helices and 2 short β -turns, in a three layer conformation, forming an antiparallel “ α -helical sandwich”. *N*-terminus (green), *C*-terminus (yellow) and DHT (grey) shown.

Known steroidal agonists and antagonists generally interact with the AR ligand-binding cavity through hydrophobic interactions. Furthermore the 3-keto-group of steroidal agonists interacts through hydrogen bonding with residues Gln711 and Arg752 whilst the 17 β -OH group hydrogen-bonds with residues Asn705 and Thr877 (Figure 1.19). The interactions with these residues are considered crucial for the induction of the conformational changes of the protein.^{4d,e,31}

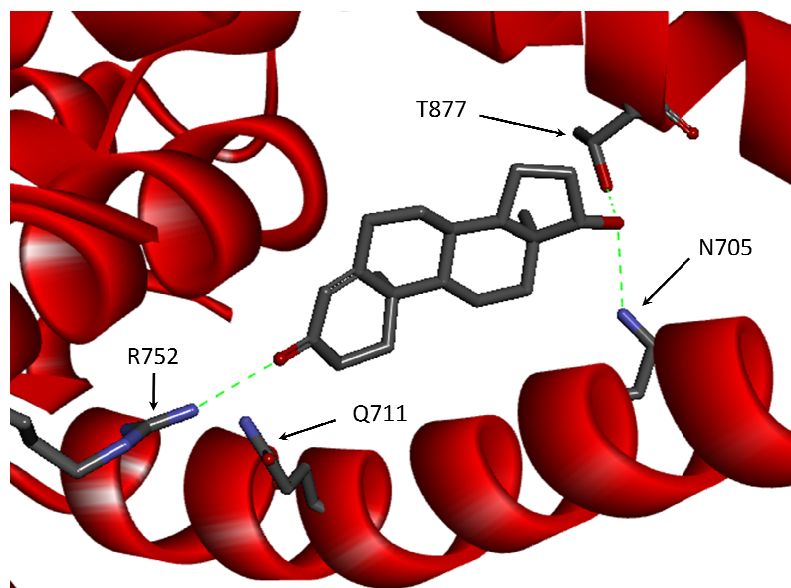


Figure 1.19: Crystal structure of AR-LBD (Resolution: 2.0 Å) with DHT bound (PDB: 1I37), depicting key hydrogen bonding interactions with R752, Q711, T877 and N705.

Apart from its genomic pathway as a transcription regulation factor, the AR takes part in a non-genomic pathway involving either a rapid activation of kinase-signaling cascades or the modulation of intracellular calcium levels. This non-genomic pathway has been reported in oocytes, skeletal muscle cells, osteoblasts, and prostate cancer cells.³⁰

1.5.2. Androgen receptor ligands: agonists, antagonists and Selective AR modulators (SARMs)

Androgen receptor ligands are classed as agonists or antagonists based on their ability to activate or inhibit the transcription of androgen receptor target genes. Agonists upregulate gene expression by inducing a conformation which favours co-regulator binding. Testosterone (TE, **I**) and 5 α -dihydrotestosterone (DHT, **II**) (Figure 1.20) are endogenous agonists of the AR. Antagonists are ligands that compete with TE and DHT for binding onto the AR and induce a conformation which promotes co-repressor binding. Due to their wide clinical use, development of novel AR ligands began with modifications of the steroidal scaffold of TE and DHT, such as stanozolol (**III**).³² However, subsequently, non-steroidal ligands which had better pharmacological properties, such as *R*-bicalutamide (**IV**)³² and analogues of flufenamic acid,³¹ were discovered (Figure 1.20).

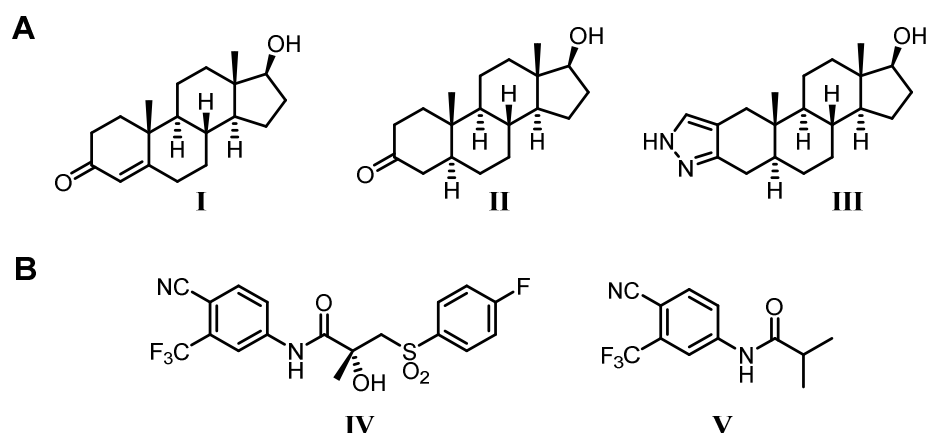


Figure 1.20: Chemical structures of known steroidal and non-steroidal AR ligands. **A:** Agonists (left to right): Testosterone **I**, 5 α -dihydrotestosterone **II** and stanozolol **III**. **B:** Antagonists: *R*-bicalutamide **IV** and flutamide **V**.

It has been shown through SAR studies^{30,33} that in flutamide analogues and derivatives, the electron-withdrawing substituents of the phenyl ring (Figure 1.21) favour AR binding. Binding of flutamide and bicalutamide analogues mainly occurs through hydrophobic interactions and less through hydrogen bonding. However, certain hydrogen bonding interactions have been identified occurring through residues Q711 and N705 (Figure 1.22).³³

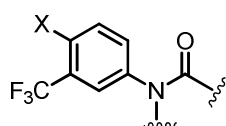


Figure 1.21: Phenyl-amide moiety of flutamide and bicalutamide analogues shown to favor AR binding (X = Cl, CN, NO₂).

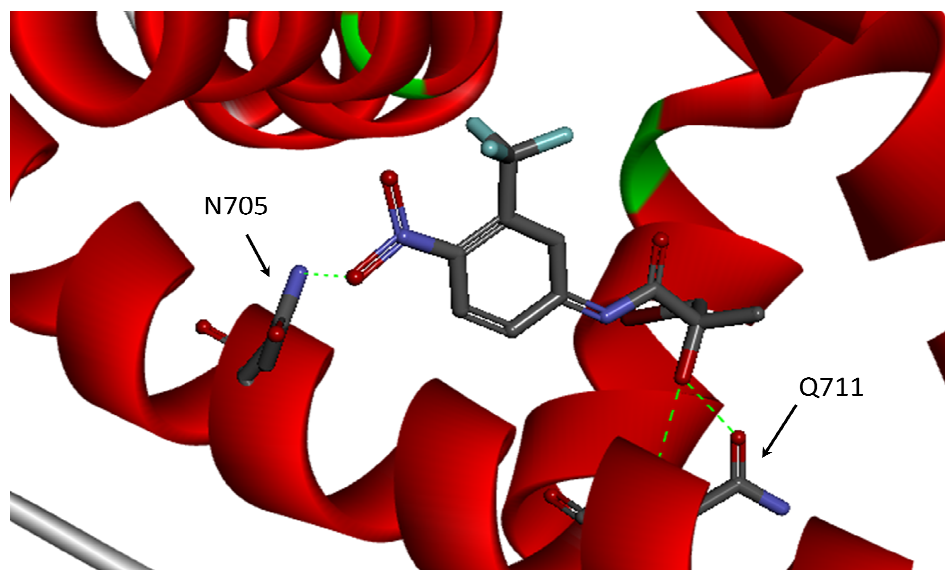


Figure 1.22: Crystal structure (Resolution: 1.65 Å) of flutamide analogue bound to the AR-LBD (PDB: 2AX9). Binding occurs mostly through hydrophobic interactions. Key hydrogen bonding residues N705 and Q711 are depicted. Certain non-interacting sections of the protein have been omitted for clarity.

As demonstrated in a recent report,³⁴ the trifluoromethyl aryl fragment (depicted in Figure 1.21) provides a good starting point for the design and development of novel AR antagonists. The authors had attached the 2-(trifluoro)methyl benzonitrile ring on carborane structures and observed antagonistic activity of the synthesised compounds at the micromolar region. Thus, this fragment would serve as a good starting point in order to showcase Activity-Directed Synthesis and to discover novel chemotypes of modulators of the Androgen Receptor.

Apart from agonists and antagonists, certain compounds display agonistic action in muscle tissue whilst they display an antagonistic action in the prostate. Such compounds are classed as selective androgen receptor modulators (SARMs) and act by inducing a conformation which lies between agonism and antagonism. Zhi and co-workers have reported the discovery of a novel class of orally available SARMs.^{4d,e}

Given the fact that the structural and chemical biology of the AR, including the numerous SAR reports on non-steroidal AR ligands,^{4c,e,31,33-34} the AR is an ideal biological target for the demonstration of the applicability of the methodology to be developed by this project. In addition, the

screening methodology is well established. Invitrogen has developed a commercially available time-resolved fluorescence resonance energy transfer (TR-FRET) biochemical assay, allowing the identification of both agonists and antagonists for the AR, which provides a reliable screening methodology (see Chapter 3 for details).

1.6. Project Outline

Having chosen an appropriate chemical toolbox and biological target an experimental outline was developed, to develop and exemplify the Activity-Directed Synthesis approach. First, the structure of the intra- or intermolecular diazo-substrates was decided (Figure 1.23). These substrates would bear the phenyl-amide motif as a minimal pharmacophore unit which would provide a starting point for active AR modulators. The *N*-appended R groups would be chosen such that they would either enable multiple possible carbenoid transformations (in the case of intramolecular substrates), or minimise intramolecular reactivity (in the case of intermolecular substrates).

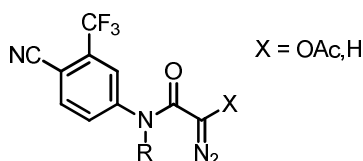


Figure 1.23: Common central structure for the diazo-substrates. The *N*-appended group would be chosen accordingly for intra- or intermolecular substrates.

These diazo-substrates would need to be tested for their activity against the AR, using the TR-FRET assay, in order to establish that any background signal or interference does not stem from these compounds before being used in the reaction arrays. Scavenging studies also needed to be undertaken to establish the degree to which the metal could be removed from the crude product mixture prior to the latter being biologically tested. Removal of the metal would minimise any effects the metal might have on either the functionality of the protein or the read-out of the screening method. The TR-FRET assay itself would need to be established and all its parameters optimised to assure its functionality and reliability. Successfully assaying known AR modulators, ideally an agonist such as testosterone and

an antagonist such as cyproterone acetate, was deemed as sufficient testing.

Reactions would need to be performed in custom made PTFE 96-well plates as regular plastic well plates would disintegrate with the use of most organic solvents. The well would have a minimum volume of 200 μL in order to accommodate a reaction solution of 100 μL and residual space for sealing. The reactants could be easily pipetted into the reaction well using finite volumes of concentrated stock solutions of the diazo-substrates any co-substrates and finally the metal catalyst which would also initiate the reaction. The reactions could be monitored by LC-MS and TLC to establish a reaction end-point. In order to scavenge the metal, the crude mixtures would need to be pipetted into wells preloaded with the appropriate amount of scavenging resin. After scavenging, the crude product mixtures would be left to evaporate at room temperature and then under reduced pressure to remove the solvent, before being assayed (Figure 1.24).

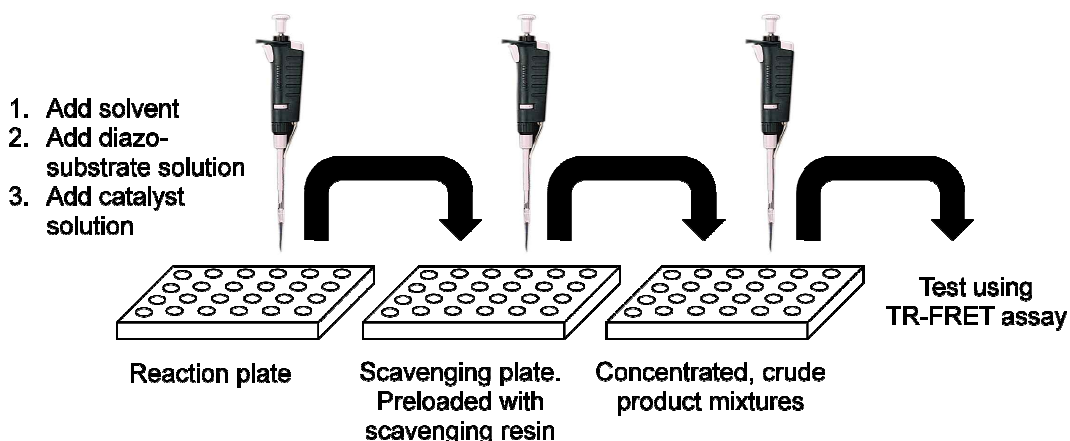


Figure 1.24: Graphical illustration of the experimental process, from performing arrays of reactions to testing them using the TR-FRET assay.

The concentrated crude product mixtures, could then be rediluted in DMSO to prepare a stock solution which could be further diluted accordingly in DMSO and assay buffer to screen the product mixtures in more than one concentrations. Screening at a lower concentration e.g. 2-fold or 10-fold, would be an efficient manner of imposing selection pressure onto the system and could facilitate the selection of conditions which would dictate the design of a subsequent reaction array. These iterative rounds of screening,

selection and redesign would continue until a total concentration of products which is low enough is met, e.g. 500-100 nM. Ideally, there should be no more than three or four reaction arrays in order to demonstrate the efficiency of the approach.

1.7. Summary

In order to overcome the limitations of conventional approaches for the discovery of small bio-active molecules, a new approach, Activity-Directed synthesis was envisaged. This approach aimed to focus on active molecules rather than treating every molecule with the same significance. Exploiting promiscuous reactivity to generate mixtures of products and crude testing would enable the use of evolutionary feedback and through iterative rounds of screening and redesign it would be possible to optimise both the structure of the active molecule and the route to its synthesis simultaneously.

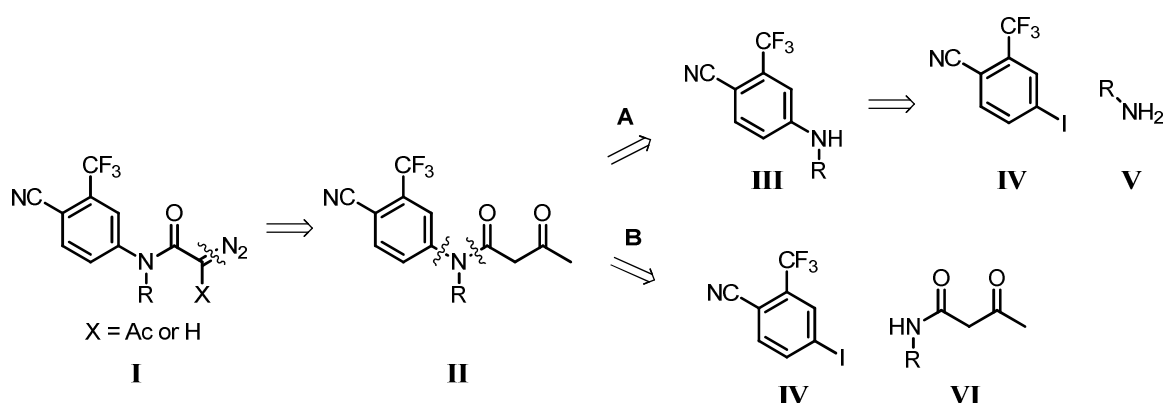
2. Chapter 2

Synthesis of diazo substrates for intramolecular metal-catalysed carbenoid reactions

This chapter will describe the development of the synthetic routes employed for the preparation of the diazo substrates for intramolecular metal-catalysed carbenoid reactions. After establishing a reliable synthetic route on a model system (Section 2.1), sixteen *N*-aryl α -diazo amides were prepared (Section 2.2).

2.1. Development of methods for the preparation of diazo-compounds

As outlined in Chapter 1 (see Section 1.2.2 and Section 1.3) the substrates for intramolecular carbenoid reactions would be diazo-butanamides and acetamides bearing the trifluoromethyl benzonitrile fragment. These diazo substrates would have the general structure **I** (Scheme 2.1, see Chapter 1). Scheme 2.1 provides an overview of two potential approaches to the synthesis of these compounds.



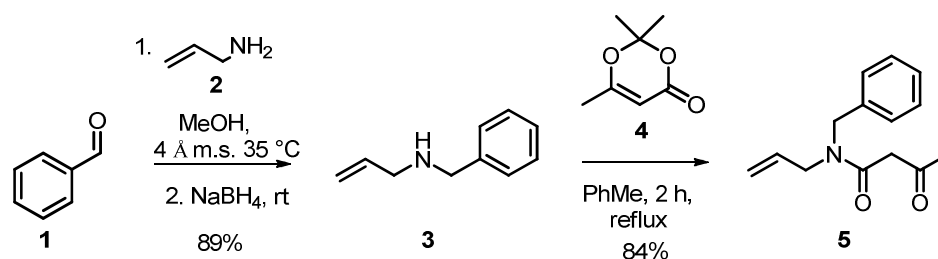
Scheme 2.1: Retrosynthetic analysis of aryl diazo amides.

The parent acetoacetamide **II** might be synthesised by acylation of the corresponding aniline **III** (route A), prepared by metal-catalysed cross-coupling between the appropriate aryl halide **IV** and an amine **V**.³⁵ Alternatively, **II** might be prepared by a metal-catalysed cross-coupling

reaction between the appropriate aryl halide **IV** and an amide **VI**,³⁶ derived by the acylation of a suitable primary amine (route B). Literature precedent for both approaches is fairly abundant.³⁵⁻³⁶

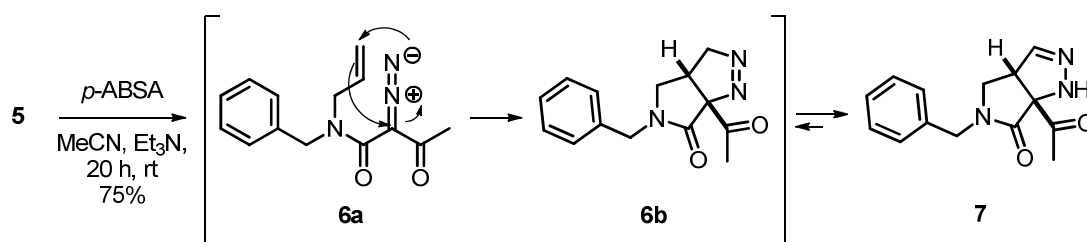
2.1.1. Development of a synthetic approach using a model system

In order to develop a robust synthetic route for the synthesis of the desired aryl diazo-acetamides, a model compound, the butanamide **5**, was prepared (Scheme 2.2). Reductive amination of benzaldehyde by treatment with allylamine and NaBH₄ in MeOH and 4 Å molecular sieves, produced the secondary amine **3**. **3** was then acylated³⁷ by reaction with **4** in refluxing toluene to afford the amide **5**.



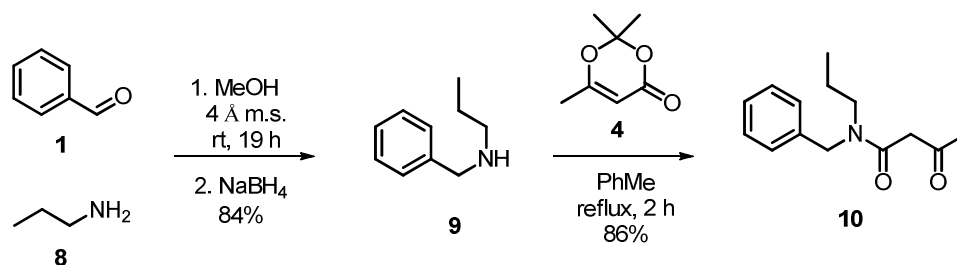
Scheme 2.2: Synthesis of the model compound, the butanamide **5**.

The amide **5** was treated with triethylamine and *para*-acetamidobenzenesulfonylazide (*p*-ABSA),³⁷⁻³⁸ however, the reaction yielded the unexpected product **7**. This product was hypothesised to be formed by a [3+2] cycloaddition reaction between the alkene and the diazo moiety, followed by subsequent tautomerisation of the intermediate **6b** (Scheme 2.3).



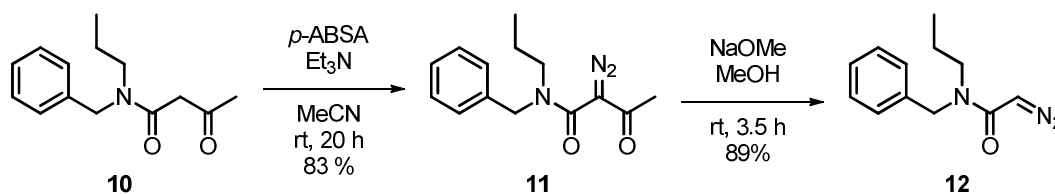
Scheme 2.3: Rationale for the formation of product **7**.

The structure of the dihydropyrazole **7** was elucidated by spectroscopic analysis. Key to the determination of its structure were the peaks corresponding to the imine-like proton (6.64 ppm) and the proton at the ring junction (3.24 ppm). Additional confirmation was provided by the IR spectrum: there were clear absorbance peaks for the N-H bond (3285 cm^{-1}) as well as the amide and ketone carbonyl groups (1665 cm^{-1} and 1702 cm^{-1}). In order to prevent the subsequent cycloaddition reaction, the saturated analogue, amide **10** was prepared. The amine **9** was synthesised *via* a reductive amination, using propylamine and benzaldehyde with NaBH_4 in MeOH. The amine **9** was then acylated by treatment with **4** in refluxing toluene, to afford the amide **10** (Scheme 2.4).



Scheme 2.4: Preparation of the amide **10**.

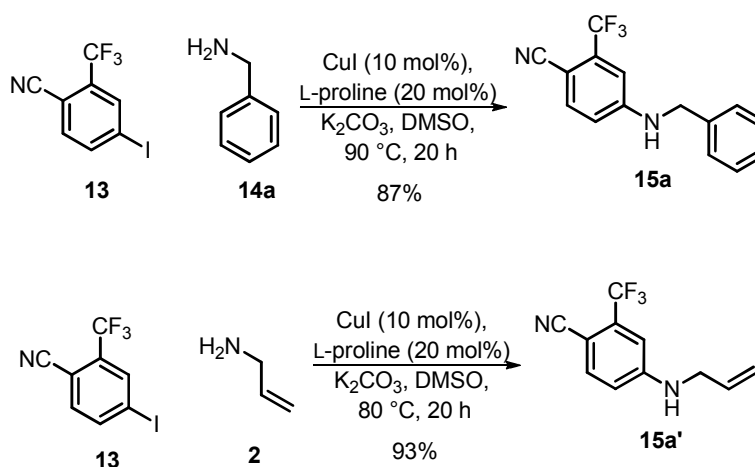
With butanamide **10** in hand, the synthesis of diazo-butanamides and diazo-acetamides was investigated. Treatment of **10** with *p*-ABSA and triethylamine in acetonitrile gave the diazo-butanamide **11**, which was subsequently deacetylated under basic conditions to give diazo-acetamide **12** (Scheme 2.5).³⁸ These results verified the applicability of the approach for the preparation of the *N*-aryl diazo-butanamide and acetamide substrates.



Scheme 2.5: Synthesis of the diazo-butanamide **11** and diazo-acetamide **12**.

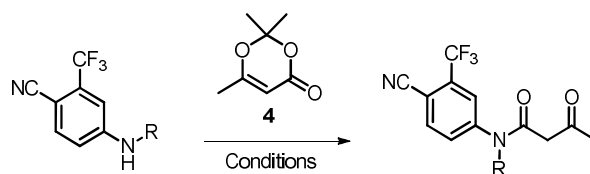
2.1.2. Development of a synthetic methodology for the preparation of aryl diazo-acetamides

Following the proposed retrosynthetic route A, (Scheme 2.1) the commercially available benzonitrile **13** was employed as a starting material. Cu^(I) catalysed cross-coupling^{36a} of **13** with benzylamine and propylamine, produced respectively the *N*-benzyl and the *N*-allyl anilines **15a** and **15a'** (Scheme 2.6).



Scheme 2.6: Cu^(I) catalysed cross-couplings to yield the anilines **15a** and **15a'**.

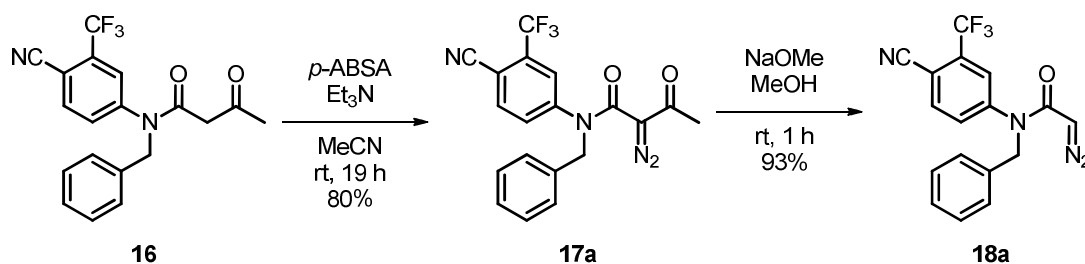
Acylation of anilines **15a** and **15a'** was attempted using the dioxinone **4** by refluxing in toluene (110 °C) or xylene (140 °C). Unfortunately, these procedures were initially unsuccessful, as summarised in Table 2.1, presumably due to the very poor nucleophilicity of the aniline. The acylation of anilines with dioxinone derivatives has been reported to proceed successfully with microwave irradiation.³⁹ The aniline **15a** was successfully acylated by treatment with dioxinone **4** under microwave irradiation to afford butanamide **16** in 74% yield.

Table 2.1: Optimisation of the acylation of the anilines **15** and **16**.

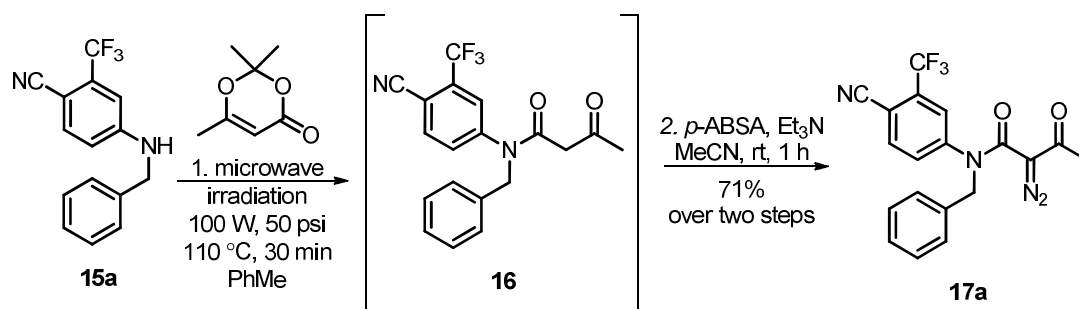
Entry	Aniline substrate	Solvent (Temperature)	Time	Outcome
1	15a (R = Bn)	Toluene (110 °C)	3 d	No reaction
2	15a (R = Bn)	Xylene (140 °C)	2 d	No reaction ^a
3	15a' (R = allyl)	Toluene (110 °C)	2 d	No reaction
4	15a' (R = allyl)	Xylene (140 °C)	2 d	No reaction
5	15a (R = Bn)	Toluene (110 °C, μ w irradiation)	1 h	16 , 74%

a: 88% of the starting material (aniline **15**) was recovered after flash chromatography.

The β -keto-butanamide **16** was treated with *p*-ABSA and triethylamine, in acetonitrile, and afforded the diazo-butanamide **17a**. This product was subsequently deacylated using NaOMe in MeOH, to yield the diazo-acetamide **18a** (Scheme 2.7).

**Scheme 2.7:** Preparation of the diazo-butanamide **17a** and the diazo-acetamide **18a**.

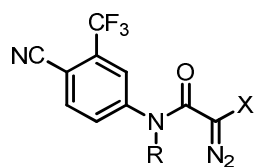
The microwave-assisted acylation and subsequent diazo-transfer step were successfully merged into a telescoped process, which did not require the isolation of the intermediate butanamide (Scheme 2.8). This telescoped synthesis afforded the diazo-butanamide **17a** in 71% yield from the aniline **15a** over two steps.



Scheme 2.8: Telescoped approach for the synthesis of **17a**.

2.2. Preparation of the diazo-butanamide and acetamide precursors

Having established a robust synthetic methodology for the preparation of aryl diazo-butanamides and their corresponding acetamides, twelve diazo-compounds were selected as initial substrates for intramolecular metal-catalysed carbenoid reactions. Different *N*-appended groups, (Figure 2.1) were selected to enable a wide range of possible reaction outcomes from the same substrate. Substrates with alkyl chains (**17b**, **18b**, **17d** and **18d**) were selected to allow the possibility of alkyl C-H insertions. Aryl groups (**17a**, **18a**, **17c** and **18c**) were chosen to enable aryl C-H insertions on different aryl rings (cyano-trifluoromethyl or phenyl) as well as the formation of different ring sizes. Unsaturated groups (**17e** and **18e**) were selected to allow the possibility of cyclopropanation. Finally, the compounds **17f** and **18f** were chosen to enable the possibility of carbonyl-ylide formation and subsequent cascade reactions (See Chapter 1). Following the results of the second reaction round (see Chapter 4) a set of four additional diazo butanamides was also prepared (Figure 2.1).



Compound No.	R =	X =	Compound No.	R =	X =
17a		Ac	17e		Ac
18a		H	18e		H
17b		Ac	17f		Ac
18b		H	18f		H
17c		Ac	17g		Ac
18c		H	17h		Ac
17d		Ac	17i		Ac
18d		H	17j		Ac

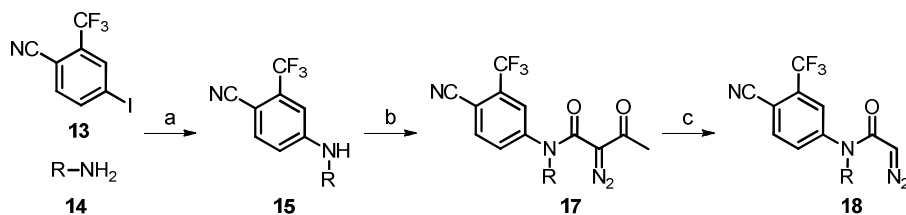
Figure 2.1: Structures of the designed diazo substrates for intramolecular carbenoid reactions.

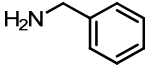
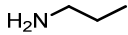
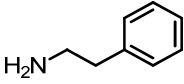
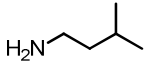
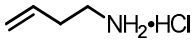
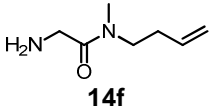
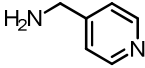
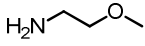
2.2.1. Preparation of the diazo-compounds

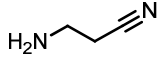
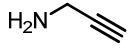
Diazo-compounds **17a** – **18e** and **17g** – **17i** were prepared from commercially available amines, using the established synthetic methodology (Table 2.2). In each case the appropriate amine precursor was heated with CuI, L-proline and K₂CO₃ in DMSO, to produce the corresponding aniline. The anilines were subsequently acylated using the dioxinone **4** under microwave conditions, and treated with *p*-ABSA and triethylamine in acetonitrile to afford the diazo-butanamides. The required diazo butanamides were deacetylated using NaOMe in MeOH to afford the corresponding diazo-acetamides.

For the preparation of the aniline **17e**, the amount of K₂CO₃ used in the Cu^(I)-catalysed coupling was increased by two equivalents because the necessary amine was only available as the hydrochloride salt. The diazo-butanamide **17e** and the diazo-acetamide **18e**, fortunately did not undergo the same [3+2] cyclisation as did the model compound intermediate **6a**. This can be attributed to two distinct differences between the two systems. The extra length of the homologated butenyl chain might inhibit optimal orbital overlap disfavouring the cyclisation. Also, the *N*-benzylamide is more free to rotate around the amide bond compared to the *N*-arylamide. This ability to rotate more freely could allow the allyl chain to be placed at the optimal position for the cyclisation to occur.

Table 2.2: Preparation of diazo-butanamides and acetamides from commercially available amines.

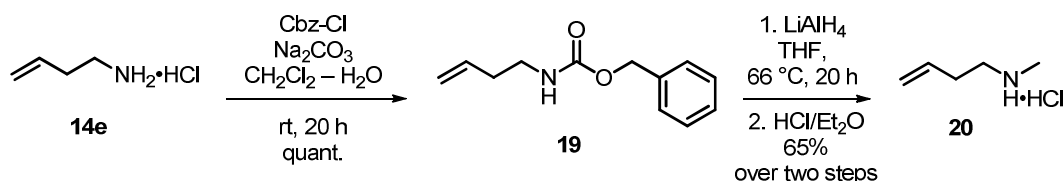


Entry	Amine	Aniline (Yield)	Diazo-butanamide (Yield) ^b	Diazo-acetamide (Yield) ^c
1	 14a	15a (87%)	17a (77%)	18a (93%)
2	 14b	15b (93%)	17b (70%)	18b (91%)
3	 14c	15c (87%)	17c (71%)	18c (82%)
4	 14d	15d (90%)	17d (70%)	18d (75%)
5	 14e	15e^d (86%)	17e (77%)	18e (93%)
6	 14f	15f (72%)	17f (63%)	18f (76%)
7	 14g	15g (67%)	17g (54%)	N.A.
8	 14h	15h (89%)	17h (97%)	N.A.

9		15i (63%)	17i (69%)	N.A.
	14i			
10		15j (15%) ^e	17j (91%)	N.A.
	14j			

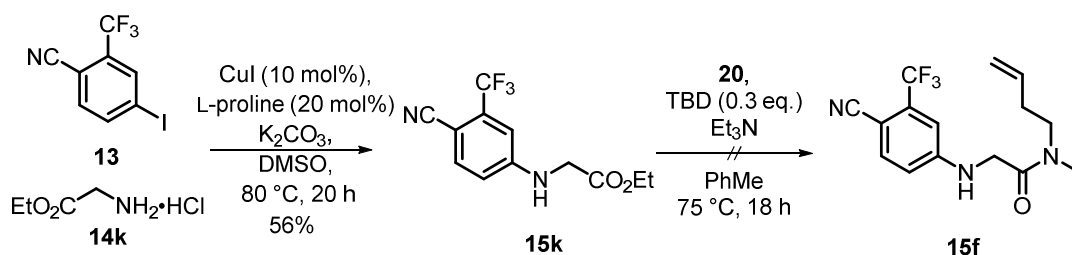
a: CuI (10 mol%), L-proline (20 mol%), K₂CO₃ (3 equiv.), DMSO, 90 °C, 20 h; b: i) Dioxinone **4**, microwave irradiation, 100 W, 50 psi, PhMe, 110 °C, 45 min, ii) *p*-ABSA, Et₃N, MeCN, rt, 1 h; c: NaOMe, MeOH, 0 °C, 3 h; d: amount of K₂CO₃ increased to five equivalents; e: prepared *via* alternative route.

Preparation of diazo-butanamide **17f** and diazo-acetamide **18f** required the preparation of the *N*-methylamine **20**. The amine was prepared, as the hydrochloride salt, from the available 3-butenylamine hydrochloride **14e** by reduction of the carbamate **19** using LiAlH₄ (Scheme 2.9).



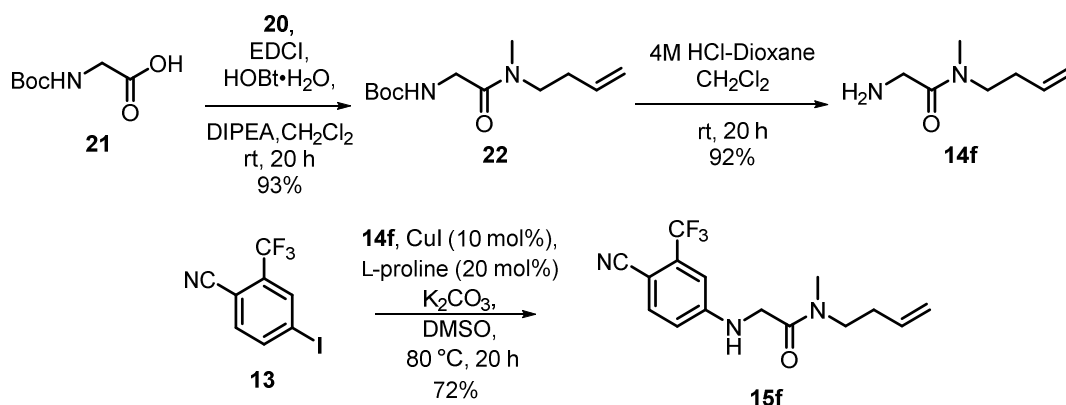
Scheme 2.9: Preparation of the *N*-methyl 3-butenylamine hydrochloride salt, **20**.

Two synthetic approaches were investigated for the preparation of the aniline **15f** (Scheme 8.13). Amide coupling reactions with esters, catalysed by triazabicyclo[4.4.0]dec-5-ene (TBD), have been reported.⁴⁰ The ester **15k** was prepared from aryl iodide **13** and glycine ethyl ester hydrochloride **14k**, treating with CuI, L-proline and K₂CO₃ in DMSO. However, the TBD-catalysed reaction between the glycine ester **15k** and the amine **20** was unsuccessful (Scheme 2.10).

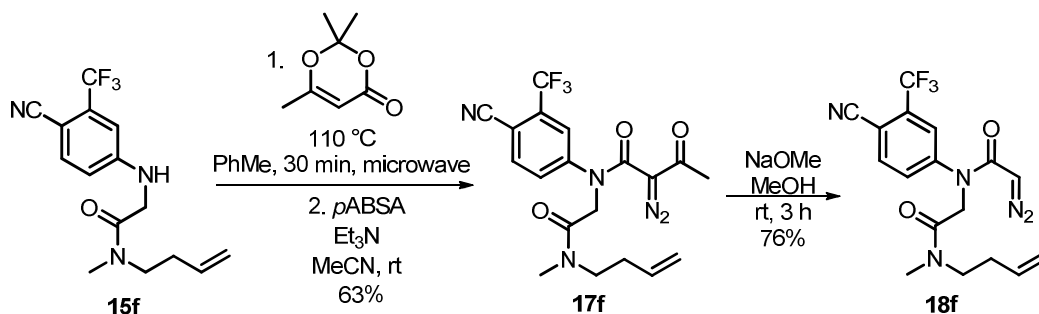


Scheme 2.10: A TBD-catalysed amide coupling between the ester **15k** and the amine **20** was not successful.

As an alternative, the amide **14f** was prepared by a EDCI/HOBt coupling between *N*-Boc glycine **21** and the amine **20** with subsequent Boc-deprotection. Treatment of the aryl iodide **13** and the amide **14f** with CuI, L-proline and K₂CO₃ in DMSO, afforded the aniline **15f** in 72% yield (Scheme 2.11). **15f** was acylated with dioxinone **4** under microwave irradiation and the crude product was treated with *p*-ABSA and Et₃N, in acetonitrile to afford the diazo-butanamide **17f**. This product was subsequently deacylated using NaOMe in MeOH, to yield the diazo-acetamide **18f** (Scheme 2.12).

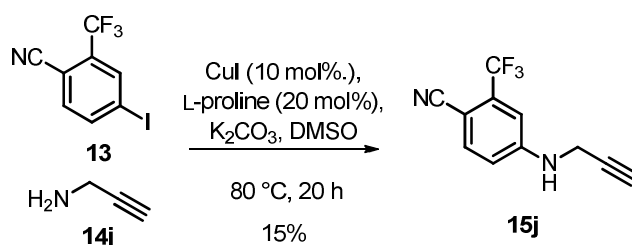


Scheme 2.11: The preparation of aniline **15f** was successful using a Cu^(I)-catalysed coupling between the aryl iodide **13** and the amide **14f**.

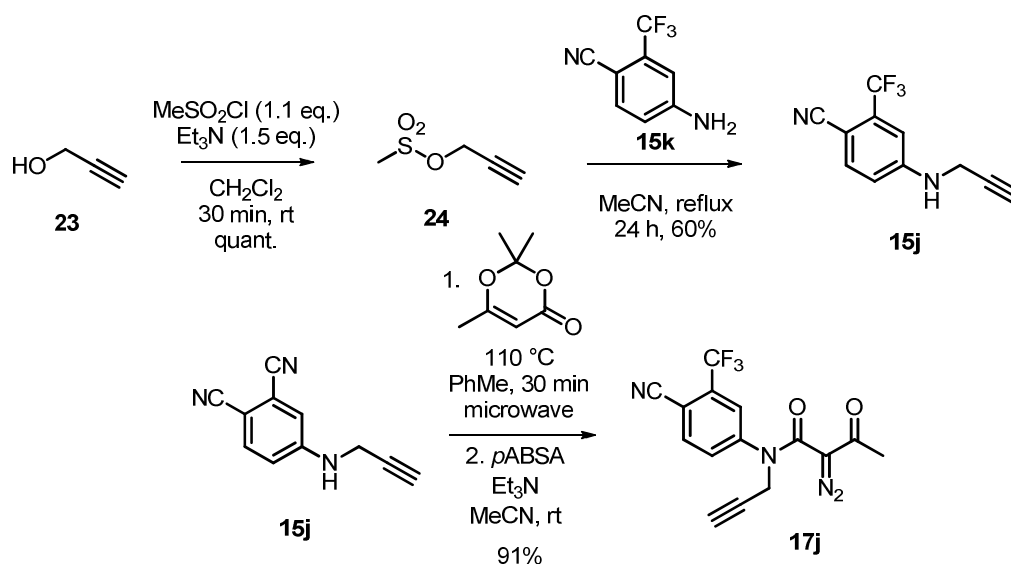


Scheme 2.12: Preparation of the diazo-butanamide **17f** and the diazo-acetamide **18f**, from the aniline **15f**.

The synthesis of diazo-butanamide **17j** proved to be more challenging as the Cu⁽⁰⁾-catalysed amine coupling was ineffective in yielding the precursor aniline **15j** in a viable amount (Scheme 2.13). An alternative route for the preparation of **15j** was hence developed: the propargyl methanesulfonate **24** was prepared by sulfonylation of the propargyl alcohol **23**. The methanesulfonate **24** was subsequently displaced by the commercially available aniline **15k** to obtain the desired aniline **15j**. The aniline **15j** was then successfully acylated with dioxinone **4** under microwave irradiation and the crude product was treated with *p*-ABSA and Et₃N, in acetonitrile to afford the diazo-butanamide **17j** in 55% yield over 3 steps (Scheme 2.14).



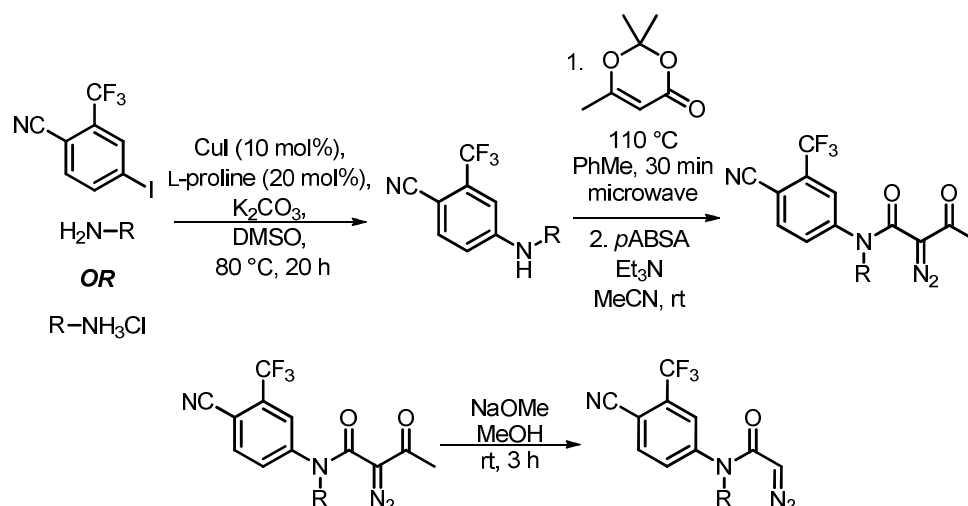
Scheme 2.13: The established route failed to afford compound **15j** in a viable yield.



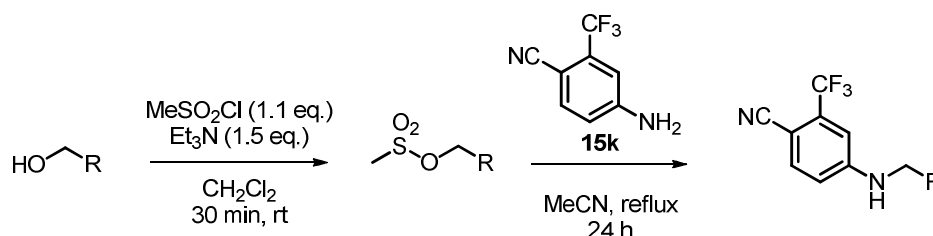
Scheme 2.14: Alternative synthetic route for the preparation of precursor **17j**.

2.3. Summary

In total, 16 diazo-butanamide and acetamide precursors for intramolecular metal-catalysed carbenoid reactions were prepared. The synthetic route developed for their preparation involved a Cu^(I)-catalysed arylation of a free amine or a corresponding amine hydrochloride salt. This step was followed by a microwave-assisted *N*-acylation, a telescoped diazo-transfer reaction and finally, an optional deacetylation reaction (Scheme 2.15). The initial Cu^(I)-catalysed coupling was substituted by a nucleophilic displacement of a suitable methanesulfonate in the case of aniline **15j**, as it was proved inadequate for the preparation of this compound (Scheme 2.16).



Scheme 2.15: The overall synthetic process; Cu^(I)-catalysed arylation followed by a microwave assisted acylation and diazotransfer reaction. The final deacetylation was only used for the preparation of the diazoacetamides.



Scheme 2.16: A nucleophilic displacement of the appropriate methanesulfonate proved to be a suitable alternative to the Cu^(I)-catalysed coupling for the preparation of the secondary anilines.

The microwave-assisted acylation and subsequent diazo-transfer reaction were successfully telescoped into one step. The telescoped process proved to be higher yielding and less time-consuming compared to isolating the intermediate butanamide. The diazo precursors prepared were successfully used in the reaction array rounds (Chapter 4).

3. Chapter 3 Establishment of a high-throughput assay

3.1. Invitrogen TR-FRET Androgen Receptor Biochemical Assay

Invitrogen has commercialised a biochemical assay for the screening of AR agonists and antagonists based on TR-FRET.⁴¹ FRET assays are commonly used in HTS systems and are fast, sensitive and reliable for screening libraries of compounds.⁴¹ As in standard FRET, when two fluorophores are in close proximity (0-10 nm) and their excitation and emission spectra overlap, excitation of the donor can result in emission by the acceptor. In TR-FRET, long-lifetime lanthanide metals are used as donors to overcome issues associated with scattered light and autofluorescent compounds with much shorter lifetimes.⁴¹

This particular assay uses a Tb⁺³-labeled anti-GST antibody as the FRET donor (excitation 340 nm, emission 495 nm), a fluorescein-labeled coactivator peptide (excitation 490 nm, emission 520 nm) and a rat recombinant GST-tagged AR LBD. When the Tb⁺³-anti-GST antibody is excited at 340 nm, it fluoresces, emitting sharp bands centred at 490 nm, 540 nm, 580 nm and 620 nm (Figure 3.1, dashed line). The emission at 490 nm is enough to excite the fluorescein which in turn emits sharply at 520 nm. The ratio of emission at 520 nm over emission at 495 nm is then used to calculate the FRET ratio.

$$FRET = \frac{Emmission_{520\text{ nm}}}{Emmission_{495\text{ nm}}}$$

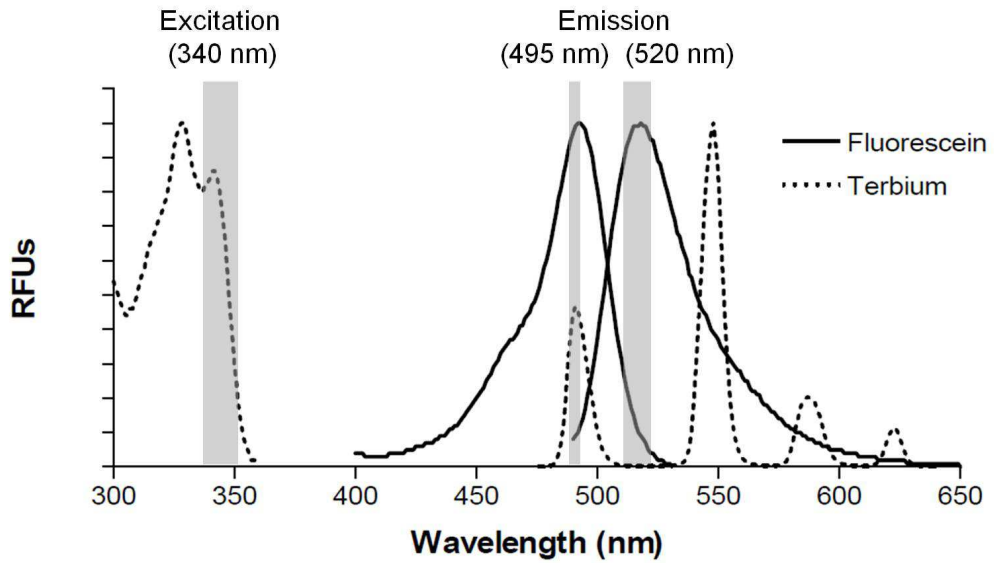


Figure 3.1: Excitation and emission spectra of the Tb³⁺-anti-GST antibody (TR-FRET donor) and fluorescein (TR-FRET acceptor).

Binding of an agonist to the AR LBD induces a series of conformational changes allowing the coactivator peptide to associate to the AR LBD. Association of the peptide to the AR LBD brings the Tb³⁺- donor in close proximity to the fluorescein acceptor allowing FRET to occur (Figure 3.2A). The same system can also be used for antagonist identification. Binding of an antagonist promotes the dissociation of the fluorescein-labeled peptide resulting in a decrease of FRET (Figure 3.2B).

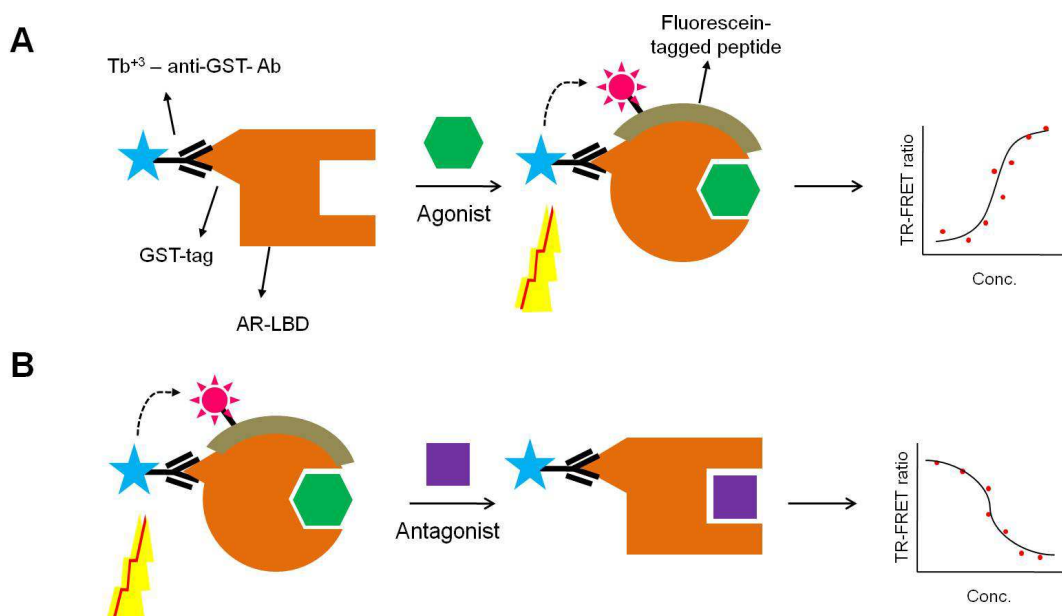


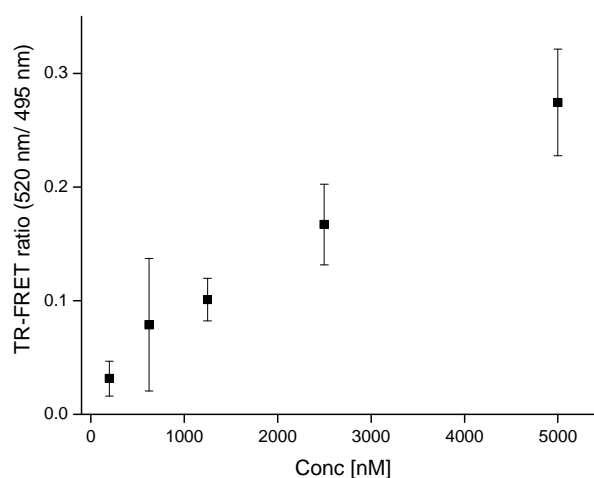
Figure 3.2: Simplified illustration of the basic principles of the Invitrogen TR-FRET assay. **A:** Agonistic mode; upon binding of an agonist conformational changes result in the association of the fluorescein-labeled coactivator peptide. The two fluorophores are brought in close proximity allowing for FRET to occur. The FRET ratio is concentration-dependent. **B:** Antagonistic mode; Displacing an agonist and binding of an antagonist inhibits the association of the fluorescein-labeled peptide resulting in a decrease of the FRET ratio in a concentration-dependent manner.

Although this was a commercially available assay, setting up the system and optimising all the parameters proved to be a challenging and laborious task. It was found that the use of the specific combination of certain 384-well plates (Corning #3676) and filters on the plate reader (Perkin-Elmer excitation filter 340 nm with 30 nm bandwidth; emission filters 520 nm with 25 nm bandwidth and 495 nm with 10 nm bandwidth) were needed to obtain reproducible results.

3.2. Establishing the plate reader set-up

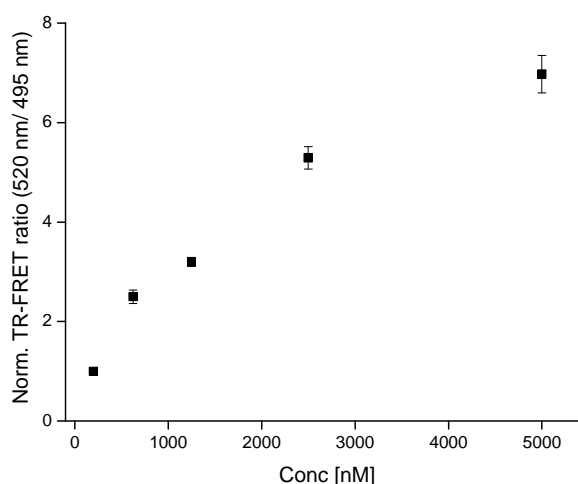
The plate reader was tested in order to verify that the combination of excitation and emission filters available to use was optimal for measuring the TR-FRET signal from the Tb³⁺-chelate donor and the fluorescein-labeled peptide acceptor. Five solutions of the acceptor in different concentrations ranging from 5 μ M to 200 nM were prepared. Aliquots from these samples were added to the wells of a 96-well plate containing a Tb³⁺-chelate donor

solution. The diffusion FRET ratio stemming from simple interactions between the two fluorophores due to Brownian motion bringing them to close proximity, estimated by dividing the emission intensity at 520 nm by the emission intensity at 495 nm, was plotted against the acceptor concentration (Plot 3.1) displaying a concentration dependent increase of FRET as expected.



Plot 3.1: Diffusion FRET ratio (520nm:495nm) against acceptor concentration.

The ratiometric signal was normalized by dividing the FRET ratio for each acceptor concentration with the FRET ratio for the lowest acceptor concentration (Plot 3.2). The results verified that the combination of excitation and emission filters used was optimal for measuring the FRET signal of the fluorescein acceptor and Tb³⁺-chelate donor supplied with the assay kit as they were consistent with the manufacturers values for these parameters.



Plot 3.2: Normalised diffusion FRET ratio against acceptor concentration.

3.2.1. Determination of the activity of known agonists and antagonists

Having established the plate reader setup, a natural AR agonist, testosterone (TE) was tested. A DMSO solution of TE (500 μ M) was prepared and then diluted in a 3-fold 12-step serial dilution manner in DMSO. These solutions were diluted further using the assay buffer and the solutions added to duplicate wells of a 384-well plate. The protein (ARLBD 1.25 μ M) and the two fluorophores (Tb⁺³-anti-GST-Ab 5 nM and Fluorescein-labeled peptide 500 nM) were added and the plate was left to equilibrate for 2 h before being read at the plate reader. A synthetic antagonist – cyproterone acetate (CPA) – was also tested. In a similar fashion, a DMSO solution of CPA (2 mM) was prepared and then diluted in a 3-fold 12-step serial dilution manner in DMSO. As with TE, these solutions were diluted further using the assay buffer and the solutions added to the wells of a 384-well plate in duplicate. The protein (ARLBD 1.25 μ M) the two fluorophores (Tb⁺³-anti-GST-Ab 5 nM and fluorescein-labeled peptide 500 nM) as well as TE (360 nM) were added and the plate was left to equilibrate for 2 - 4 h before being read at the plate reader.

Both compounds gave concentration-dependent curves consistent with literature values (Figure 3.3).^{33b} Obtaining dose response curves with EC₅₀

and IC_{50} values consistent with reported literature^{33b} provided additional confirmation for the applicability of the Invitrogen assay for the purposes of the project.

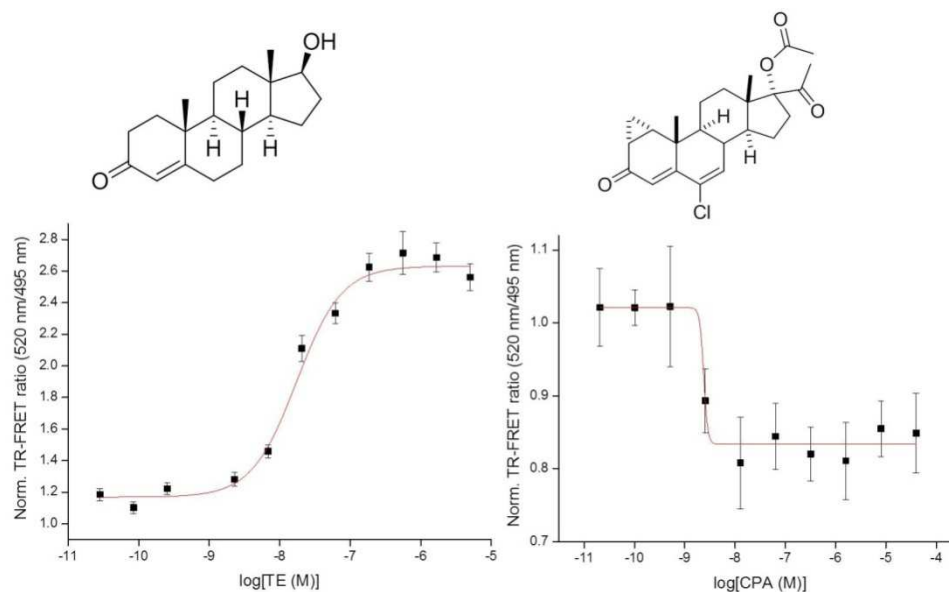


Figure 3.3: Dose-response curves for Testosterone, TE (left) and cyproterone acetate, CPA (right). EC_{50} and IC_{50} values, respectively, are consistent with literature values,¹ TE EC_{50} 17.3 nM; CPA IC_{50} 6.4 nM.

3.3. Metal scavenging studies

In order to be able to screen reactions mixtures using the Invitrogen assay, removal of the residual $Rh^{(II)}$ catalysts was required. This is readily achievable using metal-scavenging macroporous polymeric resins.⁴² Thiourea resins, such as the commercially available QuadraPure TUTM resin,⁴² (Figure 3.4) have been demonstrated to be excellent for the removal of Pd, Rh, Ru and other metals.

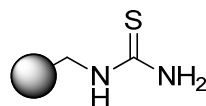
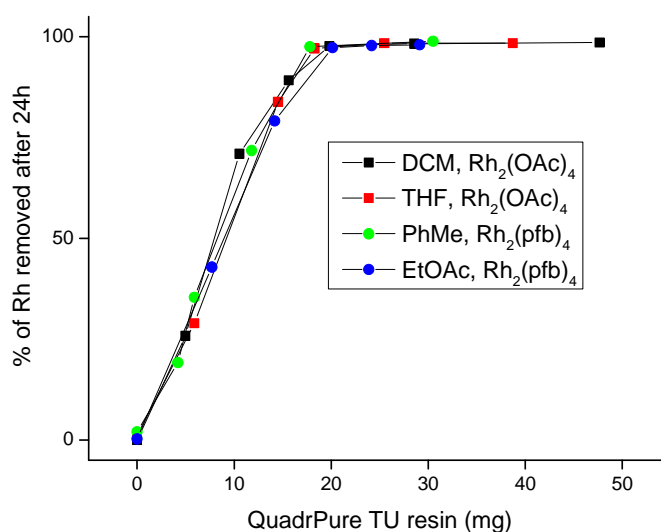


Figure 3.4: Structure of thiourea polymeric resin used to scavenge Pd, Rh, Ru, Pt and other heavy metals from reaction mixtures.

Briefly, 100 μ L of 1 mM solutions of $Rh_2(OAc)_4$ in CH_2Cl_2 and THF and $Rh_2(pfb)_4$ in toluene and EtOAc were prepared in the wells of a custom made

96-well PTFE plate. Increasing amounts of QuadraPure TU resin were added to the wells. No resin was added to the first row of each column and these wells served as negative controls. The wells were sealed using disposable sealing caps and left to scavenge. After 24 h the wells were unsealed and aliquots of the resulting solutions were analysed for heavy metal traces using an atomic absorbance microanalyser and compared against a calibration curve produced from three standard solutions (for rhodium: 5 ppm, 10 ppm and 15 ppm). As it can be observed in Plot 3.3, it was possible to remove >99% of the Rh^(III) metal added using *ca* 30 mg of the resin. The amount of Rh^(III) metal remaining in solution after scavenging was calculated to be *ca* 1 nmol per 100 μ L of reaction mixture which would be diluted down to 1 nM when screening at a total product concentration of 10 μ M (see Chapter 4). An approximate amount of 30 mg of QuadraPure TU resin thus added to the actual microreaction mixtures during the reaction arrays.

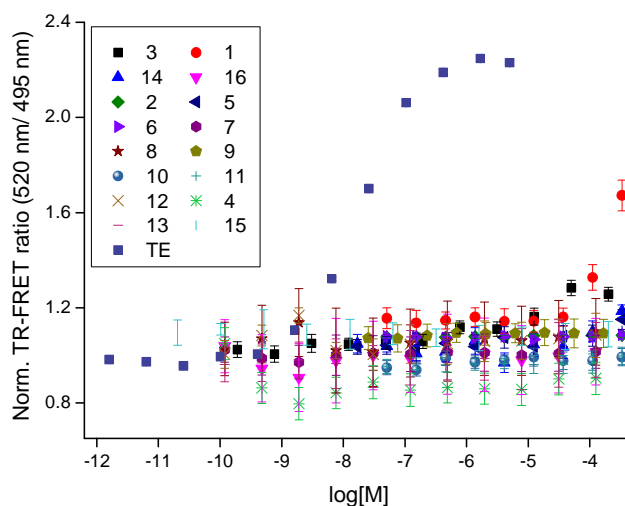


Plot 3.3: Scavenging of Rh^(III) catalysts from various solvents using the QuadraPure Thiourea resin.

3.4. Determination of the activity of the diazo precursors

It was essential to determine that the potential diazo precursors' activity would not interfere with the activity displayed by the microreaction mixtures that would be generated later during the progress of the project. Dose

response curves of the all 16 diazo precursors were recorded in a similar manner to TE and CPA (Plot 3.4). As it can be observed all of the diazo precursors were essentially inactive below 100 μM . This concentration would serve as an initial starting point for the screening of the microreaction mixtures and hence no interference from residual unreactive precursors would be observed.



Plot 3.4: Dose response curves of the 16 diazo precursors used in the reaction arrays. TE curve for comparison.

3.5. Summary

The applicability of the TR-FRET assay for the purposes of this project was confirmed by testing the plate reader setup and recording dose-response curves for two literature compounds, a natural agonist TE and a synthetic antagonist CPA. The EC_{50} and IC_{50} values determined for these compounds are consistent with reported literature values.³⁰ The ability to remove the Rh metal from the microreaction mixtures using the QuadraPure TU resin was successfully determined. A quantity of *ca.* 30 mg was determined to be ideal for the removal of the metal. Lastly, the diazo precursors were found to be inactive against the androgen receptor at concentrations lower than 100 μM . All the above findings provided confidence that the experimental setup used was optimised and could be used successfully for the purposes of the project.

4. Chapter 4

Exploitation of intramolecular reactions in the Activity-Directed Synthesis of androgen receptor agonists

This chapter describes the details of the activity-directed synthesis of androgen receptor agonists using intramolecular reactions. Subsequently, the isolated products were elucidated and biologically evaluated. In addition, the basis of the emergence of the syntheses were evaluated retrospectively. The results described in this chapter have been published in Karageorgis *et al.* in *Nature Chemistry*, 2014, **6**, 872-876.

4.1. Reaction array 1

For the first reaction array, the initial twelve α -diazo-amides **17a** – **18f** described in Chapter 2 were used. Dichloromethane was chosen as a generic solvent along with three commonly used Rh^(III) catalysts: Rh₂(OAc)₄, Rh₂(S-DOSP)₄ and Rh₂(5S-MEPY)₄ (Figure 4.1). Rh₂(OAc)₄ is the most common Rh^(III) catalyst, and Rh₂(S-DOSP)₄ and Rh₂(5S-MEPY)₄ are also commonly exploited with α -diazo-amides.⁴³ Reactions were carried out in custom made 96-well PTFE plates. Briefly, the appropriate catalyst (4 μ L of 25 mM solution in THF) was added to each well containing a solution of the relevant diazo-substrate (8 μ L of 1.25 M solution in CH₂Cl₂) in the appropriate solvent (88 μ L) and subsequently sealed. This mixture resulted in a final solution with the diazo-amide substrate at a concentration of 100 mM and the metal catalyst at a concentration of 1 mM. The product mixtures were mixed by pipetting occasionally, resealed and left to react at room temperature for 48 hours.

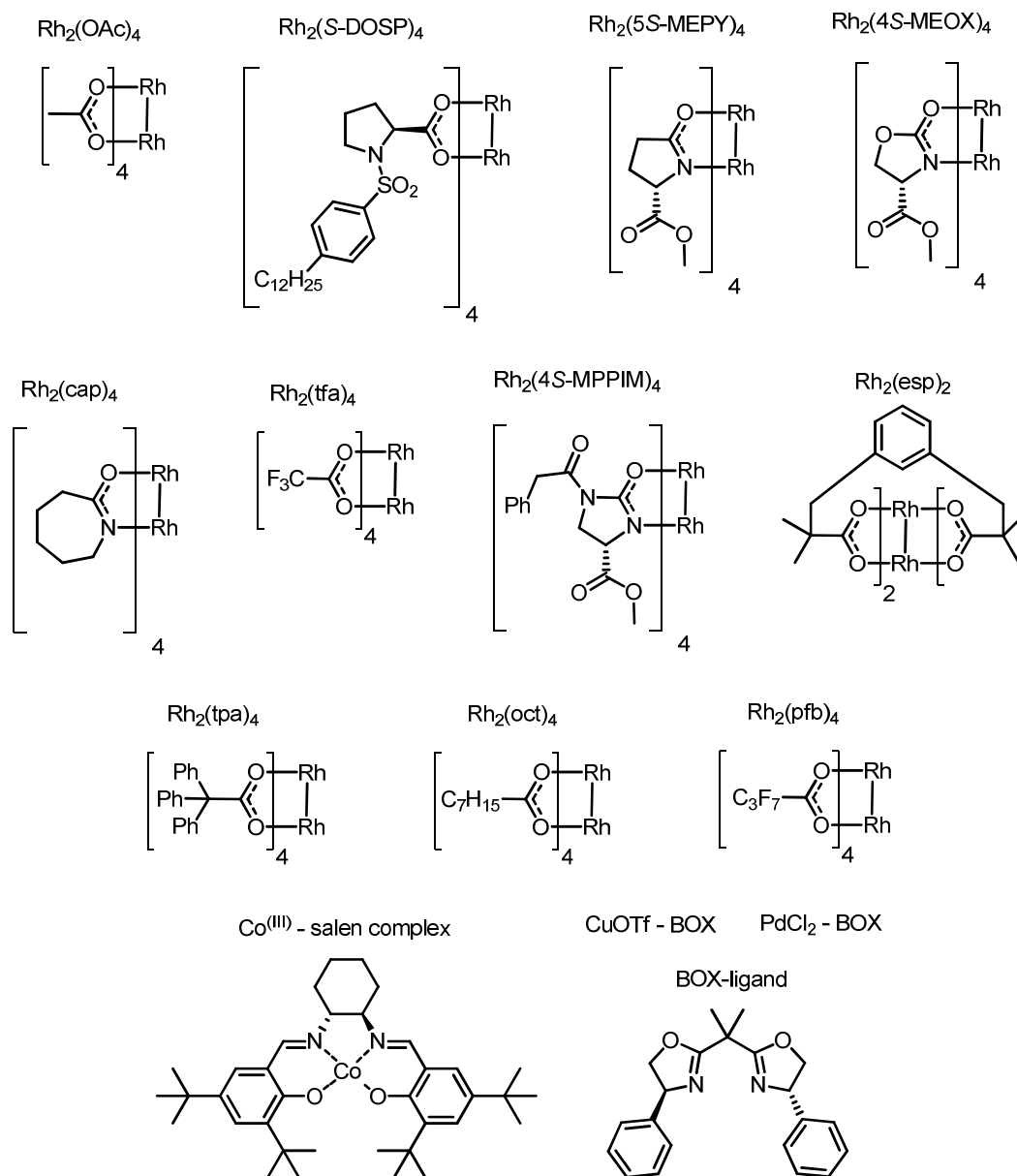


Figure 4.1: Structures of metal catalysts used in intramolecular reactions for activity-directed synthesis on androgen receptor agonists using intramolecular reactions.

After scavenging for $Rh^{(II)}$ (see Chapter 3 for metal scavenging studies), the solvent was removed by evaporation at rt and then under reduced pressure and the reaction mixture was rediluted in dimethyl sulfoxide to give a solution of total product concentration of 100 mM. The product mixtures were then diluted further in DMSO and assay buffer and screened at an initial screened total product concentration of 10 μM (10 μM 1% DMSO in buffer, see experimental for full details). The TR-FRET ratio (520 nm/495 nm) was then normalised to a percentage using the positive control

(Testosterone, TE 5 μM) as 100% and the negative control (1% DMSO in buffer, no ligand) as 0%. The results are shown in Figure 4.2.

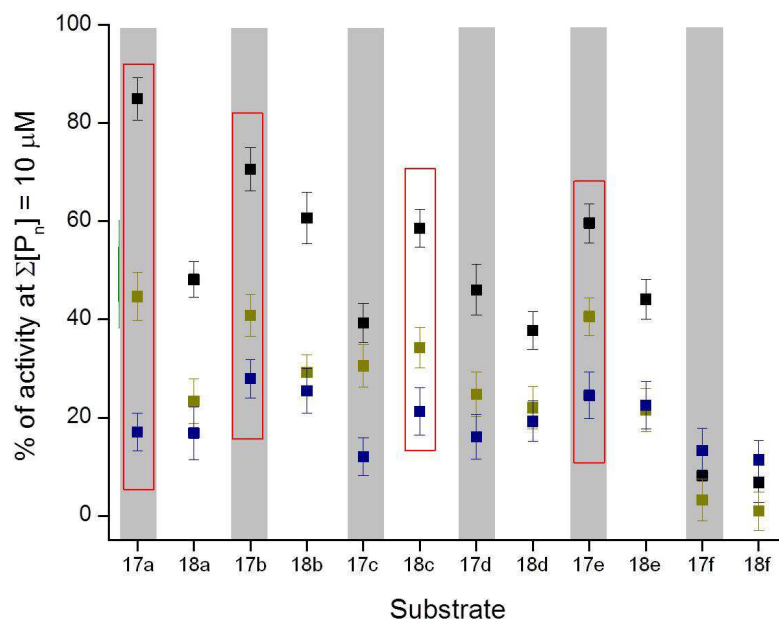


Figure 4.2: Percentage of activity (relative to 5 μM TE) of product mixtures from reaction array 1 at a total concentration of 10 μM (1% DMSO, in buffer). Different colours represent different catalysts: black Rh₂(OAc)₄, yellow Rh₂(S-DOSP)₄ and blue Rh₂(5S-MEPY)₄. Red boxes show which product mixtures were selected to inform the design of the subsequent reaction array.

Product mixtures derived from the substrates **17a**, **17b**, **18c** and **17e** (Figure 4.3) exhibited the most promising results. These product mixtures retained the high levels of activity at the screened concentration as well as across two of the catalysts used, Rh₂(OAc)₄ and Rh₂(4S-DOSP)₄. The activity of these product mixtures informed the design of the reaction array 2.

4.2. Reaction array 2

For the second array, four solvents of increasing polarity⁴⁴ and eight catalysts were chosen. CH₂Cl₂, THF, toluene and EtOAc have been previously used for metal carbenoid reactions.^{25b} Rh₂(OAc)₄, Rh₂(4S-MEOX)₄, Rh₂(cap)₄, Rh₂(tfa)₄, and Rh₂(4S-MPPIM)₄ (Figure 4.1) were chosen as readily available and reliable Rh^(II) catalysts that could enable a wide range of carbenoid reactivity. Reports of using Cu^(I), Pd^(II) and Co^(III)

based catalysts for carbenoid chemistry²⁸ prompted the use of CuOTf–bis-oxazoline, PdCl₂–bis-oxazoline and Co^(III)–salen complexes as well.

The diazo substrates **17a**, **17b**, **18c** and **17e** (Figure 4.3) were used in reaction array 2 as these substrates that yielded the most promising product mixtures in reaction array 1. The diazo substrates **17f** and **18f** were also used in reaction array 2 in order to investigate whether it would be possible to resurrect any activity from substrates that did not yield any promising product mixtures in reaction array 1.

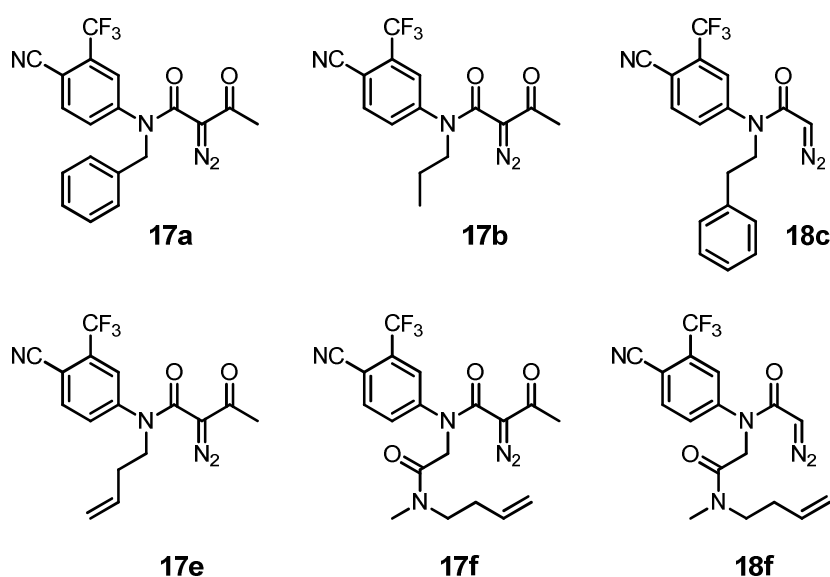


Figure 4.3 Diazo substrates exploited in reaction array 2. Substrates **17a**, **17b**, **18c** and **17e** were found to give the most active product mixtures. Substrates **17f** and **18f** were also used in the second reaction array as a control to investigate if it would be possible to resurrect any levels of activity.

The microreactions were conducted in a similar fashion as for reaction array 1: the appropriate catalyst (4 μ L of 25 mM solution in THF) was added to each well containing a solution of the relevant diazo-substrate (8 μ L of 1.25 M solution in CH₂Cl₂) in the appropriate solvent (88 μ L) and subsequently sealed. They were mixed by pipetting occasionally, resealed and left to react at room temperature for 48 hours. The product mixtures were diluted accordingly in DMSO and buffer and screened using the TR-FRET AR assay at a total concentration of 10 μ M as well as at a total concentration of 1 μ M (10 μ M and 1 μ M 1% DMSO in buffer, see experimental for full details). Screening at a lower concentration was used

as a way of imposing selection pressure onto the system as well probing any effect dilution would have on the activity displayed by each reaction mixture. As before, the TR-FRET ratio (520 nm/495 nm) was normalised to a percentage using the positive control (TE 5 μM) as 100% and the negative control (1% DMSO in buffer, no ligand) as 0%. The results are shown in Figure 4.4.

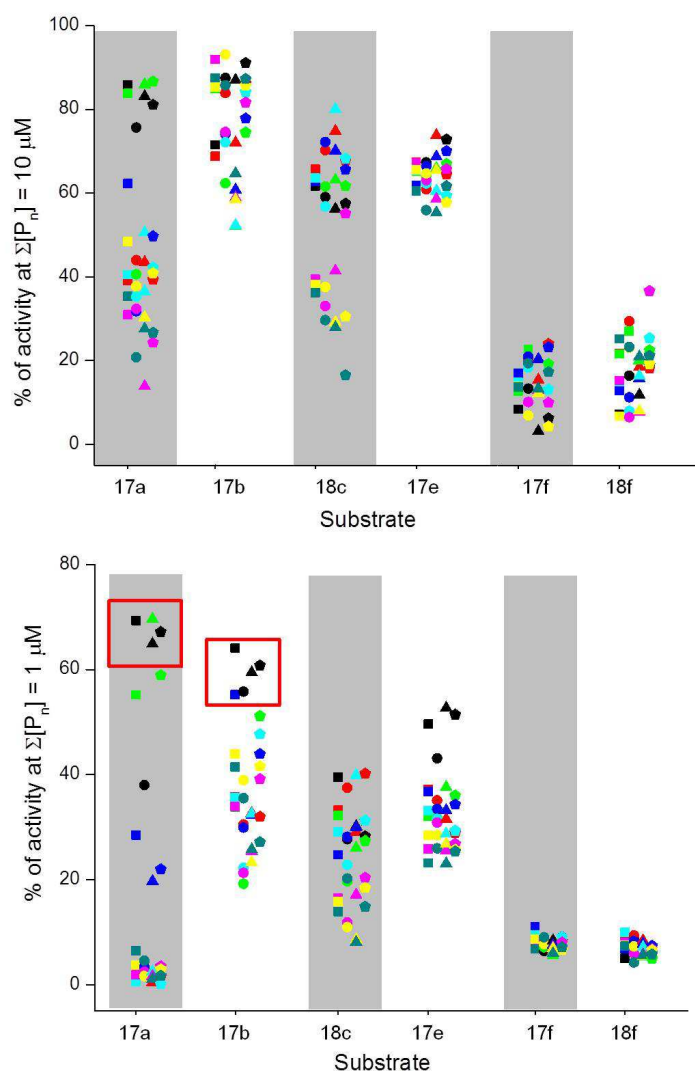


Figure 4.4: Percentage of activity (relative to 5 μM TE) of product mixtures from reaction array 2 at a total concentration of 10 μM (above) and a total concentration of 1 μM (below) (1% DMSO, in buffer). Different colours represent different catalysts (black $\text{Rh}_2(\text{OAc})_4$, bright green $\text{Rh}_2(\text{tfa})_4$ and blue $\text{Rh}_2(\text{cap})_4$) and different shapes represent different solvents (squares CH_2Cl_2 , triangles PhMe, circles THF, pentagons EtOAc). Red boxes show which product mixtures were selected to inform the design of the subsequent reaction array. Error bars omitted for clarity. Typical error 2-5%.

As it can be observed in Figure 4.4, screening at a lower concentration revealed that only few product mixtures displayed high activities. This

observation might suggest that the reactions are only steered towards the formation of active products under specific combinations of diazo substrate, catalyst and solvent. This effect is more striking in the case of substrate **17a**, where most of the product mixtures display very low activities, and only under some conditions combinations high activities are observed. Product mixtures from substrates **17a** and **17c** in combination with carboxylate Rh^(II) catalysts in CH₂Cl₂, toluene or EtOAc, gave consistently better results compared to substrates **18c** and **17e**. The Cu^(I), Pd^(II) and Co^(III) catalysts were found to yield weakly active product mixtures which lost their activity once diluted by a factor of ten. As expected, substrates **17f** and **18f** did not yield any promising product mixtures suggesting that no active products were derived from these substrates. These results informed the design of the subsequent reaction array three.

4.3. Reaction array 3

Using the above results, a focused library of four additional substrates was synthesised, based on the structural features of substrates **17a** and **17b**. The diazo substrate **17g** was a heteroaromatic analogue of diazo substrate **17a**, whilst diazo substrates **17h–17j** were functionalised analogues of diazo substrate **17b**. Substrates **17g–17j** were synthesised using the established synthetic route as described in Chapter 2 (Figure 4.5).

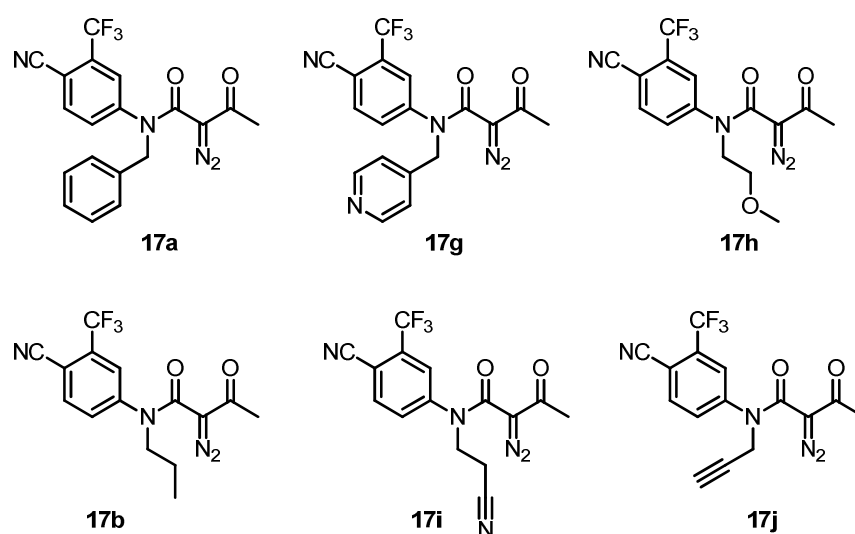


Figure 4.5: Diazo substrates exploited in reaction array 3. Substrates **17g–17j** were inspired by substrates **17a** and **17b**.

A third reaction array was carried out using the substrates **17a**, **17b** and **17g - 17j** as well. A focused set of carboxylate Rh^(III) catalysts was used as this type of catalyst had been shown to give the most active product mixtures in the previous reaction array. The reactions were conducted in CH₂Cl₂, toluene and EtOAc as all three solvents gave consistently good results in the previous array. The appropriate catalyst (4 μL of 25 mM solution in THF) was added to each well containing a solution of the relevant diazo-substrate (8 μL of 1.25 M solution in CH₂Cl₂) in the appropriate solvent (88 μL) and subsequently sealed. They were mixed by pipetting occasionally, resealed and left to react at room temperature for 48 hours. The product mixtures were subsequently diluted in DMSO and buffer accordingly and screened using the TR-FRET AR assay total concentrations of both 1 μM as well as 100 nM. As before, the TR-FRET ratio (520 nm/495 nm) was normalised to a percentage using the positive control (TE 5 μM) as 100% and the negative control (1% DMSO in buffer, no ligand) as 0%. The results are shown in Figure 4.6.

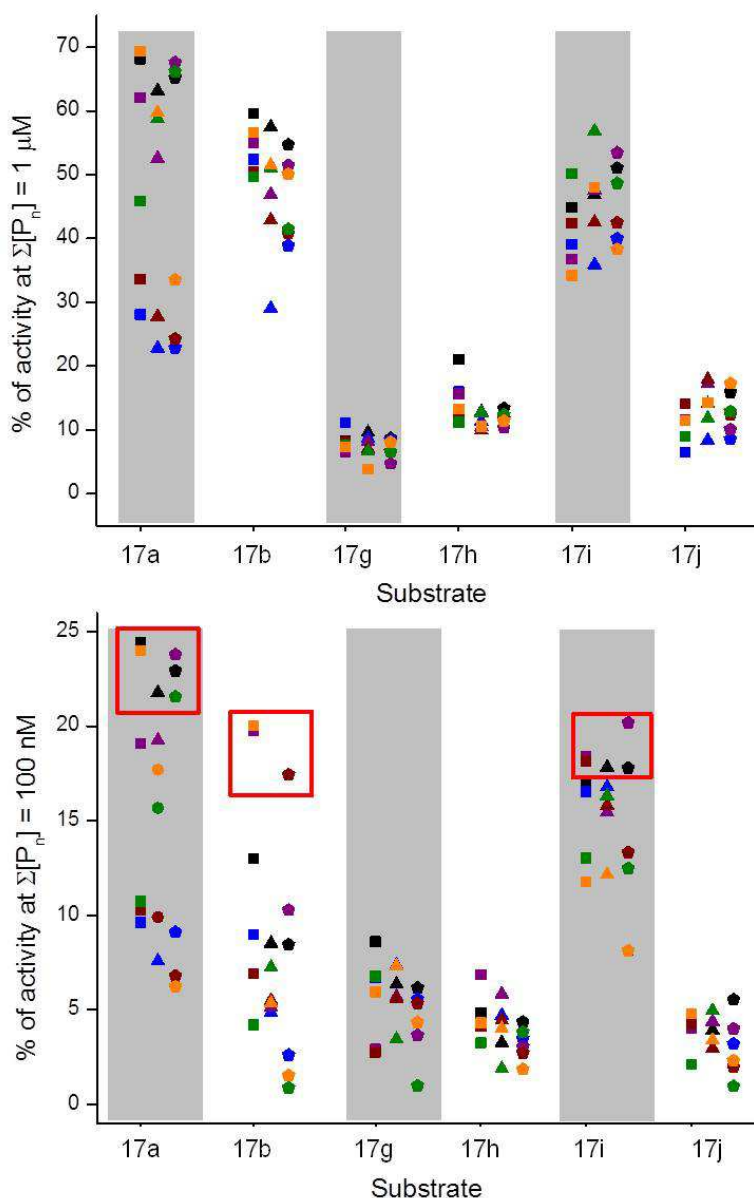


Figure 4.6: Percentage of activity (relative to 5 μM TE) of products mixtures from reaction array 3 at a total concentration of 1 μM (above) and 100 nM (below) (1% DMSO, in buffer). Different colours represent different catalysts (black Rh₂(OAc)₄, purple Rh₂(esp)₂ and orange Rh₂(oct)₄) and different shapes represent different solvents (squares: CH₂Cl₂, triangles: PhMe, pentagons: EtOAc). Red boxes show which product mixtures were selected to inform the selection of reactions to scale-up. Error bars omitted for clarity. Typical error 2-5%.

Once more, it can be observed that only specific reaction conditions yield product mixtures which displayed promising activities. At this point the most promising combinations of substrate, catalyst and solvent were selected for scale up. Their selection was based on maintaining their activity even at the lowest level of dilution, total concentration of 100 nM when screened using the TR-FRET AR assay.

4.4. Scale up

A total of eight reactions was selected for scale up; three reaction conditions using substrate **17a**, three reaction conditions using substrate **17b** and two reaction conditions using substrate **17i**. The conditions for these reactions are summarised in Table 4.1.

Table 4.1: The eight most promising reactions were selected for scale-up. The details of the combinations regarding the substrate, catalyst and solvent are shown below.

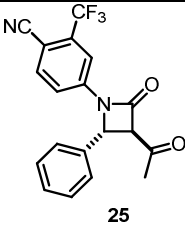
Entry	Substrate	Solvent	Catalyst
1		CH ₂ Cl ₂	Rh ₂ (oct) ₄
2		CH ₂ Cl ₂	Rh ₂ (OAc) ₄
3		EtOAc	Rh ₂ (esp) ₂
4		CH ₂ Cl ₂	Rh ₂ (oct) ₄
5		CH ₂ Cl ₂	Rh ₂ (esp) ₂
6		CH ₂ Cl ₂	Rh ₂ (OAc) ₄
7		EtOAc	Rh ₂ (esp) ₂
8		PhMe	Rh ₂ (tpa) ₄

The selected reactions were performed in a similar manner as the microreactions on a 50-fold larger scale. The appropriate diazo substrates (400 μ L of a 1.25 M solution in CH₂Cl₂) and the metal catalyst (200 μ L of a 25 mM in THF) were mixed in the appropriate solvent (4.4 mL). The final concentration for the diazo substrate was 0.1 M and for the catalyst 1 mM, in 5 mL of solvent. The reactions were sealed and left to react for 48 h, followed by TLC and LC-MS. After scavenging they were filtered, concentrated *in vacuo* and the crude mixture purified by column chromatography.

4.4.1. Reactions from diazo substrate **17a**

The diazo butanamide **17a** was treated with 1 mol% $\text{Rh}_2(\text{OAc})_4$, $\text{Rh}_2(\text{oct})_4$ or $\text{Rh}_2(\text{esp})_2$ in CH_2Cl_2 or EtOAc. The outcome of each reaction is summarised in Table 4.2. The major product isolate in all three reactions was the β -lactam **25** formed by a C-H insertion at the benzylic position. The structure was confirmed by the IR peak at 1705 cm^{-1} , indicative for a β -lactam as well as the characteristic splitting patterns of the protons at positions 3 and 4 of the azetidinone ring. The relative *trans* configuration around the ring was determined by nOe spectroscopy, observing the correlation between the proton at the 4-position of the azetidinone ring (5.55 ppm) and the methyl protons (2.40 ppm) (Figure 4.7) as well as characteristic *trans* azetidinone coupling constants of the protons at the 3- and 4- positions.

Table 4.2: Scaled-up reactions from the diazo substrate **17a**.

Entry	Catalyst	Solvent	Product	Yield (%)
1	$\text{Rh}_2(\text{oct})_4$	CH_2Cl_2	 25	71
2	$\text{Rh}_2(\text{OAc})_4$	CH_2Cl_2		68
3	$\text{Rh}_2(\text{esp})_2$	EtOAc		75

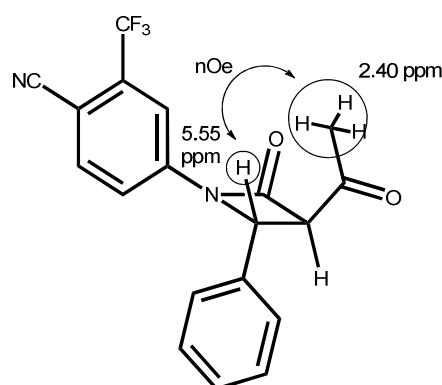
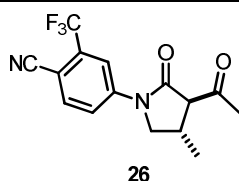


Figure 4.7: Structural confirmation about the *trans* configuration of the azetidinone ring came from the nOe correlation between the proton at the 4-position and the methyl protons.

4.4.2. Reactions from diazo substrate **17b**

The diazo butanamide **17b** was treated with 1 mol% $\text{Rh}_2(\text{OAc})_4$, $\text{Rh}_2(\text{oct})_4$ or $\text{Rh}_2(\text{esp})_2$ in CH_2Cl_2 . The outcome of each reaction is summarised in Table 4.3. The major product isolated was in all cases, the γ -lactam **26** which was formed by a C-H insertion at the 2-position of the ethyl group. Structural confirmation was, once more provided by nOe spectroscopy to determine the *trans* configuration around the five-membered lactam ring. The correlation between the proton at the 3-position of the lactam ring (3.48 ppm) and the protons of methyl group at the 4-position (1.25 ppm) was observed (Figure 4.8).

Table 4.3: Scaled-up reactions from diazo substrate **17b**.

Entry	Catalyst	Solvent	Product	Yield (%)
1	$\text{Rh}_2(\text{oct})_4$	CH_2Cl_2	 26	88
2	$\text{Rh}_2(\text{esp})_2$	CH_2Cl_2		90
3	$\text{Rh}_2(\text{OAc})_4$	CH_2Cl_2		55

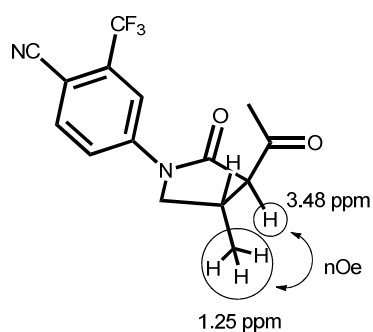
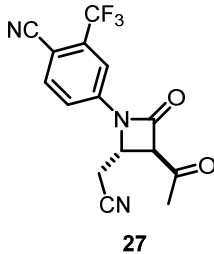
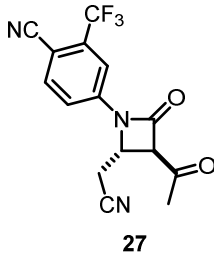


Figure 4.8: Determination of the relative configuration around the lactam ring: a nOe correlation between the proton at the 3-position and the protons of the methyl group at the 4-position was observed.

4.4.3. Reactions from diazo substrate **17i**

Diazo butanamide **17i** was treated with 1 mol% $\text{Rh}_2(\text{esp})_2$ and $\text{Rh}_2(\text{tpa})_4$ in EtOAc or toluene respectively. The outcome of the two reactions is summarised in Table 4.4. The major product isolated from both reactions the β -lactam **27** formed by a C-H insertion at the 2-position of the *N*-appended group. As in the case of β -lactam **25**, structural confirmation was provided by IR (1716 cm^{-1}) and observation of nOe interactions (Figure 4.9) between the proton at 4.42 ppm (3-position) and the protons at 3.06 ppm (methylene cyano group) as well as characteristic *trans* azetidinone coupling constants of the protons at the 3- and 4- positions.

Table 4.4: Scaled-up reactions from diazo substrate **17i**.

Entry	Catalyst	Solvent	Product	Yield (%)
1	$\text{Rh}_2(\text{esp})_2$	EtOAc		78
2	$\text{Rh}_2(\text{tpa})_4$	PhMe		70

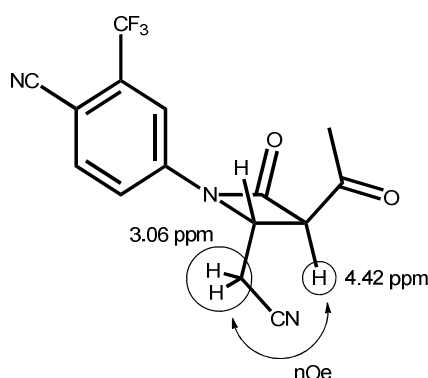


Figure 4.9: Structural confirmation about the *trans*- geometry of the azetidinone ring came from the nOe correlation between the proton at the 3-position and the protons at the 2- position of the methylene cyano group.

4.5. Evaluation of the isolated products

The three isolated products – the β -lactam **25**, the γ -lactam **26** and the β -lactam **27** were assayed in dose-dependent manner. Stock solutions of the compounds in DMSO were prepared (20 mM for **25** and **26** and 50 mM for **27**) and diluted accordingly with DMSO and assay buffer in a 12-step, 3-fold serial dilution manner. The initial assayed concentration was 50 μ M for compounds **25** and **26** and 200 μ M for compound **27** (1% DMSO in buffer) (Figure 4.10 and experimental for details).

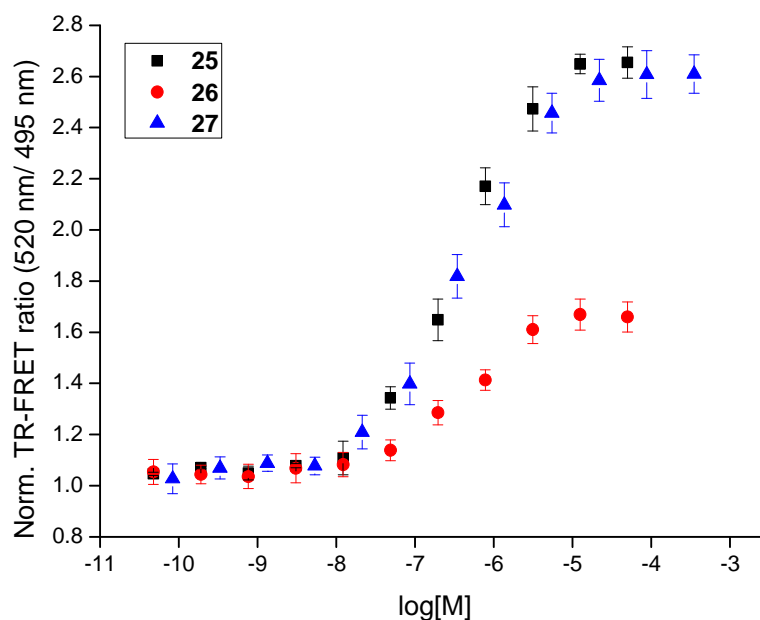


Figure 4.10: Dose-response curves obtained by assaying the isolated products from the scaled reactions β -lactam **25**, γ -lactam **26** and the β -lactam **27**.

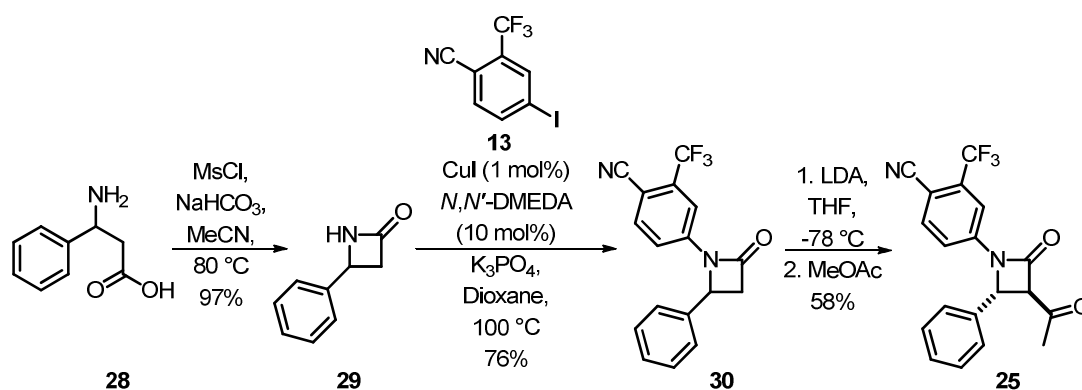
From the dose-response curves obtained, the EC_{50} value for each of the compounds was extracted by applying a non-linear fitting (logistic fit, OriginPro v. 8.6); β -lactam **25** 350 (± 60) nM, γ -lactam **26** 470 (± 78) nM and β -lactam **27** 440 (± 56) nM. The two β -lactams **25** and **27**, were found to be full agonists of the Androgen Receptor, whilst the γ -lactam **26** was found to be a partial agonist meaning that it will display a lower maximum activity compared to the maximum activity displayed by a full agonist such as testosterone. It had been previously observed that bicalutamide also acted

as a partial agonist when using this assay.⁴⁵ All three products were found to be active modulators of the Androgen Receptor with chemotypes with no previously annotated biological activity.

4.6. Synthesis of β -lactam **25** via an alternative route

An alternative synthesis of the most active compound, the β -lactam **25**, was undertaken. The alternative synthesis would prove beyond reasonable doubt that the activity observed from the isolated compound using the Rh-catalysed reaction was indeed attributed to the β -lactam **25**, and not to undetected minor impurities.

To this extent, the commercially available racemic β -phenyl alanine **28** was treated with methanesulfonyl chloride and NaHCO₃ in acetonitrile⁴⁶ to give the β -lactam **29**. The β -lactam **29** was subsequently arylated by treatment with the aryl iodide **13**, CuI, a diamine ligand and K₃PO₄ in refluxing dioxane⁴⁷ to yield the *N*-arylated β -lactam **30**. Subsequently the β -lactam **30** was successfully acylated at the 3' position by treatment with LDA and then methyl acetate⁴⁸ to afford the desired β -lactam **25** as a single diastereomer (Scheme 4.1). The NMR spectra of the product, were identical to those previously obtained.



Scheme 4.1: Alternative, synthesis of the β -lactam **25**.

A sample of the re-synthesised compound was assayed alongside a sample of the original β -lactam and the two were found to display almost identical activities within experimental error (Figure 4.11). The activity of the

resynthesised molecule demonstrated beyond reasonable doubt that the β -lactam **25** was responsible for the activity observed.

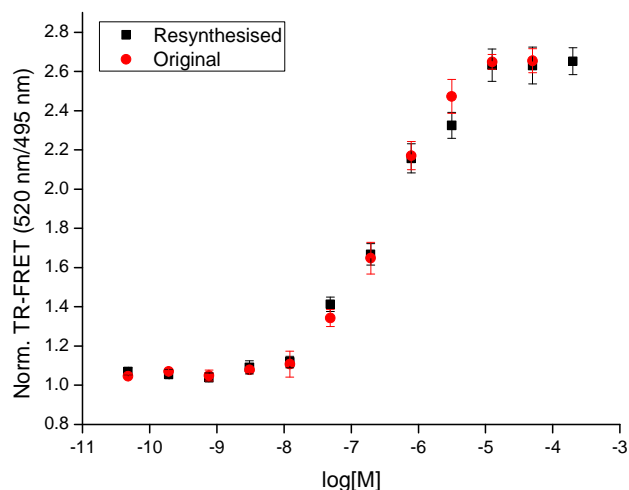


Figure 4.11: The resynthesised β -lactam was found to give an almost identical dose-response curve as the original sample. Resynthesised (black squares) 320 ± 67 nM; Original (red circles) 340 ± 42 nM.

4.7. Retrospective exploration of the basis of the emergence of Activity-Directed Synthesis

Having proved that the active components in the product mixtures were the same as the products isolated from the scaled reactions, a retrospective exploration was undertaken in order to understand the basis for the emergence of the activity-directed synthesis.

4.7.1. Quantitative HPLC

To begin, the yield of the active component **25** and the activity displayed by the crude product mixtures was correlated. Quantitative HPLC analysis of the product mixtures generated in reaction array 3 with the diazo substrate **17a** was performed, to determine the yield of the β -lactam **25** formed in each reaction (Figure 4.12). Samples of each micro-reaction were

analysed using HPLC conditions determined by HPLC analysis of a pure sample of the β -lactam **25**.

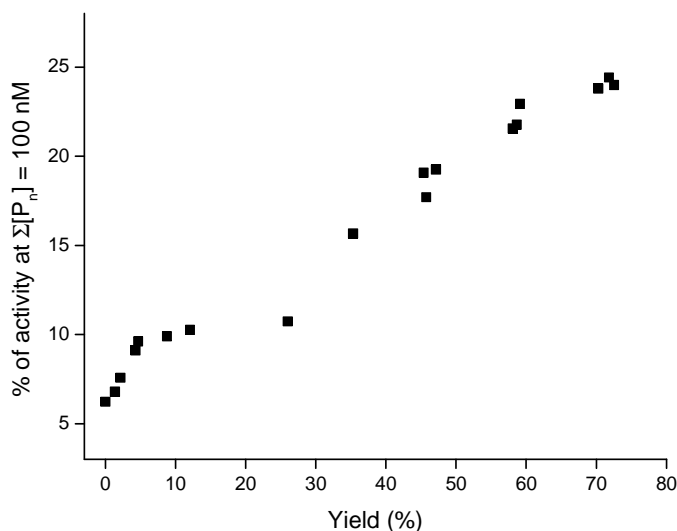


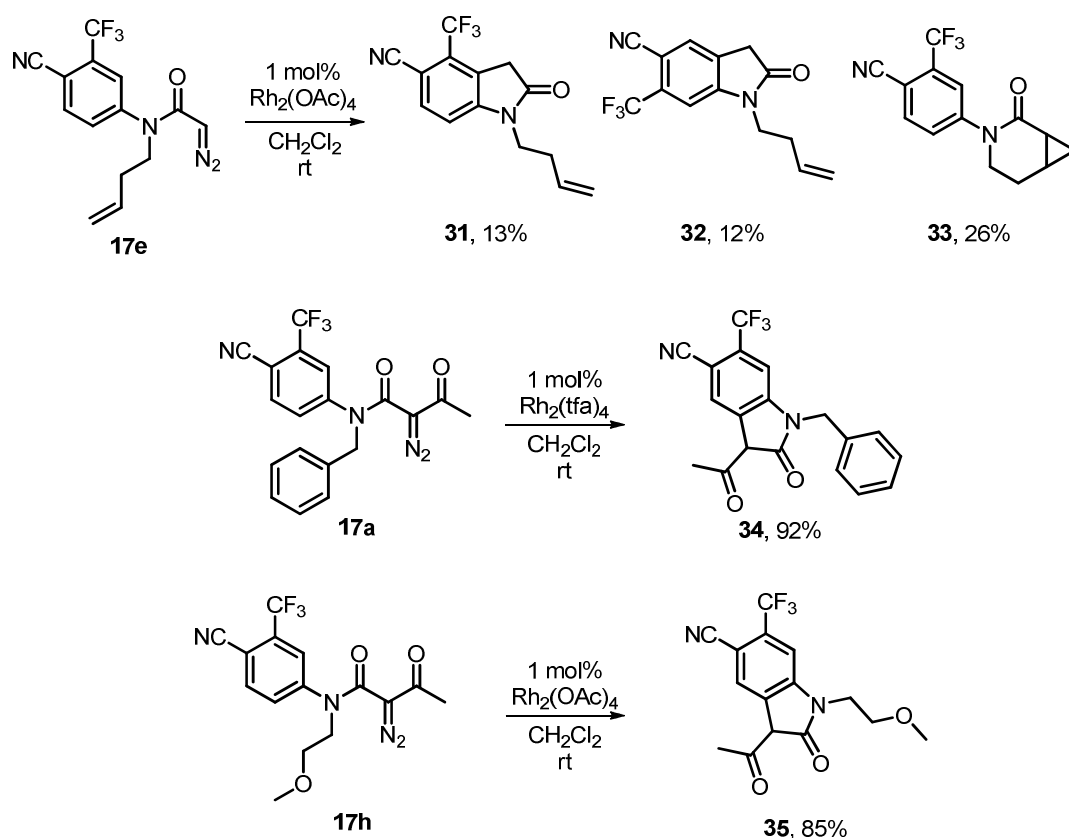
Figure 4.12: Correlation of the yield (%) of the β -lactam **25** and the activity displayed by product mixtures (relative to 5 μ M TE) from reaction array 3, screened at $\Sigma[P_n] = 100$ nM (1% DMSO in buffer).

The yield of the β -lactam **25** correlated very well with the activity displayed by the product mixtures (Figure 4.12). This analysis demonstrated that the direct assaying of the product mixtures gave an indication of the yield of the most active product *i.e.* by maximising the activity of the product mixtures, the yield of the most active product would also be optimised.

4.7.2. Diversity of products

In order to investigate whether diverse products had been generated throughout the reaction arrays, some reactions that did not display sufficiently promising activity were also scaled-up. One reaction from each reaction array was selected: from reaction array 1 the diazo substrate **17e** with $\text{Rh}_2(\text{OAc})_4$ in CH_2Cl_2 ; from reaction array 2 diazo substrate **17a** with $\text{Rh}_2(\text{tfa})_4$ in CH_2Cl_2 ; and finally, from reaction array 3 diazo substrate **17h** with $\text{Rh}_2(\text{OAc})_4$ in CH_2Cl_2 . In each reaction, the appropriate diazo substrate (400 μ L of a 1.25 M solution in CH_2Cl_2) and the necessary metal catalyst (200 μ L of a 25 mM in THF) were mixed in the appropriate solvent (4.4 mL).

The final concentration for the diazo substrate was 0.1 M and for the catalyst 1 mM, in 5 mL of solvent. The reactions were sealed and left to react for 48 h and as before followed by TLC and LC-MS. After scavenging, the crude was filtered, concentrated *in vacuo* and purified by column chromatography. The diazo substrate **17e** afforded three different products when treated with 1 mol% $\text{Rh}_2(\text{OAc})_4$ in CH_2Cl_2 at room temperature: two oxindoles, **31** and **32**, formed by C-H insertions, and a δ -lactam **33** formed by a cyclopropanation (Scheme 4.2). The diazo substrate **17a** was treated with 1 mol% $\text{Rh}_2(\text{tfa})_4$ in CH_2Cl_2 at room temperature: the reaction yielded the oxindole **34**, again via a C-H insertion. Similarly, treatment of the diazo substrate **17h** with 1 mol% $\text{Rh}_2(\text{OAc})_4$ in CH_2Cl_2 at room temperature yielded the oxindole **35**.



Scheme 4.2: Outcome of some reactions that did not yield product mixtures with sufficient activity for prioritisation.

Stock solutions of the purified products in DMSO (100 mM for compounds **31-33**, 25 mM for compound **34** and 50 mM for compound **35**) were prepared and used to assay compounds 31-25 in a dose-response manner. These solutions were further diluted in buffer resulting at an initial assayed concentration of 1 mM for compounds **31-33**, 110 μM for compound

34 and 200 μM for compound **35** (1% DMSO in buffer). When assayed all products, apart from the oxindole **32**, were found to be partial agonists of the androgen receptor. Their EC_{50} values were determined by using a logistic fit on the dose-response curve: oxindole **31** $10.0 \pm 0.9 \mu\text{M}$; δ -lactam **33** $0.7 \pm 0.1 \mu\text{M}$; oxindole **34** $2.4 \pm 0.4 \mu\text{M}$; and oxindole **35** $12.0 \pm 3.7 \mu\text{M}$. Their EC_{50} values were found to be significantly higher than the products isolated from the original eight scaled-up reactions (Figure 4.13 and Table 4.5).

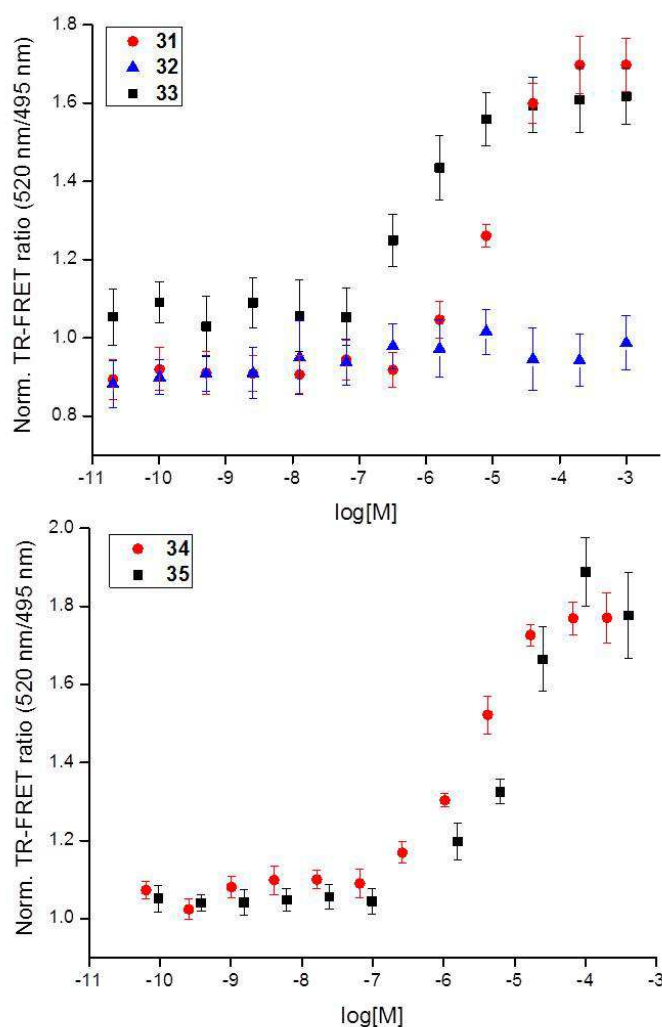
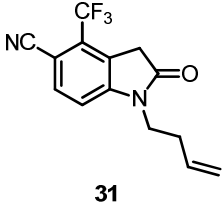
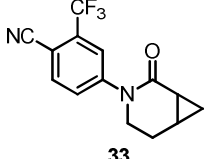
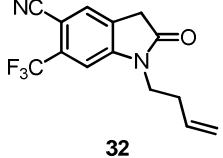
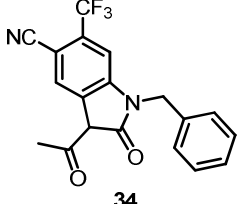
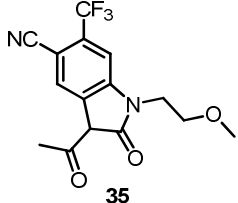


Figure 4.13: Dose-response activity of the products **31**, **33**, **34** and **35**. Compound **32** was not found to be active when assayed for agonistic activity. All compounds were found to be partial agonists of the androgen receptor. Initial assayed concentrations 1 mM for compounds **31-33**, 110 μM for compound **34** and 200 μM for compound **35** (1% DMSO in buffer).

Table 4.5: EC₅₀ values of some products obtained from reactions whose product mixtures did not display significantly promising activity for prioritisation.

Entry	Product	EC ₅₀ (μM)
1	 <p style="text-align: center;">31</p>	10.0 ± 0.9
2	 <p style="text-align: center;">33</p>	0.7 ± 0.1
3	 <p style="text-align: center;">32</p>	>200 μM
4	 <p style="text-align: center;">34</p>	2.4 ± 0.4
5	 <p style="text-align: center;">35</p>	12.0 ± 3.7

From these additional reactions, four chemotypes were identified: the oxindole **31**, the isomeric oxindole **32**, the δ-lactam **33** and the acetyl-oxindoles **34** and **35**. Apart from compound **32**, all the compounds were found to be partial agonists with higher EC₅₀ values compared to compounds **25-27**. These results may retrospectively rationalise the reason for not prioritising these reactions for the design of the subsequent reaction array. From reaction array 1, which was screened at a total product concentration of 10 μM, product mixtures stemming from diazo-substrate **17e** displayed borderline activity presumably stemming from oxindole **31** the δ-lactam **33**.

From reaction array 2, which was screened at total product concentrations of 10 μM and 1 μM , only some of the product mixtures stemming from diazo-substrate **17a** displayed promising activities whilst a few displayed only moderate activity, insufficient for prioritisation, possibly stemming from oxindole **34**. Finally in reaction array 3, which was screened at total product concentrations of 1 μM and 100 nM, product mixtures stemming from diazo-substrate **17h**, did not display promising activities, attributed to the formation of the weakly active oxindole **35**. These results indicate that the chemical space arising from each of the diazo substrates was sufficiently explored yet ultimately discarded due to either the low activity displayed by the products or the low yield in which they were formed.

4.8. Summary

Three arrays of intramolecular reactions were performed and the product mixtures from each array were screened for agonism of the Androgen Receptor, in progressively lower concentrations. This technique facilitated the selection of reaction conditions to be carried forward to the subsequent reaction array, based on the activity of product mixtures. A total of 272 micro-reactions were performed. This process allowed for the selection of eight reaction conditions for scale-up (Figure 4.14). Purifying, characterising and evaluating the biological activity of the products led to the rapid and efficient discovery of three sub-micromolar modulators of the Androgen Receptor with chemotypes with no previously annotated biological activity (Figure 4.15).

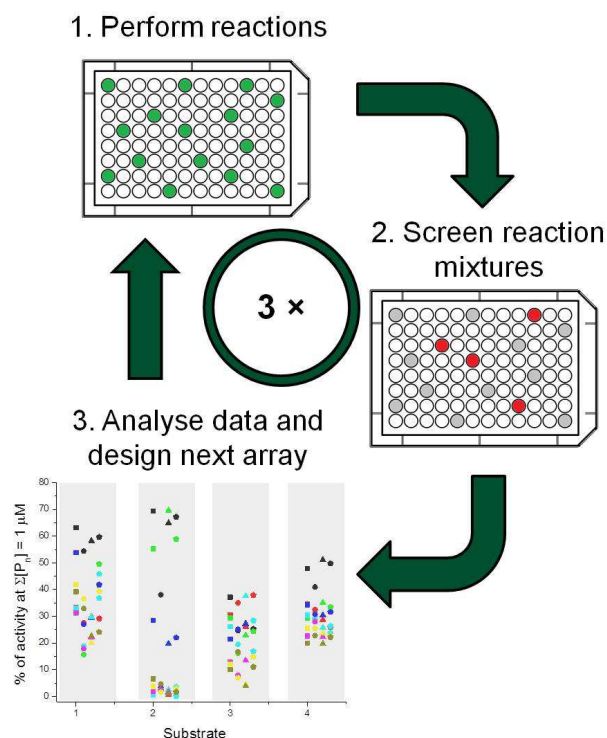


Figure 4.14: A total of 272 reactions were performed over three reaction arrays. Eight reaction conditions were selected to be scaled-up.

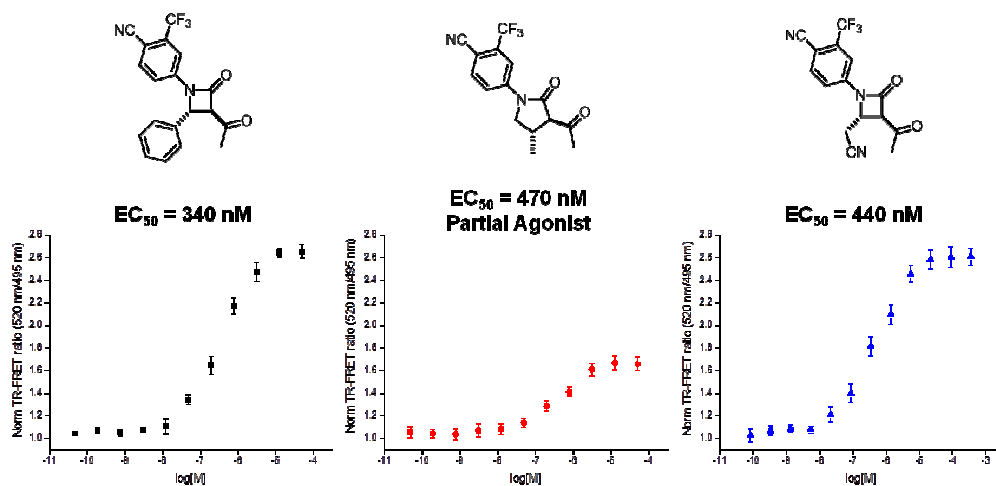


Figure 4.15: Three modulators of the Androgen Receptor with chemotypes with no previously annotated biological activity.

The retrospective exploration also provided evidence about the overall development of the approach and that the optimisation of activity-directed synthesis might lead to the simultaneous optimisation of both the yield and the structure of an active chemotype. In reaction array 1, the carbenoid reactivity was probed, evidenced by the formation of products **31**,

32, **33** and the β -lactam **25**. In reaction array 2, the combination of solvent and catalyst resulted in yielding the active component in a similar or higher yield. In some cases the formation of a different less active product e.g. oxindole **34** was observed. Finally, in reaction array 3, a new, functionally similar diazo-substrate e.g. **17i** was used to yield a novel compound, **27**, but of a similar chemotype *i.e.* a β -lactam (Figure 4.16).

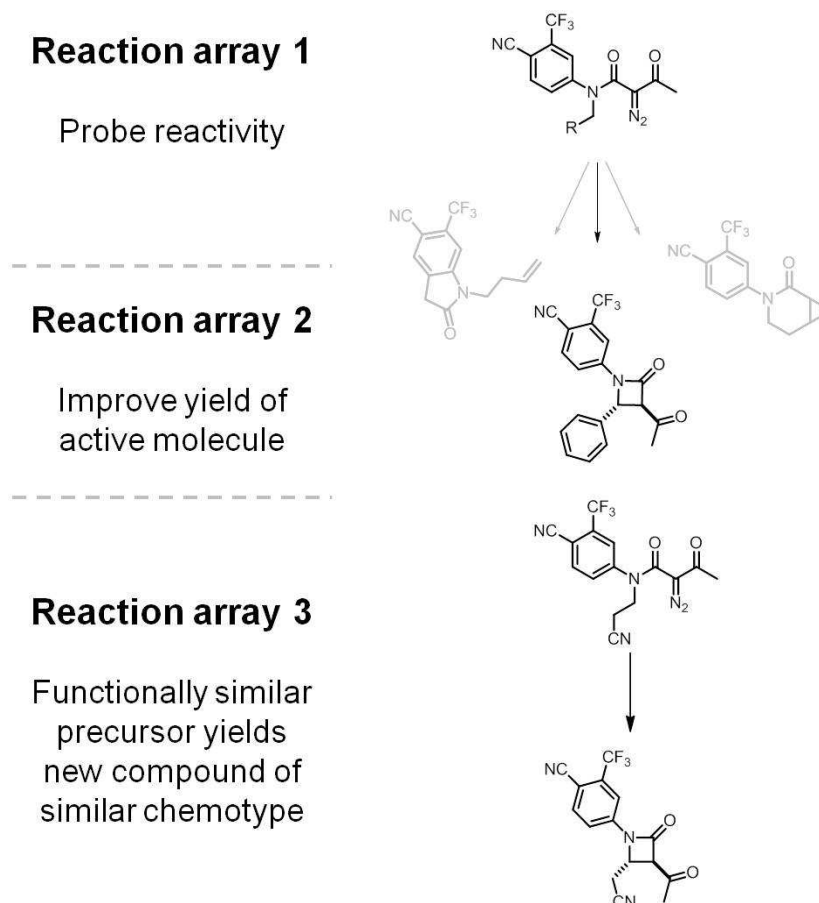


Figure 4.16: Overall development of the methodology elucidated by the retrospective exploration.

The alternative synthesis confirmed the activity of the β -lactam **25** both quantitatively and qualitatively. The HPLC analysis combined with scaling up three additional reactions elucidated the progression and overall development of the methodology demonstrating its versatility and effectiveness as a novel tool for the discovery of small bioactive molecules.

5. Chapter 5

Exploitation of Intermolecular Reactions in the Activity-Directed Synthesis of Androgen Receptor Agonists

A limitation of intramolecular reactions is that the outcome is largely determined by the diazo-substrate. Furthermore, synthetic effort was invested in the individual preparation of each substrate. For these reasons, it was decided to exploit intermolecular reactions for the activity-directed synthesis of Androgen Receptor agonists. Intermolecular reactions could, in principle, enable a far wider range of possible outcomes. In each round, a collection of possible co-substrates which were inactive against the androgen receptor, was used with diazo-amide substrates to yield product mixtures. Subsequently, selected reactions from each round were scaled-up and the isolated products from were elucidated and evaluated biologically in order to understand rationalise the emergence of activity-directed syntheses.

5.1. Synthesis of diazo amide substrates for intermolecular reactions

The diazo amide substrates for intermolecular reactions followed a similar design to the diazo amides for intramolecular reactions. However, it was decided that the *N*-appended group would be chosen such that it would minimise the possibility for intramolecular reactions. Limiting the consumption of the diazo substrate in intramolecular reactions would, in principle, promote the participation in intermolecular reactions. Four diazo amide substrates were initially used for intermolecular reactions: two diazo butanamides and two diazo acetamides (Figure 5.1). The *N*-appended group was chosen to be either methyl or cyclopropyl, as C-H insertions on unactivated methyl groups or tertiary carbon atoms have been shown to be unfavoured,⁴⁹ minimising the possibilities of intramolecular reactions.

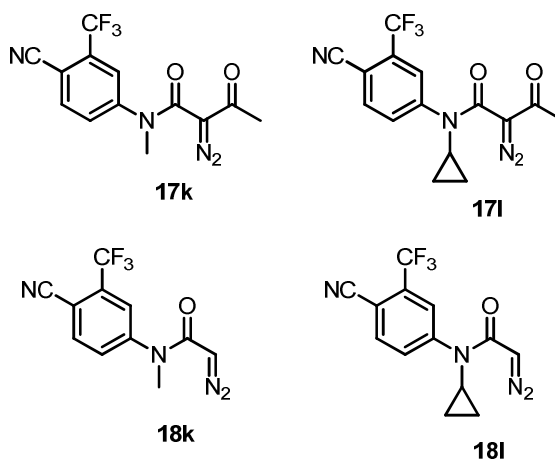
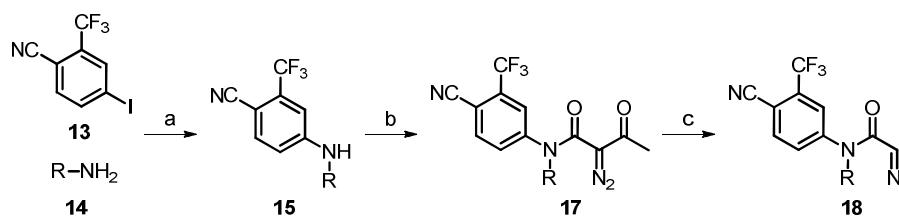
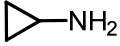


Figure 5.1: The design of the four diazo amides **17k–18l**, used in intermolecular reactions. The *N*-appended groups were selected such that possible intramolecular reactions would be minimised.

The four diazo amides were prepared using a synthetic route similar to the diazo amides for intramolecular reactions (see Chapter 2). The aryl iodide **13** was heated with either the *N*-methyl amine hydrochloride **14k** or the cyclopropylamine **14l**, and CuI, L-proline and K₂CO₃ in DMSO to afford the anilines **15k** and **15l**. The anilines **15k** and **15l** were acylated under microwave irradiation using the dioxinone **4** and subsequently diazotated by treatment with *p*-ABSA and triethyl amine in acetonitrile to yield the diazo butanamides **17k** and **17l**. Subsequently, **17k** and **17l** were deacylated by treatment with NaOMe in methanol and afforded the diazo amides **18k** and **18l**.

Table 5.1: Synthesis of diazo amide substrates **17k–18l** from available amines.

Entry	Amine	Aniline (Yield)	Diazo- butanamide (Yield) ^b	Diazo- acetamide (Yield) ^c
1	Me-NH ₂ HCl	15k^d	17k	18k
	14k	(85%)	(88%)	(64%)
2	 -NH ₂	15l	17l	18l
	14l	(81%)	(83%)	(48%)

a: CuI (10 mol%), L-proline (20 mol%), K₂CO₃ (3 equiv.), DMSO, 90 °C, 20 h; b: i) Dioxinone **4**, microwave irradiation, 100 W, 50 psi, PhMe, 110 °C, 45 min, ii) *p*-ABSA, Et₃N, MeCN, rt, 1 h; c: NaOMe, MeOH, 0 °C, 3 h; d: amount of K₂CO₃ increased to five equivalents.

Prior to being used in intermolecular microreaction arrays, the four diazo amides (**17k**, **17l**, **18k** and **18l**) were tested in a dose-dependent manner against the androgen receptor using the TR-FRET assay from at an initial concentration of 500 μM (1% DMSO, in buffer) (Figure 5.2). As it can be observed, all four diazo amide substrates were not active at concentrations lower than 50 μM, indicating that they could be used in the subsequent intermolecular microreaction arrays.

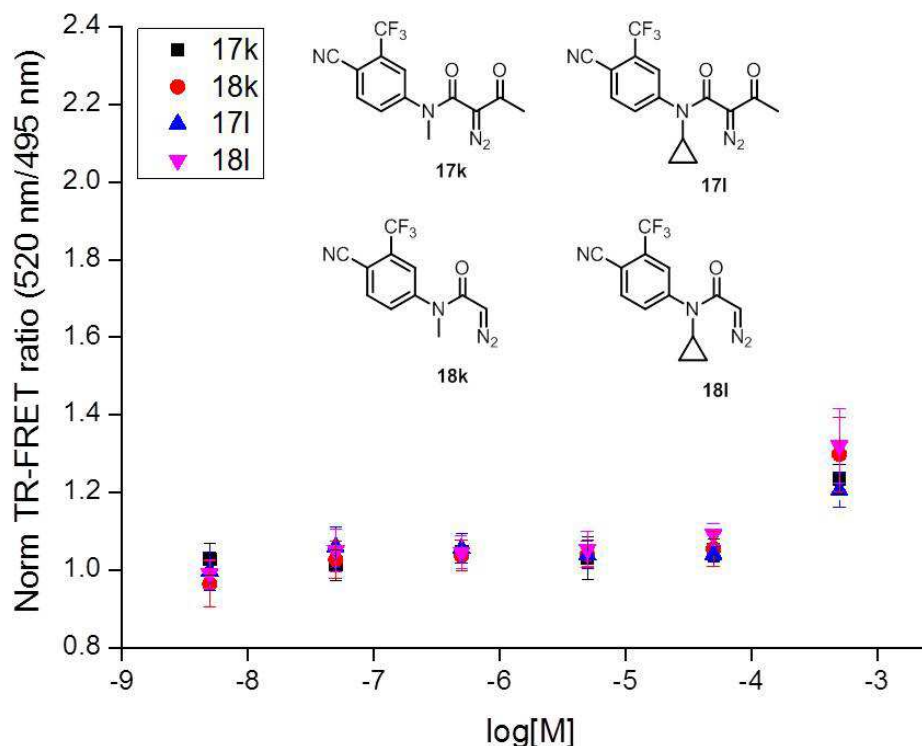


Figure 5.2: Normalised TR-FRET ratio (520 nm/495 nm) of the four diazo amide substrates **17k-18l** assayed in a dose-dependent manner from an initial concentration of 500 μM (1 % DMSO, in buffer). The diazo substrates were found to be inactive at concentrations lower than 50 μM .

5.2. Selection of co-substrates for the intermolecular reactions

Alongside the four initial diazo substrates, an initial set of 26 potential co-substrates was selected on the basis of generally being able to undergo more than one carbenoid transformations with the same diazo-substrate (Figure 5.3). To demonstrate that any unreacted co-substrate would not interfere with the assay, mock microreactions with these potential co-substrates were performed. Stock solutions of the co-substrates (8 μL of 12.5 M solution in CH_2Cl_2) were added to the wells of the custom made 96-well PTFE plates with the appropriate solvent (92 μL , either CH_2Cl_2 or toluene) to give a final concentration of 1.0 M of each co-substrate. The microreactions were mixed by pipetting sealed and left for 48 h. After scavenging for 24 h, the solutions were left to evaporate and the crude dissolved in dimethyl sulfoxide to give a final solution of 1.0 M of co-

substrate. These stock solutions were subsequently further diluted in DMSO and buffer and screened at a concentration of 1 mM (1% DMSO in buffer see experimental for details). The TR-FRET ratio (520 nm/495 nm) was then normalised to a percentage using the positive control (Testosterone, TE 5 μ M) as 100% and the negative control (1% DMSO in buffer, no ligand) as 0%. The results are shown in Table 5.2.

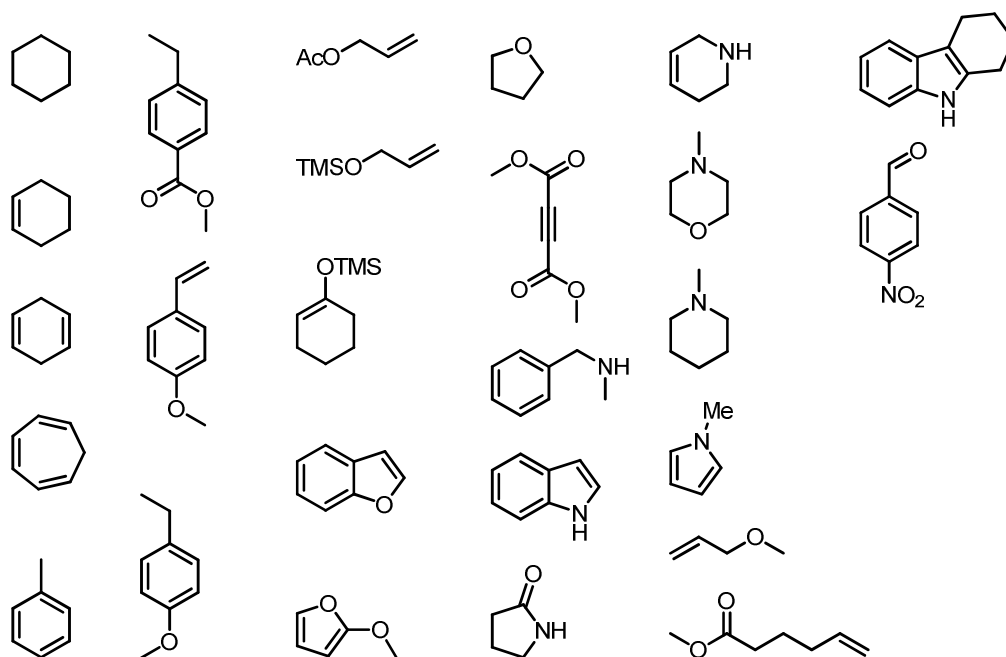

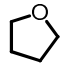

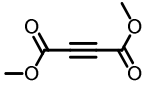

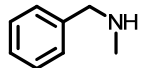
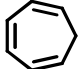
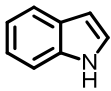
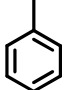
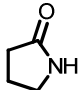
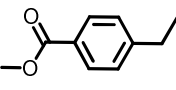
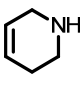
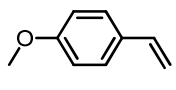
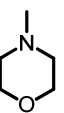
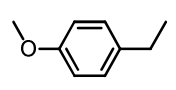
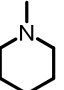
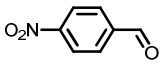
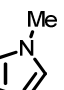
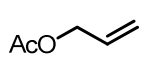
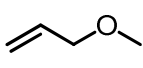
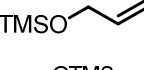
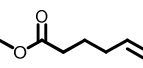
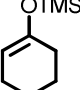
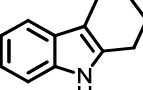
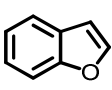
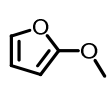


Figure 5.3: Structures of 26 commercially available potential co-substrates for intermolecular reactions. The potential co-substrates were selected on the basis of being able to undergo multiple chemical transformations with metal-carbenoid species.

Table 5.2: Percentage of activity at 1 mM of potential co-substrates.

Entry	Structure	% of activity at 1 mM	Entry	Structure	% of activity at 1 mM
1		2%	14		2%
2		3%	15		23%
3		5%	16		7%
4		6%	17		1%
5		5%	18		5%
6		2%	19		6%
7		8%	20		8%
8		7%	21		18%
9		24%	22		0%
10		7%	23		9%
11		0%	24		1%
12		6%	25		42%
13		2%	26		12%

Percentage of activity (relative to 5 μ M TE) of product mixtures from mock microreactions at a total concentration of 1 mM (1% DMSO, in buffer). Typical error 1-7%.

Most of the potential co-substrates were found to have minimal activities (lower than 7%) against the androgen receptor at a concentration of 1 mM. However some, such as *p*-nitro benzaldehyde (Table 5.2, entry 9) or tetrahydrocarbazole (Table 5.2, entry 25), were found to display moderate

activities arising either from biological effects or, more likely, interference with the assay read-out. Hence it was decided that these potential co-substrates were not to be used in the intermolecular reaction arrays. Out of the total 26 potential co substrates, nine were selected to be used as intermolecular reaction co-substrates (Figure 5.4). Their selection was based on their low activities against the androgen receptor as well as their structural features that would possibly enable more than one chemical transformations with the same diazo-substrate. For example, indole (Table 5.2, entry 17) can potentially undergo C-H insertion reactions at position 3⁴⁹ or 7,⁵⁰ or an N-H insertion⁵¹ to yield more than one potentially active products within the same product mixture.

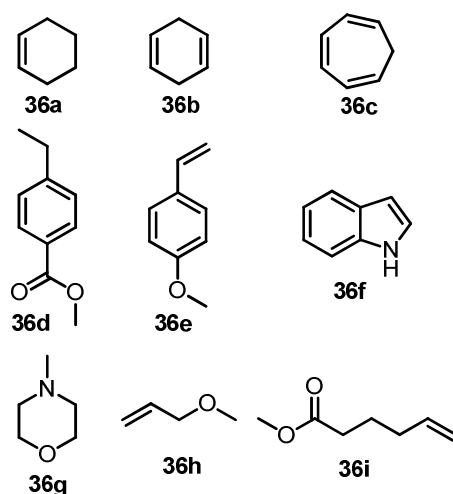


Figure 5.4: Structures of the nine selected co-substrates for the first intermolecular reaction array. Their selection was based on their low activity against the androgen receptor as well as that their structures may enable more than one carbenoid transformations.

5.3. Intermolecular reaction array 1

For the first reaction array, the four diazo amide substrates **17k-18l** and the nine co-substrates were used, in combinations with six Rh^(II) catalysts (Rh₂(S-DOSP)₄ Rh₂(TFA)₄ Rh₂(5*R*-MEPY)₄ Rh₂(Oct)₄ Rh₂(4*S*-MEOX)₄ Rh₂(cap)₄, Figure 5.5) in two solvents (CH₂Cl₂ and toluene). An additional combination of diazo substrates without co-substrate was also used as a control. It would also be possible that a pair of diazo substrate and co-substrate might have yielded the same product irrespective of the combination of solvent and catalyst used. Hence, in order to minimise redundancy, and because there was a total of 480 possible combinations, it was decided to perform a sparse array of reactions. Random combinations were investigated, covering ca. 40% of all possibilities (192 combinations) in an attempt to further the limits of small molecule discovery by activity-directed synthesis.

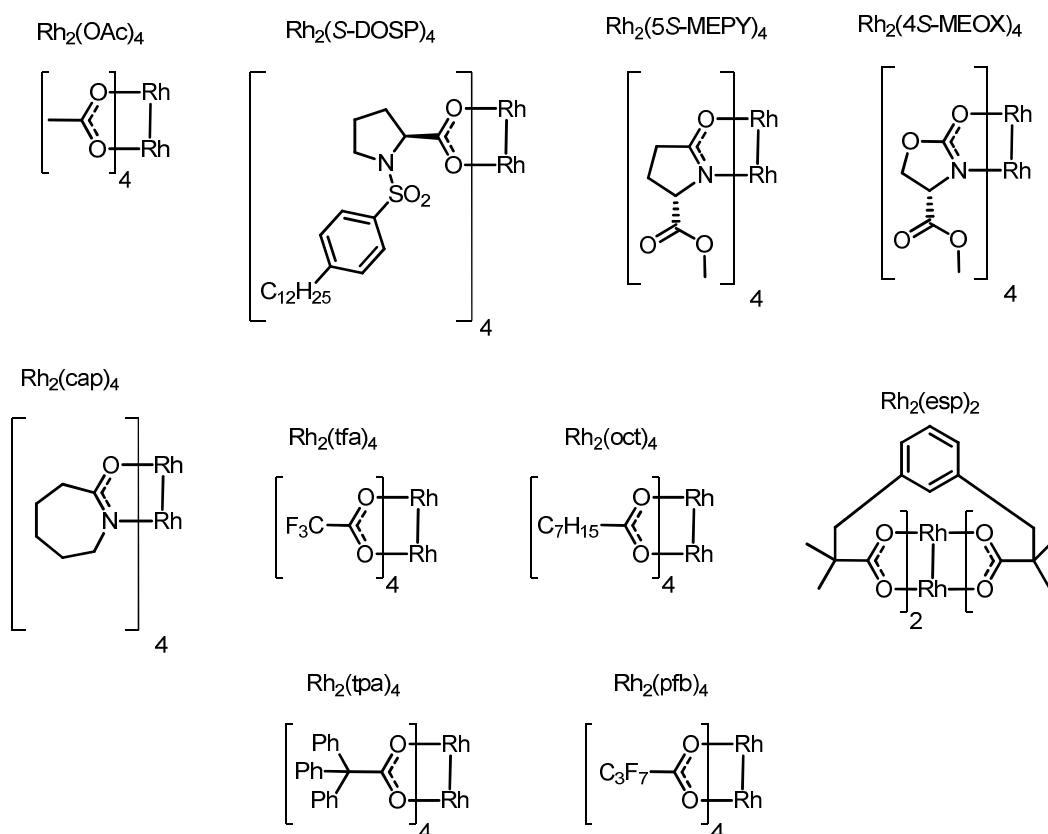


Figure 5.5: Structures of metal catalysts used in reaction arrays for activity-directed synthesis on androgen receptor agonists using intermolecular reactions.

Reactions were, as before, carried out in custom made 96-well PTFE plates. The appropriate catalyst (4 μL of 25 mM solution in THF) was added to each well containing a solution of the relevant diazo-substrate (8 μL of 1.25 M solution in CH_2Cl_2) and the appropriate co-substrate (8 μL of 12.5 M solution in CH_2Cl_2) in the appropriate solvent (80 μL) and subsequently sealed. This mixture resulted in a final solution with the diazo-amide substrate at a concentration of 0.1 M, the co-substrate at a concentration of 1.0 M and the metal catalyst at a concentration of 1 mM. The product mixtures were mixed by pipetting occasionally, resealed and left to react at room temperature for 48 hours. After scavenging for $\text{Rh}^{\text{(II)}}$ (see Chapter 3 for metal scavenging studies), the solvent was removed by evaporation at rt and then under reduced pressure and the product mixtures were rediluted in dimethyl sulfoxide to give a solution of total product concentration of 100 mM. The product mixtures were then diluted further in DMSO and assay buffer and screened initially at a total product concentration 10 μM (10 μM 1% DMSO in buffer, see experimental for full details). The TR-FRET ratio (520 nm/495 nm) was then normalised to a percentage using the positive control (Testosterone, TE 5 μM) as 100% and the negative control (1% DMSO in buffer, no ligand) as 0%. The results are shown in Figure 5.6.

It was observed that only specific combinations of catalyst, diazo-substrate, co-substrate and solvent yielded any promising product mixtures, since only two out of 192 product mixtures displayed any promising activity at the concentration screened. These mixtures were derived from diazo substrate **18k** with either cyclohexene **36a** or indole **36f** with $\text{Rh}_2(\text{S-DOSP})_4$ in CH_2Cl_2 (Figure 5.6). The results suggested that it was possible that the active product in each case was the result of an intermolecular reaction as the combinations of the diazo-substrate with no co-substrate present did not display any promising activity. These results formed the basis for the design of the second intermolecular reaction array.

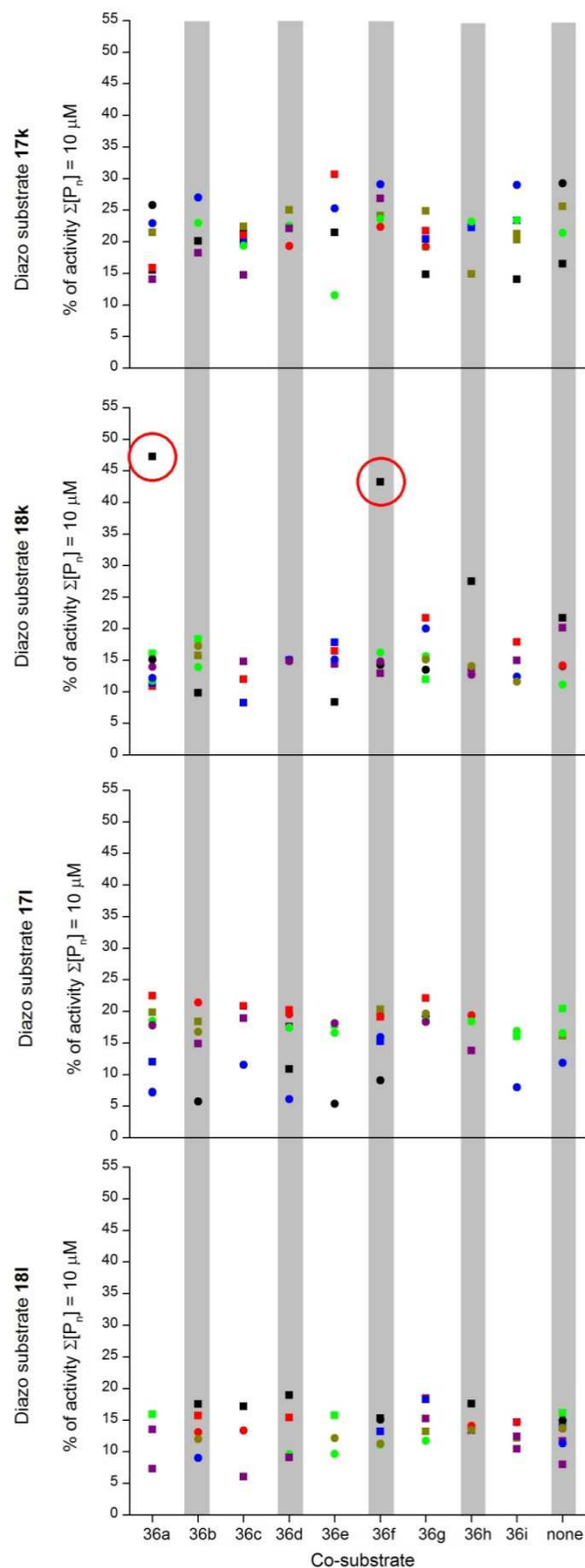


Figure 5.6: Percentage of activity (relative to 5 μM TE) of product mixtures from intermolecular reaction array 1 at a total concentration of 10 μM (1% DMSO, in buffer). Different colours represent different catalysts: black, $\text{Rh}_2(\text{S-DOSP})_4$; red, $\text{Rh}_2(\text{tfa})_4$. Different shapes represent different solvents: squares, CH_2Cl_2 ; circles Toluene. Red circles indicate combinations with promising activity. Error bars omitted for clarity. Typical error 3-7%.

5.4. Intermolecular reaction array 2

For the second reaction array, the two deacylated diazo substrates **18k** and **18l** were used. Promising activities in reaction array 1 were observed from product mixtures derived from diazo substrate **18k** only. Diazo substrate **18l** was used to investigate whether it would be possible to resurrect and activity from product mixtures derived from that substrate. The co-substrates used in this reaction array were inspired by cyclohexene and indole which were prioritised in the previous reaction array (Figure 5.7). Unsaturated and aromatic heterocycles with different ring sizes were used, again to enable more than possible reaction outcomes. Where possible, an acetyl or methyl group was incorporated on certain co-substrates such **36v** and **36w** or **36j** and **36u**. This derivatisation was incorporated to probe the effect such a group could have on the outcome of the product mixture, by either blocking a possible reaction, e.g. an N-H insertion, or enabling a different reaction, e.g. a C-H insertion.

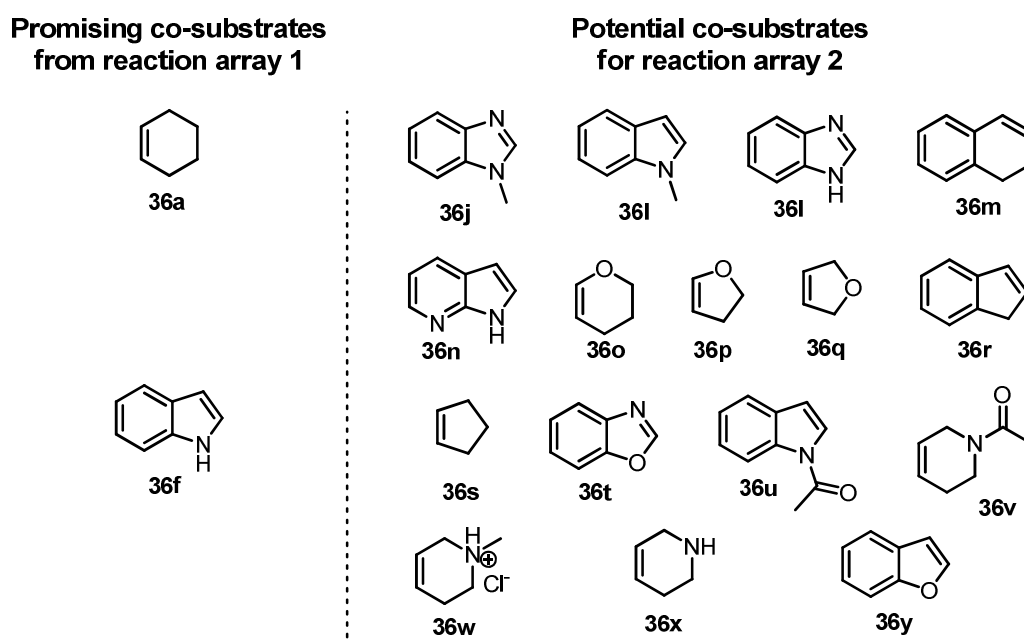
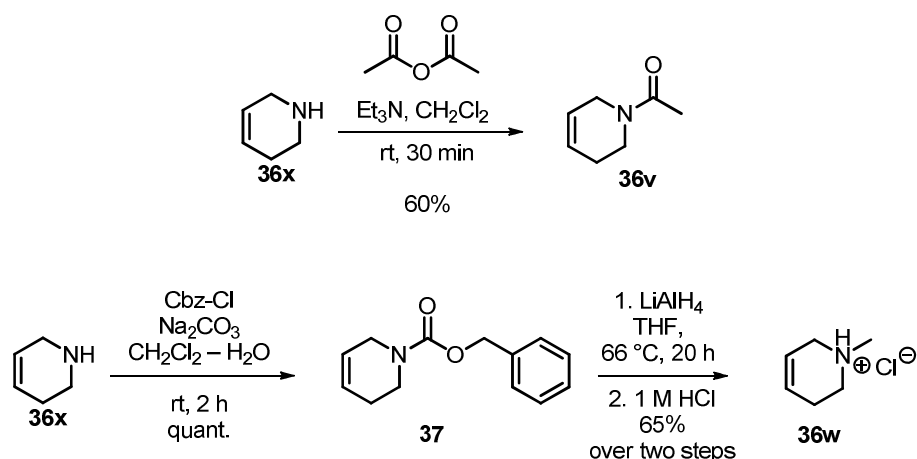


Figure 5.7: Structures of the 18 potential co-substrates selected for the second intermolecular reaction array. The structures were inspired by cyclohexene and indole.

Whilst most of these co-substrates were readily commercially available, some were prepared in one or two steps. The amide **36v** was prepared by treating **36x** with acetic anhydride in triethylamine and CH_2Cl_2 (Scheme 5.1). The methyl hydrochloride **36w** was prepared in two steps.

The amine **36x** was treated with benzyl chloroformate and Na₂CO₃ in aqueous CH₂Cl₂ which was subsequently reduced by treatment with LiAlH₄ in refluxing THF. Treatment of the crude mixture with a 1 M aqueous HCl solution afforded the hydrochloride salt of the methyl amine **36w** in 65% yield over two steps.

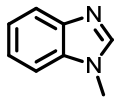
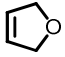
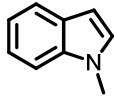
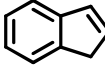
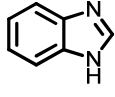
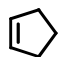
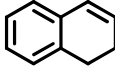
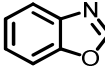
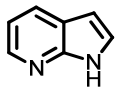
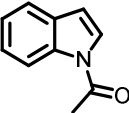
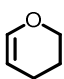
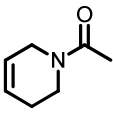
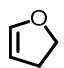
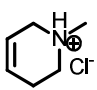


Scheme 5.1: Preparation of co-substrates **36v** and **36w** from the readily available amine **36x**.

Before they could be used, these potential co-substrates were tested as mock product mixtures similar to the potential co-substrates of the previous reaction array. Stock solutions of the co-substrates (8 μL of 12.5 M in CH₂Cl₂) were added in the wells of the custom made 96-well PTFE plates with the appropriate solvent (92 μL), either CH₂Cl₂ or toluene. This mixture resulted in a final concentration of 1.0 M of the co-substrate. The microreactions were mixed by pipetting sealed and left for 48 h. After scavenging for 24 h, the solutions were left to evaporate and the crude re-diluted in dimethyl sulfoxide to give a final solution of 1.0 M of co-substrate. These stock solutions were subsequently further diluted in DMSO and buffer and screened at a concentration of 1 mM (1% DMSO in buffer, see experimental for details). The TR-FRET ratio (520 nm/495 nm) was then normalised to a percentage using the positive control (Testosterone, TE 5 μM) as 100% and the negative control (1% DMSO in buffer, no ligand) as 0%. The results are shown in Table 5.3. As it can be seen from Table 5.3, it was possible to use all of the potential co-substrates for the second

intermolecular reaction array as they did not display any significant activity against the androgen receptor at a concentration of 1 mM.

Table 5.3: Percentage of activity at 1 mM of potential co-substrates for intermolecular reaction array 2.

Entry	Structure	% of activity at 1 mM	Entry	Structure	% of activity at 1 mM
1		2%	8		0%
2		1%	9		1%
3		1%	10		0%
4		0%	11		0%
5		1%	12		4%
6		0%	13		1%
7		1%	14		0%

Percentage of activity (relative to 5 μ M TE) of product mixtures from mock microreactions at a total concentration of 1 mM (1% DMSO, in buffer). Typical error 0.5-2%.

With the two diazo substrates and the 18 co-substrates at hand, the second reaction array was performed. Since the most promising activities from the previous reaction array arose from carboxylate type catalysts, it was decided to focus on five commonly used, Rh^(II) carboxylate catalysts (Rh₂(S-DOSP)₄, Rh₂(OAc)₄, Rh₂(pfb)₄, Rh₂(tpa)₄ and Rh₂(esp)₂). Again, instead of conducting exhaustive arrays, random combinations covering 86 of 380 possible reactions were investigated. The appropriate catalyst (4 μ L of 25 mM solution in THF) was added to each well containing a solution of the relevant diazo-substrate (8 μ L of 1.25 M solution in CH₂Cl₂) and the

appropriate co-substrate (8 μL of 12.5 M solution in CH_2Cl_2) in the appropriate solvent (80 μL CH_2Cl_2 or Toluene) and subsequently sealed. This mixture resulted in a final solution with the diazo-amide substrate at a concentration of 0.1 M, the co-substrate at a concentration of 1.0 M and the metal catalyst at a concentration of 1 mM. The product mixtures were mixed by pipetting occasionally, resealed and left to react at room temperature for 48 hours. After scavenging for $\text{Rh}^{\text{(II)}}$ (see Chapter 3 for metal scavenging studies), the solvent was removed by evaporation at rt and then under reduced pressure and the product mixtures were dissolved in dimethyl sulfoxide to give a solution of total product concentration of 100 mM. The product mixtures were then diluted further in DMSO and assay buffer and screened at total product concentrations of both 10 μM and 5 μM (10 μM and 5 μM 1% DMSO in buffer, see experimental for full details). The TR-FRET ratio (520 nm/495 nm) was then normalised to a percentage using the positive control (Testosterone, TE 5 μM) as 100% and the negative control (1% DMSO in buffer, no ligand) as 0%. The results are shown in Figure 5.8.

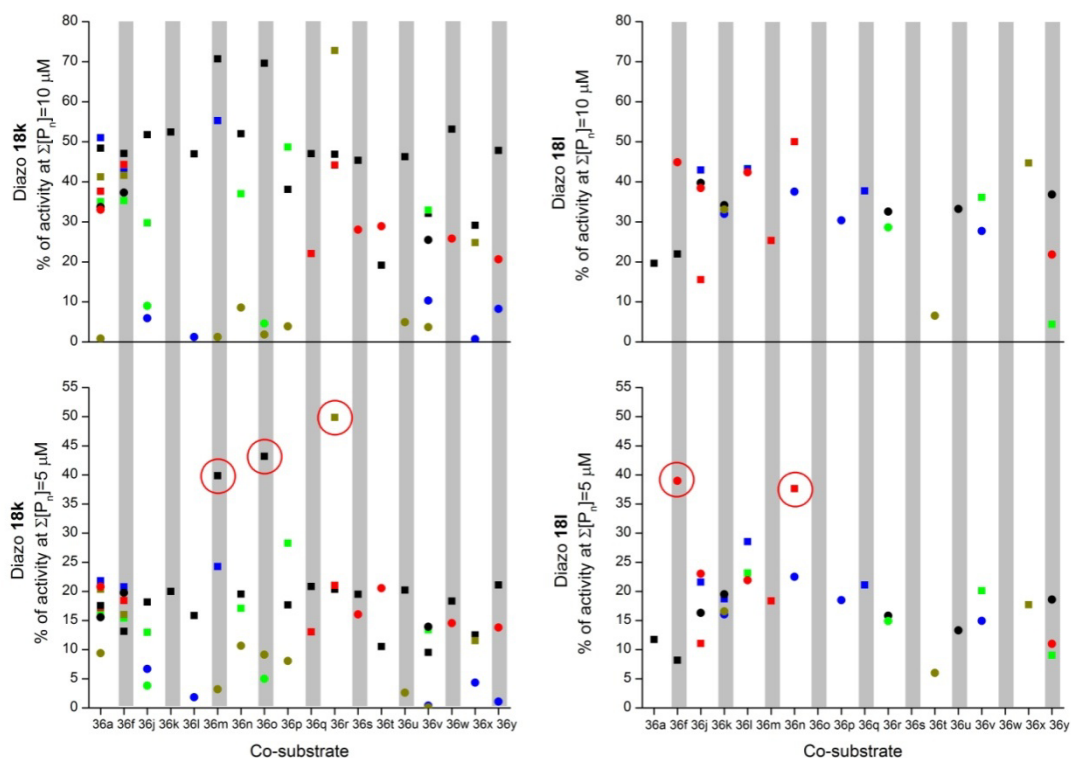


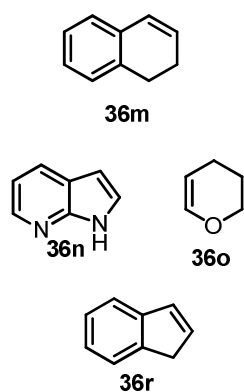
Figure 5.8: Percentage of activity (relative to 5 μM TE) of product mixtures from intermolecular reaction array 2 at a total concentration of 10 μM (above) and 5 μM (below) (1% DMSO, in buffer). Different colours represent different catalysts: black $\text{Rh}_2(\text{S-DOSP})_4$, red $\text{Rh}_2(\text{OAc})_4$; different shapes represent different solvents: squares CH_2Cl_2 , circles Toluene. Red circles indicate combinations with promising activity. Error bars omitted for clarity. Typical error 1-7%.

Similar, to the intramolecular reaction arrays (see Chapter 4), screening at a lower concentration revealed that promising activities arose only from a few product mixtures. This trend might suggest that reactions are steered towards active products only when the specific combination of reactants (diazo- and co-substrate) and conditions (catalyst and solvent) was used. Diazo substrate **18k** was observed to yield more promising product mixtures compared to diazo substrate **18l**. Product mixtures using diazo substrate **18k**, co-substrates **36m**, **36n**, **36o** and **36r** (Figure 5.9) with either $\text{Rh}_2(\text{S-DOSP})_4$ or $\text{Rh}_2(\text{esp})_2$ in CH_2Cl_2 displayed the most promising activities and were used to inform the design of the third reaction array.

5.5. Intermolecular reaction array 3

For the third reaction array, it was decided to focus on a single diazo substrate and solvent in order to investigate the scope of co-substrate and catalyst further. Promising product mixtures arose mostly from diazo substrate **18k** in CH₂Cl₂, and was thus also chosen for reaction array 3. Both enantiomers of the DOSP based catalyst were used in order to investigate the effect of catalyst configuration on the biological activity of the product mixtures. Rh₂(OAc)₄ and Rh₂(esp)₂ were also exploited as their use resulted in some promising activities in the previous reaction array. The co-substrates used in this reaction array were structurally inspired by co-substrates **36m**, **36n**, **36o** and **36r** which were prioritised from the previous reaction array (Figure 5.9). These co-substrates incorporated various substitution patterns on different positions of similar central scaffolds as co-substrates **36m**, **36n**, **36o** and **36r**.

Promising co-substrates
from reaction array 2



Potential co-substrates
for reaction array 3

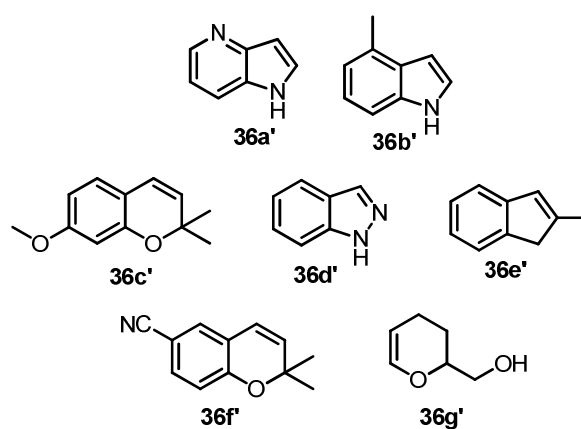
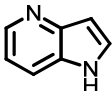
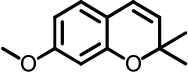
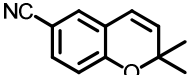
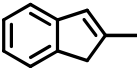
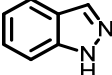
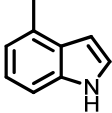
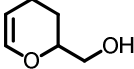


Figure 5.9: The structures of the potential co-substrates used in the third reaction array were inspired by co-substrates **36m**, **36n**, **36o** and **36r**. The potential co-substrates incorporated various substitution patterns on different positions of similar central scaffolds.

Before they could be used, these potential co-substrates were tested as mock product mixtures similar to the potential co-substrates of the previous reaction array. Stock solutions of the co-substrates (8 μL of 12.5 M in CH₂Cl₂) were added in the wells of the custom made 96-well PTFE plates with CH₂Cl₂ (92 μL). This mixture resulted in a final concentration of 1.0 M of

the co-substrate. The microreactions were mixed by pipetting sealed and left for 48 h. After scavenging for 24 h, the solutions were left to evaporate and then dissolved in dimethyl sulfoxide to give a final solution of 1.0 M of co-substrate. These stock solutions were subsequently further diluted in DMSO and buffer and screened at a concentration of 1 mM (1% DMSO in buffer, see experimental for details). The TR-FRET ratio (520 nm/495 nm) was then normalised to a percentage using the positive control (Testosterone, TE 5 μ M) as 100% and the negative control (1% DMSO in buffer, no ligand) as 0%. The results are shown in Table 5.4.

Table 5.4: Percentage of activity at 1 mM of potential co-substrates for intermolecular reaction array 3.

Entry	Structure	% of activity at 1 mM
1		36%
2		5%
3		12%
4		7%
5		5%
6		9%
7		3%

Percentage of activity (relative to 5 μ M TE) of product mixtures from mock microreactions at a total concentration of 1 mM (1% DMSO, in buffer). Typical error 0.5-3%.

As it can be observed from Table 5.4, six of the potential co-substrates could be used in the third intermolecular reaction array as they did not display any significant activity against the androgen receptor at a

concentration of 1 mM. 4-Azaindole, **36a'**, displayed a moderate activity using the TR-FRET assay and it was decided not to be used.

With the diazo substrate **18k** the co-substrates identified in the first two reaction arrays (**36a**, **36f**, **36m**, **36n**, **36o** and **36r**) as well as the six additional co-substrates at hand, the third reaction array was performed. For this reaction array, all the possible combinations were performed resulting in 48 microreactions (one diazo-substrate, 12 co-substrates, four catalysts, all in CH₂Cl₂). The appropriate catalyst (4 μL of 25 mM solution in THF) was added to each well containing a solution of the relevant diazo-substrate (8 μL of 1.25 M solution in CH₂Cl₂) and the appropriate co-substrate (8 μL of 12.5 M solution in CH₂Cl₂) in the appropriate solvent (80 μL) and subsequently sealed. This mixture resulted in a final solution with the diazo-amide substrate at a concentration of 0.1 M, the co-substrate at a concentration of 1.0 M and the metal catalyst at a concentration of 1 mM. The product mixtures were mixed by pipetting occasionally, resealed and left to react at room temperature for 48 hours. After scavenging for Rh^(III) (see Chapter 3 for metal scavenging studies), the solvent was removed by evaporation at rt and then under reduced pressure and the product mixtures were dissolved in dimethyl sulfoxide to give a solution of total product concentration of 100 mM. The product mixtures were then diluted further in DMSO and assay buffer and screened at total product concentrations of both 5 μM and 1 μM (5 μM and 1 μM 1% DMSO in buffer, see experimental for full details). The TR-FRET ratio (520 nm/495 nm) was then normalised to a percentage using the positive control (Testosterone, TE 5 μM) as 100% and the negative control (1% DMSO in buffer, no ligand) as 0%. The results are shown in Figure 5.10.

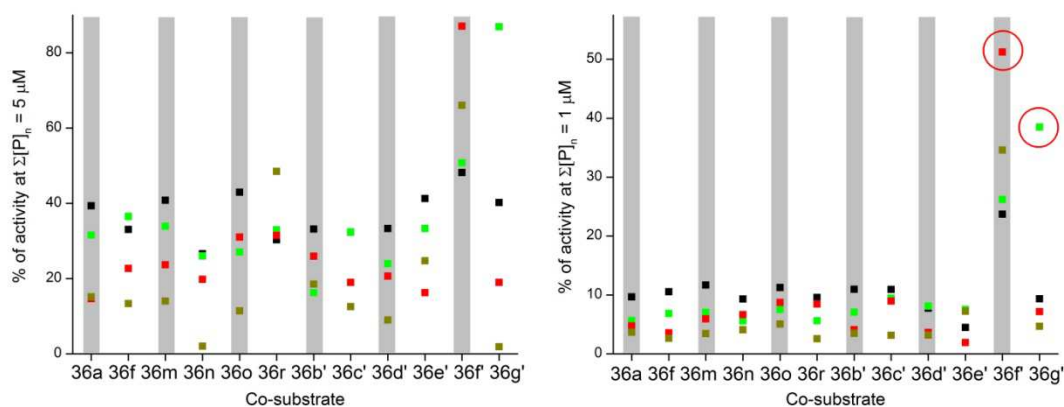


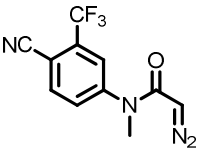
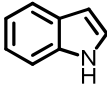
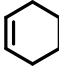
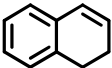
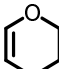
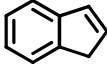
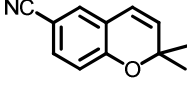
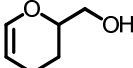
Figure 5.10: Percentage of activity (relative to 5 μM TE) of product mixtures from intermolecular reaction array 3 at a total concentration of 5 μM (above) and 1 μM (below) (1% DMSO, in buffer). Different colours represent different catalysts: black, $\text{Rh}_2(\text{S-DOSP})_4$; red, $\text{Rh}_2(\text{OAc})_4$. Red circles indicate combinations with promising activity. Error bars omitted for clarity. Typical error 1-6%.

As it can be observed in Figure 5.10, only specific reaction conditions yield product mixtures which displayed promising activities. Furthermore, in some cases, product mixtures from the *R*-DOSP ligand were observed to be more active than those from the *S*-DOSP, suggesting that the reaction is enantioselective and the product is chiral. At this point the most promising combinations of diazo substrate, co-substrate, catalyst and solvent were selected for scale up. Their selection was based on maintaining their activity even at the lowest level of dilution, total concentration of 1 μM when screened using the TR-FRET AR assay.

5.6. Scale-up

A total of seven reactions were selected for scale up; two reactions from reaction array 1, three reactions from reaction array 2 and two reactions from reaction array 3. The conditions for these reactions are summarised in Table 5.5.

Table 5.5: The seven promising reactions selected for scale-up. The details of the combinations regarding the diazo substrate, co-substrate catalyst and solvent are shown below.

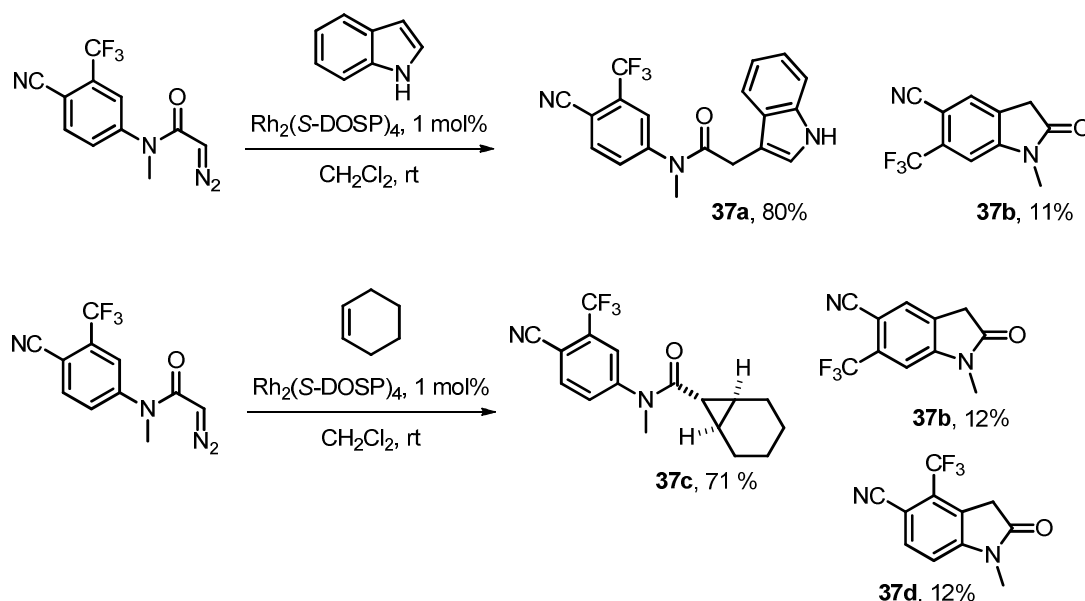
Entry	Reaction Array	Diazo substrate	Co-substrate	Catalyst	Solvent
1	1	 18k	 36f	Rh ₂ (S-DOSP) ₄	CH ₂ Cl ₂
2	1	18k	 36a	Rh ₂ (S-DOSP) ₄	CH ₂ Cl ₂
3	2	18k	 36m	Rh ₂ (S-DOSP) ₄	CH ₂ Cl ₂
4	2	18k	 36o	Rh ₂ (S-DOSP) ₄	CH ₂ Cl ₂
5	2	18k	 36r	Rh ₂ (esp) ₂	CH ₂ Cl ₂
6	3	18k	 36f'	Rh ₂ (OAc) ₄	CH ₂ Cl ₂
7	3	18k	 36g'	Rh ₂ (R-DOSP) ₄	CH ₂ Cl ₂

The selected reactions were performed in a similar manner as the microreactions on a 50-fold larger scale. The appropriate diazo substrates (400 μ L of a 1.25 M solution in CH₂Cl₂) co-substrate (400 μ L of a 12.5 M solution in CH₂Cl₂) and the metal catalyst (200 μ L of a 25 mM in THF) were mixed in the appropriate solvent (4.0 mL). The final concentration for the diazo substrate was 0.1 M, co-substrate 1.0 M and for the catalyst 1 mM, in 5 mL of solvent. The reactions were sealed and left to react for 48 h,

followed by TLC and LC-MS. After scavenging the reactions were filtered, concentrated *in vacuo* and the crude mixture purified by column chromatography.

5.6.1. Reactions identified in reaction array 1

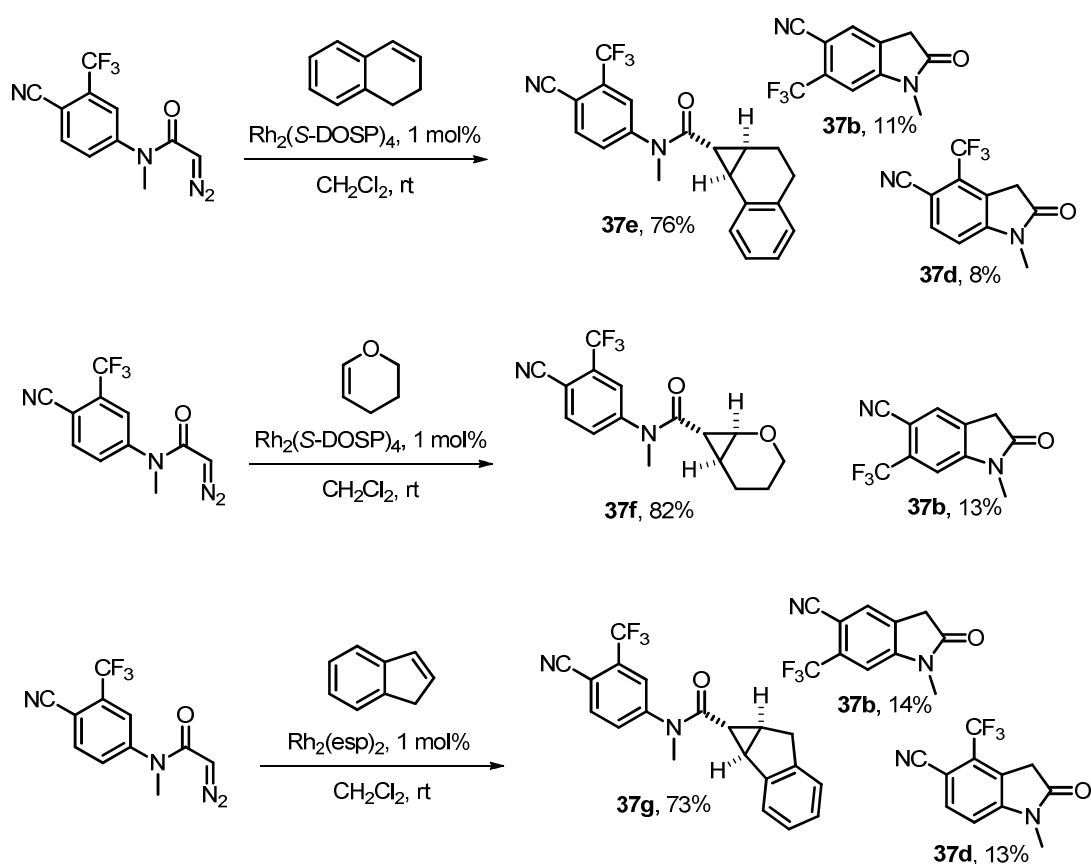
For the scale-up of the two reactions highlighted from reaction array 1, the diazo substrate **18k** was treated with 1 mol% $\text{Rh}_2(\text{S-DOSP})_4$, in CH_2Cl_2 in the presence of either the co-substrate **36f** or **36a**. The outcome of the reactions can be seen in Scheme 5.2. The major product isolated when using co-substrate **36f** was the product **37a**, of a C-H insertion at the 3' position of the indole ring. In the case of co-substrate **36a**, the major product **37c**, was formed by a cyclopropanation across the cyclohexene double bond. The *trans* configuration around the cyclopropyl ring was determined by careful analysis of the coupling constants of the protons around the cyclopropyl ring. The intramolecular products **37b** and **37d**, formed by the C-H insertion on either position 2- or 6- of the *N*-aryl ring were, also observed.



Scheme 5.2: Isolated products from the scale-up of reactions highlighted in reaction array 1. The major products isolated were formed by with a C-H insertion on the 3- position of the indole ring, **37a**, or a cyclopropanation across the cyclohexene double bond **37c**.

5.6.2. Reactions identified in reaction array 2

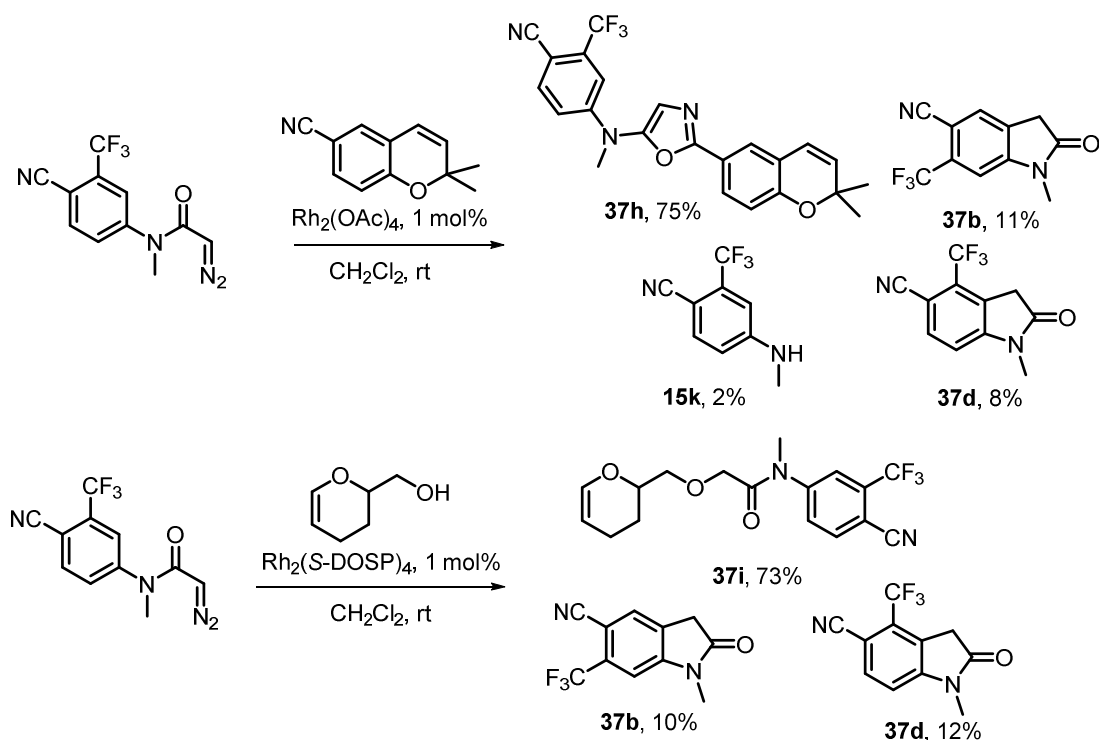
Three reactions from reaction array 2 were prioritised for scale-up. The diazo substrate **18k** was treated with 1 mol% $\text{Rh}_2(\text{S-DOSP})_4$ or $\text{Rh}_2(\text{esp})_2$ in CH_2Cl_2 in the presence of three distinct co-substrates: dihydronaphthalene **36m**, dihydropyran **36o**, or indene **36r**. The outcome of the reactions can be seen in Scheme 5.3. In all cases the major product was determined to be the result of a cyclopropanation reaction across the double bond of the co-substrate, yielding products **37e**, **37f** and **37g**. The *trans* configuration of the cyclopropyl rings was determined by careful analysis of the coupling constants of the protons around the cyclopropyl ring in each product. The formation of the intramolecular products **37b** and **37d** was also observed.



Scheme 5.3: Isolated products from the scale-up of reactions highlighted in reaction array 2. The major products isolated, **37e**, **37f** and **37g** were formed by a cyclopropanation reactions double bond of co-substrate used.

5.6.3. Reactions identified in reaction array 3

For the scale-up of the two reactions highlighted in the third reaction array, the diazo substrate **18k** was treated with 1 mol% $\text{Rh}_2(\text{S-DOSP})_4$ or $\text{Rh}_2(\text{OAc})_4$ in CH_2Cl_2 in the presence of co-substrate **36f'** or **36g'**. The outcome of the reactions can be seen in Scheme 5.4. In the presence of co-substrate **36f'**, diazo substrate **18k** afforded the oxazole **37h**, formed by a condensation between the carbenoid acetamide group of the diazo substrate and the nitrile group of the co-substrate.⁵² Key for the elucidation of the product's structure was the singlet at 6.95 ppm in its NMR spectrum, attributed to C4 proton of the oxazole ring. In the case of co-substrate **36g'**, the major product was formed by an O-H insertion of the hydroxyl group affording the acetamide **37i**. The presence of the dihydropyran ring double bond protons as well as the appearance of two diastereotopic acetamide protons (4.27 ppm and 4.23 ppm) confirmed the structure of the product. The formation of the intramolecular products **37b** and **37d** was also observed, in addition to the aniline **15k**, which was possibly formed by partial hydrolysis of the diazo substrate **18k**.



Scheme 5.4: Isolated products from the scale-up of reactions highlighted in reaction array 3. The oxazole **37h** was formed by a condensation and acetamide **37i** by an O-H insertion.

5.7. Biological and structural assessment of isolated compounds

5.7.1. Biological evaluation of isolated compounds

The intermolecular products as well as the minor intramolecular side-products isolated from the scaled-up reactions were assayed in a dose-dependent manner. Stock solutions of the compounds were prepared in DMSO and these were subsequently diluted accordingly with DMSO and assay buffer in a 12-step, 3-fold serial dilution manner (Figure 5.11 and experimental for details).

From the dose-response curves obtained, the EC_{50} value for each of the compounds was extracted by applying a non-linear fitting (logistic fit, OriginPro v. 8.6); the acetamide **37a** $8.8 (\pm 0.73) \mu\text{M}$, the cyclopropane **37c** $7.3 (\pm 0.29) \mu\text{M}$, the cyclopropane **37e** $4.9 (\pm 0.08) \mu\text{M}$, the cyclopropane **37f** $4.7 (\pm 0.07) \mu\text{M}$, the cyclopropane **37g** $3.7 (\pm 0.18) \mu\text{M}$, the oxazole **37h** $730 (\pm 28) \text{ nM}$, the acetamide **37i** $1.1 (\pm 0.07) \mu\text{M}$. EC_{50} values for the

intramolecular minor products, **37b** and **37d**, were not determined as a full dose-response curve was not obtained. However these values are predicted to be greater than 150 μM for oxindole **37b** and greater than 500 μM for oxindole **37d** (Figure 5.11).

All major products isolated from the reactions identified through the intermolecular reaction arrays, proved to be active modulators of the Androgen Receptor. These findings provide additional confirmation that Activity-Directed Synthesis is a methodology that is able to focus on active molecules.

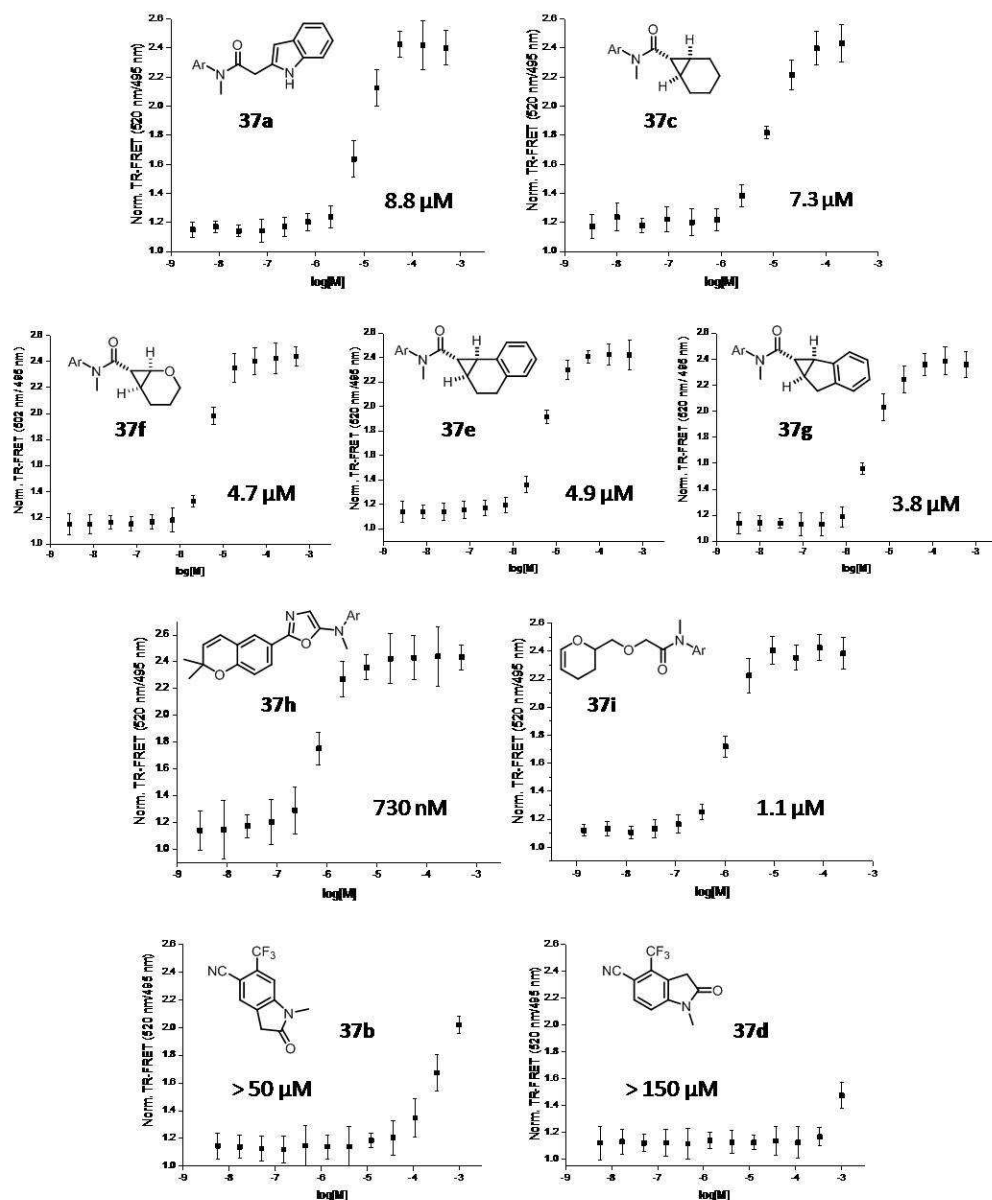


Figure 5.11: Dose-response curves obtained by assaying the isolated compounds: intermolecular products **37a**, **37c**, **37e**, **37f**, **37g**, **37h** and **37i** and intramolecular products **37b** and **37d**. Ar = 4-Cyano-3-(trifluoro)methyl-phenyl.

5.7.2. Structural evaluation of active modulators

The major products isolated from the scaled-up reactions could be classed in four distinct chemotypes stemming from different transformations: C-H insertion (**37a**); cyclopropanation (**37c**, **37e**, **37f** and **37g**); condensation (**37h**) and O-H insertion (**37i**). Oxazoles such as **37h**, have been used as biological isosteres of amide groups in drug discovery⁵³ and drug design before.⁵⁴ It is interesting that such a chemotype arose from the intermolecular activity-directed synthesis of androgen receptor modulators, as it is possible that such compounds could mimic existing chemotypes such as flutamide or bicalutamide analogues (Figure 5.12).

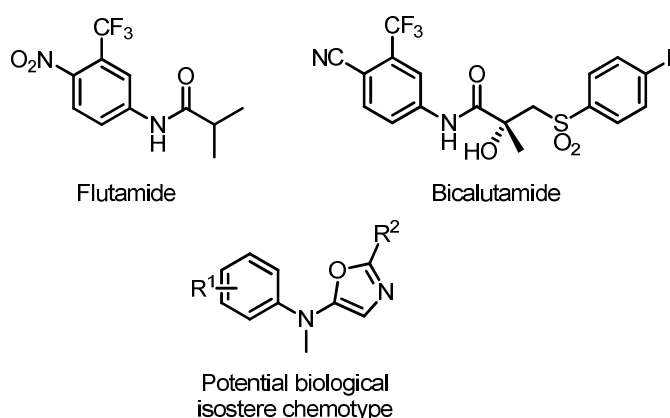


Figure 5.12: As oxazoles have been known to act as biological isosteres of amide groups, the condensation product **37h**, likely mimics existing chemotypes such as flutamide and bicalutamide.

Whilst cyclopropyl rings are often incorporated in lead or hit compounds, usually substituting a methyl group,⁵⁵ cyclopropanation reactions are rarely used in drug discovery or medicinal chemistry programmes. In this regard, the cyclopropanation products **37c**, **37e**, **37f** and **37g**, would be highly unlikely to be discovered by conventional small molecule discovery approaches. This case is emphasised by the fact that the corresponding cyclopropyl acids (Figure 5.13) in order to prepare these compounds *via* amide couplings are not commercially available. Finally, whilst compounds **37a** and **37i**, could be prepared using a less sophisticated chemical toolbox, it would be highly unlikely that they would be designed as potentially active androgen receptor modulators.

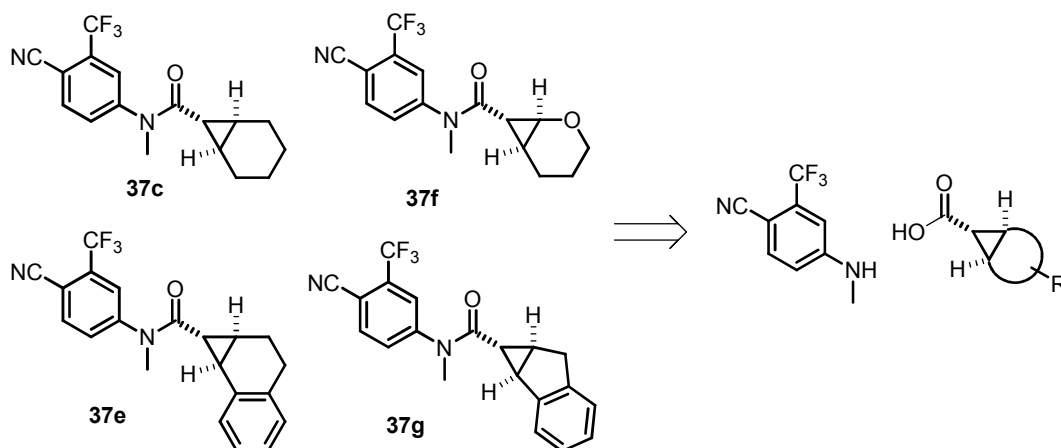


Figure 5.13: Although the cyclopropanation products **37c**, **37e**, **37f** and **37g**, could be readily prepared via simple amide couplings, the corresponding acids are not commercially available.

5.8. Summary

Three intermolecular reaction arrays have been performed and the product mixtures from each array screened at progressively lower concentrations. The biological results from one reaction array were used to select readily available co-substrates, the diazo-substrates and reaction conditions which would inform the design of the subsequent reaction array. Contrary to the intramolecular arrays, sparse combinations of reaction conditions were performed in the first two intermolecular reaction arrays. Sparse combinations minimised the possibility of redundant reactions whilst increasing the efficiency of the approach. A total of 326 reactions was performed, seven of which were prioritised for scale-up. Purifying and characterising the isolated products from each reaction, revealed that the major products formed, could be classed in four distinct chemotypes stemming from different transformations. Biological evaluation of these products revealed that these molecules are active modulators of the Androgen Receptor.

It is interesting to consider how the methodology might have developed through the intermolecular reaction arrays. Two chemotypes were identified in round 1; the acetamide, **37a** from a C-H insertion, and the cyclopropanation product **37c**. The cyclopropanation chemotype gave rise to structurally-related products **37e**, **37f** and **37g**, all formed by an intermolecular cyclopropanation, in round 2. The structural information from

co-substrates dihydronaphthalene **36m**, dihydropyran **36o** and indene **36r** inspired the use of co-substrate **36f'** and **36g'** amongst others. The use of **36f'** and **36g'** led to the formation of products **37h** and **37i**, which proved to have chemotypes not found in the previous rounds. This result suggests that in addition to optimising an identified molecular scaffold, occasionally making leaps through chemical space is another possible mechanism for the evolution of activity-directed synthesis (Figure 5.14).

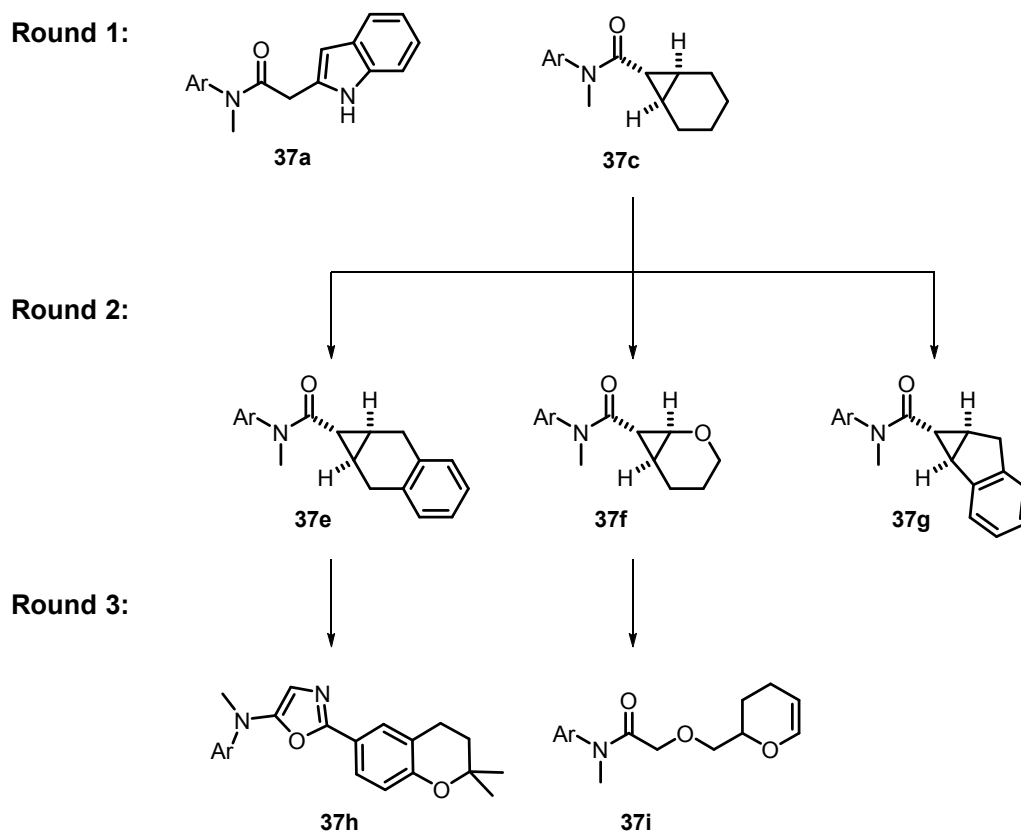


Figure 5.14: Development of Activity-Directed Synthesis through the intermolecular reaction arrays. Leaps through chemical space provide an additional mechanism for the evolution of activity-directed synthesis. Ar = 4-Cyano-3-(trifluoro)methyl-phenyl.

6. Chapter 6 Conclusions and Future Work

6.1. Conclusions

6.1.1. Activity-Directed Synthesis exploiting intramolecular reactions

The Activity-Directed Synthesis of sub-micromolar Androgen Receptor modulators with chemotypes with no previously annotated activity has been successfully developed and demonstrated. By exploiting promiscuous metal-carbenoid reactions with multiple possible outcomes, generating mixtures of products allowed the rapid and facile identification of small biologically active molecules, in a more efficient manner compared to conventional approaches. A key aspect of Activity-Directed Synthesis was the utilisation of evolutionary feedback, through the analysis of the information from the screening of one reaction array to design a subsequent reaction array. The development of the approach was retrospectively analysed and rationalised in the case of intramolecular reactions, demonstrating that Activity-Directed Synthesis is able to focus on active molecules rather than treating molecules in large collections with the same significance. The approach was demonstrated to facilitate the optimisation of both the structure of the active component as well as a route for its synthesis simultaneously.

6.1.2. Activity-Directed Synthesis exploiting intermolecular reactions

A limiting factor when exploiting intramolecular reactions was the necessity to synthetically incorporate the various reactive groups on the same substrate, increasing the synthetic effort required for their preparation and diminishing the number of possible combinations used. These issues were addressed by exploiting intermolecular reactions, as demonstrated by the greater diversity of structures and chemotypes of the major products isolated from the scale-up of selected intermolecular reactions. It was also shown that exhaustive combinations of reaction arrays were not needed, as

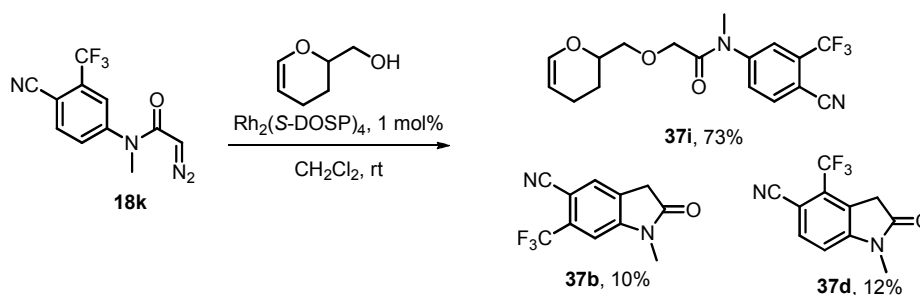
sparse combinations were enough to provide sufficient information for the design of a subsequent reaction array. In addition, it was demonstrated that structural leaps through chemical space provide an additional mechanism for the evolution Activity-Directed Synthesis.

6.2. Future work

6.2.1. Retrospective exploration of the intermolecular reaction arrays

In order to fully rationalise and understand the development of Activity-Directed Synthesis using intermolecular reactions a retrospective exploration, similar to the case of intramolecular reactions, is needed. Initially, reactions which were not prioritised from each reaction array should be scaled-up and the products isolated, characterised and evaluated biologically, in order to investigate whether products of different structural scaffolds were formed.

In the case of diazo-substrate **18k**, with co-substrate **36g'** (Scheme 6.1), two significantly different activities were observed with the use of the two enantiomers of the $\text{Rh}_2(\text{DOSP})_4$ catalyst. These results suggested that the reaction was enantioselective and the product was chiral. As the major product formed, **37i** is indeed chiral, it is possible that the catalyst is kinetically resolving the two enantiomers of the racemic co-substrate used, resulting in an enantiomerically enriched bioactive product. Performing the same reaction using the *S* enantiomer instead of the *R*, and isolating, characterising and evaluating the isolated products will aid to the verification of this hypothesis. The enantioselectivity can be determined by determining the enantiomeric excess using chiral HPLC analysis. This analysis will also help verify the above hypothesis, as well as add to the overall understanding of the methodology.



Scheme 6.1: Scaled reaction of diazo-substrate **18k** with co-substrate **36g'** with $\text{Rh}_2(\text{R-DOSP})_4$ in CH_2Cl_2 .

6.2.2. Crystallographic Studies

There is currently no evidence for the structural basis of the novel Androgen Receptor modulators discovered through this project. Although it is hypothesised that these molecules bind in the same cavity of the AR LBD as other flutamide or bicalutamide analogues,⁵⁶ it would not be surprising if the binding conformation or orientation is different. It would also be possible that these molecules act through covalent binding, as these has been previously reported for other β -lactam based molecules.⁵⁷ A crystallographic study to obtain an X-Ray crystal structure with the isolated molecules co-crystallised with the AR LBD would provide additional information and elucidate the binding site and orientation, as well as provide evidence of potentially new interactions which could be used to further optimise the activity of these molecules.

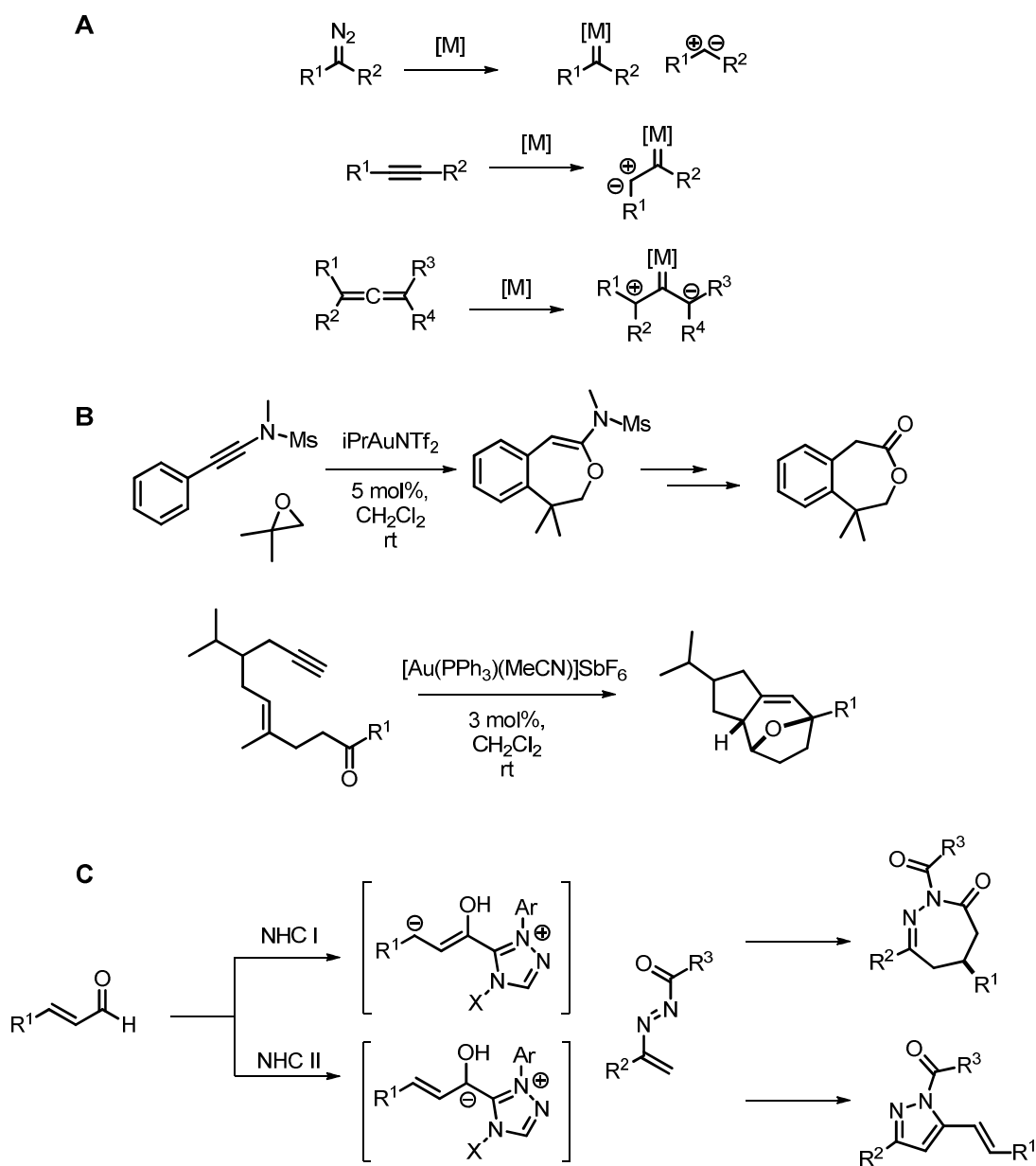
6.2.3. Further Future Work

The general applicability of Activity-Directed Synthesis as an efficient approach for the discovery of novel small bioactive molecules could be effectively demonstrated by applying this methodology on different biological targets exploiting different chemical toolbox.

The TR-FRET assay has proven to be an effective, high throughput and reliable screening method once it was established. Similar assays are commercially available for different biological targets such as PDK1 or VEGFR-2 or other kinases.⁵⁸ As they as very well studied and understood, with limited novel inhibitors reported, kinases provide an attractive target to demonstrate the applicability of Activity-Directed Synthesis.

When choosing a different chemical toolbox the same considerations should be taken into account. The chemistry needs to be equally versatile and tunable, with a demonstrated record of applicability. In this regards, both Au catalysis and *N*-heterocyclic carbene (NHC) catalysis are very attractive. Au-catalysed chemistry can be considered complementary to carbenoid chemistry as shown in Scheme 6.2A. Both intra- and intermolecular applications of this chemistry have been reported, leading to the formation of diverse molecular scaffolds with the reaction outcome critically depended on conditions used (Scheme 6.2B).⁵⁹ Similarly, NHC-catalysed cascades have been reported, where the use of either NHC-I or NHC-II type catalysed may result in different products with the use of the same starting materials (Scheme 6.2C).⁶⁰

Finally, however, in order to demonstrate the versatility, efficiency and greater potential of Activity-Directed Synthesis, it would be ideal to turn to unbiased libraries. Such an application would allow the same library of starting materials and its respective chemical toolbox to be exploited against different biological targets and ultimately turn Activity-Directed synthesis into a general methodology. This application would be far more efficient, as any synthetic preparations would need to be undertaken to a minimal extend whilst the starting materials could be used for more than one assays. Furthermore, it would be possible to extract multivariant information which would in turn facilitate SAR deduction and add to the subsequent optimisation of small molecules discovered by such an application of Activity-Directed Synthesis.



Scheme 6.2: Representative examples of the potentially attractive chemical transformations to be exploited for Activity-Directed Synthesis. **A:** Au-catalysed chemistry can be considered complementary to metal-carbenoid chemistry considering the reactive species. **B:** Representative examples of Au-catalysed transformations to prepare molecules with diverse scaffolds through either intra- or intermolecular reactions. **C:** Representative example of NHC-catalysed transformation where different molecular scaffolds are obtained by treating the same starting materials with different types of NHC catalysts.

7. Chapter 7 Experimental Section

7.1. Instrumentation and General Information

All non-aqueous reactions were carried out under an atmosphere of nitrogen. Water-sensitive reactions were performed in oven- or flame-dried glassware cooled under nitrogen before use. Solvents were removed under reduced pressure using a Büchi rotary evaporator and a Vacuubrand PC2001 Vario diaphragm pump.

Ether refers to diethyl ether and petrol refers to petroleum spirit (b.p. 40-60 °C) unless otherwise stated. All other solvents and reagents were of analytical grade and used as supplied. Commercially available starting materials were obtained from Sigma–Aldrich and Alfa Aesar.

Flash column chromatography was carried out using silica (35-70 µm particles). Thin layer chromatography was carried out on commercially available pre-coated glass or aluminium plates (Merck silica 2 8 8 0 Kieselgel 60F254).

Analytical LC-MS was performed using an Agilent 1200 series LC system comprising of a Bruker HCT Ultra ion trap mass spec, a high vacuum degasser, a binary pump, a high performance autosampler and micro well plate autosampler, an autosampler thermostat, a thermostated column compartment and diode array detector. The system used Phenomenex Luna C18 50 x 2mm 5 micron column and two solvent systems: MeCN/H₂O + 0.1% Formic acid or MeCN/H₂O.

Proton (¹H) and carbon-13 (¹³C) NMR spectra were recorded on a Bruker Avance DPX 300, Avance 500 or DRX500 spectrophotometer using an internal deuterium lock. ¹³C NMR spectra were recorded with composite pulse decoupling using the waltz 16 pulse sequence. DEPT, COSY, HMQC and HMBC pulse sequences were routinely used to aid the assignment of spectra. Chemical shifts are quoted in parts per million downfield of tetramethylsilane, and coupling constants (*J*) are given in Hz. NMR spectra were recorded at 300 K unless otherwise stated.

Melting points were determined on a Reichert hot stage microscope and are uncorrected.

Infrared spectra were recorded on a Perkin Elmer spectrum One FT-IR spectrophotometer.

Nominal mass spectrometry was routinely performed on a Bruker HCT Ultra spectrometer using electrospray (+) ionization. Nominal and accurate mass spectrometry using electrospray ionisation on a Bruker MicroTOF or a Bruker MaXis Impact spectrometer.

EC₅₀ values were obtained by performing logistic fits to the appropriate dose-response curves using the OriginPro v.8.6 software.

7.2. Experimental Procedures

7.2.1. Experimental procedures for organic compounds

General procedure A: Amination of 4-iodo-2(trifluoro)methyl benzonitrile with primary amines.

The amine (3 equiv.) was added to a stirred solution of 4-iodo-2-(trifluoro)methyl benzonitrile (1 equiv.), CuI (10 mol%), L-proline (20 mol%) and K₂CO₃ (3 equiv.) in DMSO (0.5 M) and the reaction mixture was heated to 80 °C. After 20 h the reaction mixture was allowed to cool to rt. Water (10 mL) was added and the resulting mixture was extracted with EtOAc (4 × 10 mL). The combined organic layers were washed with brine (sat. aq. sol., 20 mL), dried (Na₂SO₄), filtered and concentrated *in vacuo* to give a crude product.

General procedure B: Acylation of secondary anilines with 2,2,6-trimethyl-4*H*-1,3-dioxin-4-one *via* microwave irradiation and diazotisation of the crude reaction mixture.

2,2,6-Trimethyl-4*H*-1,3-dioxin-4-one (1.5 equiv.) was added to a solution of the appropriate secondary aniline (1 equiv.) in toluene (1 mL). The reaction mixture was irradiated under microwave conditions (100 Watts, 50 psi) at 110 °C for 45 min. The reaction mixture was concentrated *in vacuo* to give a crude product. Et₃N (1.1 equiv.) was added to a stirred solution of the crude

product in MeCN (0.5 M) at rt. *p*-ABSA (1.1 equiv.) was added portionwise to the reaction mixture. After 2 h the reaction mixture filtered through a celite pad eluting with a 1:1 mixture of CH₂Cl₂–Et₂O and concentrated *in vacuo* to give a crude product.

General Procedure C: Deacylation of diazo-butanamides.

NaOMe (1.1 equiv) was added portionwise to a stirred solution of the appropriate diazo-butanamide (1 equiv.) in MeOH (0.5 M) at 0 °C, and the reaction mixture was stirred at 0 °C. After 2-4 h the reaction mixture was poured into ice-water (10 mL), saturated with solid NaCl and extracted with Et₂O (4 × 10 mL). The combined organic layers were dried (Na₂SO₄), filtered and concentrated *in vacuo* to give a crude product.

General Procedure D: Implementation of intramolecular reaction arrays

The reaction arrays were carried out in 96-well plates (8 × 12) custom made out of PTFE (well volume ~300 μL). Diazo-substrates were dissolved in CH₂Cl₂, to give a final solution of 1.25 M. Rh^(III) catalysts were dissolved in THF to give a 25 mM solution. 8 μL of the diazo-substrate solution were added to the appropriate well followed by 88 μL of the appropriate reaction solvent and 4 μL of the appropriate catalyst solution. The final volume of the reaction mixture was 100 μL; the final concentration of diazo-substrate was 100 mM and the final concentration of catalyst was 1 mM. The reaction wells were sealed using disposable sealing caps (Qiagen, Part No. 1051163) and left to react for 48 h at rt and mixed occasionally (*ca.* 2 h) by pipetting. The product mixtures were transferred to scavenging wells pre-loaded with QuadraPure TU resin (30 mg). Each reaction well was washed with the reaction solvent (3 × 50 μL) and the washes transferred to the corresponding scavenging well. The wells were sealed and left for 24 h. The scavenged product mixtures were transferred in Eppendorf tubes (500 μL). Each well was washed with the reaction solvent (3 × 100 μL) and the washes transferred to the corresponding Eppendorf tube. The product mixtures were left to evaporate at rt for 48 h. After evaporation the tube rack was placed in a desiccator and placed under vacuum for a further 24 h. The residue was re-dissolved in 100 μL of DMSO to give a product mixture solution of Σ[P_n] = 100 mM.

General Procedure E: Implementation of intermolecular reaction arrays

The reaction arrays were carried out in 96-well plates (8 × 12) custom made out of PTFE (well volume ~300 μL). Diazo-substrates were dissolved in CH_2Cl_2 , to give a final solution of 1.25 M. Co-substrates were dissolved in CH_2Cl_2 , to give a final solution of 12.5 M. $\text{Rh}^{\text{(II)}}$ catalysts were dissolved in THF to give a 25 mM solution. 8 μL of the diazo-substrate solution were added to the appropriate well followed by 80 μL of the appropriate reaction solvent, 8 μL of the appropriate co-substrate and finally, 4 μL of the appropriate catalyst solution. The final volume of the reaction mixture was 100 μL ; the final concentration of diazo-substrate was 100 mM, the final concentration of the co-substrate was 1 M and the final concentration of catalyst was 1 mM. The reaction wells were sealed using disposable sealing caps (Qiagen, Part No. 1051163) and left to react for 48 h at rt and mixed occasionally (ca. 2 h) by pipetting. The product mixtures were transferred to scavenging wells pre-loaded with QuadraPure TU resin (30 mg). Each reaction well was washed with the reaction solvent (3 × 50 μL) and the washes transferred to the corresponding scavenging well. The wells were sealed and left for 24 h. The scavenged reaction mixtures were transferred in Eppendorf tubes (500 μL). Each well was washed with the reaction solvent (3 × 100 μL) and the washes transferred to the corresponding Eppendorf tube. The product mixtures were left to evaporate at rt for 48 h. After evaporation the tube rack was placed in a desiccator and placed under vacuum for a further 24 h. The crude was dissolved in 100 μL of DMSO to give a product mixture solution of $\Sigma[\text{P}_n] = 100 \text{ mM}$.

General Procedure F: Reaction scale-up process for intramolecular reactions.

The scale-up process was identical to the reaction array method (General Procedure D), performed on a 50-fold larger scale. Diazo-substrates were dissolved in CH_2Cl_2 , to give a final solution of 1.25 M. $\text{Rh}^{\text{(II)}}$ catalysts were dissolved in THF to give a 25 mM solution. 400 μL of the diazo-substrate solution were added to a round-bottom flask followed by 4.4 mL of the appropriate reaction solvent and 200 μL of the appropriate catalyst solution and the reaction mixture was stirred at rt. The final volume of the reaction

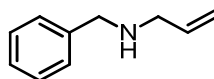
mixture was 5.0 mL; the final concentration of the diazo-substrate was 100 mM and the final concentration of catalyst was 1 mM. After 48 h QuadraPure TU resin (500 mg) was added and the mixture stirred at rt. After 24 h the mixture was filtered washing with the reaction solvent (3 × 10 mL) and concentrated *in vacuo* to give a crude product.

General Procedure G: Reaction Scale-up process for intermolecular reactions.

The scale-up process was identical to the reaction array method (General Procedure E), performed on a 50-fold larger scale. Diazo-substrates were dissolved in CH₂Cl₂, to give a final solution of 1.25 M. Co-substrates were dissolved in CH₂Cl₂, to give a final solution of 12.5 M. Rh^(II) catalysts were dissolved in THF to give a 25 mM solution. 400 μL of the diazo-substrate solution were added to a round-bottom flask followed by 4.0 mL of the appropriate reaction solvent, 400 μL of the co-substrate solution and finally, 200 μL of the appropriate catalyst solution and the reaction mixture was stirred at rt. The final volume of the reaction mixture was 5.0 mL; the final concentration of the diazo-substrate was 100 mM and the final concentration of catalyst was 1 mM. After 48 h QuadraPure TU resin (500 mg) was added and the mixture stirred at rt. After 24 h the mixture was filtered washing with the reaction solvent (3 × 10 mL) and concentrated *in vacuo* to give a crude product.

7.2.2. Compound Data

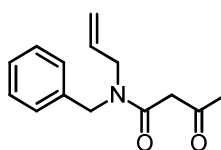
Benzyl(prop-2-en-1-yl)amine, 3



Benzaldehyde (2.0 mL, 20.0 mmol) was added to a stirred suspension of allylamine (1.0 mL, 13.3 mmol) with 4 Å molecular sieves (2.50 g) in MeOH (53.0 mL) at rt and the resulting mixture was heated at 35 °C for 24 h. The reaction mixture was cooled to rt and filtered through a pad of celite, eluting with MeOH (20 mL). The solution was concentrated to half volume *in vacuo*, cooled to 0 °C, NaBH₄ (1.01 g, 26.7 mmol) was added, the reaction mixture was allowed to warm to rt and stirred for 1.5 h. The reaction mixture was acidified to pH 2 by addition of aq. 2M HCl, concentrated to half volume *in*

vacuo and extracted with EtOAc (3 × 15 mL). The aqueous phase was basicified to pH 12 by addition of aq. sat. sol. K₂CO₃ and extracted with EtOAc (3 × 20 mL). The combined organic layers, after basification were dried (MgSO₄) and concentrated *in vacuo* to give the amine **3** (1.77 g, 89%) as a pale yellow oil which required no further purification. *R*_f: 0.79 (85:14:1 DCM—EtOH—NH₄OH); δ_H (500 MHz; CDCl₃) 7.34-7.31 (3H, m, Ar), 7.27-7.23 (2H, m, Ar), 5.93 (1H, ddt, *J* 17.2, 10.4 and 6.9, propenyl 2-H), 5.20 (1H, dd, *J* 17.2 and 6.9, propenyl 3-H_A), 5.11 (1H, dd, *J* 10.4 and 6.9, propenyl 3-H_B), 3.79 (2H, s, PhCH₂-), 3.28 (2H, d, *J* 6.9, propenyl 1-H₂), 1.50 (1H, s, b, N-H); δ_C (125 MHz; CDCl₃) 140.3 (Ar), 136.9 (propenyl C-2), 128.4 (Ar), 128.2 (Ar), 126.7 (Ar), 116.0 (propenyl C-3), 53.3 (PhCH₂-), 51.8 (propenyl C-1); $\nu_{\max}/\text{cm}^{-1}$ (film) 3311, 2816, 1949, 1872, 1811; *m/z* (EI) [M⁺] 146.1 (100%, M⁺); HRMS Found: 146.0961 (C₁₀H₁₃N requires *M* 146.0967).

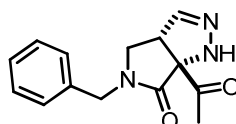
N-Benzyl-3'-oxo-N-(prop-2-en-1-yl)butanamide, 5



2,2,6-Trimethyl-4*H*-1,3-dioxin-4-one (1.08 mL, 8.2 mmol) was added to a stirred solution of the amine **3** (400 mg, 2.8 mmol) in toluene (9.00 mL) and the reaction mixture was heated at reflux for 1 h. The reaction mixture was allowed to cool to rt and concentrated *in vacuo* to give a crude product. Purification by flash chromatography, eluting with CH₂Cl₂—Et₂O (90:10), gave the *amide* **5** (508 mg, 84%) (3:2 keto:enol tautomers, 1:1 rotamers) as a bright yellow oil. *R*_f: 0.42 (9:1, CH₂Cl₂—Et₂O); δ_H (500 MHz; CDCl₃) 7.39-7.34 (20H, m, Ph), 7.34-7.22 (20H, m, Ph), 7.22-7.14 (10H, m, Ph), 5.83-5.69 (10H, m, propenyl 2-H₁ rot A and B), 5.26-5.10 (24H, m, propenyl 3-H₂ rot A and B and butanamide 2-H₁^{enol} rot A and B), 4.62 (6H, s, PhCH₂-^{keto} rot A), 4.62 (4H, s, PhCH₂-^{enol} rot A), 4.48 (6H, s, PhCH₂-^{keto} rot B) 4.47 (4H, s, PhCH₂-^{enol} rot B), 4.02 (5H, d, *J* 5.8, propenyl 1-H₂ rot A), 3.80 (5H, d, *J* 5.8, propenyl 1-H₂ rot B), 3.58 (6H, s, butanamide 2-H₂^{keto} rot A), 3.56 (6H, s, butanamide 2-H₂^{keto} rot B), 2.30 (9H, s, butanamide 4-H₃^{keto} rot A), 2.26 (9H, s, butanamide 4-H₃^{keto} rot B), 1.97 (6H, s, butanamide 4-H₃^{enol} rot A), 1.91 (6H, s, butanamide 4-H₃^{enol} rot B); δ_C (75 MHz; CDCl₃) 202.5 (butanamide C-

3^{keto} rot A), 202.4 (butanamide C- 3^{keto} rot B), 175.6 (butanamide C- 3^{enol} rot A), 175.4 (butanamide C- 3^{enol} rot B), 172.4 (butanamide C- 1^{enol} rot A), 172.4 (butanamide C- 1^{enol} rot B), 167.2 (butanamide C- 1^{keto} rot A), 167.0 (butanamide C- 1^{keto} rot B), 136.9 (Ph rot A), 136.1 (Ph rot B), 132.4 (propenyl C-2 rot A), 132.3 (propenyl C-2 rot B). 129.0 (Ph rot A), 128.7 (Ph rot B), 128.1 (Ph rot A), 127.8 (Ph rot B), 127.5 (Ph rot A), 126.3 (Ph rot B), 117.6 (1-C (enol-)), 117.9 (propenyl C- 3^{keto} rot A), 117.4 (propenyl C- 3^{enol} rot A), 117.2 (propenyl C- 3^{keto} rot B), 117.1 (propenyl C- 3^{enol} rot B), 87.0 (butanamide C- 2^{enol}), 50.8 (PhCH₂- $^{\text{keto}}$ rot B), 50.0 (butanamide C- 2^{keto} rot B), 49.9 (butanamide C- 2^{keto} rot A), 49.7 (propenyl C- 3^{keto} rot B), 49.0 (PhCH₂- $^{\text{enol}}$ rot B), 48.4 (PhCH₂- $^{\text{keto}}$ rot A), 48.1 (propenyl C- 3^{keto} rot A), 47.9 (PhCH₂- $^{\text{enol}}$ rot A), 47.5 (propenyl C- 3^{enol} rot A), 30.4 (butanamide C- 4^{keto} rot A), 30.3 (butanamide C- 4^{keto} rot B), 22.0 (30.4 (butanamide C- 4^{enol} rot A and B); $\nu_{\text{max}}/\text{cm}^{-1}$ (film) 3498, 3086, 2556, 1859, 1724, 1631; m/z (ES) [MNa⁺] 254.11 (100%, MNa⁺); HRMS Found: 254.1155, (C₁₄H₁₇NNaO₂ requires MNa 254.1151).

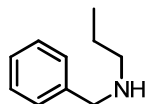
6 α -Acetyl-5-benzyl-1H,3 α H,4H,5H,6H,6 α H-pyrrolo[3,4-c]pyrazol-6-one, 7



Triethylamine (0.23 mL, 1.65 mmol) was added to a stirred solution of the amide 5 (346.0 mg, 1.5 mmol) in MeCN (2.00 mL) at 0°C. *p*-Acetamidobenzenesulfonyl azide (396.0 mg, 1.65 mmol) was added portion wise, the reaction mixture was allowed to warm to rt and stirred for a further 22 h. The reaction mixture was concentrated *in vacuo* to give a crude product. Purification by flash chromatography, eluting with Petrol—EtOAc (30:70), gave the *pyrazolone* 7 (289.5 mg, 75%) as a colourless amorphous solid, m.p. 89-92 °C (from Petrol); R_f : 0.32 (30:70, Petrol—EtOAc); δ_H (500 MHz; CDCl₃) 7.36-7.28 (3H, m, Ar), 7.15 (2H, d, J 7.6, Ar), 6.70 (1H, s, N-H), 6.64 (1H, s, 3-H), 4.51 (1H, d, J 14.8, PhCH_AH_B), 4.38 (1H, d, J 14.8, PhCH_AH_B), 3.81 (1H, d, J 7.5, 3 α -H), 3.60 (1H, dd, J 7.5 and 2.5, 4-H_A), 3.24 (1H, d, J 2.5, 4-H_B), 2.44 (3H, s, Acetyl-CH₃); δ_C (125 MHz; CDCl₃) 203.5 (Acetyl CO), 170.3 (6-C), 144.3 (3-C), 135.0 (Ar), 129.1 (Ar), 128.0 (Ar), 127.4 (Ar), 80.8 (6 α -C), 48.2 (4-C), 47.4 (3 α -C), 46.8 (PhCH₂-), 27.4 (Acetyl-

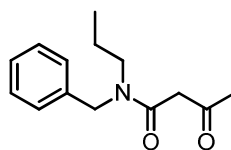
CH₃); $\nu_{\max}/\text{cm}^{-1}$ (film) 3285, 2943, 2131, 1989, 1971, 1665, 1602; m/z (ES) [MNa⁺] 280.1 (100%, MNa⁺); HRMS Found: 280.1056 (C₁₄H₁₅N₃NaO₂ requires MNa 280.1056).

Benzyl(propyl)amine, **9**



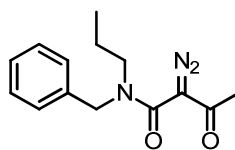
Benzaldehyde (1.22 mL, 12 mmol) was added to a stirred solution of propylamine (0.66 mL, 8 mmol) and 4 Å molecular sieves (2.50 g) in MeOH (32 mL) and the resulting mixture was stirred at rt. After 19 h the reaction mixture was filtered through a pad of celite, eluting with MeOH (50 mL). The solution was concentrated to half volume *in vacuo*, cooled to 0 °C, NaBH₄ (605 mg, 16 mmol) was added and the reaction mixture was allowed to warm to rt and stirred. After 2 h the reaction mixture was acidified to pH 2 by addition of aq. 2M HCl, concentrated to half volume *in vacuo* and extracted with EtOAc (4 × 10 mL). The aqueous layer was basified to pH 12 by addition of sat. aq. sol. K₂CO₃ and extracted with EtOAc (7 × 20 mL). The combined organic layers, after basification were dried (Na₂SO₄), filtered and concentrated *in vacuo* to give the amine **9**⁶¹ (1.0 g, 84%) as a colourless oil which required no further purification. R_f : 0.39 (9:1, CH₂Cl₂—MeOH); δ_H (500 MHz; CDCl₃) 7.32 (4H, m, Ph), 7.26-7.22 (1H, m, Ph), 3.79 (2H, s, PhCH₂), 2.60 (2H, t, J 7.3, propyl 1-H₂), 1.58-1.49 (3H, m, propyl 2-H₂ and NH), 0.92 (3H, t, J 7.7, propyl 3-H₃); δ_C (125 MHz; CDCl₃) 140.7 (Ph), 128.4 (Ph), 128.1 (Ph), 126.7 (Ph), 54.0 (PhCH₂), 51.4 (propyl C-1), 23.2 (propyl C-2), 11.8 (propyl C-3); $\nu_{\max}/\text{cm}^{-1}$ (film) 3310, 2958, 1604, 1494, 1454; m/z (EI) 149.1 (M⁺, 85%), 120.1 (77%), 91 (100%); (Found: 149.1208, C₁₀H₁₅N requires M 149.1204).

***N*-Benzyl-3-oxo-*N*-propylbutanamide, 10**



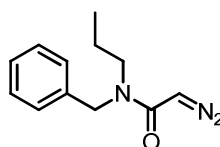
2,2,6-Trimethyl-4*H*-1,3-dioxin-4-one (1.08 mL, 8.2 mmol) was added to a stirred solution of the amine **9** (298 mg, 2.0 mmol) in toluene (7 mL) and the reaction mixture was heated at reflux for 2 h. The reaction mixture was allowed to cool to rt and concentrated *in vacuo* to give a crude product. Purification by flash chromatography, eluting with CH₂Cl₂—Et₂O (95:5), gave the *amide* **10** (400 mg, 86%) (3:1 keto:enol tautomers, 1:1 rotamers) as a yellow viscous oil. *R*_f: 0.28 (9:1, CH₂Cl₂—Et₂O); δ_H (500 MHz; CDCl₃) 7.39-7.29 (16H, m, Ph), 7.29-7.21 (16H, m, Ph), 7.17 (8H, d, *J* 6.4, Ph), 5.14 (1H, s, butanamide 2-H₁^{enol} rot A), 5.07 (2H, s, butanamide 2-H₁^{enol} rot B), 4.62 (8H, s, PhCH₂ rot A), 4.52 (8H, s, PhCH₂ rot B), 3.60 (6H, s, butanamide 2-H₂^{keto} rot A), 3.50 (6H, s, butanamide 2-H₂^{keto} rot B), 3.36 (4H, t, *J* 7.7 propyl 1-H₂ rot A), 3.13 (4H, t, *J* 7.7 propyl 1-H₂ rot B), 2.31 (9H, s, butanamide 4-H₃^{keto} rot A), 2.25 (9H, s, butanamide 4-H₃^{keto} rot B), 1.98 (3H, s, butanamide 4-H₃^{enol} rot A), 1.90 (3H, s, butanamide 4-H₃^{enol} rot B), 1.62-1.50 (16H, m, propyl 2-H₂ rot A and B), 0.94-0.83 (24H, m, propyl 3-H₃ rot A and B); δ_C (125 MHz; CDCl₃) 202.5 (butanamide C-3^{keto}), 175.2 (butanamide C-3^{enol}), 171.9 (butanamide C-1^{enol}), 167.1 (butanamide C-1^{keto} rot A) 166.8 (butanamide C-1^{keto} rot B), 137.1 (Ph rot A), 136.6 (Ph rot B), 129.0 (Ph rot A), 128.6 (Ph rot B), 127.9 (Ph rot A), 127.8 (Ph rot B), 127.4 (Ph rot A), 127.2 (Ph rot B), 126.3 (Ph rot A), 126.2 (Ph rot B), 87.2 (butanamide C-2^{enol} rot A), 86.9 (butanamide C-2^{enol} rot B), 51.6 (PhCH₂ rot B), 50.2 (butanamide C-2^{keto} rot B), 49.9 (butanamide C-2^{keto} rot A), 49.2 (propyl C-1 rot B), 48.3 (propyl C-1 rot A), 48.0 (PhCH₂ rot A), 30.3 (butanamide C-4^{keto} rot A and B), 22.2 (butanamide C-4^{enol} rot A), 21.6 (propyl C-2 rot A), 21.1 (butanamide C-4^{enol} rot B), 20.7 (propyl C-2 rot B), 11.3 (propyl C-3 rot A), 11.3 (propyl C-3 rot B); $\nu_{\max}/\text{cm}^{-1}$ (film) 3030, 2965, 1722, 1639, 1591; *m/z* (ES) [MNa⁺] 256.11 (100%, MNa⁺); HRMS Found: 256.1341 (C₁₄H₁₉NNaO₂ requires *MNa* 256.1347).

***N*-Benzyl-2-diazo-3-oxo-*N*-propylbutanamide, 11**



Et₃N (131 μ L) was added to a stirred solution of the butanamide **10** (200 mg) in MeCN (0.8 M) at 0 °C. *p*-ABSA (1.1 equiv.) was added portionwise to the reaction mixture at 0 °C and the resulting mixture was allowed to warm to rt. After 20 h the reaction mixture was concentrated *in vacuo* to give a crude product. Purification by flash chromatography eluting with CH₂Cl₂—Et₂O (95:5), gave the *diazo-butanamide* **11** (185 mg, 83%) as a bright yellow viscous oil. *R*_f: 0.32 (95:5, CH₂Cl₂—Et₂O); δ_H (500 MHz; CDCl₃) 7.38-7.33 (2H, m, Ph), 7.31-7.27 (1H, m, Ph), 7.25 (2H, d, *J* 6.8, Ph), 4.59 (2H, s, PhCH₂), 3.25 (2H, t, *J* 7.6, propyl 1-H₂), 2.35 (3H, s, butanamide 4-H₃), 1.61 (2H, ap. hex, *J* 7.5, propyl 2-H₂), 0.88 (3H, t, *J* 7.4, propyl 3-H₃); δ_C (125 MHz; CDCl₃) 190.1 (butanamide C-3), 161.5 (butanamide C-1), 136.3 (Ph), 128.9 (Ph), 127.7 (Ph), 127.3 (Ph), 73.7 (butanamide C-2), 50.6 (PhCH₂), 49.2 (propyl C-1), 27.3 (butanamide C-4), 20.9 (propyl C-2), 11.2 (propyl C-3); $\nu_{\max}/\text{cm}^{-1}$ (film) 3585, 3518, 2965, 2358, 1634, 1418; *m/z* (ES) [MNa⁺] 282.1212 (100%, MNa⁺); HRMS Found: 282.1212 (C₁₄H₁₇N₃NaO₂ requires MNa 282.1213).

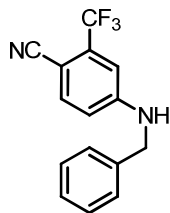
***N*-Benzyl-2-diazo-3-oxo-*N*-propylacetamide, 12**



By general procedure C, butanamide **11**, gave the *diazo-acetamide* **12** (129 mg, 89%) as a bright yellow liquid which required no further purification. *R*_f: 0.63 (95:5, CH₂Cl₂—MeOH); δ_H (500 MHz; CDCl₃) 7.34-7.28 (2H, m, Ph), 7.27-7.23 (1H, m, Ph), 7.21 (2H, d, *J* 7.7, Ph), 4.94 (1H, s, diazo-acetamide 2-H₁), 4.48 (2H, s, b, PhCH₂), 3.16 (2H, s, b, propyl 1-H₂), 1.55 (2H, ap. hex, *J* 7.5, propyl 2-H₂), 0.87 (3H, t, *J* 7.5, propyl 3-H₃); δ_C (125 MHz; CDCl₃) 166.2 (acetamide C-1), 137.4 (Ph), 128.7 (Ph), 127.4 (Ph), 50.3 (propyl C-1), 48.9 (PhCH₂), 46.7 (acetamide C-2), 21.3 (propyl C-2), 11.3 (propyl C-3); $\nu_{\max}/\text{cm}^{-1}$ (film) 3463, 3066, 2334, 2104, 1748, 1603; *m/z* (ES) [MNa⁺] 240.11

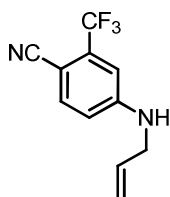
(100%, MNa^+); HRMS Found: 240.1113 ($\text{C}_{12}\text{H}_{15}\text{N}_3\text{NaO}$ requires MNa 240.1107).

4-(Benzylamino)-2-(trifluoromethyl)benzonitrile, **15a**



By general procedure A, benzylamine, followed by purification by flash chromatography eluting with Petrol—EtOAc (80:20), gave the *aniline* **15a** (240 mg, 87%) as pale yellow needles, m.p. 152-155 °C (Petrol); R_f : 0.72 (80:20, Petrol—EtOAc); δ_H (500 MHz; CDCl_3) 7.50 (1H, d, J 8.5, Ar 6-H), 7.37 (1H, m, Ph), 7.33 (2H, m, Ph), 7.30 (2H, m, Ph), 6.91 (1H, d, J 3.3, Ar 3-H), 6.69 (1H, dd, J 8.5 and 3.3, Ar 5-H), 5.02 (1H, s, br, NH), 4.40 (2H, s, PhCH_2); δ_C (125 MHz; CDCl_3) 150.9 (Ar C-4), 136.2 (Ar C-6), 135.9 (Ph), 134.0 (q, $^2J_{\text{FC}}$ 32, Ar C-2), 129.0 (Ph), 127.9 (Ph), 127.2 (Ph), 122.0 (q, $^1J_{\text{FC}}$ 274, CF_3); 117.7 (CN), 113.8 (Ar C-5), 110.2 (Ar C-3), 95.6 (Ar C-1), 47.3 (PhCH_2); $\nu_{\text{max}}/\text{cm}^{-1}$ (film) 3348, 2641, 2592, 2228, 1895, 1819; m/z (ES) [MNa^+] 299.1 (100%, MNa^+); HRMS Found: 299.0755 ($\text{C}_{15}\text{H}_{11}\text{F}_3\text{N}_2$ requires MNa 299.0767).

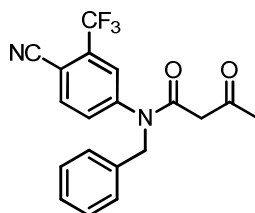
4-[(Prop-2-en-1-yl)amino]-2-(trifluoromethyl)benzonitrile, **15a'**



By general procedure A, allyl amine followed by purification by flash chromatography, eluting with Petrol—EtOAc (90:10), gave the *aniline* **15a'** (105 mg, 98%) as pale yellow needles, m.p. 128-134 °C (Petrol); R_f : 0.76 (80:20, Petrol—EtOAc); δ_H (500 MHz; CDCl_3) 7.54 (1H, d, J 8.5, Ar 6-H), 6.87 (1H, d, J 2.7, Ar 3-H), 6.70 (1H, dd, J 8.5 and 2.7, Ar 5-H), 5.89 (1H, ddt, J 17.3, 10.2 and 7.3, propenyl 2- H_1), 5.29 (1H, dd, J 17.3 and 2.7, propenyl 3- H_A), 5.24 (1H, dd, J 10.2 and 2.7, propenyl 3- H_B), 4.79 (1H, s, b, NH), 3.86 (2H, d, J 7.3, propenyl 1-H); δ_C (125 MHz; CDCl_3) 151.1 (Ar C-4),

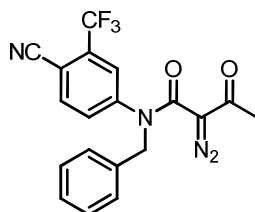
136.1 (Ar C-6), 134.2 (q, $^2J_{FC}$ 32, Ar C-2), 132.9 (propenyl C-2), 122.0 (q, $^1J_{FC}$ 276, CF_3), 117.5 (propenyl C-3), 117.2 (CN); 113.9 (Ar C-5), 110.1 (Ar C-3), 95.6 (Ar C-1), 45.7 (propenyl C-1); ν_{max}/cm^{-1} (film) 3370, 2923, 2871, 2253, 2223, 1895; m/z (ES) [MNa^+] 249.1 (100%, MNa^+); HRMS Found: 249.0608, ($C_{11}H_9F_3N_2Na$ requires MNa 249.061).

***N*-Benzyl-*N*-[4-cyano-3-(trifluoromethyl)phenyl]-3-oxobutanamide, 16**



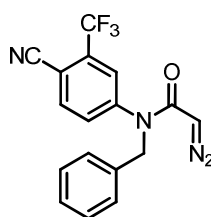
2,2,6-Trimethyl-4*H*-1,3-dioxin-4-one (103 μ L, 0.77 mmol) was added to a solution of the aniline 7 (142 mg, 0.51 mmol) in toluene (1 mL). The reaction mixture was irradiated under microwave conditions (100 Watts, 50 psi) at 110 $^{\circ}$ C for 30 mins. The crude product was concentrated *in vacuo*. Purification by flash chromatography, eluting with CH_2Cl_2 — Et_2O (98:2), gave the *amide* 16 (155 mg, 84%) (1:1 keto:enol tautomers) as a pale yellow viscous oil. R_f : 0.42 (95:5, CH_2Cl_2 — Et_2O); δ_H (500 MHz; $CDCl_3$) 7.81-7.78 (2H, m, Ar 5-H), 7.55-7.53 (2H, m, Ar 2-H), 7.39-7.47 (2H, m, Ar 6-H), 7.30-7.27 (6H, m, Ph), 7.19-7.17 (4H, m, Ph), 4.97 (2H, s, $PhCH_2^{keto}$), 4.96 (2H, s, $PhCH_2^{enol}$), 4.73 (1H, s, butanamide-2 H_1^{enol}), 3.40 (2H, s, br, butanamide 2- H_2^{keto}), 2.18 (3H, s, butanamide 4- H_3^{keto}), 1.88 (3H, s, butanamide 4- H_3^{enol}); δ_C (125 MHz; $CDCl_3$) 201.6 (butanamide C-3 keto), 177.3 (butanamide C-3 enol), 171.6 (butanamide C-1 enol), 165.9 (butanamide C-1 keto), 146.1 (Ar C-1), 136.2 (Ar C-5), 135.8 (Ph), 134.1 (q, $^2J_{FC}$ 32, Ar C-3), 131.7 (Ar C-6), 128.9 (Ph), 128.4 (Ph), 127.3 (Ph), 126.7 (Ar C-2), 121.8 (q, $^1J_{FC}$ 273, CF_3), 114.8 (CN), 108.5 (Ar C-4), 88.8 (butanamide C-2 enol), 52.2 ($PhCH_2$), 50.1 (butanamide C-2 keto), 30.6 (butanamide C-4 keto), 21.9 (butanamide C-4 enol); ν_{max}/cm^{-1} (film) 3374, 3065, 2927, 2234, 1723, 1667, 1612; m/z (ES) [MNa^+] 383.09 (100%, MNa^+); HRMS Found: 383.0974 ($C_{19}H_{15}F_3N_2NaO_2$ requires MNa 383.0978).

N-Benzyl-N-[4-cyano-3-(trifluoromethyl)phenyl]-2-diazo-3-oxobutanamide, 17a



By general procedure B, aniline **15a**, followed by purification by flash chromatography, eluting with Petrol—EtOAc (80:20), gave the *amide* **17a** (133 mg, 80%) as a bright yellow viscous oil. R_f : 0.35 (90:10, CH₂Cl₂—Et₂O); δ_H (500 MHz; CDCl₃) 7.76 (1H, d, J 8.2, Ar 5-H), 7.52 (1H, d, J 2.1, Ar 2-H), 7.39 (1H, dd, J 8.2 and 2.1, Ar 6-H), 7.33-7.27 (3H, m, Ph), 7.22-7.19 (2H, m, Ph), 5.04 (2H, s, PhCH₂), 2.34 (3H, s, butanamide 4-H₃); δ_C (125 MHz; CDCl₃) 188.1 (butanamide C-3), 161.3 (butanamide C-1), 146.6 (Ar C-1), 136.0 (Ar C-5), 135.6 (Ph), 134.3 (q, $^2J_{FC}$ 32, Ar C-3), 129.2 (Ph), 129.0 (Ar C-6), 128.3 (Ph), 128.0 (Ph), 123.8 (Ar C-2), 121.7 (q, $^1J_{FC}$ 274, CF₃), 114.7 (CN), 108.0 (Ar C-4), 75.9 (butanamide C-2), 54.1 (PhCH₂), 27.8 (butanamide C-4); ν_{max}/cm^{-1} (film) 3087, 3066, 2933, 2232, 2114, 1660, 1608; m/z (ES) [MNa⁺] 409.09 (100%, MNa⁺); HRMS Found: 409.0901, (C₁₉H₁₃F₃N₄NaO₂ requires MNa 409.0883).

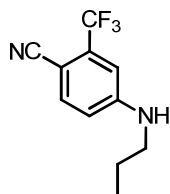
N-Benzyl-N-[4-cyano-3-(trifluoromethyl)phenyl]-2-diazo-acetamide, 18a



By general procedure C, amide **17a**, followed by purification by flash chromatography, eluting with CH₂Cl₂—EtOAc (90:10), gave the *amide* **18a** (51 mg, 93%) as a bright yellow viscous oil. R_f : 0.47 (90:10, CH₂Cl₂—Et₂O); δ_H (500 MHz; CDCl₃) 7.78 (1H, d, J 8.7, Ar 5-H), 7.59 (1H, d, J 2.6, Ar 2-H), 7.41 (1H, dd, J 8.7 and 2.6, Ar 6-H), 7.37-7.27 (3H, m, Ph), 7.19 (2H, d, J 8.5, Ph), 4.97 (2H, s, PhCH₂), 4.62 (1H, s, acetamide 2-H₁); δ_C (125 MHz; CDCl₃) 165.3 (acetamide C-1), 146.4 (Ar C-1), 136.1 (Ph), 135.9 (Ar C-5), 134.1 (q, $^2J_{FC}$ 32, Ar C-3), 130.8 (Ar C-6), 129.0 (Ph), 128.1 (Ph), 127.7

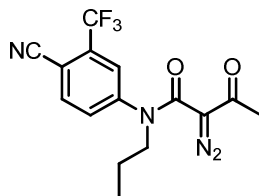
(Ph), 125.6 (Ar C-2), 121.7 (q, $^1J_{FC}$ 275, CF₃), 114.7 (CN), 108.5 (Ar C-4), 52.8 (PhCH₂), 48.5 (acetamide C-2); ν_{max}/cm^{-1} (film) 3089, 2930, 2232, 2106, 1631, 1607, 1502; m/z (ES) [MNa⁺] 367.08 (100%, MNa⁺); HRMS Found: 367.0770, (C₁₇H₁₁F₃N₄NaO requires MNa 367.0777).

4-(Propylamino)-2-(trifluoromethyl)benzonitrile, **15b**



By general procedure A, propyl amine followed by purification by flash chromatography, eluting with Petrol—EtOAc (90:10), gave the *aniline* **15b** (187 mg, 82%) as pale yellow needles, m.p. 116—119 °C (Petrol); R_f : 0.55 (50:50, Petrol—EtOAc); δ_H (500 MHz; CDCl₃) 7.54 (1H, d, J 8.7, Ar 6-H), 6.83 (1H, d, J 2.4, Ar 3-H), 6.67 (1H, dd, J 8.7 and 2.4, Ar 5-H), 4.46 (1H, s, br, NH), 3.16 (2H, t, J 7.2, propyl 1-H₂), 1.68 (2H, ap. hex, J 7.3, propyl 2-H₂), 1.02 (3H, t, J 7.3, propyl 3-H₃); δ_C (125 MHz; CDCl₃) 151.1 (Ar C-4), 136.2 (Ar C-6), 134.2 (q, $^2J_{FC}$ 31, Ar C-2), 122.0 (q, $^1J_{FC}$ 272, CF₃), 117.4 (CN), 113.7 (Ar C-5), 110.0 (Ar C-3), 95.4 (Ar C-1), 45.0 (propyl C-1), 22.2 (propyl C-2), 11.4 (propyl C-3); ν_{max}/cm^{-1} (film) 3357, 2878, 2224, 1893, 1615; m/z (ES) [MNa⁺] 251.08 (100%, MNa⁺); HRMS Found: 251.0773, (C₁₁H₁₁F₃N₂Na requires MNa 251.0767).

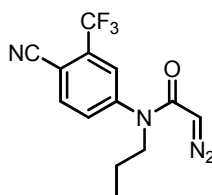
N-[4-Cyano-3-(trifluoromethyl)phenyl]-2-diazo-3-oxo-*N*-propylbutanamide, **17b**



By general procedure B, aniline **15b**, followed by purification by flash chromatography, eluting with Petrol—EtOAc (80:20), gave the *amide* **17b** (129 mg, 89%) as bright yellow needles. R_f : 0.83 (95:5, CH₂Cl₂—MeOH); δ_H (500 MHz; CDCl₃) 7.88 (1H, d, J 8.4, Ar 5-H), 7.62 (1H, d, J 2.0, Ar 2-H), 7.53 (1H, dd, J 8.4 and 2.0, Ar 6-H), 3.81 (2H, t, J 7.8, propyl 1-H₂), 2.33 (3H, s, butanamide 4-H₃), 1.62 (2H, ap. hex, J 7.5, propyl 2-H₂), 0.94 (3H, t,

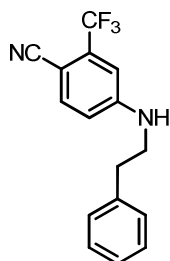
J 7.5, propyl 3-H₃); δ_C (125 MHz; CDCl₃) 188.4 (butanamide C-3), 160.9 (butanamide C-1), 146.8 (Ar C-1), 136.2 (Ar C-5), 134.4 (q, $^2J_{FC}$ 32, Ar C-3), 129.2 (Ar C-6), 123.8 (Ar C-2), 121.7 (q, $^1J_{FC}$ 276, CF₃), 114.7 (CN), 107.8 (Ar C-4), 75.8 (butanamide C-2), 52.6 (propyl C-1), 27.7 (butanamide C-4), 21.4 (propyl C-2), 11.1 (propyl C-3); ν_{max}/cm^{-1} (film) 3084, 2934, 2235, 2095, 1777, 1682, 1503; m/z (ES) [MNa⁺] 361.09 (100%, MNa⁺); HRMS Found: 361.0890, (C₁₅H₁₃F₃N₄NaO₂ requires *MNa* 361.0883).

***N*-[4-Cyano-3-(trifluoromethyl)phenyl]-2-diazo-*N*-propylacetamide, 18b**



By general procedure C, amide **17b**, followed by purification by flash chromatography, eluting with CH₂Cl₂—EtOAc (90:10), gave the *amide* **18b** (65 mg, 91%) as a bright yellow viscous oil. R_f : 0.49 (95:5, CH₂Cl₂—MeOH); δ_H (500 MHz; CDCl₃) 7.89 (1H, d, J 8.2, Ar 5-H), 7.67 (1H, d, J 2.1, Ar 2-H), 7.57 (1H, dd, J 8.2 and 2.1, Ar 6-H), 4.61 (1H, s, acetamide 2-H), 3.74 (2H, t, J 7.6, propyl 1-H₂), 1.58 (2H, ap. hex, J 7.6, propyl 2-H₂), 0.92 (3H, t, J 7.6, propyl 3-H₃); δ_C (125 MHz; CDCl₃) 164.9 (acetamide C-1), 146.4 (Ar C-1), 136.2 (Ar C-5), 134.4 (q, $^2J_{FC}$ 32, Ar C-3), 131.0 (Ar C-6), 125.8 (Ar C-2), 122.0 (q, $^1J_{FC}$ 276, CF₃), 114.8 (CN), 108.3 (Ar C-4), 51.1 (propyl C-1), 48.4 (acetamide C-2), 21.7 (propyl C-2), 11.1 (propyl C-1); ν_{max}/cm^{-1} (film) 3110, 2939, 2229, 2109, 1735, 1594, 1504; m/z (ES) [MH⁺] 297.1 (100%, MH⁺); HRMS Found: 297.0951 (C₁₃H₁₁F₃N₄O requires *MH* 297.0958).

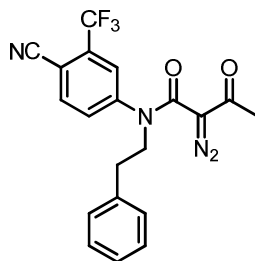
4-[(2-Phenylethyl)amino]-2-(trifluoromethyl)benzonitrile, 15c



By general procedure A, phenylethylamine followed by purification by flash chromatography, eluting with Petrol—EtOAc (80:20), gave the *aniline* **15c** (203 mg, 87%) as pale yellow needles, m.p. 132-136 °C (Petrol); R_f : 0.89

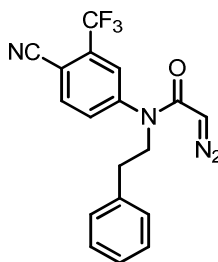
(95:5, CH₂Cl₂—MeOH); δ_H (500 MHz; CDCl₃) 7.54 (1H, d, *J* 8.5, Ar 6-H), 7.37-7.31 (2H, m, Ph), 7.29-7.24 (2H, m, Ph), 7.21 (1H, d, *J* 7.7, Ph), 6.82 (1H, d, *J* 2.4, Ar 3-H), 6.66 (1H, dd, *J* 8.5 and 2.4, Ar 5-H), 4.48 (1H, s, br, NH), 3.48 (2H, t, *J* 6.8, CH₂N), 2.95 (2H, t, *J* 6.8, PhCH₂); δ_C (125 MHz; CDCl₃) 150.8 (Ar C-4), 138.0 (Ph), 136.2 (Ar C-6), 134.2 (q, ²*J*_{FC} 32, Ar C-2), 128.9 (Ph), 128.7 (Ph), 127.0 (Ph), 122.6 (q, ¹*J*_{FC} 272, CF₃), 117.1 (CN), 113.9 (Ar C-5), 110.1 (Ar C-3), 95.4 (Ar C-1), 44.3 (CH₂N), 35.1 (PhCH₂); $\nu_{\max}/\text{cm}^{-1}$ (film) 3351, 2925, 2224, 1615, 1528; *m/z* (ES) [MNa⁺] 313.1 (100%, MNa⁺); HRMS Found: 313.0921 (C₁₆H₁₃F₃N₂Na requires *MNa* 313.0923).

***N*-[4-Cyano-3-(trifluoromethyl)phenyl]-2-diazo-3-oxo-*N*-(2-phenylethyl)butanamide, 17c**



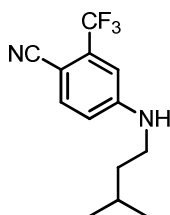
By general procedure B, aniline **15c**, followed by purification by flash chromatography, eluting with Petrol—EtOAc (80:20), gave the *amide* **17c** (125 mg, 76%) as a bright yellow viscous oil *R*_f: 0.49 (90:10, CH₂Cl₂—Et₂O); δ_H (500 MHz; CDCl₃) 7.75 (1H, d, *J* 8.4, Ar 5-H), 7.35-7.24 (3H, m, Ph and Ar 2-H), 7.22 (1H, d, *J* 8.4 and 2.2, Ar 6-H), 7.16-7.12 (3H, m, Ph), 4.06 (2H, t, *J* 7.8, CH₂N), 3.00 (2H, t, *J* 7.8, PhCH₂), 2.37 (3H, s, butanamide 4-H₃); δ_C (125 MHz; CDCl₃) 189.3 (butanamide C-3), 160.8 (butanamide C-1), 147.0 (Ar C-1), 138.0 (Ph), 136.2 (Ar C-5), 134.1 (q, ²*J*_{FC} 32, Ar C-3), 129.0 (Ar C-6), 127.2 (Ph), 123.9 (Ar C-2), 121.5 (q, ¹*J*_{FC} 276, CF₃), 114.6 (CN), 107.7 (Ar C-4), 75.9 (butanamide C-2), 53.7 (CH₂N), 34.2 (PhCH₂), 28.2 (butanamide C-4); $\nu_{\max}/\text{cm}^{-1}$ (film) 3029, 2232, 2113, 1660, 1607, 1501; *m/z* (ES) [MNa⁺] 423.11 (100%, MNa⁺); HRMS Found: 423.1057, (C₂₀H₁₅F₃N₄NaO₂ requires *MNa* 423.1039).

N*-[4-Cyano-3-(trifluoromethyl)phenyl]-2-diazo-*N*-(2-phenylethyl)acetamide, **18c*



By general procedure C, amide **17c**, followed by purification by flash chromatography, eluting with CH₂Cl₂—EtOAc (90:10), gave the *amide* **18c** (36 mg, 89%) as a bright yellow viscous oil. *R*_f: 0.49 (90:10, CH₂Cl₂—Et₂O); δ_H (500 MHz; CDCl₃) 7.77 (1H, d, *J* 8.5, Ar 6-H), 7.32-7.20 (4H, m, Ph and Ar 2-H), 7.17-7.09 (3H, m, Ph and Ar 5-H), 4.51 (1H, s, acetamide 2-H), 4.03 (2H, t, *J* 7.3, CH₂N), 2.96 (2H, t, *J* 7.3, PhCH₂); δ_C (125 MHz; CDCl₃) 164.9 (acetamide C-1), 138.0 (Ph), 146.8 (Ar C-1), 135.9 (Ar C-5), 134.3 (q, ²*J*_{FC} 32, Ar C-3), 130.9 (Ph and Ar C-6), 128.7 (Ph), 126.9 (Ph), 125.8 (Ar C-2), 121.7 (q, ¹*J*_{FC} 278, CF₃), 114.8 (CN), 108.2 (Ar C-4), 51.9 (CH₂N), 48.5 (acetamide C-2), 34.7 (PhCH₂); ν_{max}/cm^{-1} (film) 3500, 3086, 2232, 2108, 1726, 1634, 1606; *m/z* (ES) [MNa⁺] 381.09 (100%, MNa⁺); HRMS Found: 381.0934, (C₁₈H₁₃F₃N₄NaO requires *MNa* 381.0934).

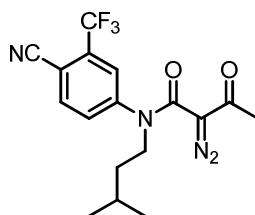
4-[Isopentylamino]-2-(trifluoromethyl)benzonitrile, **15d**



By general procedure A, isopentyl amine, followed by purification by flash chromatography, eluting with Petrol—EtOAc (80:20) gave the *aniline* **15d**, (460 mg, 90%) as pale yellow oil; *R*_f: 0.90 (95:5, CH₂Cl₂—MeOH); δ_H (500 MHz; CDCl₃) 7.53 (1H, d, *J* 8.7, Ar 6-H), 6.83 (1H, d, *J* 2.5, Ar 3-H), 6.67 (1H, dd, *J* 8.7 and 2.5, Ar 5-H), 4.47 (1H, s, b, NH), 3.19 (2H, dt, *J* 7.6 and 2.2, ⁱpentyl 1-H₂), 1.72 (1H, ap. sept, *J* 6.7, ⁱpentyl 3-H₁), 1.54 (2H, q, *J* 7.2, ⁱpentyl 2-H₂), 0.97 (6H, d, *J* 6.7, ⁱpentyl 4-H₃ and 4'-H₃); δ_C (125 MHz; CDCl₃) 151.2 (Ar C-4), 136.1 (Ar C-6), 134.3 (q, ²*J*_{FC} 33, Ar C-2), 122.7 (q, ¹*J*_{FC} 279, CF₃), 117.2 (CN), 113.6 (Ar C-5), 110.0 (Ar C-3), 95.1 (Ar C-1);

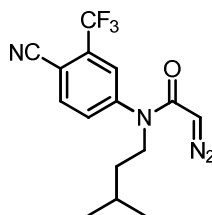
41.5 (¹pentyl C-1), 37.8 (¹pentyl C-2), 25.9 (¹pentyl C-3), 22.4 (¹pentyl C-4); $\nu_{\max}/\text{cm}^{-1}$ (film) 3367, 2960, 2219, 1711, 1616, 1533; m/z (ES) [MNa^+] 279.11 (100%, MNa^+); HRMS Found: 279.1087 ($\text{C}_{13}\text{H}_{15}\text{F}_3\text{N}_2\text{Na}$ MNa requires 279.1080).

***N*-(Isopentyl)-*N*-[4-cyano-3-(trifluoromethyl)phenyl]-2-diazo-3-oxobutanamide, 17d**



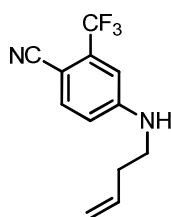
By general procedure B, aniline **15d**, followed by purification by flash chromatography, eluting with Petrol—EtOAc (80:20) gave the *amide* **17d** (425 mg, 65 %) as a bright yellow oil; R_f : 0.61 (90:10, CH_2Cl_2 — Et_2O); δ_H (500 MHz; CDCl_3) 7.87 (1H, d, J 8.6, Ar 5-H), 7.58 (1H, d, J 2.5, Ar 2-H), 7.49 (1H, dd, J 8.6 and 2.5, Ar 6-H), 3.84 (2H, t, J 8.1, ¹pentyl 1-H₂), 2.33 (3H, s, butanamide 4-H₃), 1.59 (1H, ap. sept, J 6.8, ¹pentyl 3-H₂), 1.47 (2H, dt, J 6.8 and 8.1, ¹pentyl 2-H), 0.92 (6H, d, J 6.8, ¹pentyl 4-H₃ and 4'-H₃); δ_C (125 MHz; CDCl_3) 189.0 (butanamide C-3), 160.9 (butanamide C-1), 146.8 (Ar C-1), 136.2 (Ar C-5), 134.8 (q, $^2J_{\text{FC}}$ 31, Ar C-3), 129.1 (Ar C-2), 123.8 (Ar C-6), 121.7 (q, $^2J_{\text{FC}}$ 276, CF_3), 114.7 (CN), 107.1 (Ar C-4), 75.8 (butanamide C-2), 49.8 (¹pentyl C-1), 36.8 (¹pentyl C-2), 27.7 (butanamide C-4), 26.1 (¹pentyl C-3), 22.3 (¹pentyl C-4); $\nu_{\max}/\text{cm}^{-1}$ (film) 3083, 2958, 2873, 2232, 2111, 1675; m/z (ES) [MNa^+] 389.12 (100%, MNa^+); HRMS Found: 389.1207 ($\text{C}_{16}\text{H}_{13}\text{F}_3\text{N}_4\text{NaO}_2$ requires, MNa 389.1196).

N*-(Isopentyl)-*N*-[4-cyano-3-(trifluoromethyl)phenyl]-2-diazo-acetamide, **18d*



By general procedure C, amide **17d**, followed by purification by flash chromatography, eluting with Petrol—EtOAc (70:30) gave the *amide* **18d** (87 mg, 75 %) , as a bright yellow oil; R_f : 0.32 (70:30, Petrol—EtOAc); δ_H (500 MHz; $CDCl_3$) 7.89 (1H, d, J 8.4, Ar 5-H), 7.65 (1H, d, J 2.8, Ar 2-H), 7.55 (1H, dd, J 8.4 and 2.8, Ar 6-H), 4.56 (1H, s, acetamide 2-H₁), 3.78 (2H, t, J 7.0, ¹pentyl-1H₂), 1.59 (1H, ap. sept, J 6.7, ¹pentyl 3-H₁), 1.43 (2H, dt, J 7.0 and 6.7, ¹pentyl 2-H₂), 0.91 (6H, d, J 7.0, ¹pentyl 4-H₃ and 4'-H₃); δ_C (125 MHz; $CDCl_3$) 164.9 (acetamide C-1), 146.5 (Ar C-1), 136.0 (Ar C-5), 134.6 (q, ² J_{FC} 31, Ar C-3), 130.9 (Ar C-6), 125.7 (Ar C-2), 121.8 (q, ¹ J_{FC} 269, CF₃), 114.7 (CN), 108.3 (Ar C-4), 48.4 (acetamide C-2), 48.2 (¹pentyl C-1), 37.2 (¹pentyl C-2), 26.0 (¹pentyl C-3), 22.4 (¹pentyl C-4); ν_{max}/cm^{-1} (film) 3096, 2959, 2236, 2107, 1630; m/z (ES) [MNa^+] 347.11 (100%, MNa^+); HRMS Found: 347.1093 (C₁₅H₁₅F₃N₄NaO requires MNa 347.1090).

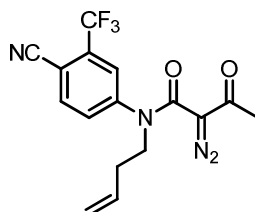
4-[(But-3-en-1-yl)amino]-2-(trifluoromethyl)benzonitrile, **15e**



By general procedure A, 3-butenylamine hydrochloride and two extra equiv. of K_2CO_3 followed by purification by flash chromatography, eluting with Petrol—EtOAc (80:20), gave the *aniline* **15e** (197 mg, 87%) as a pale yellow viscous oil. R_f : 0.67 (50:50, Petrol—EtOAc); δ_H (500 MHz; $CDCl_3$) 7.53 (1H, d, J 8.2, Ar 6-H), 6.86 (1H, d, J 2.1, Ar 3-H), 6.69 (1H, dd, J 8.2 and 2.1, Ar 5-H), 5.81 (1H, ddt, J 17.0, 10.4 and 3.2, butenyl 3-H₁), 5.18 (1H, dd, J 17.0 and 3.2, butenyl 4-H_A), 5.15 (1H, dd, J 10.4 and 3.2, butenyl 4-H_B), 4.76 (1H, s, br, NH), 3.26 (2H, ap. q, J 6.5, butenyl 1-H₂), 2.42 (2H, ap. q, J 6.8,

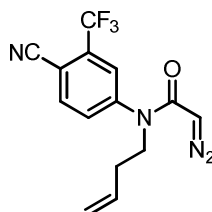
butenyl 2-H₂); δ_C (125 MHz; CDCl₃) 151.3 (Ar C-4), 136.1 (Ar C-6), 134.5 (butenyl C-3), 134.1 (q, $^2J_{FC}$ 32, Ar C-2), 122.6 (q, $^1J_{FC}$ 274, CF₃), 117.9 (butenyl C-4), 117.8 (CN), 113.8 (Ar C-5), 110.2 (Ar C-3), 94.8 (Ar C-1), 42.0 (butenyl C-1), 39.4 (butenyl C-2); ν_{max}/cm^{-1} (film) 3367, 2926, 2220, 1615, 1531; m/z (ES) [MNa⁺] 263.08 (100%, MNa⁺); HRMS Found: 263.0769 (C₁₂H₁₁F₃N₂Na, requires MNa 263.0767).

***N*-(But-3-en-1-yl)-*N*-[4-cyano-3-(trifluoromethyl)phenyl]-2-diazo-3-oxobutanamide, 17e**



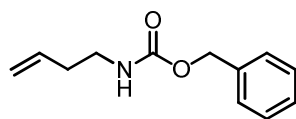
By general procedure B, aniline **15e**, followed by purification by flash chromatography, eluting with Petrol—EtOAc (80:20), gave the *amide* **17e** (162 mg, 91%) as bright yellow needles. R_f : 0.47 (90:10, CH₂Cl₂—Et₂O); δ_H (500 MHz; CDCl₃) 7.87 (1H, d, J 8.2, Ar 5-H), 7.61 (1H, d, J 2.3, Ar 2-H), 7.51 (1H, dd, J 8.2 and 2.3, Ar 6-H), 5.75 (1H, ddt, J 17.3, 10.2 and 7.3, butenyl 3-H₁), 5.09 (1H, dd, J 10.2 and 3.0, butenyl 4-H_A), 5.06 (1H, dd, J 17.3 and 3.0, butenyl 4-H_B), 3.93 (2H, t, J 7.1, butenyl 1-H₂), 2.37 (2H, dt, J 7.3 and 7.1, butenyl 2-H₂), 2.33 (3H, s, butenamide 4-H₃); δ_C (125 MHz; CDCl₃) 188.4 (butenamide C-3), 161.1 (butenamide C-1) 146.4 (Ar C-1), 136.1 (Ar C-5), 134.7 (q, $^2J_{FC}$ 34, Ar C-3), 134.1 (butenyl C-3), 129.3 (Ar C-6), 124.0 (Ar C-2), 121.7 (q, $^1J_{FC}$ 274, CF₃), 118.0 (butenyl C-4), 114.6 (CN), 108.0 (Ar C-4); 75.8 (butenamide C-2), 50.3 (butenyl C-1), 32.5 (butenyl C-2), 27.7 (butenamide C-4); ν_{max}/cm^{-1} (film) 3277, 3087, 2228, 2113, 1759, 1645, 1503; m/z (ES) [MNa⁺] 373.09 (100%, MNa⁺); HRMS Found: 373.0892, (C₁₆H₁₃F₃N₄O₂ requires MNa 373.0883).

N*-(But-3-en-1-yl)-*N*-[4-cyano-3-(trifluoromethyl)phenyl]-2-diazoacetamide, **18e*



By general procedure C, amide **17e**, followed by purification by flash chromatography, eluting with Petrol—EtOAc (80:20), gave the amide **18e** (75 mg, 93%) as a bright yellow viscous oil. R_f : 0.56 (90:10, CH₂Cl₂—Et₂O); δ_H (500 MHz; CDCl₃), 7.91 (1H, d, J 8.5, Ar 5-H), 7.67 (1H, d, J 2.2, Ar 2-H), 7.57 (1H, dd, J 8.5 and 2.2, Ar 6-H), 5.73 (1H, ddt, J 17.3, 10.4 and 7.3, butenyl 3-H₁), 5.08 (1H, dd, J 10.4 and 2.3, butenyl 4-H_A), 5.06 (1H, dd, J 17.3 and 2.3, butenyl 4-H_B), 4.57 (1H, s, b, acetamide 2-H₁), 3.87 (2H, t, J 7.4, butenyl 1-H₂), 2.32 (2H, ap. q, J 7.4, butenyl 2-H₂); δ_C (125 MHz; CDCl₃) 165.0 (acetamide C-1), 146.2 (Ar C-1), 136.0 (Ar C-5), 134.6 (q, $^2J_{FC}$ 32, Ar C-3), 134.3 (butenyl C-3), 131.4 (Ar C-6), 126.2 (Ar C-2), 121.9 (q, $^1J_{FC}$ 274, CF₃), 117.9 (butenyl C-4), 114.7 (CN), 108.6 (Ar C-4), 48.7 (butenyl C-1), 48.5 (acetamide C-2), 32.8 (butenyl C-2); ν_{max}/cm^{-1} (film) 3083, 2934, 2233, 2112, 1633, 1503, 1393; m/z (ES) [MNa⁺] 331.08 (100%, MNa⁺); HRMS Found: 331.0778, (C₁₄H₁₁F₃N₄O requires MNa 331.0777).

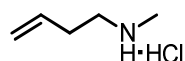
Benzyl but-3-enylcarbamate, **19⁶²**



By the method of Taillier *et al.*,⁶² a solution of Na₂CO₃ in H₂O (3 mL, 4 M) was added to a stirred suspension of 3-butenyl amine hydrochloride (403 mg, 3.75 mmol) in CH₂Cl₂ (40 mL) at rt and the reaction mixture was cooled to 0 °C. Benzyl chloroformate (0.85 mL, 6.0 mmol) was added dropwise to the reaction mixture and allowed to warm to rt. After 3 h H₂O (50 mL) was added and layers separated. The aqueous layer was extracted with CH₂Cl₂ (3 × 20 mL). The combined organic layers were washed with H₂O (20 mL), dried over Na₂SO₄, filtered and concentrated *in vacuo* to give the carbamate **19**⁶² as a clear oil (769 mg, 95 %) which required no further

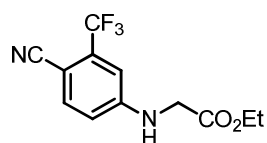
purification. R_f : 0.52 (80:20, Petrol—EtOAc); δ_H (500 MHz; CDCl_3) 7.34 (5H, m, Ph), 5.74 (1H, ddt, J 17.1, 10.2, and 6.6, butenyl 2-H), 5.10 (4H, m, butenyl 1- H_2 and PhCH_2), 3.26 (2H, q, J 6.6, butenyl 3- H_1), 2.26 (2H, q, J 6.6, butenyl 4- H_2); δ_C (125 MHz; CDCl_3) 156.4 (carbamate C-1); 136.7 (Ph), 135.1 (butenyl C-2), 133.3 (Ph), 128.8 (Ph), 128.1 (Ph), 117.3 (butenyl C-1); 66.6 (PhCH_2), 40.1 (butenyl C-3), 34.1 (butenyl C-4); $\nu_{\text{max}}/\text{cm}^{-1}$ (film) 3332, 2940, 1953, 1870, 1776, 1692, 1547; m/z (ES) [MNa^+] 228.1 (100%, MNa^+).

N-Methyl but-3-enyl amine hydrochloride, 20⁶³



The carbamate **19** was added, as a solution in THF (4 mL) to a stirred suspension of LiAlH_4 in THF (4 mL) at 0 °C. The syringe was washed with THF (2 mL) and the reaction mixture was allowed to warm to rt and then heated to reflux. After 4 h the reaction mixture was cooled to 0 °C and H_2O (0.8 mL), NaOH (15% aq. sol., 0.8 mL) and H_2O (2.4 mL) were added sequentially and the reaction mixture was allowed to warm to rt. After 2.5 h the reaction mixture was filtered through a pad of celite eluting with Et_2O (100 mL). The organic layer was extracted with 1 M HCl (3 x 20 mL) and the combined aqueous layers were concentrated *in vacuo* to give the amine hydrochloride salt **20⁶³** (395 mg, 65%) as a pale yellow amorphous solid. m.p. 164-167 °C (lit.⁶³ 178-180 °C); δ_H (500 MHz; D_2O) 5.74 (1H, ddt, J 17.4, 10.2 and 3.4, butenyl 3- H_1), 5.18 (1H, dd, J 10.2 and 3.4, butenyl 4- H_A), 5.15 (1H, dd, J 17.4 and 3.4, butenyl 4- H_B), 4.68 (2H, s, b, NH_2^+), 3.05 (2H, t, J 7.0, butenyl 1- H_2), 2.63 (3H, s, NMe), 2.39 (2H, ap. q, J 7.0, butenyl 2- H_2); δ_C (125 MHz; D_2O) 132.8 (butenyl C-3), 119.0 (butenyl C-4), 48.1 (butenyl C-1), 32.7 (NMe), 29.9 (butenyl C-2); m/z (ES) [MH^+] 86.09 (100%, MH^+).

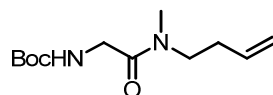
Ethyl 2-[(4-cyano-3-(trifluoromethyl)phenyl)amino]acetate, 15k



By general procedure A, glycine ethyl ester hydrochloride and two extra equiv. of K_2CO_3 followed by purification by flash chromatography, eluting

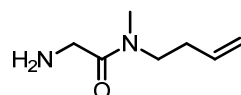
with Petrol—EtOAc (60:40), gave the *aniline* **42** (304 mg, 56%) as a colourless amorphous solid. R_f : 0.22 (70:30, Petrol—EtOAc); δ_H (500 MHz; CDCl₃) 7.59 (1H, d, J 8.5, Ar 5-H), 6.88 (1H, d, J 2.4, Ar 2-H), 6.70 (1H, dd, J 8.5 and 2.4, Ar 6-H), 5.13 (1H, s, b, NH), 4.29 (2H, q, J 7.1, ethyl 1-H₂), 3.96 (2H, d, J 5.1, glycinic 1-H₂), 1.32 (3H, t, J 7.1, ethyl 2-H₃); δ_C (125 MHz; CDCl₃) 169.4 (glycinic C-2), 149.8 (Ar C-1), 136.6 (Ar C-5), 134.5 (q, $^2J_{CF}$ 33, Ar C-3), 122.3 (q, $^1J_{CF}$ 278, CF₃), 116.7 (CN), 114.2 (Ar C-6), 110.4 (Ar C-2), 96.8 (Ar C-4), 62.1 (ethyl C-1), 44.7 (glycinic C-1), 14.1 (ethyl C-2); ν_{max}/cm^{-1} (film) 3360, 2996, 2221, 1713, 1615; m/z (ES) [MH⁺] 273.09 (100%, MH⁺); HRMS Found: 273.0854, (C₁₂H₁₁F₃N₂O₂ requires MH 273.0845).

tert*-Butyl *N*-[[(but-3-en-1-yl)(methyl)carbamoyl]methyl]carbamate, **22*



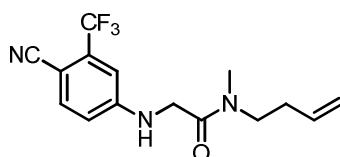
DIPEA (1.4 mL, 8.9 mmol) was added to a stirred solution of EDCI·HCl (468 mg, 2.4 mmol) and HOBt·H₂O (324 mg, 2.4 mmol) in CH₂Cl₂ (20 mL). The amine **20** (392 mg, 2.4 mmol) and *N*-Boc glycine (385 mg, 2.2 mmol) were added sequentially to the reaction mixture. After 20 h the reaction mixture was concentrated *in vacuo*. Purification by flash chromatography eluting with Petrol—EtOAc (1:1) gave the *amide* **22** (494 mg, 93%; 1:1 mixture of rotamers) as a colourless oil. R_f : 0.85 (90:10, CH₂Cl₂—MeOH); δ_H (500 MHz; CDCl₃) 5.75 (1H, m, butenyl 3-H₁), 5.53 (1H, s, b, NH), 5.08 (2H, m, butenyl 4-H_A and 4-H_B), 3.97 (1H, d, J 4.3, glycinic-H rot A), 3.92 (1H, d, J 4.3, glycinic-H rot B), 3.47 (1H, t, J 7.3, butenyl 1-H₂ rot A), 3.28 (1H, t, J 7.3, butenyl 1-H₂ rot B), 2.96 (1.5H, s, *NMe* rot A), 2.93 (1.5H, s, *NMe* rot B), 2.31 (2H, m, butenyl 2-H₂), 1.45 (9H, s, Boc); δ_C (125 MHz; CDCl₃) 168.2 (Boc C-1); 155.8 (glycine amide C-2), 135.1 (butenyl C-3 rot A), 133.7 (butenyl C-3 rot B), 118.2 (butenyl C-4 rot A), 117.0 (butenyl C-4 rot B); 48.2 (butenyl C-1 rot A), 47.6 (butenyl C-1 rot B), 42.4 (glycine amide C-1 rot A), 42.2 (glycine amide C-1 rot B), 34.2 (*NMe* rot A), 33.5 (*NMe* rot B), 32.4 (butenyl C-2 rot A), 31.8 (butenyl C-2 rot B), 28.4 (Boc C-3); ν_{max}/cm^{-1} (film) 3418, 3332, 2978, 2933, 1714, 1658, 1487; m/z (EI) [M⁺] 242.16 (100%, M⁺); HRMS Found: 242.1639, (C₁₂H₂₂N₂O₃ requires M 242.1630).

2-Amino-*N*-(but-3-en-1-yl)-*N*-methylacetamide, **14f**⁶³



HCl (4 M in Dioxane, 2 mL) was added dropwise over 5 min to a stirred solution of the amide **34** (506 mg, 2.1 mmol) in CH₂Cl₂ (10 mL). After 17 h the reaction mixture was concentrated *in vacuo* to give a crude product. The crude was diluted in Et₂O—MeOH (20:1, 80 mL) and the organic layer was extracted with H₂O (2 × 20 mL) and 1 M HCl (2 × 20 mL). The combined aqueous layers were concentrated *in vacuo* until half volume and basified by the addition of 2 M NaOH until pH 14. The aqueous layer was extracted with EtOAc (10 × 20 mL). The combined organic layers were dried over Na₂SO₄, filtered and concentrated *in vacuo* to give the amide **14f**⁶³ as a pale yellow oil (248 mg, 92%) which required no further purification (1:1 mixture of rotamers). R_f: 0.21 (90:10, CH₂Cl₂—MeOH); δ_H (500 MHz; CDCl₃) 5.52 (1H, m, butenyl 3-H₁), 4.82 (2H, m, butenyl 4-H₂), 3.21 (1H, t, *J* 7.1, butenyl 1-H₂ rot A), 3.19 (2H, s, acetamide 2-H₂), 3.04 (1H, t, *J* 7.1, butenyl 1-H₂ rot B), 2.70 (1.5H, s, NMe rot A), 2.68 (1.5H, s, NMe rot B), 2.06 (2H, m, butenyl 2-H₂), 1.96 (2H, s, b, NH₂); δ_H (125 MHz; CDCl₃) 172.1 (acetamide C-1), 135.1 (butenyl C-3 rot A), 133.9 (butenyl C-3 rot B), 117.6 (butenyl C-4 rot A), 116.7 (butenyl C-4 rot B), 47.8 (butenyl C-1 rot A), 47.4 (butenyl C-1 rot B), 43.0 (acetamide C-2 rot A), 42.7 (acetamide C-2 rot B), 33.9 (NMe rot A), 33.3 (NMe rot B), 32.3 (butenyl C-2 rot A), 31.6 (butenyl C-2 rot B); *m/z* (EI) [MH⁺] 143.1 (100%, MH⁺); HRMS Found: 143.1181, (C₁₂H₂₂N₂O₃ requires *MH* 143.1148).

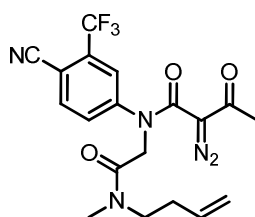
N-(But-3-en-1-yl)-2-[(4-cyano-3-(trifluoromethyl)phenyl)amino]-*N*-methylacetamide, **15f**



By general procedure A, amide **14f**, followed by purification by flash chromatography eluting with CH₂Cl₂—Et₂O (95:5), gave the *aniline* **15f** (112 mg, 72%) as a colourless amorphous solid (1:1 mixture of rotamers); R_f: 0.62 (90:10, CH₂Cl₂—Et₂O); δ_H (500 MHz; CDCl₃) 7.55 (1H, d, *J* 8.3, Ar 5-H),

6.88 (1H, d, J 3.1, Ar 2-H), 6.72 (1H, dd, J 8.3 and 3.1, Ar 6-H), 5.93 (1H, s, b, NH), 5.79 (1H, m, butenyl 3-H₁), 5.11 (2H, m, butenyl 4-H₂), 3.93 (1H, d, J 4.1, acetamide 2-H₂ rot A), 3.89 (1H, d, J 4.1, acetamide 2-H₂ rot B), 3.55 (1H, t, J 7.1, butenyl 1-H₂ rot A), 3.38 (1H, t, J 7.1, butenyl 1-H₂ rot B), 3.04 (1.5H, s, NMe rot A), 3.03 (1.5H, s, NMe rot B), 2.40 (1H, ap q, J 7.1, butenyl 2-H₂ rot A), 2.34 (1H, ap. q, J 7.1, butenyl 2-H₂ rot B); δ_C (125 MHz; CDCl₃) 167.1 (acetamide C-1 rot A), 167.0 (acetamide C-1 rot B), 149.9 (Ar C-1), 136.1 (Ar C-5), 134.8 (butenyl C-3 rot A), 134.2 (q, $^2J_{FC} = 279$ Ar C-3), 133.5 (butenyl C-3 rot B), 122.7 (q, $^1J_{FC} = 38$ CF₃); 118.6 (butenyl C-4 rot A), 117.1 (butenyl C-4 rot B); 114.4 (CN), 114.3 (Ar C-6), 110.4 (Ar C-2), 95.6 (Ar C-4), 48.1 (butenyl C-1 rot B), 47.8 (butenyl C-1 rot A), 44.1 (acetamide C-2 rot B), 43.9 (acetamide C-2 rot A), 34.1 (NMe rot A), 33.6 (NMe rot B), 32.3 (butenyl C-2 rot A), 31.7 (butenyl C-2 rot B); m/z (ES) [MH⁺] 312.13 (100%, MH⁺); HRMS Found: 312.1312, (C₁₅H₁₆F₃N₂O requires MH 312.1318).

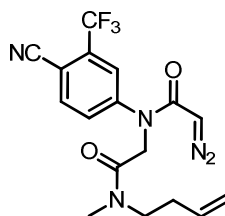
***N*-(But-3-en-1-yl)-*N*-[4-cyano-3-(trifluoromethyl)phenyl]-*N*-methylacetamide-2-diazo-3-oxobutanamide, 17f**



By general procedure B, aniline **15f**, followed by purification by flash chromatography eluting with CH₂Cl₂—Et₂O (90:10) gave the *amide* **17f** (101 mg, 63 %) as bright yellow oil (1:1 mixture of rotamres); R_f : 0.26 (90:10, CH₂Cl₂—Et₂O); δ_H (500 MHz; CDCl₃) 7.83 (1H, d, J 8.5, Ar 5-H), 7.69 (1H, d, J 2.4, Ar 2-H), 7.64 (1H, dd, J 8.5 and 2.4, Ar 6-H), 5.76 (1H, ddt, J 17.3, 10.7 and 7.3, butenyl 3-H₁), 5.12-5.07 (2H, m, butenyl 4-H₂), 4.61 (1H, s, acetamide 2-H₂ rot A), 4.57 (1H, s, acetamide 2-H₂ rot B), 3.46 (1H, t, J 7.3, butenyl 1-H₂ rot A), 3.36 (1H, t, J 7.3, butenyl 1-H₂ rot B), 3.02 (1.5H, s, NMe rot A), 2.96 (1.5H, s, NMe rot B), 2.39 (1H, ap q, J 7.1, butenyl 2-H₂ rot A), 2.37 (3H, s, butanamide 4-H₃), 2.30 (1H, ap q, J 7.1, butenyl 2-H₂ rot B); δ_C (125 MHz; CDCl₃) 188.9 (butanamide C-3), 166.4 (acetamide C-1), 161.3 (butanamide C-1), 147.3 (Ar C-1), 136.0 (Ar C-5), 134.6 (q, $^2J_{FC} = 35$, Ar C-3), 133.6 (butenyl C-3 rot A), 132.8 (butenyl C-3 rot B), 128.9 (Ar C-6), 123.9

(Ar C-2), 121.6 (q, $^2J_{FC} = 275, CF_3$), 118.4 (butenyl C-4 rot A), 116.9 (butenyl C-4 rot B), 114.6 (CN), 108.1 (Ar C-4), 75.6 (butanamide C-2), 53.3 (acetamide C-2 rot A), 51.9 (acetamide C-2 rot B), 48.8 (butenyl C-1 rot A), 48.1 (butenyl C-1 rot B), 34.7 (NMe rot A), 33.8 (NMe rot B), 32.4 (butenyl C-2 rot A), 31.7 (butenyl C-2 rot B), 27.7 (butanamide C-4); ν_{max}/cm^{-1} (film) 3320, 2926, 2232, 2117, 1653; m/z (ES) [MNa⁺] 444.13 (100%, MNa⁺); HRMS Found: 444.1269, (C₁₉H₁₈F₃N₅NaO₃ requires MNa 444.1254).

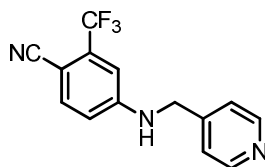
N*-(But-3-en-1-yl)-*N*-[4-cyano-3-(trifluoromethyl)phenyl]-2-diazoacetamide-*N*-methylglycineamide, **18f*



By general procedure C, amide **17f**, followed by purification by flash chromatography eluting with Petrol—EtOAc (1:1) gave the *amide* **18f** (84 mg, 76%) as bright yellow oil (1:1 mixture of rotamers); R_f : 0.32 (90:10, CH₂Cl₂—Et₂O); δ_H (500 MHz; CDCl₃) 7.87 (1H, d, J 8.7, Ar 5-H), 7.84 (1H, d, J 2.9, Ar 2-H), 7.79 (1H, dd, J 8.7 and 2.9, Ar 6-H), 5.75 (1H, m, butenyl 3-H₁ rot A and B), 5.06 (2H, m, butenyl 4-H₂ rot A and B), 4.62 (1H, s, acetamide 2-H₁), 4.53 (1H, s, glycineamide 1-H₂ rot A), 4.49 (1H, s, glycineamide 1-H₂ rot B), 3.46 (1H, t, J 7.3, butenyl 1-H₂ rot A), 3.36 (1H, t, J 7.3, butenyl 1-H₂ rot B), 3.01 (1.5H, s, NMe rot A), 2.96 (1.5H, s, NMe rot B), 2.39 (1H, ap. q, J 7.3, butenyl 2-H₂ rot A), 2.30 (1H, ap. q, J 7.3, butenyl 2-H₂ rot B); δ_C (125 MHz; CDCl₃) 168.8 (glycineamide C-2 rot A), 167.0 (glycineamide C-2 rot B), 166.9 (acetamide C-1 rot A), 165.4 (acetamide C-1 rot B), 146.9 (Ar C-1); 135.9 (Ar C-5), 134.9 (butenyl C-3 rot A), 134.3 (Ar C-3), 133.8 (butenyl C-3 rot B), 131.5 (Ar C-6), 126.0 (Ar C-2), 121.7 (CF₃); 118.1 (butenyl C-4 rot A), 116.8 (butenyl C-4 rot B), 114.7 (CN), 108.7 (Ar C-4), 50.9 (glycine amide C-1 rot A), 50.8 (glycine amide C-1 rot B), 48.9 (butenyl C-1 rot A), 48.3 (acetamide C-2), 48.0 (butenyl C-1 rot B), 34.7 (NMe rot A), 33.8 (NMe rot B), 32.4 (butenyl C-2 rot A), 31.7 (butenyl C-2 rot B); ν_{max}/cm^{-1} (film) 3084,

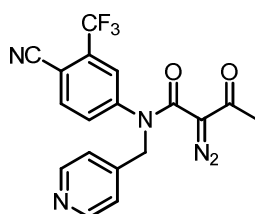
2926, 2232, 2110, 1654, 1606, 1501; m/z (ES) $[MNa^+]$ 402.12 (100%, MNa^+); HRMS Found: 402.1159, ($C_{17}H_{16}F_3N_5NaO_2$ requires MNa 444.1148).

4-[(Pyridin-4-ylmethyl)amino]-2-(trifluoromethyl)benzonitrile, **15g**



By general procedure A, pyridinyl amine, followed by purification by flash chromatography, eluting with Petrol—EtOAc (50:50), gave the *aniline* **15g**, (369 mg, 67%) as a colorless amorphous solid, R_f : 0.68 (80:20, CH_2Cl_2 — Et_2O); δ_H (500 MHz; $CDCl_3$) 8.59 (2H, d, J 6.0, pyr 3-H), 7.55 (1H, d, J 8.5, Ar 6-H), 7.25 (2H, d, J 6.0, pyr 2-H), 6.91 (1H, d, J 2.5, Ar 3-H), 6.67 (1H, dd, J 8.5 and 2.5, Ar 5-H), 5.19 (1H, s, b, NH), 4.48 (2H, d, J 6.0, pyr CH_2 NH); δ_C (125 MHz; $CDCl_3$) 150.5 (Ar C-4), 150.4 (pyr C-3), 146.3 (pyr C-1), 136.4 (Ar C-6), 134.4 (q, $^2J_{FC}$ 33, Ar C-2), 122.4 (q, $^1J_{FC}$ 282, CF_3), 121.8 (pyr C-2), 116.7 (CN), 114.0 (Ar C-5), 110.8 (Ar C-3); 96.9 (Ar C-1), 46.3 (pyr CH_2 NH); ν_{max}/cm^{-1} (film) 3236, 2253, 2220, 1945, 1615; m/z (ES) $[MH^+]$ 278.09 (100%, MH^+); HRMS Found: 278.0912, ($C_{14}H_{10}F_3N_3$ MH requires 278.0900).

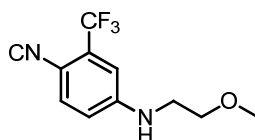
N-[4-Cyano-3-(trifluoromethyl)phenyl]-*N*-(pyridin-4-ylmethyl)-2-diazo-3-oxobutanamide, **17g**



By general procedure B, aniline **15g**, followed by purification by flash chromatography, eluting with EtOAc— Et_2O (75:25), gave the *amide* **17g** (270 mg, 54%), as a colorless amorphous solid, R_f : 0.44 (95:5, EtOAc—MeOH); δ_H (500 MHz; $CDCl_3$) 8.59 (2H, d, J 6.0, pyr 2-H), 7.81 (1H, d, J 8.2, Ar 5-H), 7.57 (1H, d, J 2.3, Ar 2-H), 7.43 (1H, dd, J 8.2 and 2.3, Ar 6-H), 7.21 (2H, d, J 6.0, pyr 3-H), 5.06 (2H, s, pyr- CH_2), 2.30 (3H, s, butanamide 4-H); δ_C (125 MHz; $CDCl_3$) 187.0 (butanamide C-3, verified in HMBC) 161.5 (butanamide C-1), 150.2 (pyr C-2), 146.7 (Ar C-1), 144.9 (pyr C-4), 136.1 (Ar

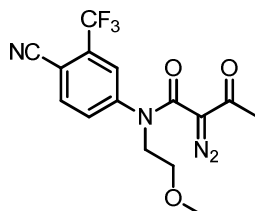
C-5), 134.6 (q, $^2J_{FC}$ 30, Ar C-3), 128.5 (Ar C-6), 123.2 (Ar C-2), 122.4 (pyr C-3), 121.5 (q, $^1J_{FC}$ 284, CF_3), 114.5 (CN), 108.2 (Ar C-4), 74.7 (butanamide C-2, verified in HMBC), 53.3 (pyr- CH_2), 27.5 (butanamide C-4); ν_{max}/cm^{-1} (film) 3338, 2234, 2114, 1687, 1649; m/z (ES) $[MH^+]$ 388.11 (100%, MH^+); HRMS Found: 388.1017, ($C_{18}H_{12}F_3N_5O_2$ MH requires 388.1016).

4-[(2-Methoxyethyl)amino]-2-(trifluoromethyl)benzonitrile, **15h**



By general procedure A, 2-methoxy ethyl amine, followed by purification by flash chromatography, eluting with CH_2Cl_2 — Et_2O (90:10), gave the *aniline* **15h** (218 mg, 89%) as pale yellow needles, m.p. 132-134 °C (Et_2O); R_f : 0.51 (50:50, CH_2Cl_2 — Et_2O); δ_H (500 MHz; $CDCl_3$) 7.55 (1H, d, J 8.5, Ar 6-H), 6.87 (1H, d, J 2.9, Ar 3-H), 6.70 (1H, dd, J 8.5 and 2.9, Ar 5-H), 4.83 (1H, s, b, NH), 3.62 (2H, t, J 5.3, ethyl 2-H), 3.41 (3H, s, methoxy- CH_3), 3.36 (2H, ap. q, J 5.3, ethyl 1-H); δ_C (125 MHz; $CDCl_3$) 151.0 (Ar C-4), 136.2 (Ar C-6), 134.3 (q, $^2J_{FC}$ 32, Ar C-2), 122.6 (q, $^1J_{FC}$ 280, CF_3), 117.0 (CN), 114.0 (Ar C-5), 111.3 (Ar C-3), 95.8 (Ar C-1), 70.1 (ethyl C-2), 58.9 (methoxy- CH_3), 42.7 (ethyl C-1); ν_{max}/cm^{-1} (film) 3340, 2226, 1618, 1542; m/z (ES) $[MH^+]$ 245.09 (100%, MH^+); HRMS Found: 245.0886, ($C_{11}H_{11}F_3N_2O$ MH requires 245.0896).

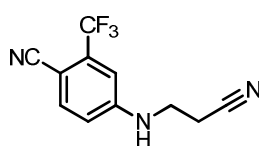
N-[4-Cyano-3-(trifluoromethyl)phenyl]-*N*-2-methoxyethyl-2-diazo-3-oxobutanamide, **17h**



By general procedure B, aniline **15h**, followed by purification by flash chromatography, eluting with CH_2Cl_2 — Et_2O (95:5), gave the *amide* **17h** (600 mg, 97%) as a viscous bright yellow liquid, R_f : 0.47 (80:20, CH_2Cl_2 — Et_2O); δ_H (500 MHz; $CDCl_3$) 7.86 (1H, d, J 8.4, Ar 5-H), 7.81 (1H, d, J 2.6, Ar 2-H), 7.63 (1H, dd, J 8.4 and 2.6, Ar 6-H), 4.01 (2H, t, J 5.0, ethyl 1-H), 3.61 (2H, t,

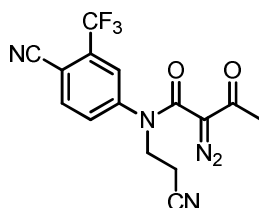
J 5.0, ethyl 2-H), 3.34 (3H, s, methoxy-CH₃), 2.37 (3H, s, butanamide 4-H); δ_C (125 MHz; CDCl₃) 188.9 (butanamide C-3), 160.9 (butanamide C-1), 147.5 (Ar C-1), 136.0 (Ar C-5), 134.4 (Ar C-3), 129.3 (Ar C-6), 124.3 (q, $^2J_{FC}$ 35, Ar C-2), 121.7 (q, $^1J_{FC}$ 275, CF₃), 114.8 (CN), 107.7 (Ar C-4), 75.8 (butanamide C-2), 69.8 (ethyl C-2), 58.9 (methoxy-CH₃), 51.4 (ethyl C-1), 27.9 (butanamide C-4); ν_{max}/cm^{-1} (film) 3083, 2898, 2232, 2115, 1659; m/z (ES) [MNa⁺] 377.09 (100%, MNa⁺); HRMS Found: 377.0850, (C₁₅H₁₃F₃N₄NaO₃ MNa requires 377.0832).

4-[(2-Cyanoethyl)amino]-2-(trifluoromethyl)benzonitrile, **15i**



By general procedure A, 3-amino propionitrile, followed by purification by flash chromatography, eluting with Petrol—EtOAc (50:50), gave the *aniline* **15i** (444 mg, 69%) as colorless needles, m.p. 146-150 °C (Petrol); R_f : 0.26 (50:50, Petrol—EtOAc); δ_H (500 MHz; CDCl₃) 7.62 (1H, d, J 8.7, Ar 6-H), 6.91 (1H, d, J 2.4, Ar 3-H), 6.76 (1H, dd, J 8.7 and 2.4, Ar 5-H), 4.85 (1H, s, b, NH), 3.61 (2H, ap. q, J 6.3, ethyl 1-H), 2.71 (2H, t, J 6.3, ethyl 2-H); δ_C (125 MHz; CDCl₃) 149.6 (Ar C-4), 136.5 (Ar C-6), 134.7 (q, $^2J_{FC}$ 31, Ar C-2), 122.3 (q, $^1J_{FC}$ 273, CF₃), 117.2 (CN), 116.5 (Ar CN), 114.2 (Ar C-5), 110.4 (Ar C-3), 97.6 (Ar C-1), 39.0 (ethyl C-1), 18.1 (ethyl C-2); ν_{max}/cm^{-1} (film) 3391, 2252, 2222, 1905, 1791; m/z (ES) [MNa⁺] 262.06 (100%, MNa⁺); HRMS Found: 262.0562, (C₁₁H₈F₃N₃Na MNa requires 262.0563).

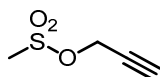
N-(2-Cyanoethyl)-*N*-[4-cyano-3-(trifluoromethyl)phenyl]-2-diazo-3-oxo-butanamide, **17i**



By general procedure B, aniline **15i**, followed by purification by flash chromatography, eluting with Petrol—EtOAc (50:50), gave the *amide* **17i** (444 mg, 69%), as a colorless needles. R_f : 0.58 (40:60, Petrol—EtOAc); δ_H (500 MHz; CDCl₃) 7.92 (1H, d, J 8.3, Ar 5-H), 7.70 (1H, d, J 2.5, Ar 2-H),

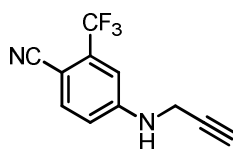
7.63 (1H, dd, J 8.3 and 2.5, Ar 6-H), 4.08 (2H, t, J 6.4, ethyl 1-H), 2.82 (2H, t, J 6.4, ethyl 2-H), 2.33 (3H, s, butanamide 4-H); δ_C (125 MHz; $CDCl_3$) 187.5 (butanamide C-3, verified in HMBC), 161.5 (butanamide C-1), 145.9 (Ar C-1), 136.5 (Ar C-5), 134.9 (q, $^2J_{FC}$ 30, Ar C-3), 129.7 (Ar C-6); 124.3 (Ar C-2), 121.5 (q, $^1J_{FC}$ 280, CF_3) 117.1 (CN), 114.4 (Ar CN), 109.1 (Ar C-4), 76.1 (butanamide C-2, verified in HMBC), 47.3 (ethyl C-1), 27.8 (butanamide C-4), 17.0 (ethyl C-2); ν_{max}/cm^{-1} (film) 3336, 3085, 2252, 2234, 2123, 1632; m/z (ES) $[MNa^+]$ 372.07 (100%, MNa^+); HRMS Found: 372.0690, ($C_{15}H_{10}F_3N_5NaO_2$ MNa requires 372.0679).

Prop-2-yn-1-yl methanesulfonate, **24**⁶⁴



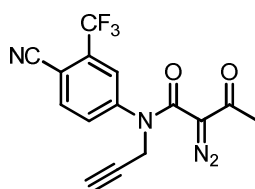
By the method of Girard *et al.*,⁶⁴ methanesulfonyl chloride was added dropwise to a stirred solution of propargyl alcohol and Et_3N in CH_2Cl_2 at 0 °C, and the reaction mixture was allowed to warm to rt. After 30 min, the reaction mixture was diluted with CH_2Cl_2 (10 mL) and HCl (aq, 1 M, 10 mL) was added and layers separated. The aqueous layer was extracted with CH_2Cl_2 (3 × 10 mL). The combined organic layers were washed with brine (sat. aq. sol 10 mL), dried (Na_2SO_4), filtered and concentrated *in vacuo*. Purification by flash chromatography eluting with Petrol—EtOAc (50:50) gave the sulfonate **24**,⁶⁴ at a quantitative yield, as a pale yellow oil which required no further purification. R_f : 0.87 (90:10, CH_2Cl_2 —MeOH); δ_H (500 MHz; $CDCl_3$) 4.86 (2H, d, J 2.5, propynyl 1-H), 3.13 (3H, s, methyl), 2.71 (1H, t, J 2.5, propynyl 3-H); δ_C (125 MHz; $CDCl_3$) 75.8 (propynyl C-3), 57.2 (methyl), 46.1 (propynyl C-2), 39.1 (propynyl C-1); m/z (EI) $[MH^+]$ 135.01 (100%, MH^+).

4-[(Prop-2-yn-1-yl)amino]-2-(trifluoromethyl)benzonitrile, **15j**



4-amino-2(trifluoromethyl)benzonitrile (930 mg, 5 mmol) was added to a stirred solution of sulfonate **24** (335 mg, 2.5 mmol), in MeCN (0.5M) at rt and the reaction mixture was heated to reflux. After 3 h, the reaction mixture was allowed to cool to rt and quenched by the addition of K₂CO₃ (sat. aq. sol. 10 mL). CH₂Cl₂ (10 mL) was added and layers separated. The organic layer was triturated using a glass rod and the precipitate was removed by filtration through a pad of celite, eluting with a CH₂Cl₂–MeOH (50:50) mixture. The solution was concentrated *in vacuo*. Purification by flash chromatography eluting with Petrol–Et₂O (50:50) gave the *aniline* **15j**, as bright yellow needles (531 mg, 60%). m.p. 126-127 °C; R_f: 0.32 (80:20, Petrol–Et₂O); δ_H (500 MHz; CDCl₃) 7.62 (1H, d, *J* 8.2, Ar 6-H), 6.96 (1H, d, *J* 2.6, Ar 3-H), 6.81 (1H, dd, *J* 8.2 and 2.6, Ar 5-H), 4.77 (1H, s, b, NH), 4.03 (2H, dd, *J* 3.5 and 2.4, propynyl 1-H), 2.30 (1H, t, *J* 2.4, propynyl 3-H); δ_C (125 MHz; CDCl₃) 149.8 (Ar C-4), 136.2 (Ar C-6), 134.3 (q, ²J_{FC} 32, Ar C-2), 122.3 (q, ¹J_{FC} 276, CF₃), 116.8 (CN), 114.6 (Ar C-5), 110.9 (Ar C-3), 91.2 (Ar C-1), 78.4 (propynyl C-2), 72.7 (propynyl C-3), 32.9 (propynyl C-1); ν_{max}/cm⁻¹ (film) 3362, 3299, 2226, 1902, 1617; *m/z* (ES) [MNa⁺] 247.05 (100%, MNa⁺); HRMS Found: 247.0461, (C₁₁H₇F₃N₂Na *MNa* requires 247.0454).

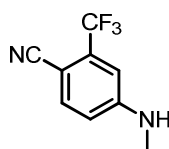
N-[4-Cyano-3-(trifluoromethyl)phenyl]-*N*-(prop-2-yn-1-yl)-2-diazo-3-oxobutanamide, **17j**



By general procedure B, aniline **15j**, followed by purification by flash chromatography, eluting with Petrol–Et₂O (40:60), gave the *amide* **17j** (444 mg, 69%), as pale yellow needles. R_f: 0.53 (60:40, EtOAc–Petrol); δ_H (500 MHz; CDCl₃) 7.92 (1H, d, *J* 8.3, Ar 5-H), 7.74 (1H, d, *J* 2.2, Ar 2-H), 7.63 (1H, dd, *J* 8.3 and 2.2, Ar 6-H), 4.60 (2H, d, *J* 2.5, propynyl 1-H), 2.37 (3H, s,

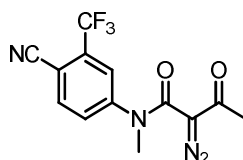
butanamide 4-H), 2.34 (1H, t, J 2.5, propynyl 3-H); δ_C (125 MHz; $CDCl_3$) 188.2 (butanamide C-3), 161.0 (butanamide C-1), 145.7 (Ar C-1), 136.2 (Ar C-5), 134.5 ($^2J_{FC}$ 32, Ar C-3), 129.7 (Ar C-6), 124.4 (Ar C-2), 121.7 (q, $^1J_{FC}$ 277, CF_3), 114.6 (CN), 108.7 (Ar C-4), 77.3 (propynyl C-2), 75.9 (butanamide C-2), 74.2 (propynyl C-3), 39.9 (propynyl C-1), 27.9 (butanamide C-4); ν_{max}/cm^{-1} (film) 3287, 2221, 2118, 1689, 1647; m/z (ES) [MNa^+] 357.06 (100%, MNa^+); HRMS Found: 357.0573, ($C_{15}H_9F_3N_4NaO_2$ MNa requires 357.0570).

4-(Methylamino)-2-(trifluoromethyl)benzonitrile, 15k



By general procedure A, methylamine HCl salt with two additional equiv of K_2CO_3 followed by purification by flash chromatography eluting with 50:50 Petrol—EtOAc to yield the *aniline* **15k** (860 mg, 86%) as a yellow solid. R_f : 0.53 (50:50, Petrol—EtOAc); δ_H (500 MHz; $CDCl_3$) 7.56 (1H, d, J 8.5, Ar 2-H), 6.84 (1H, d, J 2.1, Ar 5-H), 6.68 (1H, dd, J 8.5 and 2.1, Ar 3-H), 4.54 (1H, s, NH), 2.93 (3H, d, J 5.5, Me); δ_C (125 MHz; $CDCl_3$) 151.8 (Ar C-4), 136.1 (Ar C-2), 134.0 (q, $^2J_{FC}$ 31, Ar C-6), 122.0 (q, $^1J_{FC}$ 274, CF_3), 117.1 (CN), 113.5 (Ar C-3), 109.7 (Ar C-5), 95.0 (Ar C-1), 29.9 (Me); ν_{max}/cm^{-1} (film) 3357, 2218; m/z (ES) [MH^+] 201.1 (100%, MH^+); HRMS Found: 201.0630, ($C_9H_8F_3N_2$ requires MH 201.0634).

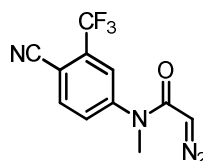
N-[4-Cyano-3-(trifluoromethyl)phenyl]-2-diazo-3-oxo-*N*-methylbutanamide, 17k



By general procedure B, aniline **15k**, followed by purification by flash chromatography, eluting with 90:10 CH_2Cl_2 — Et_2O , to yield the butanamide **17k** (1.15 g, 88%), as a yellow amorphous solid, R_f : 0.46 (90:10 CH_2Cl_2 — Et_2O); δ_H (500 MHz; $CDCl_3$) 7.86 (1H, d, J 8.4, Ar 5-H), 7.65 (1H, d, J 2.2, Ar 2-H), 7.54 (1H, dd, J 8.4 and 2.2, Ar 6-H), 3.45 (3H, s, NMe), 2.35 (3H, s,

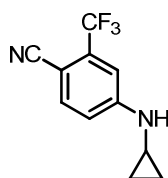
butanamide 4-H); δ_C (125 MHz; CDCl_3) 187.9 (butanamide C-3), 161.5 (butanamide C-1), 147.7 (Ar C-1), 136.1 (Ar C-6), 134.4 (q, $^2J_{\text{CF}}$ 32, Ar C-3), 128.0 (Ar C-5), 122.9 (Ar C-2), 121.8 (q, $^1J_{\text{CF}}$ 274, CF_3), 114.7 (CN), 107.6 (Ar C-4), 75.9 (butanamide C-2), 38.3 (NMe), 27.7 (butanamide C-4); $\nu_{\text{max}}/\text{cm}^{-1}$ (film) 2231, 2115, 1643, 1606; m/z (ES) [MNa^+] 333.1 (100%, MNa^+); HRMS Found: 333.0573, ($\text{C}_{13}\text{H}_9\text{F}_3\text{N}_4\text{NaO}_2$ requires MNa 333.0570).

***N*-[4-Cyano-3-(trifluoromethyl)phenyl]-2-diazo-*N*-(methyl)acetamide, 18k**



By general procedure C, amide **17k**, followed by purification by flash chromatography eluting with 90:10 CH_2Cl_2 — Et_2O , to yield the acetamide **18k**, (276 mg, 64%) as a pale yellow solid, R_f : 0.40 (90:10 CH_2Cl_2 — Et_2O); δ_H (500 MHz; CDCl_3) 7.87 (1H, d, J 8.4, Ar 5-H), 7.71 (1H, d, J 2.4, Ar 2-H), 7.60 (1H, dd, J 8.4 and 2.4, Ar 6-H), 4.80 (1H, s, acetamide 2-H), 3.37 (3H, s, NMe); δ_C (125 MHz; CDCl_3) 165.0 (acetamide C-1), 147.4 (Ar C-1), 135.8 (Ar C-5), 134.0 (q, $^2J_{\text{CF}}$ 33, Ar C-3), 129.2 (Ar C-6), 124.2 (Ar C-2), 122.0 (q, $^1J_{\text{CF}}$ 288, CF_3), 114.9 (CN), 108.0 (Ar C-4); 448.3 (acetamide C-2), 28.6 (NMe); $\nu_{\text{max}}/\text{cm}^{-1}$ (film) 2235, 2115, 1604; m/z (ES) [MNa^+] 291.0 (100%, MNa^+); HRMS Found: 291.0465, ($\text{C}_{11}\text{H}_7\text{F}_3\text{N}_4\text{NaO}$ requires MNa 291.0464).

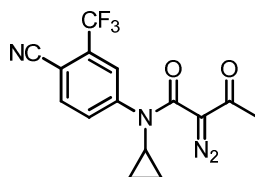
4-(Cyclopropylamino)-2-(trifluoromethyl)benzonitrile, 15I



By general procedure A, cyclopropyl amine, followed by purification by flash chromatography, eluting with 70:30 Petrol— EtOAc , gave the *aniline* **15I** (910 mg, 81%) as a pale yellow solid, m.p. 80-84 °C; R_f : 0.75 (50:50 Petrol— EtOAc); δ_H (500 MHz; CDCl_3) 7.56 (1H, d, J 8.7, Ar 6-H), 7.03 (1H, d, J 2.1, Ar 3-H), 6.89 (1H, dd, J 8.7 and 2.1, Ar 5-H), 4.96 (1H, s, b, NH), 2.51 (1H, ttd, J 6.8, 3.6 and 1.4, cp 1-H), 0.87 (2H, td, J 6.8 and 4.9, cp 2-Ha), 0.58

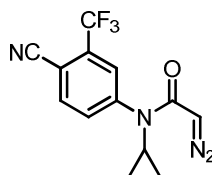
(2H, td, J 4.9 and 3.6, cp 2-Hb); δ_C (125 MHz; $CDCl_3$) 151.8 (Ar C-4), 135.9 (Ar C-6), 134.0 (q, $^2J_{CF}$ 34, Ar C-2), 122.7 (q, $^1J_{CF}$ 284, CF_3), 117.2 (CN), 114.6 (Ar C-5), 110.6 (Ar C-3), 96.1 (Ar C-1), 24.6 (cp C-1), 7.7 (cp C-2); ν_{max}/cm^{-1} (film) 3351, 2213; m/z (ES) $[MH^+]$ 227.1 (100%, MH^+); HRMS Found: 227.0795, ($C_{11}H_{10}F_3N_2$ requires MH 227.0790).

***N*-(Cyclopropyl)-*N*-[4-cyano-3-(trifluoromethyl)phenyl]-2-diazo-3-oxobutanamide, 17I**



By general procedure B, aniline **15I**, followed by purification by flash chromatography, eluting with 70:30 Petrol—EtOAc, to yield the *butanamide* **17I** (560 mg, 83%), as a pale yellow solid; R_f : 0.34 (50:50 Petrol—EtOAc); δ_H (500 MHz; $CDCl_3$) 7.91 (1H, d, J 1.9, Ar 2-H), 7.83 (1H, d, J 8.6, Ar 6-H), 7.77 (1H, dd, J 8.6 and 1.9, Ar 5-H), 3.09 (1H, tt, J 7.0 and 3.8, cp 1-H), 2.46 (3H, s, butanamide 4-H), 1.15 (2H, td, J 7.0 and 1.4, cp 2-Ha), 0.80 (2H, td, J 3.8 and 1.4, cp 2-Hb); δ_C (125 MHz; $CDCl_3$) 189.7 (butanamide C-3), 162.7 (butanamide C-1), 146.4 (Ar C-1), 135.3 (Ar C-6), 133.5 (q, $^2J_{CF}$ 32, Ar C-3), 127.4 (Ar C-5), 122.4 (Ar C-3), 121.6 (q, $^1J_{CF}$ 286, CF_3), 115.1 (CN), 106.6 (Ar C-4), 75.9 (butanamide C-2), 31.9 (cp C-1), 28.2 (butanamide C-4), 11.1 (cp C2); ν_{max}/cm^{-1} (film) 2228, 2114, 1642; m/z (ES) $[MNa^+]$ 359.1 (100%, MNa^+); HRMS Found: 359.0729 ($C_{15}H_{11}F_3N_4NaO_2$ requires MNa 359.0726).

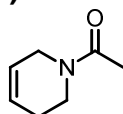
***N*-(Cyclopropyl)-*N*-[4-cyano-3-(trifluoromethyl)phenyl]-2-diazoacetamide, 18I**



By general procedure C, amide **17I**, followed by purification by flash chromatography eluting with 60:40 Petrol—EtOAc, to yield the acetamide **18I**, (232 mg, 48%) as a pale yellow solid, R_f : 0.30 (60:40 Petrol—EtOAc); δ_H (500 MHz; $CDCl_3$) 7.85 (1H, d, J 1.9, Ar 2-H), 7.79 (1H, d, J 8.4, Ar 6-H),

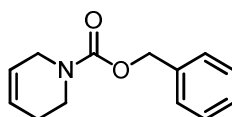
7.68 (1H, dd, J 8.4 and 1.9, Ar 5-H), 5.64 (1H, s, acetamide 2-H), 2.97 (1H, tt, J 6.9 and 3.8, cp 1-H), 1.13 (2H, td, J 6.9 and 1.2, cp 2-Ha), 0.71 (2H, td, J 3.8 and 1.2, cp 2-Hb); δ_C (125 MHz; CDCl₃) 167.6 (acetamide C-1), 146.1 (Ar C-1), 134.7 (Ar C-6), 133.1 (q, $^2J_{CF}$ 32, Ar C-3), 127.9 (Ar C-5), 123.1 (Ar C-2), 122.1 (q, $^1J_{CF}$ 276, CF₃), 115.5 (CN), 105.5 (Ar C-4), 49.0 (acetamide C-2), 29.4 (cp C-1), 11.4 (cp C2); ν_{max}/cm^{-1} (film) 2230, 2111, 1636; m/z (ES) [MNa⁺] 317.2 (100%, MNa⁺); HRMS Found: 295.0805 (C₁₃H₁₀F₃N₄O requires *MH* 295.0801).

1-(1,2,3,6-Tetrahydropyridin-1-yl)ethan-1-one, 36v⁶⁵



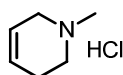
By the method of Stille *et al.*,⁶⁵ acetic anhydride (340 μ L, 3.6 mmol) was added dropwise to a solution of 1,2,3,6-tetrahydropyridine (274 μ L, 3 mmol) and Et₃N (830 μ L, 6 mmol) in CH₂Cl₂ (6 mL, 0.5 M) at 0 °C over ten min. After the addition was completed the mixture was allowed to warm to rt and stirred. After 30 min, sat. aq. NH₄Cl solution (1 mL) was added and layers separated. The organic layer was washed with sat. aq. NaHCO₃ solution (2 \times 3 mL), dried (Na₂SO₄), filtered and concentrated *in vacuo*. Purification by flash chromatography eluting with 95:5 CH₂Cl₂—MeOH gave the ethanone **36v⁶⁵** (223 mg, 60%) as a pale yellow oil, R_f : 0.45 (95:5 CH₂Cl₂—MeOH); δ_H (500 MHz; CDCl₃) 5.93-5.76 (1H, m, 5-H), 5.73-5.59 (1H, m, 4-H), 4.03 (1H, q, J 2.7, 6-H rot A), 3.92 (1 H, q, J 2.7, 6-H rot B), 3.65 (1 H, t, J 5.7, 2-H rot A), 3.50 (1 H, t, J 5.7, 2-H rot B), 2.22-2.11 (2H, m, 3-H), 2.10 (1.6H, s, N-acetyl), 2.08 (1.4H, s, N-acetyl); δ_C (125 MHz; CDCl₃) 169.4 (C=O rot A), 169.2 (C=O rot B), 126.5 (C-5 rot A), 124.8 (C-5 rot B), 124.5 (C-4 rot A), 123.2 (C-4 rot B), 45.6 (C-6 rot A), 43.2 (C-2 rot A), 41.8 (C-6 rot B), 37.9 (C-2 rot A), 25.7 (C-3 rot A), 24.8 (C-3 rot B), 21.9 (N-acetyl rot A), 21.4 (N-acetyl rot B); m/z (ES) [MNa⁺] 148.4 (100%, MNa⁺).

Benzyl 1,2,3,6-tetrahydropyridine-1-carboxylate, **37**⁶⁶



By the method of Larock *et al.*,⁶⁶ benzyl chloroformate (1.14 mL, 8.0 mmol) was added dropwise over ten min to a stirred solution of 1,2,3,6-tetrahydropyridine (457 μ L, 5.0 mmol) in CH_2Cl_2 (50 mL, 0.1 M) and aqueous NaHCO_3 (10.5 mmol, 4 M) at 0 °C. After the addition was completed the mixture was allowed to warm to rt and stirred. After 2 h, H_2O (40 mL) was added and layers separated. The aqueous layer was extracted with CH_2Cl_2 (3 \times 40 mL) and the combined organic layers were dried (Na_2SO_4), filtered and concentrated *in vacuo*, to yield the carbamate **37**,⁶⁶ as a colourless oil which required no further purification. R_f : 0.42 (80:20 Petrol—EtOAc); δ_H (500 MHz; CDCl_3) 7.40-7.37 (2H, m, Ph), 7.36-7.30 (3H, m, Ph), 5.84 (1H, ap. s, b, 5-H), 5.67 (1H, app d, b, J 21, 4-H), 5.16 (2H, s, benzyl-H), 3.97 (2H, quint, J 3.2, 6-H), 3.58 (2H, t, J 5.9, 2-H), 2.16 (2H, s, b, 3-H); δ_C (125 MHz; CDCl_3) 155.6 (C=O), 136.9 (Ph), 135.2 (C-5), 128.7 (Ph), 127.6 (Ph), 126.9 (Ph), 125.4 (C-4), 67.0 (C-6), 40.3 (C-2), 24.9 (C-3); m/z (ES) $[\text{MH}^+]$ 218.3 (100%, MH^+).

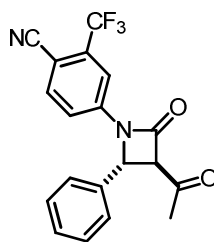
1-methyl-1,2,3,6-tetrahydropyridine hydrochloride, **36w**⁶⁷



The carbamate **37** (650 mg, 3.0 mmol) in THF (1 mL) was added dropwise, over 30 min, to a solution of LiAlH_4 in THF (6 mL, 1M) at 0 °C. The reaction mixture was allowed to warm to rt and then heated to reflux. After 2 h, the reaction mixture was cooled to 0 °C and H_2O (0.5 mL), NaOH (aq, sol., 15% w/v, 0.5 mL) and H_2O (0.5 mL) were sequentially added dropwise. The mixture was allowed to warm to rt and after 15 min filtered through a celite pad eluting with Et_2O (30 mL). The organic layer was extracted with 1 M HCl aqueous solution (2 \times 10mL) and H_2O (2 \times 10mL) and the combined aqueous layers were concentrated *in vacuo* to give the amine HCl salt **36w**,⁶⁷ as a crystalline solid which required no further purification. δ_H (500 MHz; MeOD) 6.06-5.98 (1H, m, 5-H), 5.83-5.74 (1H, m, 4-H), 3.90 (1H, d, J 16.4, 6Ha), 3.70 (1H, d, J 16.4, 6-Hb), 3.59 (1H, dd, J 6.1, 2-Ha), 3.29 (1H,

dt, J 5.1 and 11.8, 2-Hb), 2.99 (3H, s, NMe), 2.71-2.59 (1H, m, 3-Ha), 2.44 (1H, ap d, J 18, 3-Hb); δ_C (125 MHz; MeOD) 126.3 (C-5), 121.0 (C-4), 52.9 (C-6), 51.6 (C-2), 43.2 (NMe), 23.5 (C-3); m/z (ES) [MNa⁺] 120.2 (100%, MNa⁺).

4-(3-Acetyl-2-oxo-4-phenylazetididin-1-yl)-2-(trifluoromethyl)benzonitrile, **25**

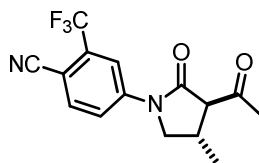


By general procedure F, diazo butanamide **17a** with Rh₂(Oct)₄ in CH₂Cl₂ followed by purification by flash chromatography, eluting with 30:70 Petrol—Et₂O gave the β -lactam **25** as a colourless amorphous solid (128 mg, 71%). R_f : 0.56 (80:20, Et₂O-Hexane); δ_H (500 MHz; CDCl₃) 7.79 (1H, d, J 2.1, Ar 3-H), 7.69 (1H, d, J 8.4, Ar 6-H), 7.45-7.32 (6H, m, Ar 5-H and Ph), 5.55 (1H, d, J 2.8, azetidiny 3-H), 4.29 (1H, d, J 2.8, azetidiny 4-H), 2.40 (3H, s, acetyl H); δ_C (125 MHz; CDCl₃) 197.5 (acetyl C=O), 160.9 (azetidiny C=O), 140.6 (Ar C-4), 136.0 (Ar C-6), 134.8 (Ph), 134.4 (q, ² J_{FC} 33, Ar C-2), 129.7 (Ph), 129.6 (Ph), 126.1 (Ph), 121.8 (q, ¹ J_{FC} 277, CF₃), 119.4 (Ar C-5), 115.3 (Ar C-3), 115.2 (CN), 104.7 (Ar C1), 72.3 (azetidiny C-3), 56.5 (azetidiny C-4), 29.9 (acetyl CH₃); ν_{max}/cm^{-1} (film) 3427, 2927, 2231, 1784, 1705, 1615; m/z (ES) [MNa⁺] 381.08 (100%, MNa⁺); HRMS Found: 381.0825, (C₁₉H₁₃F₃N₂O₂ MNa requires 381.0821).

By general procedure F, diazo butanamide **17a** with Rh₂(OAc)₄ in CH₂Cl₂ followed by purification by flash chromatography, eluting with 30:70 Petrol—Et₂O gave the β -lactam **25** as a colourless amorphous solid (122 mg, 68%).

By general procedure F, diazo butanamide **17a** with Rh₂(esp)₂ in EtOAc followed by purification by flash chromatography, eluting with 30:70 Petrol—Et₂O gave the β -lactam **25** as a colourless amorphous solid (134 mg, 75%).

4-(3-Acetyl-4-methyl-2-oxopyrrolidin-1-yl)-2-(trifluoromethyl)benzonitrile, **26**

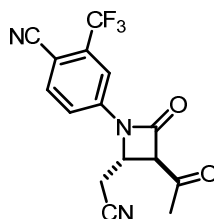


By general procedure F, diazo butanamide **17b** with $\text{Rh}_2(\text{Oct})_4$ in CH_2Cl_2 followed by purification by flash chromatography, eluting with 80:20 Petrol—EtOAc gave the γ -lactam **26** as a pale yellow amorphous solid (136 mg, 88%). R_f : (90:10, CH_2Cl_2 — Et_2O); δ_H (500 MHz; CDCl_3) 8.13 (1H, d, J 2.1, Ar 3-H), 7.93 (1H, dd, J 8.6 and 2.1, Ar 5-H), 7.82 (1H, d, J 8.6, Ar 6H), 4.04 (1H, dd, J 9.6 and 8.1, 5- H_a), 3.46 (2H, m, 5- H_b and 3-H), 3.04 (1H, ap. sept, J 7.2, 4-H), 2.47 (3H, s, acetyl CH_3), 1.24 (3H, d, J 7.2, CH_3); δ_C (125 MHz; CDCl_3) 201.8 (acetyl C=O), 169.9 (C-2), 142.8 (Ar C-4), 135.5 (Ar C-6), 133.7 (q, $^2J_{\text{FC}}$ 30, Ar C-2), 122.1 (q, $^1J_{\text{FC}}$ 275, CF_3), 121.6 (Ar C-5), 117.0 (Ar C-3), 115.4 (CN), 106.1 (Ar C-5), 104.8 (Ar C-1), 64.5 (C-4), 53.4 (C-2), 30.5 (acetyl CH_3), 27.9 (C-3), 18.5 (methyl CH_3); $\nu_{\text{max}}/\text{cm}^{-1}$ (film) 2921, 2236, 1696; m/z (ES) [MNa^+] 333.08 (100%, MNa^+); HRMS Found: 333.08259, ($\text{C}_{15}\text{H}_{13}\text{F}_3\text{N}_2\text{O}_2$ MNa requires 333.0821).

By general procedure F, diazo butanamide **17b** with $\text{Rh}_2(\text{esp})_2$ in CH_2Cl_2 followed by purification by flash chromatography, eluting with 80:20 Petrol—EtOAc gave the γ -lactam **26** as a pale yellow amorphous solid (140 mg, 90%).

By general procedure F, diazo butanamide **17b** with $\text{Rh}_2(\text{OAc})_4$ in CH_2Cl_2 followed by purification by flash chromatography, eluting with 80:20 Petrol—EtOAc gave the γ -lactam **26** as a pale yellow amorphous solid (85 mg, 55%).

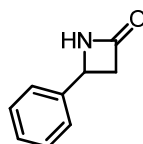
4-[3-Acetyl-2-(cyanomethyl)-4-oxoazetid-1-yl]-2-(trifluoromethyl)benzonitrile, **27**



By general procedure F, diazo butanamide **17i** with $\text{Rh}_2(\text{esp})_2$ in EtOAc followed by purification by flash chromatography, eluting with 50:50 Et_2O — CH_2Cl_2 gave the β -lactam **27** as a pale yellow viscous oil (122 mg, 78%). R_f : 0.35 (50:50, CH_2Cl_2 — Et_2O); δ_H (500 MHz; CDCl_3) 7.86 (1H, d, J 8.6, Ar 6-H), 7.73 (1H, d, J 2.1, Ar 3-H), 7.62 (1H, dd, J 8.6 and 2.1, Ar 5-H), 4.93 (1H, ddd, J 4.6, 2.6 and 2.1, azetidiny 4-H), 4.42 (1H, d, J 2.6, azetidiny 3-H), 3.06 (2H, ap dd, J 5.9 and 4.6, methylene CH_2), 2.44 (3H, s, acetyl CH_3); δ_C (125 MHz; CDCl_3) 196.4 (acetyl C=O), 158.9 (azetidiny C-2), 139.6 (Ar C-4), 136.4 (Ar C-6), 134.8 (q, $^2J_{\text{FC}}$ 33, Ar C-2), 121.8 (q, $^1J_{\text{FC}}$ 277, CF_3), 119.6 (Ar C-5), 114.9 (Ar C-3), 114.3 (Ar CN and CN), 105.7 (Ar C1); 67.9 (azetidiny C-3), 48.7 (azetidiny C-4), 29.7 (acetyl CH_3), 20.3 (methylene CH_2); $\nu_{\text{max}}/\text{cm}^{-1}$ (film) 2922, 2851, 2231, 1767, 1716, 1611; m/z (ES) [MNa^+] 344.06 (100%, MNa^+); HRMS Found: 344.0616, ($\text{C}_{15}\text{H}_{10}\text{F}_3\text{N}_3\text{O}_2$ MNa requires 344.0617).

By general procedure F, diazo butanamide **17i** with $\text{Rh}_2(\text{tpa})_4$ in toluene followed by purification by flash chromatography, eluting with 50:50 Et_2O — CH_2Cl_2 gave the β -lactam **27** as a pale yellow viscous oil (109 mg, 70%).

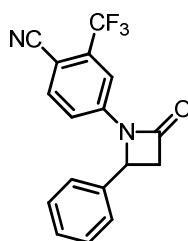
4-Phenylazetid-2-one, **29⁴⁶**



By the method of Lowew *et al.*,⁴⁶ methane sulfonyl chloride (680 μL , 8.8 mmol) was added to a suspension of NaHCO_3 (4.4 g, 48 mmol) in MeCN (44 mL) and the resulting mixture was heated to reflux. Solid (\pm)-3-amino 3-phenyl propionic acid (1.3 g, 8 mmol) was added portionwise to the reaction mixture over a period of 3 h and the reaction mixture was stirred at 80 °C. After 2 h the reaction was allowed to cool to rt, filtered eluting with MeCN

(2 × 75 mL) and concentrated *in vacuo* to give the β -lactam **29**⁴⁶ as a light yellow amorphous solid (1.14 g, 97%) which required no further purification. δ_H (500 MHz; CDCl₃) 7.40-7.35 (4H, m, Ph), 7.35-7.29 (1H, m, Ph), 6.40 (1H, s, b, NH), 4.72 (1H, ap q, *J* 2.6, azetidiny 4-H), 3.44 (1H, dq, *J* 14.8 and 2.6, azetidiny 3-H_a), 2.87 (1H, dd, *J* 14.8 and 2.6, azetidiny 3-H_b); δ_C (125 MHz; CDCl₃) 168.1 (C=O), 140.2 (Ph), 128.9 (Ph), 128.3 (Ph), 125.6 (Ph), 50.4 (azetidiny C-4), 48.0 (azetidiny C-3); $\nu_{\max}/\text{cm}^{-1}$ (film) 3203, 1737, 1704, 1644; *m/z* (EI) [MH⁺] 148.19 (100%, MH⁺).

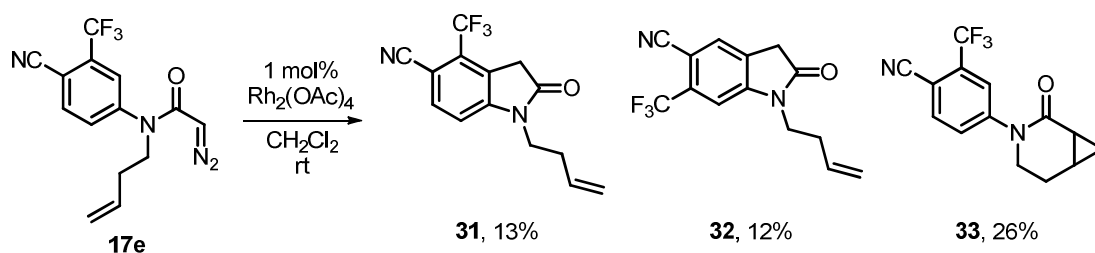
4-(2-Oxo-4-phenylazetid-1-yl)-2-(trifluoromethyl)benzonitrile, **30**



4-Iodo-2(trifluoro)methyl benzonitrile (594 mg, 2.0 mmol) as a solution in dioxane (1 mL) was added to a stirred suspension of the lactam **29** (353 mg, 2.4 mmol), CuI (19 mg, 0.1 mmol), *N,N*-dimethylethylenediamine (22 μ L, 0.2 mmol) and K₃PO₄ (849 mg, 4.0 mmol) in dioxane (1 mL). The reaction mixture was heated to reflux. After 23 h the reaction mixture was allowed to cool to rt and concentrated *in vacuo*. Purification by flash chromatography eluting with 50:40:10 CHCl₃–Hexane–Et₂O gave the arylated *lactam* **30** (481 mg, 76%) as a pale yellow viscous oil. *R*_f: 0.48 (50:50, Hexane-EtOAc); δ_H (500 MHz; CDCl₃) 7.82 (1H, d, *J* 2.1, Ar 3-H), 7.65 (1H, d, *J* 8.5, Ar 6-H), 7.46-7.33 (6H, m, Ar 5-H and Ph), 5.12 (1H, ap q, *J* 2.8, azetidiny 4-H), 3.69 (1H, dd, *J* 15.9 and 6.0, azetidiny 3-H_a), 3.11 (1H, dd, *J* 15.9 and 2.8, azetidiny 3-H_b); δ_C (125 MHz; CDCl₃) 165.1 (C=O), 141.1 (Ar C-4), 136.5 (Ph), 135.9 (Ar C-6), 134.0 (q, ²*J*_{FC} 32, Ar C-2), 129.6 (Ph), 129.3 (Ph), 125.9 (Ph), 121.7 (q, ¹*J*_{FC} 278, CF₃), 118.8 (Ar C-5), 115.5 (Ar C-3), 115.1 (CN); 103.9 (Ar C-1), 54.9 (azetidiny C-4), 47.82 (azetidiny C-3); $\nu_{\max}/\text{cm}^{-1}$ (film) 2224, 1767, 1605; *m/z* (ES) [MNa⁺] 339.07 (100%, MNa⁺); HRMS Found: 339.0718, (C₁₇H₁₁F₃N₂O, MNa requires 339.0716).

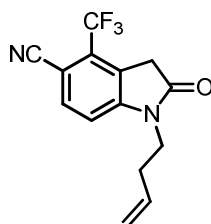
4-(3-Acetyl-2-oxo-4-phenylazetididin-1-yl)-2-trifluoromethyl)benzonitrile, **25 (via alternative route)**

LDA (670 μ L as a 2 M solution in THF/hexane, 1.3 mmol) was added to a stirred solution of the arylated β -lactam **30** (318 mg, 1.0 mmol) in THF at -78 $^{\circ}$ C. After 30 min, MeOAc (315 μ L, 4 mmol) was added and the reaction mixture was stirred at -78 $^{\circ}$ C. After 1 h the reaction mixture was allowed to warm to rt. After 1.5 h, sat. aq. NH_4Cl solution (16 mL) was added and the mixture extracted with Et_2O (3 \times 20 mL). The combined organic layers were dried (Na_2SO_4), filtered and concentrated *in vacuo*. Purification by flash chromatography eluting with 50:40:10 CHCl_3 -Hexane- Et_2O gave the β -lactam **25** (208 mg, 58%) as a colourless amorphous solid.



By general procedure F, diazo butanamide **17e** with $\text{Rh}_2(\text{OAc})_4$ in CH_2Cl_2 followed by purification by flash chromatography, eluting with 95:5 CH_2Cl_2 - Et_2O gave the oxindole **31** (17.9 mg, 13%), the oxindole **32** (16.6 mg, 12%) and the δ -lactam **33** (36.6 mg, 26%). Characterisation data for these compounds is given below.

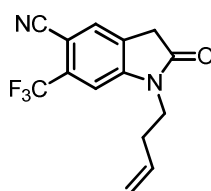
1-(But-3-en-1-yl)-2-oxo-4-(trifluoromethyl)-2,3-dihydro-1H-indole-5-carbonitrile, **31**



R_f : 0.83 (90:10, CH_2Cl_2 - Et_2O); δ_H (500 MHz; CDCl_3) 7.78 (1H, d, J 8.5, 6-H), 7.05 (1H, d, J 8.5, 7-H), 5.78 (1H, ddt, J 16.6, 9.7 and 7.3, butenyl 3-H),

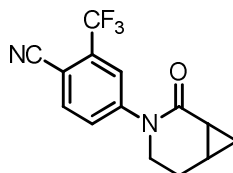
5.09 (1H, dd, J 16.6 and 3.4, butenyl 4-H_A), 5.06 (1H, dd, J 9.7 and 3.4, butenyl 4-H_B), 3.83 (2H, t, J 7.3, butenyl 1-H₂), 3.74 (2H, indole 3-H₂), 2.43 (2H, ap q, J 7.3, butenyl 2-H₂); δ_C (125 MHz; CDCl₃) 173.8 (C-2), 149.0 (C-7a), 135.9 (C-6), 133.5 (C-4), 129.5 (CF₃), 124.3 (C-3a), 118.2 (butenyl C-4), 116.0 (CN), 110.8 (Ar C-1), 102.9 (Ar C-5), 39.8 (butenyl C-1), 35.3 (C-3), 31.5 (butenyl C-2); m/z (ES) [MNa⁺] 303.1 (100%, MNa⁺); HRMS Found: 303.0713 (C₁₄H₁₁F₃N₂O requires MNa 303.0716).

1-(But-3-en-1-yl)-2-oxo-6-(trifluoromethyl)-2,3-dihydro-1H-indole-5-carbonitrile, 32



R_f: 0.52 (9:1, CH₂Cl₂—Et₂O); δ_H (500 MHz; CDCl₃) 7.65 (1H, s, 4-H), 7.15 (1H, s, 7-H), 5.78 (1H, ddt, J 16.7, 9.7 and 7.9, butenyl 3-H₁), 5.08 (1H, dd, J 16.7 and 3.1, butenyl 4-H_A), 5.06 (1H, dd, J 9.7 and 3.1, butenyl 4-H_B), 3.84 (2H, t, J 7.9, butenyl 1-H₂), 3.62 (2H, s, indole 3-H₂), 2.45 (2H, ap. q, J 7.4, butenyl 2-H₂); δ_C (125 MHz; CDCl₃) 173.8 (C-2), 148.7 (C-5), 133.6 (C-7), 129.9 (C-3a), 128.4 (C-4), 118.4 (butenyl C-4), 115.8 (CN), 106.5 (C-6), 102.9 (C-7a), 39.9 (butenyl C-1), 34.9 (C-3), 31.7 (butenyl C-2); m/z (ES) [MNa⁺] 303.1 (100%, MNa⁺); HRMS Found: 303.0707 (C₁₄H₁₁F₃N₂O requires MNa 303.0716).

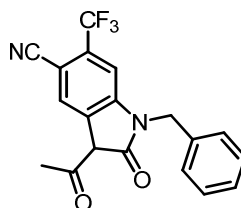
4-[2-Oxo-3-azabicyclo[4.1.0]heptanyl]3-2-(trifluoromethyl)benzonitrile, 33



R_f: 0.24 (9:1, CH₂Cl₂—Et₂O); δ_H (500 MHz; CDCl₃) 7.80 (1H, d, J 8.4, Ar 6-H), 7.75 (1H, d, J 2.5, Ar 3-H), 7.64 (1H, dd, J 8.4 and 2.5, Ar 5-H), 3.62 (1H, ap. ddt J 6.6, 5.6 and 5.2, 4-H_A), 3.54-3.49 (1H, m, 4-H_B), 2.28-2.17 (2H, m 5-H_A and 5-H_B), 1.96 (1H, dddd, J 4.4, 2.8 2.2 and 1.8, 6-H_A), 1.84-1.78 (1H, m, 6-H_B), 1.36 (1H, ap. q, J 4.4 7-H_A), 1.18-1.12 (1H, m, 7-H_B); δ_C (125 MHz;

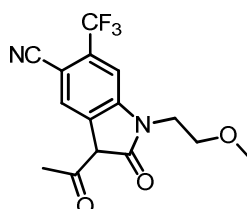
CDCl₃) 171.0 (C-2), 147.2 (Ar C-4), 135.1 (Ar C-6), 133.4 (q ²J_{FC} 33, Ar C-3), 128.2 (Ar C-5), 123.3 (Ar C-3), 121.4 (q ¹J_{FC} 273, CF₃), 115.3 (CN), 106.3 (Ar C-1), 44.6 (C-4), 21.4 (C-5), 18.0 (C-6), 14.6 (C-1), 7.4 (C-7); *m/z* (ES) [MNa⁺] 307.1 (100%, MNa⁺); HRMS Found: 307.0708, (C₁₄H₁₁F₃N₂O requires *MNa* 307.0716).

3-Acetyl-1-benzyl-2-oxo-6-(trifluoromethyl)-2,3-dihydro-1H-indole-5-carbonitrile, **34**



By general procedure F, diazo butanamide **17a** with Rh₂(tfa)₄ in CH₂Cl₂ followed by purification by flash chromatography, eluting with 90:10 CH₂Cl₂—MeOH gave the *dihydroindole* **34** as a colourless amorphous solid (166 mg, 92%). *R_f*: 0.15 (95:5, CH₂Cl₂—MeOH); δ_H (500 MHz; CDCl₃) 7.75 (1H, s, 4-H), 7.37-7.29 (3H, m, Ph), 7.28-7.24 (2H, m, Ph), 7.20 (1H, s, 7-H), 5.11 (2H, s, CH₂-Ph), 2.58 (3H, s, acetyl CH₃) (3-H not observed); δ_C (125 MHz; CDCl₃) 178.6 (acetyl C=O), 170.9 (NH-C=O), 140.2 (C-7a), 134.6 (Ph), 130.4 (C-6), 129.2 (Ph), 128.3 (Ph), 127.6 (q, ¹J_{FC} 278, CF₃), 127.3 (C-3a), 124.7 (C-4), 116.4 (CN), 107.2 (C-7), 105.1 (Ph), 103.1 (C-5), 99.9 (C-3), 43.8 (CH₂-Ph), 21.1 (acetyl CH₃); ν_{max}/cm⁻¹ (film) 3031, 2228, 1661, 1606, 1455; *m/z* (ES) [MNa⁺] 376.1 (100%, MNa⁺); HRMS Found: 359.1001, (C₁₉H₁₃F₃N₂O₂ *MH* requires 359.1002).

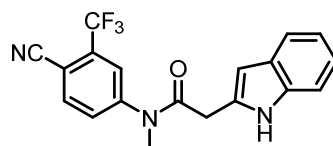
3-Acetyl-1-(2-methoxyethyl)-2-oxo-6-(trifluoromethyl)-2,3-dihydro-1H-indole-5-carbonitrile, **35**



By general procedure F, diazo butanamide **17h** with Rh₂(OAc)₄ in CH₂Cl₂ followed by purification by flash chromatography, eluting with 90:10 CH₂Cl₂—MeOH gave the *dihydroindole* **35** as a pale yellow viscous oil (139

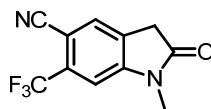
mg, 85%). R_f : 0.10 (95:5, CH₂Cl₂—MeOH); δ_H (500 MHz; CDCl₃) 7.74 (1H, s, 4-H), 7.51 (1H, s, 7-H), 4.10 (2H, t, J 5.6, ethyl-2-H), 3.67 (2H, t, J 5.6, ethyl-1-H), 3.31 (3H, s, OMe), 2.56 (3H, s, acetyl-CH₃) (3-H not observed); δ_C (300 MHz; CDCl₃) 178.4 (acetyl C=O), 171.2 (NH-C=O), 141.1 (C-7a), 129.5 (q, $^2J_{FC}$ 31, C-6), 125.3 (C-3a), 124.5 (C-4), 122.7 (q, $^1J_{FC}$ 278, CF₃), 116.5 (CN), 108.1 (C-7), 102.7 (C-5), 99.9 (C-3), 70.6 (ethyl-C-1), 58.9 (OMe), 40.5 (ethyl-C-2), 20.8 (acetyl-CH₃); ν_{max}/cm^{-1} (film) 3057, 2923, 2230, 1679, 1630; m/z (ES) [MH⁺] 327.1 (100%, MH⁺); HRMS Found: 327.0995, (C₁₅H₁₃F₃N₂O₃ *MH* requires 327.0987).

***N*-[4-Cyano-3-(trifluoromethyl)phenyl]-2-(1H-indol-3-yl)-*N*-methylacetamide, 37a**



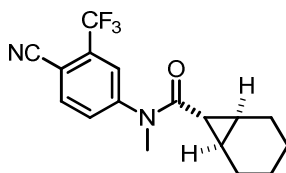
By general procedure G, the diazo-substrate **18k** and co-substrate **36f** with Rh₂(S-DOSP)₄ in CH₂Cl₂ followed by flash chromatography, eluting with 90:10 CH₂Cl₂—Et₂O gave the *acetamide* **37a** as a brown viscous oil (143 mg, 80%). R_f : 0.35 (90:10 CH₂Cl₂—Et₂O); δ_H (500 MHz; CDCl₃) 8.39 (1H, s, br, NH), 7.71 (1H, d, J 8.2, Ar 5-H), 7.48 (1H, s, br, Ar 6-H), 7.40 (2H, ap. d, J 8, Indole 7-H and Ar 2-H), 7.32 (1H, d, J 8.1, Indole 4-H), 7.19 (1H, dt, J 8.2 and 1, Indole 5-H), 7.09 (1H, dt, J 7.5 and 1.0, Indole 6-H), 6.83 (1H, s, br, Indole 3-H), 3.79 (2H, s, CH₂), 3.35 (3H, s, NMe); δ_C (125 MHz; CDCl₃) 171.3 (C=O), 148.0 (Ar C-1), 136.1 (Indole C-3a), 135.7 (Ar C-5), 133.8 (q, $^2J_{CF}$ 33 Ar C-3), 130.1 (Ar C-2), 126.7 (Indole C-7a), 125.02 (Ar C-6), 122.9 (Indole C-3), 122.4 (Indole C-5), 121.6 (q, $^1J_{CF}$ 276 CF₃), 119.8 (Indole C-6), 118.3 (Indole C-7), 114.9 (CN), 111.4 (Indole C-4), 108.0 (Ar C-4), 107.9 (Indole C-2), 37.7 (NMe), 32.3 (CH₂); ν_{max}/cm^{-1} (film) 3466, 3055, 2234, 1664, 1609; m/z (ES) [MH⁺] 358.1 (100%, MH⁺); HRMS Found: 358.1175 (C₁₉H₁₄F₃N₃O *MH* requires 358.1162)

1-(Methyl)-2-oxo-6-(trifluoromethyl)-2,3-dihydro-1H-indole-5-carbonitrile, 37b



By general procedure G, the diazo-substrate **18k** and co-substrate **36f** with $\text{Rh}_2(\text{S-DOSP})_4$ in CH_2Cl_2 followed by flash chromatography, eluting with 90:10 CH_2Cl_2 — Et_2O gave the oxindole **37b** as a colourless amorphous solid (13.1 mg, 11 %). R_f : 0.62 (90:10 CH_2Cl_2 — Et_2O); δ_H (500 MHz; CDCl_3) 7.66 (1H, s, 4-H), 7.16 (1H, s, 7-H), 3.64 (2H, s, 3-H), 3.29 (3H, s, NMe); δ_C (125 MHz; CDCl_3) 174.0 (C-2), 150.0 (C-7a), 129.8 (C-3a), 135.0 (C4), 133.0 (q, $^2J_{\text{CF}}$ 34 C-6), 124.0 (C-7), 121.0 (q, $^1J_{\text{CF}}$ 274, CF_3), 116.0 (CN), 106.0 (C-5), 34.9 (C-3), 26.6 (NMe); $\nu_{\text{max}}/\text{cm}^{-1}$ (film) 2227, 1719; m/z (ES) $[\text{MH}^+]$ 146.0 (100%, MH^+); HRMS Found: 137.0025, ($\text{C}_{11}\text{H}_6\text{N}_2\text{Na}_4\text{O}$ requires MH 137.0029).

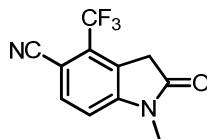
N-[4-Cyano-3-(trifluoromethyl)phenyl]-N-methylbicyclo[4.1.0]heptane-7-carboxamide, 37c



By general procedure G, the diazo-substrate **18k** and co-substrate **36a** with $\text{Rh}_2(\text{S-DOSP})_4$ in CH_2Cl_2 followed by flash chromatography, eluting with 60:40 Petrol—EtOAc gave the carboxamide **37c** (114 mg, 71%). R_f : 0.51 (60:40 Petrol—EtOAc); δ_H (500 MHz; CDCl_3) 7.89 (1H, d, J 8.2, Ar 5-H), 7.70 (1H, d, J 2.2, Ar 2-H), 7.57 (1H, dd, J 8.2 and 2.2, Ar 6-H), 3.40 (3H, s, NMe), 1.92 (2H, ap. q, 2-Ha and 2'-Ha), 1.77-1.71 (2H, m, 1-H and 1'-H), 1.54 (2H, app quint, 2-Hb and 2'-Hb), 1.34-1.20 (2H, m, 3-Ha and 3'-Ha), 1.16 (1H, t, J 4.2, 7-H), 1.07-0.96 (2H, m, 3-Hb and 3'-Hb); δ_C (300 MHz; CDCl_3) 173.7 (C=O), 148.6 (Ar C-1), 135.7 (Aryl C-5), 133.8 (q, $^1J_{\text{CF}}$ 32, Ar C-3), 129.2 (Ar C-6), 124.6 (Ar C-2), 121.9 (q, $^1J_{\text{CF}}$ 276 CF_3), 115.0 (CN), 107.0 (Ar C-4), 37.0 (NMe); 26.5 (C-7), 22.8 (C-1 and C-1'), 22.4 (C-2 and C-2'), 20.9 (C-3 and C-3'); $\nu_{\text{max}}/\text{cm}^{-1}$ (film) 2928, 2855, 2230; m/z (ES) $[\text{MH}^+]$

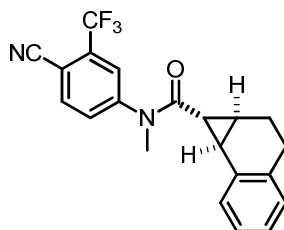
323.2 (100%, MH^+); HRMS Found: 323.1373 ($C_{17}H_{18}F_3N_2O$ requires MH 323.1366).

1-Methyl-2-oxo-4-(trifluoromethyl)-2,3-dihydro-1H-indole-5-carbonitrile, 37d



By general procedure G, the diazo-substrate **18k** and co-substrate **36a** with $Rh_2(S-DOSP)_4$ in CH_2Cl_2 followed by flash chromatography, eluting with 60:40 Petrol—EtOAc gave the oxindole **37d** as a yellow solid (14.2 mg, 12 %). R_f : 0.28 (60:40 Petrol—EtOAc); δ_H (500 MHz; $CDCl_3$) 7.81 (1H, d, J 8.2, 6-H), 7.04 (1H, d, J 8.2, 7-H), 3.76 (2H, s, 3-H), 3.28 (3H, s, NMe); δ_C (125 MHz; $CDCl_3$) 173.2 (C-2), 149.9 (C-7a), 136.2 (C-6), 128.2 (q, $^2J_{CF}$ 30, C4), 124.3 (C-3a), 115.8 (CN), 110.5 (C-7), 102.8 (C-5), 35.1 (C-3), 26.5 (NMe) (CF_3 not observed); ν_{max}/cm^{-1} (film) 2921, 2229, 1752; m/z (ES) [MH^+] 145.1 (100%, MH^+); HRMS Found: 145.1331 ($C_7H_{17}F_3N_2O$ requires MH 145.1335).

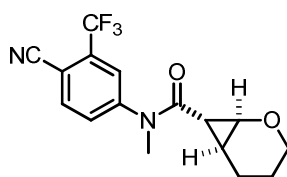
N-[4-cyano-3-(trifluoromethyl)phenyl]-N-methyl-1H,1aH,2H,3H,7bH-cyclopropa[a]naphthalene-1-carboxamide, 37e



By general procedure G, the diazo-substrate **18k** and co-substrate **36m** with $Rh_2(S-DOSP)_4$ in CH_2Cl_2 followed by flash chromatography, eluting with 6:4 Petrol—EtOAc gave the carboxamide **37e** (141 mg, 76%) as a colourless amorphous solid. R_f : 0.39 (60:40 Petrol—EtOAc); δ_H (500 MHz; $CDCl_3$) 7.79 (1H, d, J 8.3, Ar 5-H), 7.66 (1H, d, J 2.0, Ar 2-H), 7.52 (1H, dd, J 8.3 and 2.0, Ar 6-H), 7.28 (1H, dd, J 7.5 and 1.4, Ph 7-H), 7.15 (1H, ddt, J 7.5, 1.4 and 0.8, Ph 6-H), 7.10 (1H, dt, J 7.5 and 1.4, Ph 5-H), 6.97 (1H, d, J 7.5, Ph 4-H), 3.42 (3H, s, NMe), 2.72 (1H, dd, J 8.7 and 3.5, 1-H), 2.63 (1H, dt, J 14.5 and 4.5, 3-Ha), 2.35-2.29 (1H, m, 3-Hb), 2.18-2.10 (2H, m, 2-Ha and 1-aH), 1.93-1.80 (2H, m, 7b-H and 2-Hb); δ_C (125 MHz; $CDCl_3$) 171.6 (C=O),

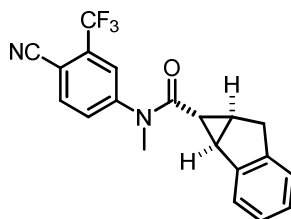
148.1 (Ar C-1), 135.7 (Ar C-5), 134.6 (Ph C-3a), 133.9 (q, $^2J_{CF}$ 33, Ar C-3), 133.4 (Ph-C-7a), 129.1 (Ar C-6), 128.7 (Ph C-7 and C-4), 126.5 (Ph C-6), 126.2 (Ph C-5), 124.4 (Ar C-2), 121.8 (q, $^1J_{CF}$ 274, CF_3), 114.9 (CN), 107.2 (Ar C-4), 37.0 (NMe), 27.11 (C-1), 25.3 (C-2 and C-1a), 24.1 (C-7b), 18.3 (C-3); ν_{max}/cm^{-1} (film) 3022, 2924, 2231, 1661, 1608; m/z (ES) $[MH^+]$ 371.0 (100%, MH^+); HRMS Found: 371.1368 ($C_{21}H_{18}F_3N_2O$ requires MH 371.1366).

N*-[4-cyano-3-(trifluoromethyl)phenyl]-*N*-methyl-2-oxabicyclo[4.1.0]heptane-7-carboxamide, **37f*



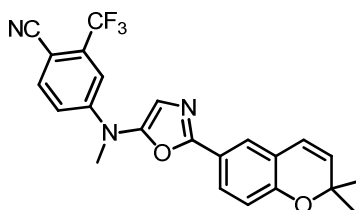
By general procedure G, the diazo-substrate **18k** and co-substrate **36o** with $Rh_2(S-DOSP)_4$ in CH_2Cl_2 followed by flash chromatography, eluting with 1:1 Petrol—EtOAc gave the carboxamide **37f** (133 mg, 82%) as a pale yellow amorphous solid. R_f : 0.15 (60:40 Petrol—EtOAc); δ_H (500 MHz; $CDCl_3$) 7.89 (1H, d, J 8.5, Ar 5-H), 7.71 (1H, d, J 2.3, Ar 2-H), 7.60 (1H, dd, J 8.5 and 2.3, Ar 6-H), 3.96 (1H, dd, J 7.2 and 1.7, Heptane 1-H), 3.53 (1H, dt, J 10.9 and 3.2, Heptane 3-Ha), 3.40 (3H, s, NMe), 3.35 (1H, td, J 11.3 and 1.7, Heptane 3-Hb), 2.04-1.85 (3H, m, Heptane 4-Ha and 4-Hb and Heptane 6-H), 1.58 (1H, d, J 4.7, Heptane 7-H), 1.53-1.46 (1H, m, Heptane 5-Ha), 1.29-1.20 (1H, m, Heptane 5-Hb); δ_C (125 MHz; $CDCl_3$) 171.0 (C=O), 148.2 (Ar C-1), 135.7 (Ar C-5), 133.9 (q, $^2J_{CF}$ 32, Ar C-3); 129.4 (Ar C-6); 124.4 (Ar C-2), 121.6 (q, $^2J_{CF}$ 289, CF_3), 114.9 (CN), 107.2 (Ar C-4), 64.4 (Heptane C-3), 60.8 (Heptane C-1), 36.9 (NMe), 27.1 (Heptane C-7), 22.8 (Heptane C-6), 21.9 (Heptane C-5), 18.6 (Heptane C-4) ν_{max}/cm^{-1} (film) 2933, 2859, 2231, 1655, 1608; m/z (ES) $[MH^+]$ 325.3 (100%, MH^+); HRMS Found: 325.1166 ($C_{16}H_{16}F_3N_2O_2$ requires MH 325.1166).

N*-[4-cyano-3-(trifluoromethyl)phenyl]-*N*-methyl-1*H*,1*aH*,6*H*,6*aH*-cyclopropa[α]indene-1-carboxamide, **37g*



By general procedure G, the diazo-substrate **18k** and co-substrate **36r** with $\text{Rh}_2(\text{esp})_2$ in CH_2Cl_2 followed by flash chromatography, eluting with 60:40 Petrol—EtOAc gave the carboxamide **37g** (130.1 mg, 73%) as a colourless amorphous solid. R_f : 0.35 (60:40 Petrol—EtOAc); δ_H (500 MHz; CDCl_3) 7.81 (1H, d, J 8.3, Ar 5-H), 7.69 (1H, d, J 2.2, Ar 2-H), 7.55 (1H, dd, J 8.3 and 2.2, Ar 6-H), 7.34-7.30 (1H, m, Ph), 7.16-7.09 (3H, m, Ph), 3.41 (3H, s, NMe), 3.31 (1H, dd, J 17.6 and 6.4, 6-Hb), 3.12 (1H, dq, J 6.4 and 1.3, 1a-H), 2.90 (1H, d, J 17.6, 6-Ha), 2.59 (1H, tdd, J 6.5, 3.3 and 0.4, 1-H), 1.00 (1H, s, br, 7-H); δ_C (125 MHz; CDCl_3) 174.2 (C=O), 148.1 (Ar C-1), 143.4 (Ph), 141.8 (Ph), 135.8 (Ar C-5), 133.9 (q, $^2J_{\text{CF}}$ 34, Ar C-3), 129.2 (Ar C-6), 126.5 (Ph), 125.4 (Ph), 124.4 (Ar C-2), 123.8 (Ph), 121.8 (q, $^1J_{\text{CF}}$ 289, CF_3), 114.9 (CN), 107.4 (Ar C-4), 37.2 (NMe), 35.5 (C-6a), 35.1 (C-6), 31.8 (C-1a), 27.5 (C7); $\nu_{\text{max}}/\text{cm}^{-1}$ (film) 2921, 2230, 1665, 1609; m/z (ES) $[\text{MH}^+]$ 357.4 (100%, MH^+); HRMS Found: 379.1039 ($\text{C}_{20}\text{H}_{15}\text{F}_3\text{N}_2\text{NaO}$ requires $M\text{Na}$ 379.1029).

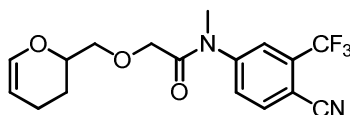
4-[(2-(2,2-Dimethyl-2H-chromen-6-yl)-1,3-oxazol-5-yl)(methyl)amino]-2-(trifluoromethyl)benzonitrile, **37h**



By general procedure G, the diazo-substrate **18k** and co-substrate **36f'** with $\text{Rh}_2(\text{OAc})_4$ in CH_2Cl_2 followed by flash chromatography, eluting with 50:50 Petrol—EtOAc gave the oxazole **37g** (159 mg, 75%) as a bright yellow oil. R_f : 0.62 (50:50 Petrol—EtOAc); δ_H (500 MHz; CDCl_3) 7.74 (1H, dd, J 8.5 and 2.1, chromene 7-H), 7.67 (1H, d, J 8.7, Ar 6-H), 7.62 (1H, d, J 2.1, chromene 5-H), 7.18 (1H, d, J 2.6, Ar 3-H), 7.02 (1H, dd, J 8.7 and 2.6, Ar 5-H), 6.93

(1H, s, oxazole 4-H), 6.84 (1H, d, *J* 8.5, chromene 8-H), 6.36 (1H, d, *J* 9.8, chromene-4H), 5.69 (1H, d, *J* 9.8, chromene 5-H), 3.43 (3H, s, *NMe*), 1.46 (6H, s, chromene 2-*Me*); δ_C (125 MHz; CDCl₃) 159.4 (oxazole C-2), 155.4 (chromene C-8a), 150.1 (Ar C-4), 148.7 (oxazole C-5), 135.9 (Ar C-6), 134.3 (q, $^2J_{CF}$ 33, Ar C-2), 131.6 (chromene C-3), 127.3 (chromene C-7), 124.3 (chromene C-5), 122.2 (q, $^1J_{CF}$ 276, CF₃), 121.6 (chromene C-4), 121.5 (chromene C-4a), 120.1 (oxazole C-4); 116.8 (chromene C-8), 116.5 (Ar C-5), 116.2 (CN), 111.7 (q, $^3J_{CF}$ 5, Ar C-3), 105.0 (chromene C-6), 99.6 (Ar C-1), 77.2 (chromene C-2), 39.6 (*NMe*), 28.2 (Chromene 2-*Me*); ν_{max}/cm^{-1} (film) 2976, 2923, 2224, 1602; *m/z* (ES) [MH⁺] 426.0 (100%, MH⁺); HRMS Found: 426.1428 (C₂₃H₁₉F₃NO₂ requires *MH* 426.1424).

N*-[4-cyano-3-(trifluoromethyl)phenyl]-2-(3,4-dihydro-2*H*-pyran-2-ylmethoxy)-*N*-methylacetamide, **37i*



By general procedure G, the diazo-substrate **18k** and co-substrate **36g'** with Rh₂(*S*-DOSP)₄ in CH₂Cl₂ followed by flash chromatography, eluting with 95:5 CH₂Cl₂—Et₂O gave the carboxamide **37i** (129.3 mg, 73%) as a colourless oil. *R_f*: 0.18 (50:50 Petrol—EtOAc); δ_H (500 MHz; CDCl₃) 7.89 (1H, d, *J* 8.3, Ar 5-H), 7.75 (1H, d, *J* 1.7, Ar 2-H), 7.64 (1H, dd, *J* 8.3 and 1.7, Ar 6-H), 6.33 (1H, d, *J* 6.2, pyran 6-H), 4.69 (1H, ddd, *J* 6.2, 1.4 and 3.2, pyran 5-H), 4.20 (2H, ap. q, *J* 12.6, acetamide 2-H), 3.93 (1H, ddd, *J* 5.6, 3.3 and 2.5, pyran 2-H), 3.58 (2H, ap. d, *J* 5.6, methoxy CH₂), 3.40 (3H, s, *NMe*), 2.14-2.04 (1H, m, pyran 4-Ha), 1.96 (1H, ap. d, *J* 17.4, pyran 4-Hb), 1.77 (1H, ap. dd, *J* 13.5 and 5.8, pyran 3-Ha), 1.67-1.56 (1H, m, pyran 3-Hb); δ_C (125 MHz; CDCl₃) 168.9 (acetamide C-1), 147.2 (Ar C-1), 143.2 (Pyran C-6), 135.8 (Ar C-5), 134.1 (q, $^2J_{CF}$ 34, Ar C-3), 129.3 (Ar C-6), 124.3 (Ar C-2), 121.9 (q, $^1J_{CF}$ 274, CF₃), 114.9 (CN), 107.9 (Ar C-4), 100.6 (pyran C-5), 74.0 (methoxy CH₂), 73.9 (pyran C-2), 70.6 (acetamide C-2), 37.0 (*NMe*), 24.2 (pyran C-3), 19.3 (pyran C-4); ν_{max}/cm^{-1} (film) 3060, 2952, 2231, 1675, 1609; *m/z* (ES) [MNa⁺] 377.0 (100%, MNa⁺); HRMS Found: 377.1094 (C₁₇H₁₇F₃N₂NaO₃ requires *MNa* 377.1083).

7.2.3. Experimental procedures for assaying individual compounds or reaction mixtures from intra- or intermolecular reaction arrays

General Procedure H: Assaying individual compounds using the Invitrogen TR-FRET Androgen Receptor co-activator assay kit – agonist mode.

The assay kit was purchased from Invitrogen and used as instructed. The kit contained the protein, AR LBD-His-GST, the fluorescein-tagged peptide, the Tb³⁺-anti-GST-Ab, co-regulator buffer and DDT.

The biochemical assay was performed in black 384-well plates from Corning (#3676). The plate type was found to be important for high quality reproducible assay results.

Reagents:

Fluorescein-tagged peptide: 100 µM in 50 mM HEPES buffer, pH 7.5, sequence: VESGSSRFMQLFMANDLLT.

AR LBD GST: Rat AR LBD in a buffer pH 7.5, containing protein, stabilising reagents and glycerol (batches were typically supplied at a concentration ranging between 450-550 nmol).

Tb³⁺-anti-GST antibody: 3.3-3.7 µM in 10 mM HEPES buffered saline 137 mM NaCl, 2.7 mM KCl, pH 7.5.

TR-FRET Coregulator buffer: proprietary buffer, pH 7.5, 20% glycerol.

DTT: 1 M in water.

Complete co-regulator buffer A: A solution of 5 mM DTT in TR-FRET co-regulator buffer was prepared freshly before each assay. This solution was then used as the dilution buffer for all materials.

The assay includes three additions per well, in which AR-LBD is added to agonist dilutions or controls, followed by the addition of a pre-mixed fluorescein-tagged peptide/Tb³⁺-anti-GST antibody solution.

A solution of compound in DMSO at 100× the desired maximum assay concentration was prepared (e.g. for testosterone the 100x concentration was 500 µM giving a maximum assay concentration of 5 µM).

A 12-step, 4-fold serial dilution of the compound stock was prepared in DMSO and 1 µL of each dilution point was added to 49 µL of complete co-regulator buffer A. 10 µL of the resulting solution were added to each well in rows A to C, columns 1-12 of a 384 well plate.

Positive Control: A 10 µM solution of testosterone was prepared by adding 2 µL of 500 µM of testosterone in DMSO to 98 µL of complete co-regulator buffer A and 5 µL of this solution were added to each well in row D columns 5 to 8 of the 384 well plate.

Negative Control: A solution of 2% DMSO in complete co-regulator buffer A was prepared and 5 µL of this solution were added to each well in row D, columns 1 to 4 and 9 to 12 of the 384 well plate.

Diffusion TR-FRET baseline control: 10 µL of complete co-regulator buffer A were added to each well in row D, columns 9 to 12 of the 384 well plate.

A 5 nM solution of the AR-LBD in complete co-regulator buffer A was prepared. 5 µL of this solution were added to each well rows A to C, columns 1 to 12 and row D columns 1 to 8, of the 384 well plate.

A solution with a final concentration of 500 nM of the fluorescein-tagged peptide and 5 nM of the Tb³⁺-anti-GST antibody respectively in complete co-regulator buffer A was prepared. 5 µL of this solution were added to each well rows A to D, columns 1 to 12 of the 384 well plate.

Representative 384-well plate layout:

	1	2	3	4	5	6	7	8	9	10	11	12
A	Agonist in serial dilution in triplicate											
B												
C												
D	Negative Control				Positive Control				Diffusion TR-FRET Control			

The plate was left to equilibrate for 2-4 h and read using a Perkin-Elmer Envision 2103 Multilabel Reader with a 340 nm excitation filter (14 nm bandwidth for the Tb³⁺) and 495nm (14 nm bandwidth, for the Tb³⁺) and 520 nm (10 nm bandwidth, for the fluorescein) emission filters and a 400 nm dichroic mirror, with a delay window of 100 μ s and an integration window of 200 μ s. 5 repeat measurements were obtained and the results of each measurement were averaged during data processing. Each assay was performed at least twice with a z' factor > 0.85.

The results were normalised by dividing the TR-FRET ratio of each well (emission at 520 nm / emission at 495 nm) by the average baseline TR-FRET ratio.

General Procedure I: Assaying reaction mixtures from the microreaction arrays using the Invitrogen TR-FRET Androgen Receptor co-activator assay kit – agonist mode.

Stock solutions were prepared as indicated in General Procedure H (above).

Each microreaction stock solution of $\Sigma[P_n] = 100$ mM in DMSO was diluted to give a stock assay solutions of $\Sigma[P_n] = 1$ mM, 0.1 mM and 0.01 mM in DMSO, appropriately, for the intramolecular reaction arrays one, two and three, respectively. This solution was used as the 100x agonist solution. Similarly, for the intermolecular reaction arrays, each stock solution was diluted to give a stock assay solutions of $\Sigma[P_n] = 1$ mM, 5 mM and 0.1 mM in DMSO, appropriately for the intermolecular reaction arrays one, two and three, respectively.

1 μL of each 100 \times agonist solution was added to 49 μL of complete co-regulator buffer A. 10 μL of the resulting solution were added to duplicate wells in a 384 well plate

Positive Control: A 5 μM solution of testosterone was prepared by adding 2 μL of 500 μM of testosterone in DMSO to 98 μL of complete co-regulator buffer A and 5 μL of this solution were added to each well in row D columns 5 to 8 of the 384 well plate.

Negative Control: A solution of 2% DMSO in complete co-regulator buffer A was prepared and 5 μL of this solution were added to each well in row A, columns 1 to 4 and 9 to 12 of the 384 well plate.

Diffusion TR-FRET baseline control: 10 μL of complete co-regulator buffer A were added were added to each well in row A, columns 9 to 12 of the 384 well plate.

A 5 nM solution of the AR-LBD in complete co-regulator buffer A was prepared. 5 μL of this solution were added to each well of the plate with the exception of row A, columns 9 to 12 (Diffusion TR-FRET baseline control).

A solution with a final concentration of 500 nM of the fluorescein-tagged peptide and 5 nM of the Tb^{3+} -anti-GST antibody respectively in complete co-regulator buffer A was prepared. 5 μL of this solution were added to each well of the 384 well plate.

Intramolecular reaction arrays:

For the first reaction array the final assay concentration was $\Sigma[\text{P}_n] = 10 \mu\text{M}$.

For the second reaction array the final assay concentrations were $\Sigma[\text{P}_n] = 10 \mu\text{M}$ and 1 μM .

For the third reaction array the final assay concentrations were $\Sigma[\text{P}_n] = 1 \mu\text{M}$ and 100 nM.

Intermolecular reaction arrays:

For the first reaction array the final assay concentration was $\Sigma[\text{P}_n] = 10 \mu\text{M}$.

For the second reaction array the final assay concentrations were $\Sigma[\text{P}_n] = 10 \mu\text{M}$ and 5 μM .

For the third reaction array the final assay concentrations were $\Sigma[P_n] = 5 \mu\text{M}$ and $1 \mu\text{M}$.

The plate was left to equilibrate for 2-4 h and read using a Perkin-Elmer Envision 2103 Multilabel Reader (see General Method F for optical configuration). 5 repeat measurements were obtained and the results of each measurement were averaged during data processing. Each assay was performed at least twice with a z' factor > 0.85 .

The results were normalised by dividing the TR-FRET ratio of each well (emission at 520 nm / emission at 495 nm) by the average baseline TR-FRET ratio. These results were transformed into an activity percentage, by setting the normalised TR-FRET ratio of the positive control as 100% and the normalised TR-FRET ratio of the negative control as 0%.

7.2.4. Experimental procedure for the metal scavenging studies

1 mM solutions of $\text{Rh}_2(\text{OAc})_4$ in CH_2Cl_2 and THF and $\text{Rh}_2(\text{pfb})_4$ in toluene and EtOAc were prepared. 100 μL of $\text{Rh}_2(\text{OAc})_4$ in CH_2Cl_2 were added to the wells of column A, rows 1-7 of a custom made 96-well PTFE plate. 100 μL of $\text{Rh}_2(\text{OAc})_4$ in THF were added to the wells of column B, rows 1-6 of the 96-well plate. 100 μL of $\text{Rh}_2(\text{pfb})_4$ in toluene were added to the wells of column C, rows 1-6 of the 96-well plate. 100 μL of $\text{Rh}_2(\text{pfb})_4$ in EtOAc were added to the wells of column D, rows 1-6 of the 96-well plate. Increasing amounts of QuadraPure TU resin were added to the wells in column A, rows 2-7, column B, rows 2-6, column C rows 2-6 and column D, rows 2-6. In the wells in columns A, B, C and D of row 1 no resin was added and served as negative control. The wells were sealed using disposable sealing caps and left to scavenge. After 24 h the wells were unsealed and aliquots of the resulting solutions were run through the microanalyser and compared against a calibration curve produced from three standard solutions (for rhodium: 5 ppm, 10 ppm and 15 ppm).

Table 7.1: Percentage of metal removed by the addition of different amounts of QuadraPure TU resin in different solutions of Rh^(II) catalysts.

Entry	QP TU resin (mg)	Metal conc in solution (ppm)	% of metal removed	Solvent	Catalyst
1	0	475	1	THF	Rh ₂ (OAc) ₄
2	5.91	342	29	THF	Rh ₂ (OAc) ₄
3	14.53	78	84	THF	Rh ₂ (OAc) ₄
4	18.29	14	97	THF	Rh ₂ (OAc) ₄
5	25.47	8	98	THF	Rh ₂ (OAc) ₄
6	38.72	8	98	THF	Rh ₂ (OAc) ₄
7	0	341	0	CH ₂ Cl ₂	Rh ₂ (OAc) ₄
8	4.97	253	26	CH ₂ Cl ₂	Rh ₂ (OAc) ₄
9	10.55	99	71	CH ₂ Cl ₂	Rh ₂ (OAc) ₄
10	15.62	37	89	CH ₂ Cl ₂	Rh ₂ (OAc) ₄
11	19.83	8	98	CH ₂ Cl ₂	Rh ₂ (OAc) ₄
12	28.56	6	98	CH ₂ Cl ₂	Rh ₂ (OAc) ₄
13	47.68	5	99	CH ₂ Cl ₂	Rh ₂ (OAc) ₄
14	0	1210	2	Toluene	Rh ₂ (pfb) ₄
15	4.2	998	19	Toluene	Rh ₂ (pfb) ₄

16	5.9	798	35	Toluene	Rh ₂ (pfb) ₄
17	11.8	349	72	Toluene	Rh ₂ (pfb) ₄
18	17.8	31	97	Toluene	Rh ₂ (pfb) ₄
19	30.5	14	99	Toluene	Rh ₂ (pfb) ₄
20	0	1176	0	EtOAc	Rh ₂ (pfb) ₄
21	7.7	672	43	EtOAc	Rh ₂ (pfb) ₄
22	14.18	246	79	EtOAc	Rh ₂ (pfb) ₄
23	20.13	32	97	EtOAc	Rh ₂ (pfb) ₄
24	24.17	26	98	EtOAc	Rh ₂ (pfb) ₄
25	29.11	24	98	EtOAc	Rh ₂ (pfb) ₄

7.2.5. Experimental procedure for quantitative HPLC analysis of product mixtures containing the β -lactam **25**

Three solutions of the β -lactam **25** in MeOH–DMSO (50:50), 0.8 mg/mL, 0.4 mg/mL and 0.15 mg/mL, were prepared and used as standard solutions to produce a calibration curve. These solutions were run on an Agilent 1290 Infinity LC system, equipped with a PHENOMENEX LUNA 3 μ Phenyl-Hexyl column (75x46 mm), eluting with a 5-95% gradient over 32 minutes of a MeCN–water–0.1% TFA solution, with a flow rate of 0.5 mL/min. The product was identified to have a retention time of 21.2 minutes ($\lambda_{\text{abs}} = 254$ nm) and a peak area of 253.7 mAUxmin (96%) for the 0.8 mg/mL sample. Aliquots from the intramolecular reaction array 3 were diluted in MeOH–DMSO (50:50) accordingly, analysed using the above conditions and the yield of the product determined.

% of activity at $\Sigma[\text{P}_n] = 100$ nM	Yield 25 %	Solvent	Catalyst
24.4	71.8	DCM	Rh ₂ (OAc) ₄
9.6	4.7	DCM	Rh ₂ (tfa) ₄
19.1	45.4	DCM	Rh ₂ (esp) ₂
10.3	12.1	DCM	Rh ₂ (pfb) ₄
10.7	26.0	DCM	Rh ₂ (tpa) ₄
24.0	72.5	DCM	Rh ₂ (oct) ₄
21.8	58.7	PhMe	Rh ₂ (OAc) ₄
7.6	2.2	PhMe	Rh ₂ (tfa) ₄
19.3	47.1	PhMe	Rh ₂ (esp) ₂
9.9	8.8	PhMe	Rh ₂ (pfb) ₄
15.7	35.3	PhMe	Rh ₂ (tpa) ₄
17.7	45.8	PhMe	Rh ₂ (oct) ₄
22.9	59.1	EtOAc	Rh ₂ (OAc) ₄
9.1	4.3	EtOAc	Rh ₂ (tfa) ₄
23.8	70.3	EtOAc	Rh ₂ (esp) ₂
6.8	1.4	EtOAc	Rh ₂ (pfb) ₄
21.6	58.1	EtOAc	Rh ₂ (tpa) ₄
6.2	0.0	EtOAc	Rh ₂ (oct) ₄

8. References

- (1) (a) Zheng, X. S.; Chan, T.-F.; Zhou, H. H. *Chem. Biol.* **2004**, *11*, 609; (b) Rix, U.; Superti-Furga, G. *Nat. Chem. Biol.* **2009**, *5*, 616.
- (2) Walsh, D. P.; Chang, Y.-T. *Chem. Rev.* **2006**, *106*, 2476.
- (3) Lipinski, C.; Hopkins, A. *Nature* **2004**, *432*, 855.
- (4) (a) Bonfanti, J.-F.; Doublet, F.; Fortin, J.; Lacrampe, J.; Guillemont, J.; Muller, P.; Queguiner, L.; Arnoult, E.; Gevers, T.; Janssens, P.; Szel, H.; Willebrords, R.; Timmerman, P.; Wuyts, K.; Janssens, F.; Sommen, C.; Wigerinck, P.; Andries, K. *J. Med. Chem.* **2007**, *50*, 4572; (b) Bonfanti, J.-F.; Meyer, C.; Doublet, F.; Fortin, J.; Muller, P.; Queguiner, L.; Gevers, T.; Janssens, P.; Szel, H.; Willebrords, R.; Timmerman, P.; Wuyts, K.; van Remoortere, P.; Janssens, F.; Wigerinck, P.; Andries, K. *J. Med. Chem.* **2008**, *51*, 875; (c) Ishioka, T.; Kubo, A.; Koiso, Y.; Nagasawa, K.; Itai, A.; Hashimoto, Y. *Bioorg. Med. Chem.* **2002**, *10*, 1555; (d) Martinborough, E.; Shen, Y.; van Oeveren, A.; Long, Y. O.; Lau, T. L. S.; Marschke, K. B.; Chang, W. Y.; López, F. J.; Vajda, E. G.; Rix, P. J.; Viveros, O. H.; Negro-Vilar, A.; Zhi, L. *J. Med. Chem.* **2007**, *50*, 5049; (e) van Oeveren, A.; Motamedi, M.; Mani, N. S.; Marschke, K. B.; López, F. J.; Schrader, W. T.; Negro-Vilar, A.; Zhi, L. *J. Med. Chem.* **2006**, *49*, 6143.
- (5) Lovering, F.; Bikker, J.; Humblet, C. *J. Med. Chem.* **2009**, *52*, 6752.
- (6) Dow, M.; Fisher, M.; James, T.; Marchetti, F.; Nelson, A. *Org. Biomol. Chem.* **2012**, *10*, 17.
- (7) (a) Hotchkiss, T.; Kramer, H. B.; Doores, K. J.; Gamblin, D. P.; Oldham, N. J.; Davis, B. G. *Chem. Commun.* **2005**, 4264; (b) Zameo, S.; Vauzeilles, B.; Beau, J.-M. *Angew. Chem. Int. Ed.* **2005**, *44*, 965.
- (8) Horswill, A. R.; Savinov, S. N.; Benkovic, S. J. *Proc. Natl. Acad. Sci. U.S.A.* **2004**, *101*, 15591.
- (9) Naumann, T. A.; Tavassoli, A.; Benkovic, S. J. *ChemBioChem* **2008**, *9*, 194.
- (10) Tavassoli, A.; Benkovic, S. J. *Angew. Chem. Int. Ed.* **2005**, *44*, 2760.

- (11) Clark, M. A.; Acharya, R. A.; Arico-Muendel, C. C.; Belyanskaya, S. L.; Benjamin, D. R.; Carlson, N. R.; Centrella, P. A.; Chiu, C. H.; Creaser, S. P.; Cuozzo, J. W.; Davie, C. P.; Ding, Y.; Franklin, G. J.; Franzen, K. D.; Gefter, M. L.; Hale, S. P.; Hansen, N. J. V.; Israel, D. I.; Jiang, J.; Kavarana, M. J.; Kelley, M. S.; Kollmann, C. S.; Li, F.; Lind, K.; Mataruse, S.; Medeiros, P. F.; Messer, J. A.; Myers, P.; O'Keefe, H.; Oliff, M. C.; Rise, C. E.; Satz, A. L.; Skinner, S. R.; Svendsen, J. L.; Tang, L.; van Vloten, K.; Wagner, R. W.; Yao, G.; Zhao, B.; Morgan, B. A. *Nat. Chem. Biol.* **2009**, *5*, 647.
- (12) (a) Melkko, S.; Zhang, Y.; Dumelin, C. E.; Scheuermann, J.; Neri, D. *Angew. Chem. Int. Ed.* **2007**, *46*, 4671; (b) Melkko, S.; Scheuermann, J.; Dumelin, C. E.; Neri, D. *Nat. Biotech.* **2004**, *22*, 568.
- (13) Scheuermann, J.; Dumelin, C. E.; Melkko, S.; Zhang, Y.; Mannocci, L.; Jaggi, M.; Sobek, J.; Neri, D. *Bioconjugate Chem.* **2008**, *19*, 778.
- (14) Dumelin, C. E.; Scheuermann, J.; Melkko, S.; Neri, D. *Bioconjugate Chem.* **2006**, *17*, 366.
- (15) (a) Rozenman, M. M.; Liu, D. R. *ChemBioChem* **2006**, *7*, 253; (b) Rozenman, M. M.; Kanan, M. W.; Liu, D. R. *J. Am. Chem. Soc.* **2007**, *129*, 14933.
- (16) Gartner, Z. J.; Grubina, R.; Calderone, C. T.; Liu, D. R. *Angew. Chem. Int. Ed.*, **2003**, *42*, 1370.
- (17) (a) Gartner, Z. J.; Kanan, M. W.; Liu, D. R. *Angew. Chem. Int. Ed.*, **2002**, *41*, 1796; (b) Gartner, Z. J.; Tse, B. N.; Grubina, R.; Doyon, J. B.; Snyder, T. M.; Liu, D. R. *Science* **2004**, *305*, 1601.
- (18) Snyder, T. M.; Tse, B. N.; Liu, D. R. *J. Am. Chem. Soc.* **2008**, *130*, 1392.
- (19) Doyon, J. B.; Snyder, T. M.; Liu, D. R. *J. Am. Chem. Soc.* **2003**, *125*, 12372.
- (20) Driggers, E. M.; Hale, S. P.; Lee, J.; Terrett, N. K. *Nat. Rev. Drug Discov.* **2008**, *7*, 608.
- (21) Gartner, Z. J.; Liu, D. R. *J. Am. Chem. Soc.* **2001**, *123*, 6961.
- (22) (a) Quinton, J.; Kolodych, S.; Chaumonet, M.; Bevilacqua, V.; Nevers, M.-C.; Volland, H.; Gabillet, S.; Thuéry, P.; Créminon, C.; Taran, F. *Angew. Chem. Int. Ed.* **2012**, *51*, 6144; (b) Sambasivan, R.; Ball, Z. T.

- Angew. Chem. Int. Ed.* **2012**; (c) McNally, A.; Prier, C. K.; MacMillan, D. W. C. *Science* **2011**, 334, 1114; (d) Robbins, D. W.; Hartwig, J. F. *Science* **2011**, 333, 1423.
- (23) Huang, Y.-L.; Bode, J. W. *Nat. Chem.* **2014**, 6, 877.
- (24) Fox, S.; Farr-Jones, S.; Sopchak, L.; Boggs, A.; Nicely, H. W.; Khoury, R.; Biros, M. *J. Biomol. Screen.* **2006**, 11, 864.
- (25) (a) Padwa, A.; Weingarten, M. D. *Chem. Rev.* **1996**, 96, 223; (b) Padwa, A.; Bur, S. K. *Tetrahedron* **2007**, 63, 5341.
- (26) Davies, H. M. L.; Coleman, M. G.; Ventura, D. L. *Org. Lett.* **2007**, 9, 4971.
- (27) Padwa, A.; Austin, D. J.; Price, A. T.; Semones, M. A.; Doyle, M. P.; Protopopova, M. N.; Winchester, W. R.; Tran, A. *J. Am. Chem. Soc.* **1993**, 115, 8669.
- (28) Davies, H. M. L.; Beckwith, R. E. J. *Chem. Rev.* **2003**, 103, 2861.
- (29) Doyle, M. P.; Duffy, R.; Ratnikov, M.; Zhou, L. *Chem. Rev.* **2009**, 110, 704.
- (30) Gao, W.; Bohl, C. E.; Dalton, J. T. *Chem. Rev.* **2005**, 105, 3352.
- (31) Féau, C. m.; Arnold, L. A.; Kosinski, A.; Zhu, F.; Connelly, M.; Guy, R. K. *ACS Chem. Biol.* **2009**, 4, 834.
- (32) Christiansen, R. G.; Bell, M. R.; D'Ambra, T. E.; Mallamo, J. P.; Herrmann, J. L.; Ackerman, J. H.; Opalka, C. J.; Kullnig, R. K.; Winneker, R. C. *J. Med. Chem.* **1990**, 33, 2094.
- (33) (a) Singh, S. M.; Gauthier, S.; Labrie, F. *Curr. Med. Chem.* **2000**, 7, 211; (b) Fang, H.; Tong, W.; Branham, W. S.; Moland, C. L.; Dial, S. L.; Hong, H.; Xie, Q.; Perkins, R.; Owens, W.; Sheehan, D. M. *Chem. Res. Toxicol.* **2003**, 16, 1338; (c) Gao, W.; Dalton, J. T. *Drug Discovery Today* **2007**, 12, 241.
- (34) Fujii, S.; Ohta, K.; Goto, T.; Oda, A.; Masuno, H.; Endo, Y.; Kagechika, H. *Med. Chem. Commun.* **2012**, 3, 680.
- (35) (a) Ghosh, A.; Sieser, J. E.; Caron, S.; Couturier, M.; Dupont-Gaudet, K.; Girardin, M. *J. Org. Chem.* **2005**, 71, 1258; (b) Wolfe, J. P.; Buchwald, S. L. *J. Org. Chem.* **1997**, 62, 6066; (c) Wolfe, J. P.; Buchwald, S. L. *J. Org. Chem.* **2000**, 65, 1144.

- (36) (a) Zhang, H.; Cai, Q.; Ma, D. *J. Org. Chem.* **2005**, *70*, 5164; (b) Yin, J.; Buchwald, S. L. *J. Am. Chem. Soc.* **2002**, *124*, 6043.
- (37) Padwa, A.; Hertzog, D. L.; Nadler, W. R.; Osterhout, M. H.; Price, A. T. *J. Org. Chem.* **1994**, *59*, 1418.
- (38) Maier, M. E.; Evertz, K. *Tetrahedron Lett.* **1988**, *29*, 1677.
- (39) Miriyala, B.; Williamson, J. S. *Tetrahedron Lett.* **2003**, *44*, 7957.
- (40) Sabot, C.; Kumar, K. A.; Meunier, S.; Mioskowski, C. *Tetrahedron Lett.* **2007**, *48*, 3863.
- (41) Ozers, M. S.; Marks, B. D.; Gowda, K.; Kupcho, K. R.; Ervin, K. M.; De Rosier, T.; Qadir, N.; Eliason, H. C.; Riddle, S. M.; Shekhani, M. S. *Biochemistry* **2006**, *46*, 683.
- (42) Sigma-Aldrich
<http://www.sigmaaldrich.com/catalog/product/aldrich/655422>
Accessed 04/03/2015.
- (43) Davies, H. M. L.; Hedley, S. J. *Chem. Soc. Rev.* **2007**, *36*, 1109.
- (44) Snyder, L. R. *J. Chrom. Sci.* **1978**, *16*, 223.
- (45) Tran, C.; Ouk, S.; Clegg, N. J.; Chen, Y.; Watson, P. A.; Arora, V.; Wongvipat, J.; Smith-Jones, P. M.; Yoo, D.; Kwon, A.; Wasielewska, T.; Welsbie, D.; Chen, C. D.; Higano, C. S.; Beer, T. M.; Hung, D. T.; Scher, H. I.; Jung, M. E.; Sawyers, C. L. *Science* **2009**, *324*, 787.
- (46) Loewe, M. F.; Cvetovich, R. J.; Hazen, G. G. *Tetrahedron Lett.* **1991**, *32*, 2299.
- (47) Klapars, A.; Antilla, J. C.; Huang, X.; Buchwald, S. L. *J. Am. Chem. Soc.* **2001**, *123*, 7727.
- (48) Kim, B. J.; Park, Y. S.; Beak, P. *J. Org. Chem.* **1999**, *64*, 1705.
- (49) Davies, H. M. L.; Morton, D. *Chem. Soc. Rev.* **2011**, *40*, 1857.
- (50) Kennedy, A. R.; Taday, M. H.; Rainier, J. D. *Org. Lett.* **2001**, *3*, 2407.
- (51) Wenkert, E.; Alonso, M. E.; Gottlieb, H. E.; Sanchez, E. L.; Pellicciari, R.; Cogolli, P. *J. Org. Chem.* **1977**, *42*, 3945.
- (52) Doyle, M. P.; Buhro, W. E.; Davidson, J. G.; Elliott, R. C.; Hoekstra, J. W.; Oppenhuizen, M. *J. Org. Chem.* **1980**, *45*, 3657.
- (53) (a) Gordon, T.; Hansen, P.; Morgan, B.; Singh, J.; Baizman, E.; Ward, S. *Bioorg. Med. Chem. Lett.* **1993**, *3*, 915; (b) McBriar, M. D.; Clader, J. W.; Chu, I.; Del Vecchio, R. A.; Favreau, L.; Greenlee, W. J.; Hyde,

- L. A.; Nomeir, A. A.; Parker, E. M.; Pissarnitski, D. A.; Song, L.; Zhang, L.; Zhao, Z. *Bioorg. Med. Chem. Lett.* **2008**, *18*, 215; (c) Meanwell, N. A. *J. Med. Chem.* **2011**, *54*, 2529.
- (54) (a) McBriar, M. D.; Clader, J. W.; Chu, I.; Del Vecchio, R. A.; Favreau, L.; Greenlee, W. J.; Hyde, L. A.; Nomeir, A. A.; Parker, E. M.; Pissarnitski, D. A. *Bioorg. Med. Chem. Lett.* **2008**, *18*, 215; (b) TulasíaKirla, K.; SingháDeora, G. *Org. Biomol. Chem.* **2013**, *11*, 3103.
- (55) (a) Cecchetti, V.; Fravolini, A.; Palumbo, M.; Sissi, C.; Tabarrini, O.; Terni, P.; Xin, T. *J. Med. Chem.* **1996**, *39*, 4952; (b) Suckling, C. J. *Angew. Chem. Int. Ed.* **1988**, *27*, 537; (c) Wentland, M. P.; Lesher, G. Y.; Reuman, M.; Gruett, M. D.; Singh, B.; Aldous, S. C.; Dorff, P. H.; Rake, J. B.; Coughlin, S. A. *J. Med. Chem.* **1993**, *36*, 2801.
- (56) (a) Axerio-Cilies, P.; Lack, N. A.; Nayana, M. R. S.; Chan, K. H.; Yeung, A.; Leblanc, E.; Guns, E. S. T.; Rennie, P. S.; Cherkasov, A. *J. Med. Chem.* **2011**, *54*, 6197; (b) Sack, J. S.; Kish, K. F.; Wang, C.; Attar, R. M.; Kiefer, S. E.; An, Y.; Wu, G. Y.; Scheffler, J. E.; Salvati, M. E.; Krystek, S. R. *Proc. Natl. Acad. Sci. U.S.A.* **2001**, *98*, 4904.
- (57) (a) Ehmann, D. E.; Jahić, H.; Ross, P. L.; Gu, R.-F.; Hu, J.; Kern, G.; Walkup, G. K.; Fisher, S. L. *Proc. Natl. Acad. Sci. U.S.A.* **2012**, *109*, 11663; (b) Hugonnet, J.-E.; Blanchard, J. S. *Biochemistry* **2007**, *46*, 11998.
- (58) (a) Inglese, J.; Johnson, R. L.; Simeonov, A.; Xia, M.; Zheng, W.; Austin, C. P.; Auld, D. S. *Nat. Chem. Biol.* **2007**, *3*, 466; (b) Moshinsky, D. J.; Ruslim, L.; Blake, R. A.; Tang, F. *J. Biomol. Screen.* **2003**, *8*, 447.
- (59) (a) Fürstner, A.; Alcarazo, M.; Goddard, R.; Lehmann, C. W. *Angew. Chem. Int. Ed.* **2008**, *47*, 3210; (b) Harrak, Y.; Blaszykowski, C.; Bernard, M.; Cariou, K.; Mainetti, E.; Mouriès, V.; Dhimane, A.-L.; Fensterbank, L.; Malacria, M. *J. Am. Chem. Soc.* **2004**, *126*, 8656; (c) Karad, S. N.; Bhunia, S.; Liu, R.-S. *Angew. Chem. Int. Ed.* **2012**, *51*, 8722.
- (60) Guo, C.; Sahoo, B.; Daniliuc, C. G.; Glorius, F. *J. Am. Chem. Soc.* **2014**, *136*, 17402.

- (61) Sato, S.; Sakamoto, T.; Miyazawa, E.; Kikugawa, Y. *Tetrahedron* **2004**, *60*, 7899.
- (62) Taillier, C.; Hameury, T.; Bellosta, V.; Cossy, J. *Tetrahedron* **2007**, *63*, 4472.
- (63) Koziara, A.; Osowska-Pactwicka, K.; Zawadzki, S.; Zwierzak, A. *Synthesis* **1985**, *1985*, 202.
- (64) Girard, A.-L.; Lhermet, R.; Fressigné, C.; Durandetti, M.; Maddaluno, J. *Eur. J. Org. Chem.* **2012**, *2012*, 2895.
- (65) Stille, J. K.; Becker, Y. *J. Org. Chem.* **1980**, *45*, 2139.
- (66) Larock, R. C.; Wang, Y. *Tetrahedron Lett.* **2002**, *43*, 21.
- (67) Assaad, T.; Mavel, S.; Parsons, S. M.; Kruse, S.; Galineau, L.; Allouchi, H.; Kassiou, M.; Chalon, S.; Guilloteau, D.; Emond, P. *Bioorg. Med. Chem. Lett.* **2006**, *16*, 2654.

Efficient discovery of bioactive scaffolds by activity-directed synthesis

George Karageorgis^{1,2}, Stuart Warriner^{1,2*} and Adam Nelson^{1,2*}

The structures and biological activities of natural products have often provided inspiration in drug discovery. The functional benefits of natural products to the host organism steers the evolution of their biosynthetic pathways. Here, we describe a discovery approach—which we term activity-directed synthesis—in which reactions with alternative outcomes are steered towards functional products. Arrays of catalysed reactions of α -diazo amides, whose outcome was critically dependent on the specific conditions used, were performed. The products were assayed at increasingly low concentration, with the results informing the design of a subsequent reaction array. Finally, promising reactions were scaled up and, after purification, submicromolar ligands based on two scaffolds with no previous annotated activity against the androgen receptor were discovered. The approach enables the discovery, in tandem, of both bioactive small molecules and associated synthetic routes, analogous to the evolution of biosynthetic pathways to yield natural products.

The astonishing functional and structural diversity of natural products continues to provide tremendous inspiration in drug discovery and chemical biology^{1–3}. Natural products arise through the evolution of biosynthetic pathways, driven by functional benefit to the host organism^{4,5}. In stark contrast, synthetic routes to bioactive small molecules are almost always developed in isolation from the assessment of their function.

In many discovery programmes, bioactive small molecules are initially identified by high-throughput screening, and, to facilitate this approach, cheminformatic approaches have been developed to assess the scaffold diversity of screening libraries⁶. The annotated bioactivity of known scaffolds can also facilitate the exploration of chemical space, and can provide inspiration in the design of bioactive molecules based on related scaffolds^{7,8}. The optimization of small-molecule function is generally undertaken through iterative rounds of design, synthesis and assaying⁹. To expedite ligand optimization, a narrow toolkit of reliable synthetic methods with predictable outcomes has emerged to support medicinal chemistry^{10,11}. Established medicinal chemistry approaches¹² may have inadvertently steered molecular design towards a subset of molecular scaffolds, and tended to exacerbate chemists' exceptionally uneven historic exploration of chemical space¹³. The emergence of diversity-oriented synthesis^{14–16} has expanded the diversity of small-molecule screening collections, but is still reliant on an expanded toolkit of synthetic methods with inherently predictable outcomes.

Although function has steered the directed evolution of biosynthetic pathways, for example to produce carotenoids with specific colours¹⁷, the emergence of chemical syntheses has rarely been directed by the function of the resulting products. Chemical strategies that link structure and function include the *in situ* synthesis of enzyme inhibitors from building blocks within active sites^{18–20}. In addition, dynamic combinatorial chemistry exploits reversible reactions to template the formation of cognate ligands for specific molecular targets²¹. To apply such approaches in bioactive small-molecule discovery, the challenge of developing reactions that operate efficiently under buffered aqueous conditions must be met. To date, only a few reactions have been developed that operate efficiently under conditions compatible with folded

proteins, fundamentally limiting the chemical diversity of the small molecules that may be discovered.

Here, we describe a novel discovery approach in which bioactive small-molecule function directs the emergence of an associated synthetic route. We specifically chose to exploit catalysed reactions with alternative possible outcomes that might be steered by the specific catalyst and reaction conditions used. It was anticipated that such reactions would enable the efficient exploration of the relevance of a wide range of molecular scaffolds to a required biological function.

In each round, an array of reactions was designed and, after scavenging, the products were assayed at increasingly low concentration for agonism of the androgen receptor. The results informed the design of a subsequent reaction array until, finally, promising reactions were scaled up to reveal, after purification, bioactive small-molecule ligands (Fig. 1a).

Crucially, the approach enabled the discovery of ligands with submicromolar activity, based on two scaffolds with no previously annotated activity against the androgen receptor. To our knowledge, the study constitutes the first example in which the emergence of synthetic routes conducted under non-aqueous conditions was directed by the biological activity of the resulting small-molecule products.

Results

Rationale for selection of chemistry. We chose to exploit catalysed reactions of diazo compounds because alternative outcomes are possible with many substrates, and yet may often be controlled through judicious choice of catalyst and reaction conditions. For example, α -diazo carbonyl compounds are well known to participate in many intermolecular²² reactions (for example, C–H, N–H and O–H insertions, cyclopropanations, ylide formation/cycloaddition) as well as intramolecular variants that form alternative ring sizes^{23–25}. Such inherently unpredictable reactions are generally unsuitable in current ligand discovery approaches, which typically involve the synthesis and purification of arrays of small molecules. However, such reactions are ideal in activity-directed synthesis because their outcome may often be controlled by appropriate catalysts and ligands^{26,27}, and

¹Astbury Centre for Structural Molecular Biology, University of Leeds, Leeds LS2 9JT, UK, ²School of Chemistry, University of Leeds, Leeds LS2 9JT, UK.
*e-mail: a.s.nelson@leeds.ac.uk; s.l.warriner@leeds.ac.uk

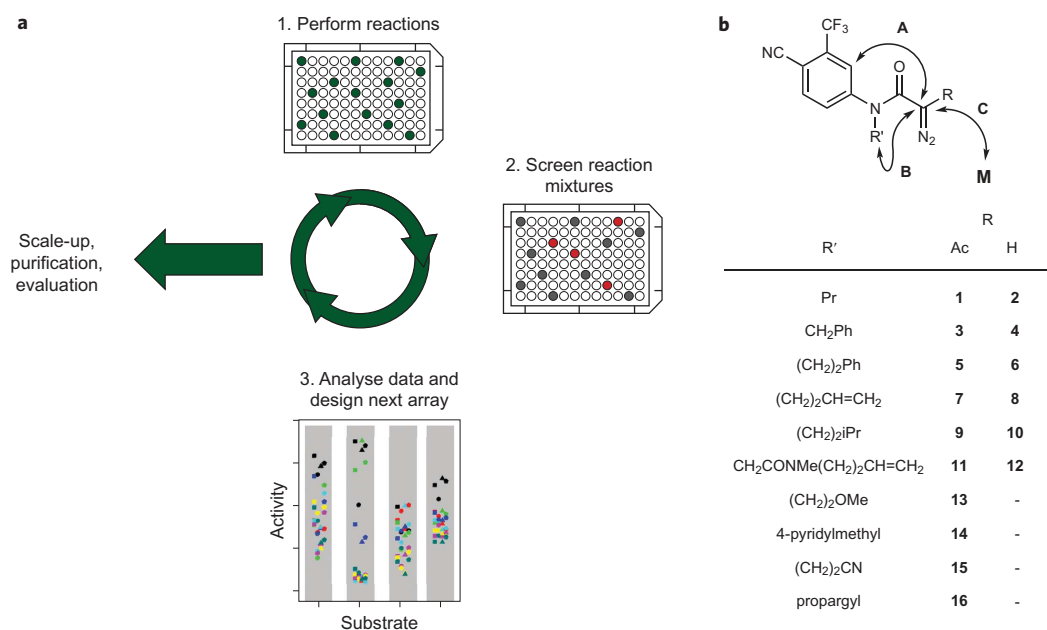


Figure 1 | Application of activity-directed synthesis to the discovery of androgen receptor agonists. **a**, Overview of activity-directed synthesis. In each round, arrays of reactions are performed in which the substrate, catalyst and solvent are varied. The resulting product mixtures are scavenged and then assayed at increasingly low concentrations to identify combinations that yield bioactive products. Analysis of the screening results can inform the design of the reaction array in the subsequent round. Finally, promising reactions are scaled up, and the products are purified, identified and evaluated. **b**, Design of α -diazo amide substrates that may react to yield androgen receptor agonists. Each substrate bears a 4-cyano-3-trifluoromethylphenyl group, a fragment that is found in a range of androgen receptor modulators. Possible fates of catalysed reactions of the substrates include intramolecular reaction with the appended *N*-aryl ring (A), intramolecular reaction with the R' side chain (B), and intermolecular reaction with a different molecule **M** (C).

synthetically accessible bioactive molecules based on alternative scaffolds might be discovered.

Three rounds of activity-directed synthesis. We investigated whether activity-directed synthesis could enable the discovery of novel chemotypes from a fragment found in a wide range of androgen receptor modulators^{28–32}. Initially, we prepared³³ twelve α -diazo amides **1–12**, which each bear the 4-cyano-3-trifluoromethylphenyl group and a variable R' group. Some possible intra- and intermolecular reactions that these substrates might undergo are outlined in Fig. 1b. The range of R' substituents was chosen to increase the scaffold diversity of possible cyclization products (for example, formed by intramolecular C–H insertion, cyclopropanation or ylide formation/cycloaddition). We performed an array of reactions in a 96-well plate in which the diazo substrate (100 mM in dichloromethane) and catalyst (1 mol%; for structures see Supplementary Fig. 1) were varied. After 48 h, the crude reactions were scavenged to remove metal contaminants (for optimization see Supplementary Fig. 2), evaporated and assayed for agonism of the androgen receptor (total concentration of products: 10 μ M in 1% dimethylsulfoxide (DMSO) in pH 7.5 aqueous buffer) (Fig. 2a and Supplementary Table 1). Activity was determined using a commercially available assay with a time-resolved Förster resonance energy transfer (FRET) readout³⁴. Crucially, we had already established that the diazo substrates were all inactive under the conditions of the assay (Supplementary Fig. 3). Four substrates (**1**, **3**, **6** or **7**) yielded products that were highly active. These substrates were fed into the design of the subsequent reaction array, together with, as a control, two substrates (**11** and **12**) that had not yielded active product mixtures.

In round two we performed an array of reactions in which the substrate (**1**, **3**, **6**, **7**, **11** and **12**), catalyst (1 mol%) and solvent (dichloromethane, THF, toluene or ethyl acetate) were varied. The

reactions were evaporated, scavenged and assayed at tenfold lower concentration (total concentration of products: 1 μ M in 1% DMSO in pH 7.5 aqueous buffer). Crucially, substrates **11** and **12**, which were included as controls, did not yield active product mixtures in round two. Furthermore, the activity of the product mixtures derived from the other substrates was critically dependent on the specific catalyst and reaction conditions used. For example, the most active product mixtures were derived from reactions of substrates **1** and **3**, but only when a specific class of catalyst (rhodium carboxylates) was used in specific solvents (dichloromethane, toluene or ethyl acetate) (Fig. 2b, Supplementary Table 2). These data suggest that the fate of these substrates may depend critically on the catalyst used, with only a specific class of catalyst steering the reaction towards active products.

In round three we exploited substrates **1** and **3**, as well as four additional structurally related substrates **13–16**. We performed a reaction array in which these six substrates were varied, together with the solvent (dichloromethane, toluene or ethyl acetate) and catalyst (six rhodium carboxylates including the two most promising catalysts from the previous round). The reaction products were assayed at tenfold lower concentration (total concentration of products: 100 nM in 1% DMSO in pH 7.5 aqueous buffer) (Fig. 2c, Supplementary Table 3). Again, for three substrates (**1**, **3** and **15**), reactions were only steered towards active products by a narrow range of catalysts and reaction conditions.

Identification and characterization of bioactive products. Finally, on the basis of active product mixtures identified in round 3, we scaled up eight reactions whose products had had the most promising biological activity (Table 1). In each case, a major product was purified, and its structure was elucidated. The three distinct major products were assayed at a range of concentrations for agonism of the androgen receptor (Table 1, Fig. 3) (for the

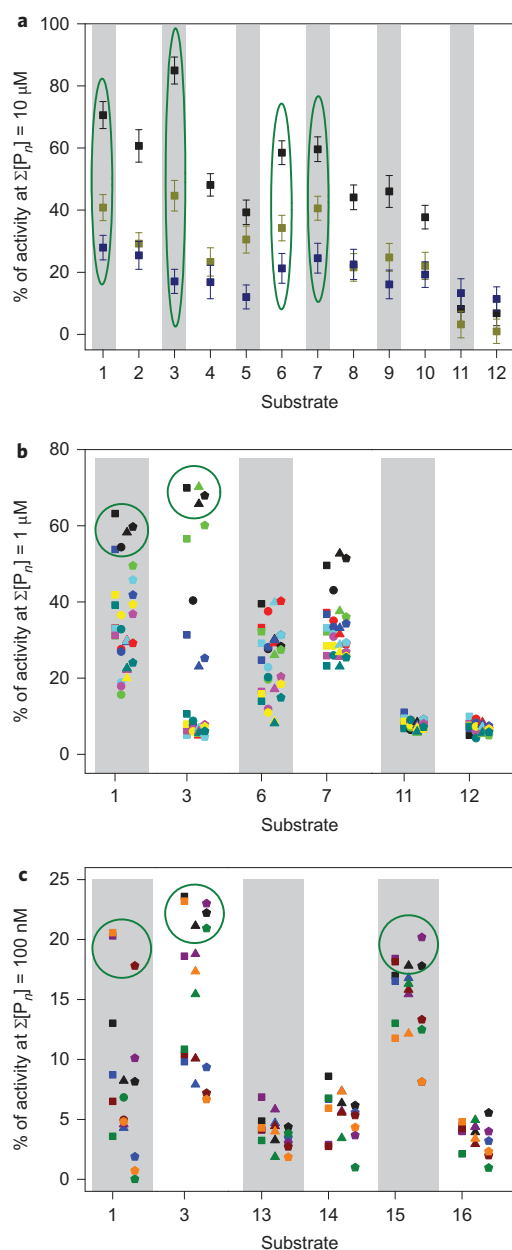


Figure 2 | Activity of product mixtures derived from reaction arrays.
a, In round 1, substrates **1**, **3**, **6** and **7** yielded active product mixtures. These substrates were fed into round 2, together with, as a control, two substrates, **11** and **12**, that had not yielded active product mixtures. **b**, In round 2, substrates **1** and **3** yielded active product mixtures when treated with rhodium carboxylate catalysts in dichloromethane, toluene or ethyl acetate. **c**, In round 3, the combinations of substrates, catalysts and solvents used were informed by the results from round 2. Specifically, we exploited the two most promising substrates (**1** and **3**) and four structurally related substrates (**13–16**); three promising solvents; and the two most promising catalysts and four related rhodium carboxylates. Eight promising reactions were selected for scale up on the basis of the activity of their products. Biological activity is expressed relative to 5 μ M testosterone. See Supplementary Tables 1–3 for the catalysts (represented by different colours, including $\text{Rh}_2(\text{OAc})_4$, black; $\text{Rh}_2(\text{tfa})_4$, dark blue; $\text{Rh}_2(\text{cap})_4$, light green) and solvents (represented by different shapes). Experiments were performed in duplicate. The error bars represent the standard deviation between replicates, and are omitted from **b** and **c** for clarity (typical error 1.5–4.5%, Supplementary Tables 1–3). tfa = trifluoroacetate; cap = caprolactamate.

Table 1 | Yield and activity of the products of reactions that were scaled up.

Entry	Reaction conditions*	Product	Yield (%)	EC ₅₀ (nM)
1	3 , 1 mol% $\text{Rh}_2(\text{esp})_2$, EtOAc	 17	75	340 \pm 30 (agonist)
2	3 , 1 mol% $\text{Rh}_2(\text{oct})_4$, CH_2Cl_2		71	
3	3 , 1 mol% $\text{Rh}_2(\text{OAc})_4$, CH_2Cl_2		68	
4	1 , 1 mol% $\text{Rh}_2(\text{esp})_2$, CH_2Cl_2	 18	90	470 \pm 40 (partial agonist [†])
5	1 , 1 mol% $\text{Rh}_2(\text{oct})_4$, CH_2Cl_2		88	
6	1 , 1 mol% $\text{Rh}_2(\text{OAc})_4$, CH_2Cl_2		55	
7	15 , 1 mol% $\text{Rh}_2(\text{esp})_2$, EtOAc	 19	78	440 \pm 60 (agonist)
8	15 , 1 mol% $\text{Rh}_2(\text{tpa})_4$, PhMe		70	

*esp = α,α,α' -tetramethyl-1,3-benzenedipropionate; tpa = triphenylacetate; oct = octanoate; [†]maximum activity was 50% that of testosterone.

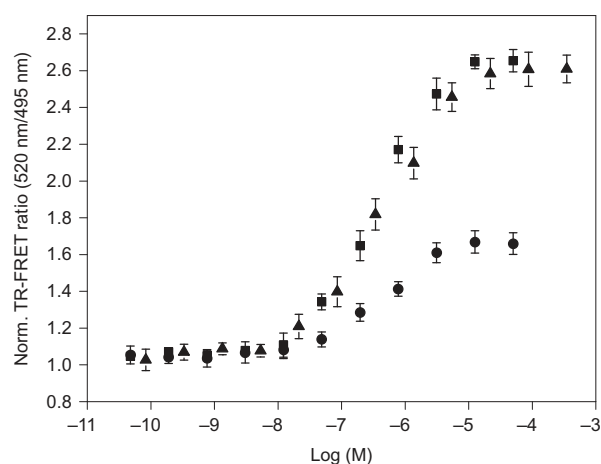


Figure 3 | Dose-dependent agonism of the androgen receptor by compounds **17, **18** and **19**.** The major products of reactions described in Table 1 were tested as agonists at a range of concentrations to show a dose-dependent effect. **17** (squares), **18** (circles) and **19** (triangles).

structure and activity of the reference ligands testosterone and flutamide, see Supplementary Fig. 4). To confirm its activity, the most potent ligand, **17**, was also prepared using an independent synthetic route (Supplementary Fig. 5a). This sample was found to have identical activity to that prepared by $\text{Rh}_2(\text{esp})_2$ -catalysed cyclization of substrate **3** (Supplementary Fig. 5b). The β -lactams **17** and **19** were full agonists of the androgen receptor, whereas γ -lactam **18** functioned as a partial agonist.

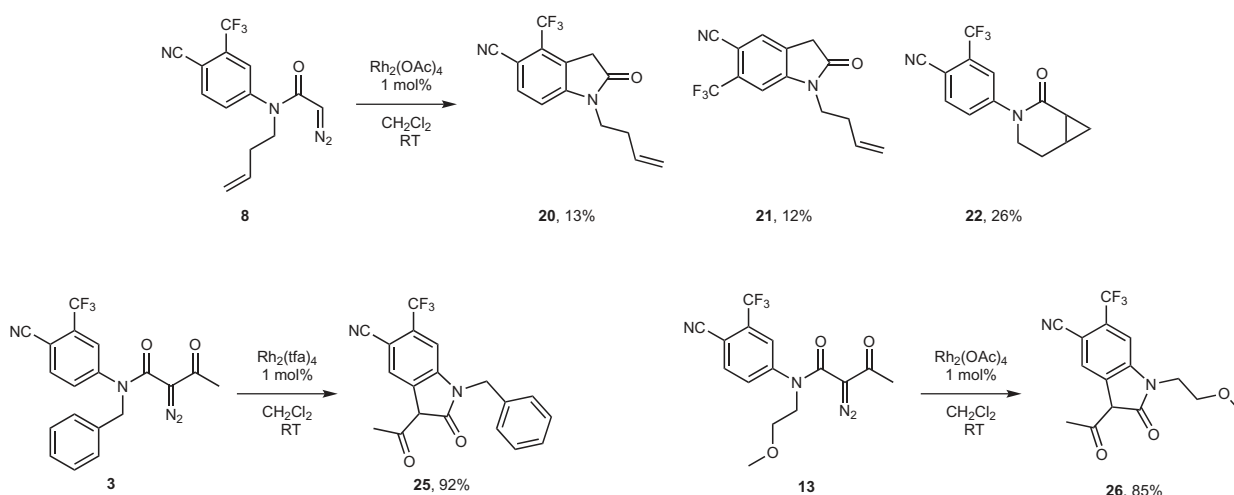


Figure 4 | A selection of the alternative products accessible from α -diazo amides **8**, **3** and **13**, which were explored in rounds one, two and three. The chemical space occupied by the products—oxindoles **20**, **21**, **25** and **26** and δ -lactam **22**—was explored yet ultimately discarded in the search for bioactive, synthetically accessible compounds. The activity of the product mixtures derived from these reactions is discussed in the main text.

Discussion

Activity-directed synthesis provides a novel and highly efficient approach to the discovery of bioactive small molecules, together with associated synthetic routes. The discovery of reactions that yield active products is undertaken in parallel through iterative rounds of reactions and screening. Only reactions that yield highly active products are scaled up, and the products then purified, identified and characterized. Resources are thus highly focused on bioactive reaction products. Conventional ligand optimization approaches tend to invest similar resources in all compounds prepared. Although parallel synthesis techniques are often exploited, purification of the resulting arrays of compounds is usually undertaken in series (often using mass-directed liquid chromatography) before assays are undertaken in parallel and structure–activity relationships are formulated.

To enable the discovery of alternative bioactive chemotypes, activity-directed synthesis requires methods where the outcome may be varied through the choice of specific catalyst and reaction conditions. We deliberately chose to exploit metal-catalysed reactions of diazo compounds on the basis of the range of intra- and intermolecular reaction types that are possible. To demonstrate the fitness of diazo chemistry for activity-directed synthesis we showed that the fate of α -diazo amide **3** varies widely, with three distinct compounds being observed in total, the distribution of which depends critically on the specific catalyst and reaction conditions used (Supplementary Fig. 6, Supplementary Table 4).

Promising reactions were identified solely on the basis of the activity of the resulting product mixtures. To demonstrate that the activity of the product mixtures provides insights into the activity of individual components, we purified and assayed the products of a limited number of reactions (Fig. 4, Supplementary Fig. 7). The $\text{Rh}_2(\text{OAc})_4$ -catalysed reaction of **8** (from round 1) gave low yields of oxindole **20** (yield, 13%; $\text{EC}_{50} = 10.1 \pm 0.1 \mu\text{M}$), oxindole **21** (yield, 12%; inactive up to 1 mM) and δ -lactam **22** (yield, 26%; $\text{EC}_{50} = 0.71 \pm 0.14 \mu\text{M}$; partial agonist); the activity of this product mixture was determined (Supplementary Table 1), but did not quite reach the threshold used to select substrates for round 2. The $\text{Rh}_2(\text{tfa})_4$ -catalysed reaction of **3** in CH_2Cl_2 (from round 2, screened at a total product concentration of 1 μM) and the $\text{Rh}_2(\text{OAc})_4$ -catalysed reaction of **13** in CH_2Cl_2 (from round 3, screened at a total product concentration of 100 nM) gave oxindoles **25** (yield, 92%; $\text{EC}_{50} = 2.4 \pm 0.5 \mu\text{M}$) and **26** (yield, 85%; $\text{EC}_{50} = 12.0 \pm 0.3 \mu\text{M}$), respectively. In each case the activity of the

product mixture was low (Supplementary Tables 2 and 3), reflecting the expected activity of these compounds at the concentrations screened. Thus, in addition to the active β - and γ -lactams (**17**–**19**) prepared from **1**, **3** and **15**, significant chemical space accessible to the substrates was thus explored, yet ultimately discarded, in the search for synthetically accessible, bioactive compounds.

We analysed the impact of screening at tenfold lower concentration in each round of activity-directed synthesis. Accordingly, we retrospectively assayed the product mixtures from rounds 2 and 3 at the total product concentrations used in the previous round (that is, 10 μM and 1 μM , respectively) (compare Fig. 2b,c with Supplementary Fig. 8b₁,c₁). At the lower concentration, the dynamic range of the assay was greater, improving confidence that the most promising reactions were taken forward, either to feed into round 3 (from round 2) or for scale up (from round 3).

The screening of mixtures has already been adopted in discovery programmes³⁵, and approaches to help identify the active components have been developed³⁶. However, in activity-directed synthesis, the activity observed would probably be influenced not only by the activities of the individual components, but also by their yield. It was therefore expected that the approach would allow the identification of reactions in which a substrate was steered towards the most active product. To test this, and to understand the basis of the discovery of the most active ligand **17**, we correlated, retrospectively, the activity of the product mixtures derived from **3** with its yield (Supplementary Fig. 9, Supplementary Tables 5 and 6). In round 2, a low level of activity was observed for most product mixtures at a total product concentration of 1 μM , usually because the reaction had been steered towards the poorly active oxindole **25** ($\text{EC}_{50} = 2.4 \pm 0.5 \mu\text{M}$) (Supplementary Fig. 8). However, under specific reaction conditions, a high level of activity was observed that correlated with a high yield of β -lactam **17** ($\text{EC}_{50} = 340 \pm 30 \text{ nM}$). Optimization of the yield of active components (such as **17**) greatly facilitated their purification and structural elucidation.

In addition to optimizing the yield of active products, activity-directed synthesis also enabled the discovery of structurally related bioactive small molecules. The reactions performed in round 3 were inspired by the most promising substrates, catalysts and solvents used in round 2. Two of the reactions selected for scale up involved substrate **15**, which had first been introduced in round 3, and both reactions gave the active β -lactam **19** in good yield (78% and 70%, Table 1). The discovery of this bioactive molecule thus

stemmed from a reaction in round 2 that had yielded the structurally related β -lactam (19).

Activity-directed synthesis was exploited in the discovery of bioactive small molecules by the development of a fragment. A directed approach enabled the discovery of three bioactive small molecules with submicromolar activity: β -lactam 17 (EC_{50} = 340 nM), γ -lactam 18 (EC_{50} = 470 nM) and β -lactam 19 (EC_{50} = 440 nM). In each case, it was simple to identify the most active component from the product mixture, a process that was greatly facilitated by the emergence of a high-yielding synthesis (highest yield of 17, 75% from 3; highest yield of 18, 90% from 1; highest yield of 19, 78% from 15). Notably, the optimal catalyst for the synthesis of the most active ligands (17–19)— $Rh_2(esp)_2$ —was designed rationally to catalyse C–H aminations³⁷, and would have been unlikely to have been exploited in a deliberate synthesis of β - or γ -lactams.

Activity-directed synthesis is broadly analogous to the evolution of a biosynthetic pathway, because bioactive small molecules emerge in tandem with routes for their synthesis. Because the approach was underpinned by reactions with alternative outcomes, the discovery of bioactive compounds based on two distinct scaffolds was possible. Remarkably, neither of these chemotypes had previously annotated activity against the androgen receptor. In addition to metal-catalysed reactions of diazo compounds, it is likely that many other reactions that have alternative possible outcomes—such as metal- and organo-catalysed inter- and intramolecular reactions—may also have value in activity-directed synthesis. By liberating chemists to exploit the most powerful transformations at their disposal, we anticipate that this highly general approach could be applied in the discovery of novel and diverse chemotypes with a very broad range of biological functions.

Received 15 January 2014; accepted 16 July 2014;
published online 24 August 2014

References

- Newman, D. J. & Cragg, G. M. Natural products as sources of new drugs over the last 25 years. *J. Nat. Prod.* **70**, 461–477 (2007).
- Beghyn, T., Deprez-Poulain, R., Willand, N., Folleas, B. & Deprez, B. Natural compounds: leads or ideas? Bioinspired molecules for drug discovery. *Chem. Biol. Drug Des.* **72**, 3–15 (2008).
- Wetzel, S., Bon, R. S., Kumar, K. & Waldmann, H. Biology-oriented synthesis. *Angew. Chem. Int. Ed.* **50**, 10800–10826 (2011).
- Maplestone, R. A., Stone, M. J. & Williams, D. H. The evolutionary role of secondary metabolites—a review. *Gene* **115**, 151–157 (1992).
- Firn, R. D. & Jones, C. G. Natural products—a simple model to explain chemical diversity. *Nat. Prod. Rep.* **20**, 382–391 (2003).
- Krier, M., Bret, G. & Rognan, D. Assessing the scaffold diversity of screening libraries. *J. Chem. Inf. Model.* **46**, 512–524 (2006).
- Wetzel, S. *et al.* Interactive exploration of chemical space with Scaffold Hunter. *Nature Chem. Biol.* **5**, 581–583 (2009).
- Renner, S. *et al.* Bioactivity-guided mapping and navigation of chemical space. *Nature Chem. Biol.* **5**, 585–592 (2009).
- Kishirsagar, T. (ed.) *High-Throughput Lead Optimization in Drug Discovery* (CRC, 2008).
- Roughley, S. D. & Jordan, A. M. The medicinal chemist's toolbox: an analysis of reactions used in the pursuit of drug candidates. *J. Med. Chem.* **54**, 3451–3479 (2011).
- Cooper, T. W. J., Campbell, I. B. & Macdonald, S. J. F. Factors determining the selection of organic reactions by medicinal chemists and the use of the reactions in arrays (small focused libraries). *Angew. Chem. Int. Ed.* **49**, 8082–8091 (2010).
- Walters, W. P., Green, J., Weiss, J. R. & Murcko, M. A. What do medicinal chemists actually make? A 50-year retrospective. *J. Med. Chem.* **54**, 6405–6416 (2011).
- Lipkus, A. H. *et al.* Structural diversity of organic chemistry. A scaffold analysis of the CAS registry. *J. Org. Chem.* **73**, 4443–4451 (2008).
- Trabocchi, A. (ed.) *Diversity-Oriented Synthesis: Basics and Applications in Organic Synthesis, Drug Discovery and Chemical Biology* (Wiley, 2013).
- Burke, M. D. & Schreiber, S. L. A planning strategy for diversity-oriented synthesis. *Angew. Chem. Int. Ed.* **43**, 46–58 (2004).
- Galloway, W. R. J. D., Isidro-Llobet, A. & Spring, D. R. Diversity-oriented synthesis as a tool for the discovery of novel biologically active small molecules. *Nature Commun.* **1**, 80 (2010).
- Umeno, D., Tobias, A. V. & Arnold, F. H., Diversifying carotenoid biosynthetic pathways by directed evolution. *Microbiol. Mol. Biol. Rev.* **69**, 51–78 (2005).
- Lewis, W. G. *et al.* Click chemistry *in situ*: acetylcholinesterase as a reaction vessel for the selective assembly of a femtomolar inhibitor from an array of building blocks. *Angew. Chem. Int. Ed.* **41**, 1053–1057 (2002).
- Hirose, T. *et al.* Observation of the controlled assembly of preclick components in the *in situ* click chemistry generation of a chitinase inhibitor. *Proc. Natl. Acad. Sci. USA* **110**, 15892–15897 (2013).
- Mamidyala S. K. & Finn, M. G. *In situ* click chemistry: probing the binding landscapes of biological molecules. *Chem. Soc. Rev.* **39**, 1252–1261 (2010).
- Corbett, P. T. *et al.* Dynamic combinatorial chemistry. *Chem. Rev.* **106**, 3652–3711 (2006).
- Davies, H. M. & Morton, D. Guiding principles for site selective and stereoselective intermolecular C–H functionalization by donor/acceptor rhodium carbenes. *Chem. Soc. Rev.* **40**, 1857–1869 (2011).
- Padwa, A. & Weingarten, D. M. Cascade processes of metallo carbenoids. *Chem. Rev.* **96**, 223–269 (1996).
- Doyle, M. P. & Forbes, D. C. Recent advances in asymmetric catalytic metal carbene transformations. *Chem. Rev.* **98**, 911–935 (1998).
- Davies, H. M. L. & Beckwith, R. E. J. Catalytic enantioselective C–H activation by means of metal–carbenoid-induced C–H insertion. *Chem. Rev.* **103**, 2861–2903 (2003).
- Nadeau, E., Ventura, D. L., Brekan, J. A. & Davies H. M. L. Controlling factors for C–H functionalization versus cyclopropanation of dihydronaphthalenes. *J. Org. Chem.* **75**, 1927–1939 (2010).
- Davies, H. M. L., Matasi, J. J. & Ahmed G. Divergent pathways in the intramolecular reactions between rhodium-stabilized vinylcarbenoids and pyrroles: construction of fused tropanes and 7-azabicyclo[4.2.0]octadienes. *J. Org. Chem.* **61**, 2305–2313 (1996).
- Gao, W., Bohl, C. E. & Dalton, J. T. Chemistry and structural biology of androgen receptor. *Chem. Rev.* **105**, 3352–3370 (2005).
- Fang, H. *et al.* Study of 202 natural, synthetic, and environmental chemicals for binding to the androgen receptor. *Chem. Res. Toxicol.* **16**, 1338–1358 (2003).
- Gao, W. & Dalton, J. T. Expanding the therapeutic use of androgens via selective androgen receptor modulators (SARMs). *Drug Discov. Today* **12**, 241–248 (2007).
- Mitchell, L. H. *et al.* Rational design of a topical androgen receptor antagonist for the suppression of sebum production with properties suitable for follicular delivery. *J. Med. Chem.* **53**, 4422–4427 (2010).
- Tong, Y. Androgen receptor antagonists and uses thereof. PCT patent WO 2012/119559 A1 (2012).
- Gauthier, D., Dodd, R. H. & Dauban, P. Regioselective access to substituted oxindoles via rhodium-catalyzed carbene C–H insertion. *Tetrahedron* **65**, 8542–8555 (2009).
- Ozers, M. S. *et al.* The androgen receptor T877A mutant recruits LXXLL and FXXLF peptides differently than wild-type androgen receptor in a time-resolved fluorescence resonance energy transfer assay. *Biochemistry* **46**, 683–695 (2007).
- Kyranos, J. (ed.) *High Throughput Analysis For Early Drug Discovery* (Elsevier, 2004).
- Cawse, J. N., Wroczynski, S. & Darchun, B. Y. Method for defining an experimental space and method and system for conducting combinatorial high throughput screening of mixtures. US patent 6,826,487 B1 (2004).
- Espino, C. G., Fiori, K. W., Kim, M. & Du Bois, J. Expanding the scope of C–H amination through catalyst design. *J. Am. Chem. Soc.* **126**, 15378–15379 (2004).

Acknowledgements

The authors acknowledge funding from the University of Leeds and from the EPSRC (for equipment). The authors also thank K. Krishenbaum, P. M. Levine (both New York University) and S. Bartlett (University of Leeds) for discussions.

Author contributions

A.N. and S.W. conceived, designed and supervised the project. G.K. undertook the experimental work. A.N., S.W. and G.K. analysed the results and wrote the paper.

Additional information

Supplementary information and chemical compound information are available in the online version of the paper. Reprints and permissions information is available online at www.nature.com/reprints. Correspondence and requests for materials should be addressed to S.W. and A.N.

Competing financial interests

The authors declare no competing financial interests.